Identification et modélisation des processus à l'origine des transferts de phosphore dissous dans un bassin versant agricole

Rémi Dupas

N° ordre : 2015-23
N° Série : D-78

THESE / AGROCAMPUS OUEST

Sous le label de l'Université Européenne de Bretagne

pour obtenir le diplôme de :

DOCTEUR DE L'INSTITUT SUPERIEUR DES SCIENCES AGRONOMIQUES, AGRO-ALIMENTAIRES, HORTICOLES ET DU PAYSAGE

Spécialité : Sciences de l'environnement

Ecole Doctorale : Sciences de la matière

présentée par :

Rémi Dupas

Identification et modélisation des processus à l'origine des transferts de phosphore dissous dans un bassin versant agricole

soutenue le 16 novembre 2015 devant la commission d'Examen

Composition du jury :
Rapporteur : Phil Jordan - Professeur - School of environmental Sciences, Irlande
Rapporteur : Sylvain Payraudeau - Maître de conférences - ENGEES Strasbourg
Président : Christian Walter - Professeur - AGROCAMPUS OUEST Rennes
Examinatrice : Ophélie Fovet - Chercheur - INRA Rennes
Examinateur : Sylvain Pellerin - Directeur de recherche - INRA Bordeaux
Directrice de thèse : Chantal Gascuel - Odoux - Directrice de recherche - INRA Rennes

Laboratoire d'accueil :
UMR INRA – Agrocampus Ouest, Sol Agro et hydrosystème Spatialisation (Rennes)

Avant-propos

Cette thèse a été réalisée à l'UMR Sol, Agro et hydrosystème, Spatialisation (SAS) entre juin 2013 et septembre 2015, sous contrat Agrocampus Ouest. Elle a été encadrée par Chantal Gascuel-Odoux (DR INRA, Rennes) et s'est inscrite dans le projet Trans-P, portant sur les transferts de phosphore dans la région Bretagne, financé par l'agence de l'eau Loire Bretagne. Elle repose en grande partie sur les données de l'Observatoire de Recherche en Environnement AgrHys.

Elle a bénéficié des conseils d'un comité de pilotage composé de Jean-Marcel Dorioz (DR INRA, Thonon), Josette Garnier (DR CNRS, Paris), Gérard Gruau (DR CNRS, Rennes) et Bruno Ringeval (CR INRA, Bordeaux), et a été enrichie par un séjour scientifique de 3 mois 1/2 à l'Université de Lancaster (Royaume-Uni) sur invitation de Phil Haygarth.

Remerciements

Une thèse est l'aboutissement d'un effort individuel mais surtout d'un travail collectif. C'est particulièrement le cas de celle-ci, puisque ce travail s'appuie sur un jeu de données et un socle de connaissance acquis avant mon arrivée à l'UMR SAS.

Je remercie donc en premier lieu les personnes qui ont participé à l'acquisition des données et au développement des connaissances préalables sur les transferts de solutés sur le site de Kervidy-Naizin (ORE AgrHyS). L'ensemble de l'UMR SAS est donc à remercier, en particulier l'équipe de techniciens de terrain et de laboratoire.

Je remercie aussi l'ensemble de l'équipe du projet Trans-P et notamment Chantal Gascuel pour avoir eu la bonne idée de lancer un projet de recherche sur le phosphore. Merci Chantal de m'avoir proposé cette thèse et de m'avoir fait confiance depuis 2011. Merci aux collègues de Géosciences Rennes, de l'université de Tours et de l'UMR SAS pour les discussions que nous avons eues autour des trois axes du projet Trans-P.

Je remercie les collègues des autres projets portant sur les cycles de l'azote et du carbone sur le même site d'étude : MOSAIC, ESCAPE. Ensemble la recherche sur les trois éléments majeurs carbone, azote et phosphore a bien avancé au cours des trois dernières années, et les travaux à venir sur l'intégration des trois cycles vont en être facilités.

Je remercie les collègues de l'université de Lancaster qui m'ont accueilli pendant 3 mois 1/2 notamment Phil Haygarth, Michael Hollaway et Keith Beven.

Je remercie les membres du jury : Phil Jordan, Sylvain Payraudeau, Christian Walter, Ophélie Fovet et Sylvain Pellerin ainsi que les membres du comité de thèse : Jean-Marcel Dorioz, Josette Garnier, Gérard Gruau et Bruno Ringeval.

Un grand merci aux collègues CDD, thésards post-doc pour les moments de convivialité.

Enfin, un énorme merci à mes proches pour leur soutien !

Résumé

Le phosphore est, avec l'azote, un facteur de contrôle de l'eutrophisation. Le phosphore présent dans les masses d'eau provient d'émissions ponctuelles, d'origine domestique et industrielle, et d'émissions diffuses, principalement d'origine agricole. Avec la diminution des émissions ponctuelles dans les pays occidentaux, la part du phosphore d'origine agricole augmente. En Bretagne, les teneurs élevées en phosphore des sols, combinées à la forte vulnérabilité des masses d'eau, nécessitent de mieux comprendre les mécanismes à l'origine des transferts de phosphore diffus. L'objectif de cette thèse a été d'identifier et de quantifier les mécanismes à l'origine des transferts de phosphore, par une démarche intégrant analyse de données d'observations multi-échelle et modélisation.

L'analyse d'une chronique de chimie de l'eau à l'exutoire d'un petit bassin versant à dominance de terres arables a révélé que les formes particulaires et dissoutes du phosphore avaient des origines différentes dans le paysage, et étaient transférées par des mécanismes généralement indépendants. Le phosphore particulaire provient de la remise en suspension de sédiments présents dans le cours d'eau, de l'érosion des berges et occasionnellement d'épisodes érosifs dans les versants. Le phosphore dissous provient des sols de la zone riparienne, d'extension variable en fonction de l'état d'humidité du bassin versant ; il est transféré par écoulement de subsurface lorsque les fluctuations de nappe créent une connexion hydrologique entre sol et rivière. Ces mécanismes ont été confirmés par une étude comparée des transferts de phosphore particulaire et dissous en crue dans deux bassins versants, en mettant en œuvre une méthode de clustering de crues reposant sur l'algorithme Dynamic Time Warping.

Le suivi multi-site de la concentration en phosphore dans l'eau des sols ripariens a permis de préciser le rôle de la nappe dans les transferts de phosphore dissous. Les données collectées ont mis en évidence que les fluctuations de nappe agissaient non seulement sur le transfert, mais aussi sur les mécanismes biogéochimiques à l'origine de la solubilisation du phosphore dans les sols. Deux moments importants ont été identifiés : la période de sécheresse estivale est favorable à la constitution d'un pool de phosphore mobile dans les sols, exporté à l'automne et en début d'hiver ; lorsque la nappe stagne dans les sols sans apport d'oxygène, la dissolution en condition réductrice des oxydes de Fer provoque un second relargage de phosphore. Ces deux épisodes de mobilisation dans les sols produisent un signal visible dans la rivière.

Un modèle couplé hydrologie-biogéochimie a permis de confirmer les hypothèses formulées suite à l'analyse de données d'observation sur le rôle de la nappe, de la teneur en phosphore des sols et des variations de température et d'humidité. Une analyse de l'incertitude dans les données et sa propagation dans le modèle ont permis d'assortir les prédictions

d'un intervalle de crédibilité, et de proposer des pistes pour réduire cette incertitude. L'utilisation d'analyseurs de phosphore sur site permettrait d'améliorer deux aspects du suivi : la fréquence de mesure et le délai entre prélèvement et analyse des échantillons.

Finalement, cette thèse a permis d'ajouter de la connaissance sur les flux d'éléments majeurs dans les bassins agricoles intensifs, en ajoutant le phosphore aux connaissances déjà existantes sur le carbone et l'azote. Des perspectives de recherche et de gestion se profilent en développant une vision intégrée des trois éléments.

Abstract

Phosphorus is, together with nitrogen, a controlling factor of eutrophication. Phosphorus in water bodies originates both from point-source emissions, of domestic and industrial origin, and diffuse emissions, mainly of agricultural origin. In western countries, reduction of point source emissions in the last two decades has resulted in a proportionally increasing contribution of agricultural phosphorus. In Brittany, the high phosphorus content of soils, combined with the high vulnerability of water bodies, asks for a better understanding of the processes controlling diffuse transfer. The objective of this thesis was to identify and quantify the processes controlling phosphorus transfer, with an approach combining analysis of multi-scale observation data and modelling.

Analysis of a water chemistry time series acquired at the outlet of a small arable catchment revealed that particulate and dissolved phosphorus forms had different spatial origin within the landscape, and were transferred through distinct mechanisms. Particulate phosphorus originates from resuspension of stream bed sediments, bank erosion and occasionally from erosion on hillslopes. Dissolved phosphorus originates from riparian soils, with a contributing area varying in size according to the catchments' wetness ; dissolved phosphorus is transferred via subsurface flow when the water table fluctuations create a hydrological connection between soils and the stream. These mechanisms were confirmed by a comparative study of storm transfer of dissolved and particulate phosphorus in two catchments, with a clustering method involving the use of the Dynamic Time Warping.

Multi-site monitoring of phosphorus concentration in the soil pore water of the riparian zone enabled a clarification of the role of groundwater in dissolved phosphorus transfer. The data showed that groundwater fluctuations controlled not only phosphorus transfer, but also the biogeochemical mechanisms controlling phosphorus solubilisation in soils. Two critical moments were identified : the summer dry period is favourable for the build-up of a pool of mobile phosphorus forms in soils, which is transferred in the autumn and the beginning of winter ; when groundwater stagnates in soil in anoxic conditions, reductive dissolution of iron oxides causes a second phosphorus release. These two critical moments of phosphorus mobilisation in the soils produce a clearly visible signal in the stream.

A coupled hydrological-biogeochemical model confirmed the hypotheses derived from the analysis of observation data, regarding the role of groundwater fluctuation, the soil phosphorus content and variability in soil temperature and moisture. An assessment of the information content in the data and the propagation of uncertainty enabled the addition of a credibility interval to model predictions, and the suggestion of options to reduce this uncertainty. Using bankside analysers would improve two aspects of the monitoring : the monitoring frequency and the delay between sampling and sample analysis.

Finally, this thesis brings forth new knowledge about fluxes of major elements (carbon, nitrogen, phosphorus) in intensively farmed agricultural catchments. Major research and management perspectives are made possible with an integrated vision of these three elements.

Sommaire

Table des figures

Liste des tableaux

Chapitre 1

Introduction générale

1.1 Le phosphore, un élément au centre d'enjeux mondiaux et locaux

1.1.1 Un élément essentiel à la vie

Le phosphore est le onzième élément le plus abondant de la croûte terrestre. C'est un élément essentiel à la vie. Il entre dans la composition et permet le fonctionnement de tous les organismes vivants, animaux, végétaux, microorganismes (Bundy *et al.*, 2005). Les acides nucléiques (ADN, ARN), supports de l'information génétique, contiennent du phosphore, tout comme les molécules impliquées dans les processus énergétiques (ATP). Le phosphore entre aussi dans la composition des tissus du vivant ; par exemple, l'enveloppe cellulaire est constituée en grande partie de phospholipides, et les os et les dents sont riches en phosphore, principalement sous forme de phosphate de calcium (Hyland *et al.*, 2005).

1.1.2 L'enjeu de la ressource

Contrairement à d'autres éléments majeurs (Carbone, Oxygène, Azote), le cycle du phosphore ne comporte pas de composante gazeuse en quantité significative. La disponibilité du phosphore dans les écosystèmes terrestres dépend donc de l'altération des roches à l'origine de la formation des sols, ainsi qu'aux apports anthropiques (Delmas *et al.*, 2015). L'exploitation des gisements de phosphate par l'homme depuis le XIX^{e} siècle (Figure 1.1) a contribué à l'augmentation des rendements agricoles (Ringeval *et al.*, 2014). Elle a aussi eu pour effet de modifier le cycle du phosphore à l'échelle de la planète, de par l'enrichissement déséquilibré de certaines régions par rapport à d'autres (Cordell *et al.*, 2009).

Du fait de l'absence d'une composante gazeuse dans son cycle, le phosphore est considéré comme une ressource non renouvelable à une échelle de temps humaine. La constitution des gisements de phosphate de roche exploitables s'aborde à une échelle de temps géologique. Les réserves actuelles en phosphate de roche se répartissent principalement entre cinq grands pays producteurs, Chine, Maroc, Etats-Unis, Afrique du sud et Jordanie, qui assurent 85% de la production mondiale (Schroder *et al.*, 2011). Avec l'actuelle poussée démographique mondiale, associée à une évolution des régimes alimentaires incluant de plus en plus de produits d'origine animale, la demande alimentaire, et donc

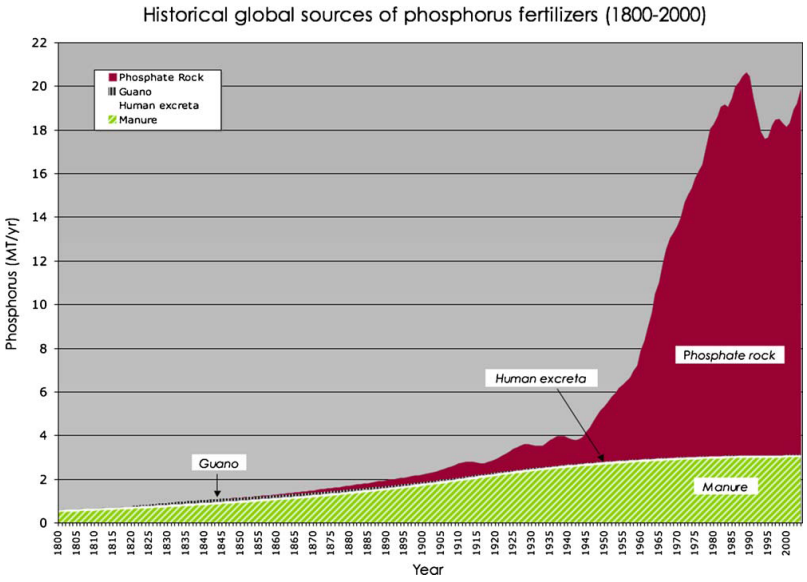

FIGURE 1.1 – Evolution historique des sources mondiales d'engrais phosphatés (Cordell et al., 2009)

la demande en engrais phosphatés, augmente et devrait continuer d'augmenter dans les prochaines décennies (Neset et Cordell, 2012). Cette prise de conscience d'une pression croissante sur une ressource non renouvelable a amené certains experts à prévoir un « pic de phosphore » à moyen terme (Figure 1.2). Il existe actuellement une grande incertitude sur la date estimée de ce pic, prévu dans quelques décennies à quelques siècles (Cordell et White, 2011).

Une chose est sûre : les ressources futures seront plus coûteuses à extraire et à purifier. On peut s'attendre à ce que cette pression croissante sur une ressources non renouvelable et inégalement répartie soit à l'origine de tensions géopolitiques et d'instabilité sur les prix, avec des conséquences sur la sécurité alimentaire mondiale (Cordell et White, 2011). Un épisode récent permet de présager de la future volatilité des prix : en 2008, le prix du phosphate de roche a augmenté soudainement de 800% (Schroder *et al.*, 2011). Si l'étude de ces enjeux géopolitiques n'est pas l'objet de cette thèse, celle-ci doit permettre de répondre à un enjeu de gestion souvent mis en avant dans les études de bilan de flux de phosphore mondiaux : celui de limiter les pertes et de favoriser les recyclages à toutes les échelles, y compris celles des bassins versants (Senthilkumar *et al.*, 2012a, b).

1.1.3 L'enjeu de l'eutrophisation

Le phosphore est un élément limitant, avec l'azote, de la production primaire des écosystèmes terrestres et aquatiques (Carpenter *et al.*, 1998 ; Correll, 1998). En contexte agricole, on cherche donc à accroître sa disponibilité pour les cultures, soit en recyclant de la matière organique, soit en important des engrais minéraux. Si une disponibilité élevée du phosphore dans les sols agricoles est souhaitable pour soutenir une demande alimen-

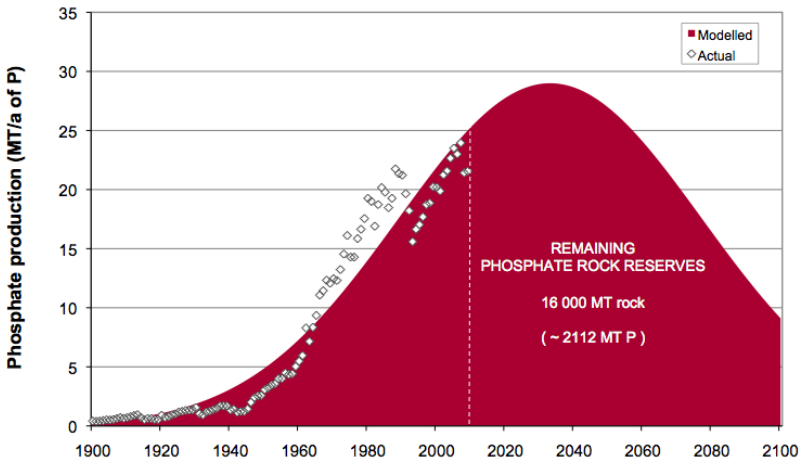

FIGURE 1.2 – Exemple de scenario d'évolution des réserves mondiales en phosphore, prédisant un pic en 2033 (scenario UGCS cité par Cordell et al., 2011)

taire mondiale croissante, elle s'accompagne souvent d'un transfert accru vers les milieux aquatiques, qui s'ajoute aux émissions ponctuelles d'origine industrielle ou domestique (Bouraoui et Grizzetti, 2011 ; Grizzetti *et al.*, 2012). Or la présence excessive de phosphore biodisponible dans les écosystèmes aquatiques représente une menace puisque le phosphore, avec l'azote, est à l'origine de l'eutrophisation, un enrichissement excessif en éléments nutritifs qui se manifeste par le développement massif de phytoplancton, d'algues et/ou de végétaux aquatiques (Smith et Schindler, 2009). Cette perturbation des écosystèmes aquatiques peut aussi être à l'origine de problèmes de santé publique, comme ceux liés à la prolifération de cyanobactéries sécrétant des toxines dangereuses pour l'homme (Serrano *et al.*, 2015). Il est généralement admis que le phosphore est l'élément limitant de l'eutrophisation en eaux douces continentales, tandis de l'azote est l'élément limitant pour les eaux côtières (Schindler *et al.*, 2008 ; Chevassus-au-Louis *et al.*, 2012). Une étude à l'échelle de la France des ratios de flux d'azote et de phosphore estimés par modélisation tend à confirmer le caractère limitant du phosphore en eaux douces continentales (Dupas *et al.*, 2015), même si de nombreux facteurs en interactions jouent un rôle difficile à appréhender : les variations saisonnières des conditions de température et de luminosité, la biodisponibilité de différentes formes de phosphore, la charge interne présente dans les masses d'eau, etc.

1.1.4 Transferts ponctuels et diffus

La part du phosphore d'origine diffuse, liée au paysage dans son ensemble, et ponctuelle, liée à des rejets, est très variable selon les régions du globe (Nemery *et al.*, 2005 ; Alexander *et al.*, 2008 ; Van Drecht *et al.*, 2009 ; Grizzetti *et al.*, 2012). En France, 46% du flux de phosphore total dans les cours d'eau provenait de transferts diffus d'origine agricole entre 2005 et 2009, contre 97% pour l'azote (Dupas *et al.*, 2015) (Figure 1.3).

En Bretagne, une analyse de chroniques basse fréquence (Legeay *et al.*, 2015) a permis

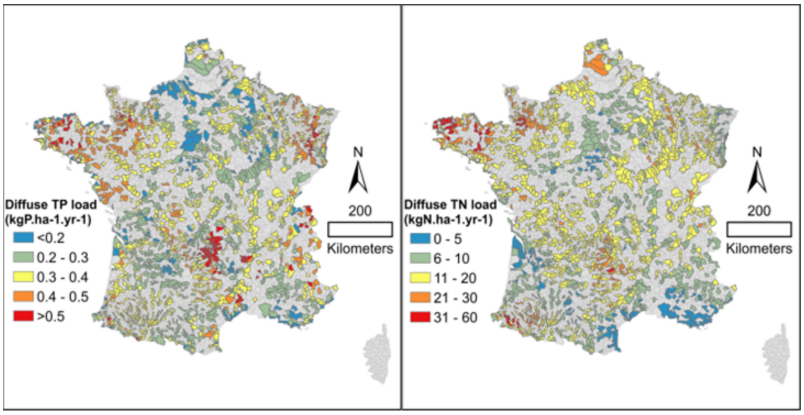

FIGURE 1.3 – Estimation des flux d'azote et de phosphore total sur l'ensemble des têtes de bassins versants en France métropolitaine entre 2005 et 2009, d'après le modele statistique Nutting (Dupas et al., 2015)

d'estimer que 70% du flux de phosphore était d'origine diffuse agricole sur la période 2007 – 2011. Si ces chiffres sont à considérer avec précaution, du fait de la forte incertitude liée à la manière de les estimer, un ordre de grandeur autour de 50% pour le flux diffus agricole est généralement admis dans les pays occidentaux (Alexander *et al.*, 2008 ; Dorioz *et al.*, 2013). L'étude bretonne a également permis de montrer que la part relative des sources ponctuelles et diffuses s'est inversée au cours des deux dernières décennies : minoritaires il y a vingt ans, les émissions diffuses agricoles sont aujourd'hui majoritaires en Bretagne (Figure 1.4).

Les raisons avancées sont l'abandon des phosphates dans les lessives, l'amélioration des techniques d'épuration et une possible augmentation des transferts diffus agricoles. La diminution des rejets ponctuels et l'augmentation des transferts diffus d'origine agricole ont été observées dans de nombreux pays occidentaux (Collins *et al.*, 2014 ; Schoumans *et al.*, 2014).

1.2 Origines spatiales et voies de transfert du phosphore diffus

Pour limiter les pertes diffuses en phosphore dans les bassins versant, il faut identifier l'origine spatiale des sources, les mécanismes à l'origine de la production de formes mobiles de phosphore et les voies de transferts (Schoumans *et al.*, 2014).

1.2.1 Cadre théorique

Dans les paysages agricoles, les transferts de phosphore ont lieu lorsque coïncident dans le temps et dans l'espace, la présence d'une « source » et l'activation de processus hydrologiques à l'origine du « transfert ». Le concept de « Critical Source Area » consiste en l'identification des facteurs source et transfert dans les paysages afin de cartographier

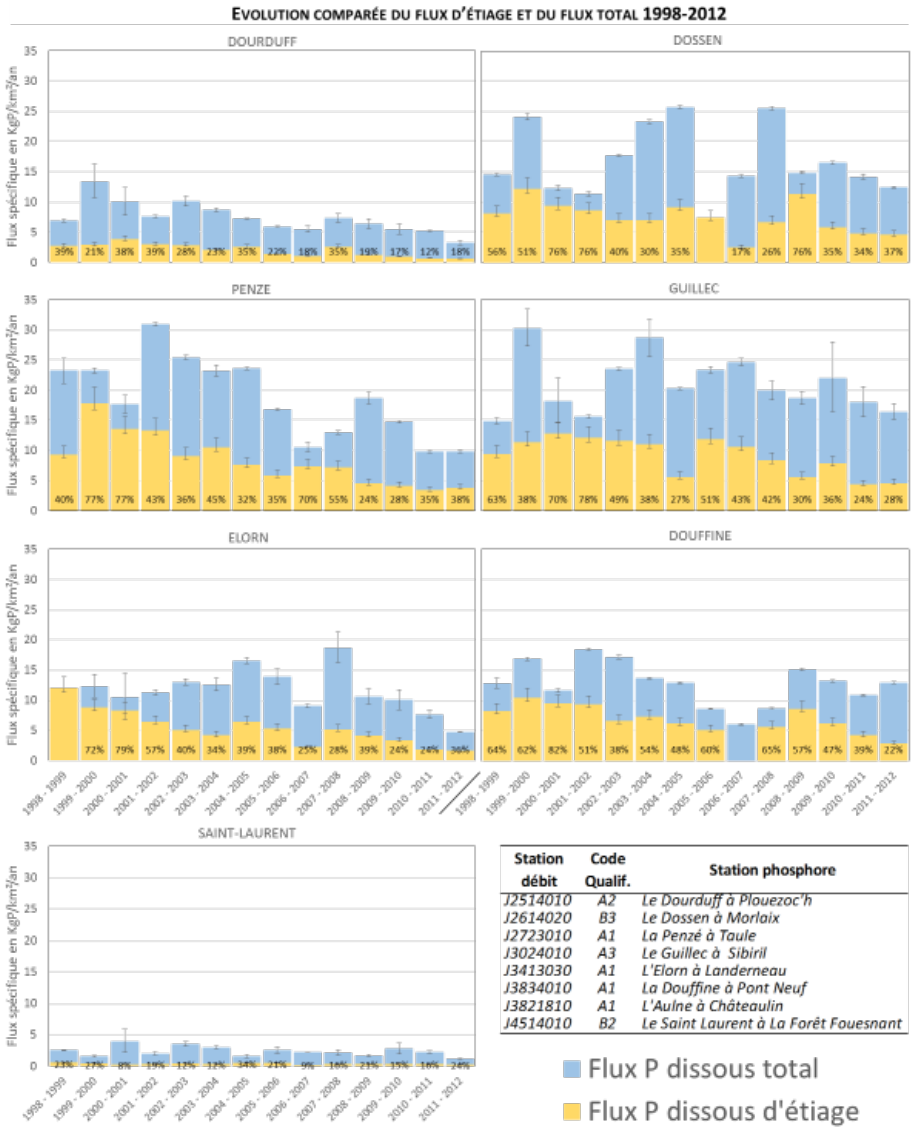

FIGURE 1.4 – Evolution du flux dissous d'étiage (représentatif des émissions ponctuelles) et du flux dissous total entre 1998 et 2012 dans sept rivières bretonnes (Legeay et al., 2015)

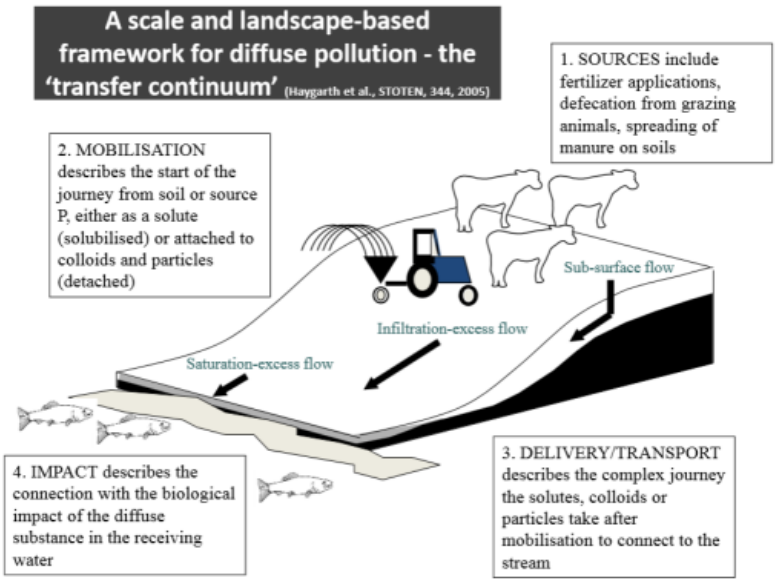

FIGURE 1.5 – Phosphorus transfer continuum, Haygarth et al. (2005)

les zones d'où provient le phosphore (Heathwaite *et al.*, 2005 ; McDowell *et al.*, 2014 ; Shore *et al.*, 2014). Ces CSA représentent généralement moins de 20% de la surface des bassins versants, mais leur surface peut varier en fonction de l'état hydrique des bassins versants.

Un autre concept utile à l'étude des transferts de phosphore dans les paysages agricoles est le « phosphorus transfer continuum », introduit par Haygarth *et al.* (2005) pour souligner le caractère interdisciplinaire et multi-échelle des approches à mettre en oeuvre. Le « phosphorus transfer continuum » comporte quatre « niveaux » : « sources », « mobilisation », « delivery », « impact » (Figure 1.5).

Les sources de phosphore peuvent être d'origine pedogénétique ou anthropique (fertilisation minérale ou organique). Parmi les sources anthropiques, il faut tenir compte des apports actuels mais aussi des apports passés, qui ont contribué à la constitution d'un pool de phosphore dans les sols, appelé « legacy phosphorus » (Jarvie *et al.*, 2013 ; Sharpley *et al.*, 2013 ; Haygarth *et al.*, 2014). Si la présence de sources de phosphore dans le bassin versant est un préalable nécessaire au transfert, il n'existe pas de relation simple entre sources et flux annuel dans les rivières (Dupas *et al.*, 2015). Des mécanismes de mobilisation et de transfert sont nécessaires. La mobilisation désigne la séparation du phosphore de sa source initiale, soit par solubilisation, soit par détachement de particules. Pour évaluer la solubilisation du phosphore, des tests agronomiques destinés à l'origine à l'estimation des besoins de fertilisation (Jordan-Meille *et al.*, 2012) peuvent être utilisés à des fins d'évaluation environnementale (Wall *et al.*, 2013). Ils sont devenus un outil législatif dans plusieurs pays d'Europe (Amery et Schoumans, 2015). En effet, il a été démontré que la concentration en phosphore dans la solution du sol augmente avec le phosphore extractible estimé par un test agronomique, parfois avec des effets de seuil importants (Heckrath *et al.*, 1995 ; Sharpley *et al.*, 2003). Pour affiner l'évaluation de la solubilisation du phosphore, des indices appelés « degré de saturation en phosphore » ont été introduit dans plusieurs pays (Beauchemin

et Simard, 1999 ; McDowell *et al.*, 2002 ; Schoumans et Chardon, 2015). Ces indices sont calculés comme le ratio entre la quantité de phosphore extractible et la quantité de sites d'adsorption présents dans les sols (Pothig *et al.*, 2010). La quantité de sites d'adsorption des sols peut être estimée grâce à des isothermes d'adsorption, ou par extraction chimique des oxydes de fer et d'aluminium. Le détachement physique de particules de sol par érosion, soit à la surface du sol, soit au niveau des parois des pores, est à l'origine des transferts de phosphore particulaire ainsi que du phosphore dissous en équilibre avec les particules. On peut estimer le risque de détachement de particules par des tests de stabilité structurale des sols (Le Bissonnais *et al.*, 2002).

Le phosphore mobilisé par des mécanismes biogéochimiques ou physiques n'est transféré vers les masses d'eau que s'il y a connectivité hydrologique entre la source et la masse d'eau. Parmi les voies de transfert possibles du phosphore, les transferts de surface sont souvent considérés comme dominants, même si la contribution des transferts de subsurface (naturels ou du fait de la présence de drains) est aujourd'hui reconnue (Heathwaite et Dils, 2000 ; Simard *et al.*, 2000 ; Jordan-Meille et Dorioz, 2004 ; van der Salm *et al.*, 2011). Dans la plupart des situations, le phosphore solubilisé va se réadsorber, le phosphore érodé va se redéposer, sans produire d'effet visible à court terme dans les masses d'eau avoisinantes. La capacité d'infiltration des sols, le niveau de la nappe, la présence de drain, la structure du paysage sont autant de facteurs qui déterminent si le phosphore mobilisé sera transféré ou non jusqu'aux masses d'eau. Les mécanismes de mobilisation produisent un signal mesurable avec des dispositifs expérimentaux dimensionnés pour des études à l'échelle du décimètre ou du mètre (simulateurs de pluie, lysimètres, test de stabilité structurale des sols), mais le signal n'est pas toujours propagé, donc observable à l'exutoire du bassin versant. Si le phosphore mobilisé est intercepté en chemin, le signal « mobilisation » ne produit pas un signal immédiatement mesurable dans le cours d'eau. Cependant, le phosphore intercepté est stocké en certains endroits du paysage, et peut être remobilisé à un autre moment pendant une durée plus ou moins longue. Tout cela contribue à rendre l'étude des dimensions temporelles et spatiales très complexes dans le cas du phosphore (Haygarth *et al.*, 2012).

La question de l'impact du phosphore transféré dans les masses d'eau est du domaine de l'écologie des milieux aquatiques. Parmi les formes de phosphore transférées, certaines sont plus biodisponibles que d'autres ; en première approche, on considère souvent que le phosphore dissous est plus biodisponible que le particulaire (Poirier *et al.*, 2012 ; Dupas *et al.*, 2015). Cette distinction entre formes dissoutes et particulaire est cependant trop simpliste pour estimer des impacts avec précision, puisqu'il existe des formes dissoutes récalcitrantes et des formes particulaires en grande partie biodisponibles (Li et Brett, 2013 ; Van Moorleghem *et al.*, 2013).

1.2.2 Approches méthodologiques

La question des transferts diffus de phosphore s'aborde à plusieurs échelles spatiales, qui ont toutes leur intérêt. Par le passé, des approches réductionnistes ont été privilégiées, avec la multiplication de travaux en batch ou utilisant des simulateurs de pluies. Ces travaux ont permis le développement de connaissances sur les processus qui produisent un signal mesurable à des échelles du millimètre au décamètre, mais pas à des échelles permettant

l'étude de bassins versants dans leur ensemble (1 – 100 km^2). Cette difficulté à passer à des échelles plus vastes a notamment été mis en évidence par l'échec des modèles de bassin versant construit par couplage de modèles développés sur la base d'observation à des échelles fines (Radcliffe *et al.*, 2009).

Plus récemment, une approche intégrée visant l'échelle des bassins versants a été privilégiée. C'est l'approche choisie dans cette thèse. Le principe de l'approche bassin versant repose sur l'idée que le signal à l'exutoire d'un bassin versant résume l'ensemble des processus qui ont eu lieu en son sein. Le signal étudié peut être constitué d'un ou plusieurs paramètres d'intérêt mesurés en un point exutoire (débit, turbidité, concentration en phosphore particulaire et dissous) dont l'évolution temporelle peut être décomposée pour faire des inférences sur des processus en jeu, y compris sur leur localisation spatiale dans le paysage du bassin versant.

Pour étudier les transferts diffus de phosphore, on se place dans des bassins ruraux, où les sources ponctuelles sont supposées négligeables ; on choisit généralement des bassins versants de petite taille ($<$10 km^2) pour minimiser l'effet des processus dans le cours d'eau et se concentrer sur les transferts entre les versants et le cours d'eau. Dans ces bassins, les concentrations en phosphore sont généralement basses et peu variables en débit de base, c'est-à-dire entre les crues, et augmentent en crue. L'élévation des concentrations en crue, combinée à l'élévation du débit, font que le transfert en crue représente une large part du flux annuel : par exemple, Gburek et Sharpley (1998) estiment que 66% du phosphore dissous est exporté en crue, Mellander *et al.* (2012) estiment que jusqu'à 50% du phosphore total est exporté en crue et Rodriguez-Blanco *et al.* (2013) estiment que 76% du phosphore particulaire et 46% du phosphore dissous est exporté en crue. Ces estimations sont très dépendantes des données utilisées (fréquence d'échantillonnage, chronique reconstituée ou non, etc) et des critères choisis pour définir une crue. Du fait de la prédominance des exportations en crue et de la faible variabilité des exportations en débit de base (en l'absence de source ponctuelle), l'étude des chroniques phosphore se concentre généralement sur les crues.

De nombreuses méthodes ont été développées pour étudier la dynamique du phosphore en crue, et en déduire des hypothèses sur l'origine spatiales des sources, les mécanismes de mobilisation et les voies de transferts, ainsi que leur variabilité intra et interannuelle. Les décalages temporels entre pic de débit et de concentration peuvent être interprétés en termes de limitation par la source ou limitation par le transport. Si le pic de concentration se produit en phase de montée du débit, on considère souvent que la source de phosphore est facilement mobilisée, et donc qu'elle se situe dans ou proche du cours d'eau. La mobilisation et le transfert de cette source sont rendus possibles par l'augmentation du débit en crue qui augmente la capacité de transport de la rivière ; en phase de descente du débit, les concentrations diminuent, soit parce que la source est temporairement épuisée, soit parce que l'énergie du cours d'eau n'est plus suffisante pour causer sa mobilisation (McDowell et Sharpley, 2002 ; Seeger *et al.*, 2004 ; Lefrancois *et al.*, 2007). Si le pic de concentration se situe en phase de descente du débit, on considère souvent que la source de phosphore est localisée dans le versant et que le délai entre pic de débit et pic de concentration est dû au temps nécessaire pour que les mécanismes hydrologiques responsables de la mise en connexion entre la source et la rivière (montée de nappe, saturation des sols) se mettent en place (Lefrancois *et al.*, 2007 ; Morel *et al.*, 2009). Enfin, il est intéressant

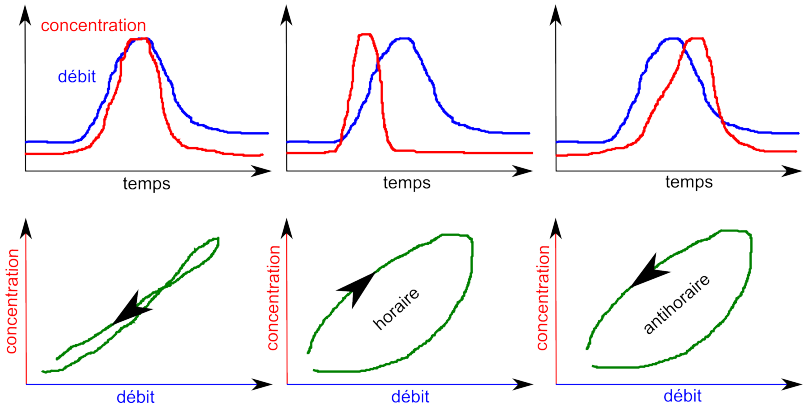

FIGURE 1.6 – Décalages temporels entre pic de concentration et pic de crue, représentés sous la forme de séries temporelles et d'hystérèses

d'étudier la synchronisation/désynchronisation entre la dynamique de plusieurs paramètres d'intérêt, par exemple entre le phosphore particulaire et le phosphore dissous, afin d'étudier si leurs transferts sont gouvernés par les mêmes mécanismes. Pour analyser les relations entre concentration et débit en crue, il est courant de représenter les séries temporelles sous la forme de graphe débit-concentration. Si le débit est représenté en abscisses et la concentration en ordonnées, un pic de concentration en phase de montée se traduira par une hystérèse horaire, tandis que si le pic de concentration a lieu en phase de descente, l'hystérèse sera antihoraire (Figure 1.6). Outre la possibilité d'une visualisation plus facile des décalages temporels crue par crue, la représentation sous forme d'hystérèse présente l'avantage de permettre de calculer des descripteurs d'hystérèses pour résumer grâce à une ou plusieurs variables quantitatives la forme, le sens et l'amplitude de l'hystérèse. L'utilisation de ces variables devient intéressante quand le nombre de crue à analyser est élevé et que l'utilisation de méthodes statistiques devient nécessaire. Un descripteur de crue couramment utilisé est le « hysteresis index » (Lawler *et al.*, 2006), calculé comme le ratio entre la concentration en phase de montée et de descente de crue à mi-chemin entre débit min et débit max. La valeur du « hysteresis index » renseigne sur le sens et l'amplitude de l'hystérèse.

Si l'analyse d'hystérèses est la méthode la plus couramment adoptée pour décrire la dynamique du phosphore en crue, d'autres méthodes existent :

- La décomposition chimique d'hydrogramme (Durand et Torres, 1996 ; Soulsby *et al.*, 2003 ; Lambert *et al.*, 2014), « end-member mixing analysis », permet de retracer l'évolution de la contribution de plusieurs compartiments du bassin versant au flux d'eau et de solutés à l'exutoire grâce à la connaissance de la concentration en éléments traceurs dans chaque compartiment (par exemple eau de pluie, eau de nappe, drains, zone humide) ;

- L'analyse de loadogramme (Mellander *et al.*, 2012 ; Mellander *et al.*, 2015), « loadograph recession analysis », s'inspire de la décomposition d'hydrogramme en crue, mais s'applique sur un loadogramme. Il s'agit de détecter des points d'inflexion dans

la courbe de flux instantané du paramètre d'intérêt, et d'interpréter les segments ainsi découpés en termes de voies de transfert ;

- Le calage de modèles empiriques concentration-débit (House et Warwick, 1998 ; Bowes *et al.*, 2005 ; Krueger *et al.*, 2009) dont les coefficients peuvent être interprétés à la manière des variables descripteur de crue. Par exemple, Krueger *et al.*, (2009) décrivent la relation concentration (C) – débit (Q) par la fonction :

$$C = a * Q^b + c * dQ/dt$$

où a, b et c sont des coefficients à calibrer. Une valeur positive de c indique une hystérèse horaire et une valeur négative une hystérèse antihoraire ;

La dynamique du phosphore en crue peut être interprétée par l'analyse de variables hydroclimatiques décrivant l'état du bassin versant (conditions antérieures et caractéristiques de l'évènement en lui-même). Par exemple, Bowes *et al.* (2005) et Ide *et al.* (2008) ont interprété les hystérèses horaires du phosphore particulaire comme résultant de la remobilisation de sédiments présents dans le cours d'eau ; ils ont aussi montré que la dynamique du phosphore particulaire dépendait de la variable dQ/dt, qui décrit l'énergie du cours d'eau en crue. D'autres auteurs (Jordan *et al.*, 2005 ; Bowes *et al.*, 2008 ; Stutter *et al.*, 2008) ont constaté qu'au cours d'une succession de crues, la quantité de phosphore particulaire exporté diminuait et s'accompagnait d'hystérèses de plus en plus aplaties ; ceci a été interprété comme l'épuisement progressif d'une source située dans le cours d'eau. A l'inverse, Bieroza et Heathwaite (2015) ont observé des hystérèses antihoraires pour le phosphore dissous, avec un contrôle par la température ; ceci a été interprété comme le résultat de transferts de subsurface en provenance des versants, avec un contrôle par la température des processus à l'origine de la solubilisation du phosphore dans les sols. Outram *et al.* (2014) ont démontré l'importance de l'alternance de périodes sèches et humides sur le transfert de phosphore dissous, en se basant sur l'analyse d'hystérèses. Avec le développement des analyseurs en continu, l'analyses de crues a pris un nouvel essor récemment (e.g. Outram *et al.*, 2014 ; Bieroza et Heathwaite, 2015 ; Perks *et al.*, 2015). Du fait du grand nombre de données à traiter, les analyses statistiques multivariées ont remplacé les méthodes basées sur la description visuelle d'un nombre limité de crues.

Pour confirmer les hypothèses formulées suite à l'analyse de chroniques, il est courant de vérifier que les mécanismes invoqués contribuent bien au transfert de phosphore en procédant à des observations ciblées dans certaines zones clés du bassin versant, ou en échantillonnant spécifiquement les différentes composantes de l'écoulement (Heathwaite et Dils, 2000 ; Siwek *et al.*, 2013). On peut aussi chercher à connaître la spéciation géochimique des formes de phosphore particulaire et dissous exportées, celle-ci pouvant permettre de tracer des sources ou des processus biogéochimiques (Cooper *et al.*, 2014). Une autre manière de vérifier ces hypothèses est de développer des modèles informatiques afin de tester si en simulant les processus identifiés comme dominants, on parvient à reproduire le signal observé à l'exutoire du bassin versant.

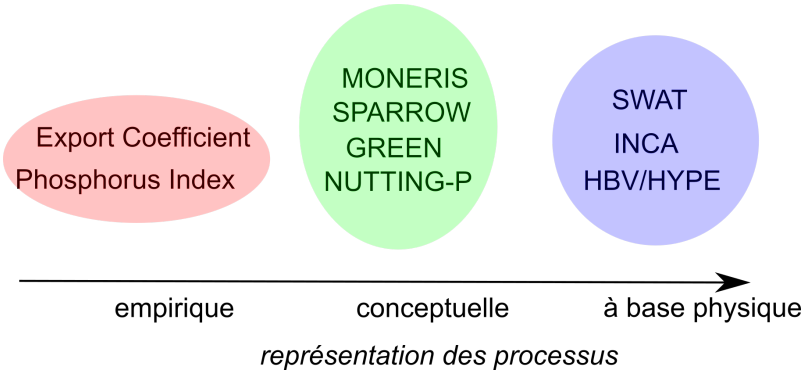

FIGURE 1.7 – Classification des modèles existants en fonction de leur complexité.

1.3 Modélisation des transferts

Le travail de modélisation doit permettre de poursuivre un objectif à définir au préalable. Krueger *et al.* (2007) distinguent deux raisons principales au développement de modèles : i) formaliser les connaissances sur les processus en jeu et tester des hypothèses ; ii) prédire des flux/concentrations sous différents scénarios, par exemple de gestion et/ou climatiques. Dans cette thèse, la modélisation fait partie intégrante de l'exploration des mécanismes à l'origine des transferts du phosphore dans les bassins versants, en lien étroit avec l'analyse de données d'observation. Elle s'inscrit donc dans le premier objectif mentionné par Krueger *et al.* (2007), puisque l'approche de modélisation choisie n'a pas vocation à produire un outil de gestion. L'état de l'art présenté dans ce paragraphe se concentre donc sur les modèles utilisés en recherche. Nous nous concentrerons sur les modèles de bassin versant dynamiques et à base physique ; les approches statiques, empiriques ou conceptuelles (Figure 1.7), ont déjà fait l'objet de synthèses bibliographiques récentes en français (Dupas *et al.*, 2011 ; Dupas et Gascuel-Odoux, 2013).

Après avoir présenté la structure de trois des modèles à base physique les plus courants, nous discuterons de questions inhérentes à la modélisation : calibration, évaluation, analyse de sensibilité et d'incertitude.

1.3.1 Représentation des processus dans les modèles

Une synthèse bibliographique récente (Wellen *et al.*, 2015) a montré que trois modèles sont principalement utilisés actuellement pour simuler les transferts de phosphore au sein des bassins versants : SWAT, INCA-P et HYPE.

SWAT

SWAT (Soil and Water Assessment Tool) est un modèle semi distribué à pas de temps journalier (Arnold *et al.*, 1998). Les Unités de Réponse Homogènes (HRU pour Homogeneous Response Units) sont découpées sur la base des types de sol, de l'occupation du sol et des itinéraires techniques types. Une interface SIG existe pour faciliter la création des fichiers d'entrée. Dans chaque HRU, le profil de sol est divisé en 10 horizons maximum,

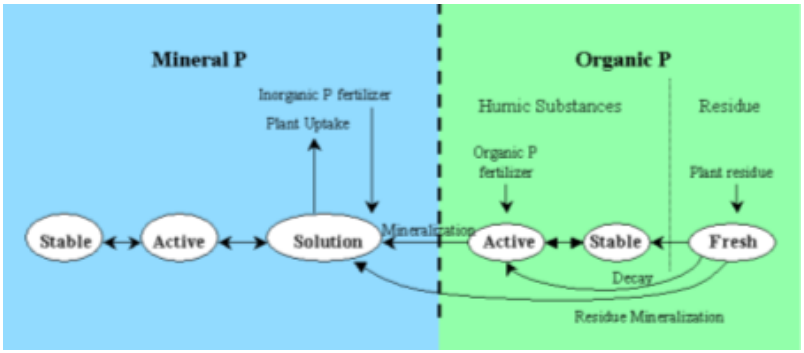

FIGURE 1.8 – Représentation des processus et des pools de phosphore dans le modèle SWAT (extrait du manuel de l'utilisateur)

auquel s'ajoute un aquifère superficiel et un aquifère profond ; les transferts d'eau entre ces compartiments et entre le sol et l'atmosphère sont représentés sur la base de bilans hydriques nécessitant des données climatiques et de caractérisation des sols.

Le cycle du phosphore dans les sols reprend les formalismes de Jones *et al.* (1984). Six pools sont pris en compte, dont trois organiques et trois minéraux (Figure 1.8). Le phosphore en solution est en équilibre rapide avec le pool actif (quelques jours) et ce dernier est en équilibre lent avec le pool stable. Vadas *et al.* (2013) reprochent au modèle SWAT, comme à de nombreux autres modèles, d'avoir peu évolué depuis les formalismes de Jones *et al.* (1984) et proposent des formalismes nouveaux pour mieux refléter les connaissances actuelles, notamment sur le devenir des effluents d'élevage (Bolster *et al.*, 2012 ; Vadas *et al.*, 2012 ; 2013 ; Vadas et White, 2010).

INCA

INCA (Integrated catchment model) est un modèle semi-distribué à pas de temps journalier (Wade *et al.*, 2002). Trois composantes de l'écoulement sont représentées : le ruissellement, les écoulements de subsurface et l'écoulement profond. Comme pour SWAT, il existe une interface SIG permettant de créer les fichiers d'entrée à partir d'un découpage en HRU ou sous bassin versant. Le nombre de pools de phosphore représentés dans les sols n'est que de trois, mais les pools et processus représentés pour les cours d'eau sont plus complexes que dans SWAT (Figure 1.9).

Malgré sa complexité, le modèle INCA-P est toujours utilisé (e.g. Jin *et al.*, 2015) et des analyses d'incertitudes ont été mises en œuvre après simplification du modèle (Dean *et al.*, 2009 ; Jackson-Blake *et al.*, 2015). Cependant, ces travaux récents posent la question de la quantité de données nécessaires pour calibrer un modèle avec autant de paramètres et Jackson-Blake *et al.* (2015) suggèrent que le modèle soit simplifié.

HYPE

HYPE est aussi un modèle semi-distribué à pas de temps journalier (Lindstrom *et al.*, 2010), plus adapté aux échelles vastes que SWAT et INCA puisqu'il a été appliqué sur des

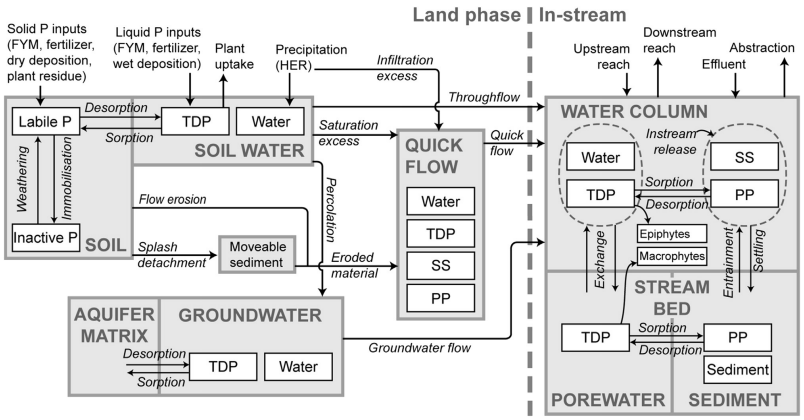

FIGURE 1.9 – Représentation des processus et des pools de phosphore dans le modèle INCA-P (Jackson-Blake et al., 2015)

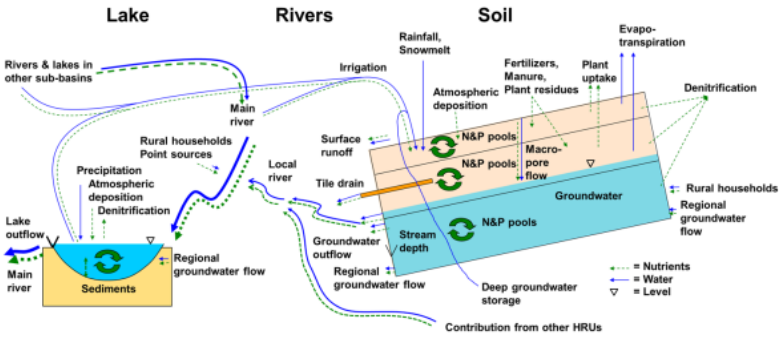

FIGURE 1.10 – Représentation des processus et des pools de phosphore dans le modèle HYPE

pays entiers (e.g. Stromqvist *et al.*, 2012). En plus des trois composantes de l'écoulement représentées dans INCA (ruissellement, écoulements de subsurface, écoulement profond), HYPE simule explicitement le drainage (Figure 1.10).

Cinq pools de phosphore dans les sols et leurs interactions, sont représentés : le phosphore organique stable, le phosphore organique labile, le phosphore adsorbé, ainsi que le phosphore dissous et particulaire dans la solution du sol.

1.3.2 Revue critique sur la démarche de modélisation

De nombreuses études de modélisation des transferts de phosphore ont révélé de mauvaises performances des modèles utilisés, notamment si on les compare aux modèles azote (Dean *et al.*, 2009 ; Jackson-Blake *et al.*, 2015 ; Wade *et al.*, 2002). Les causes possibles de ces mauvaises performances sont :

- La nature même des processus en jeu, notamment le fait qu'une part importante des transferts de phosphore se produit en crue, c'est-à-dire lors d'épisodes brefs difficiles à simuler avec des modèles. Le caractère sporadique des transferts de phosphore a rendu compliquée l'acquisition de chroniques d'observation à des fréquences suffisantes pour bien identifier les processus dominants, jusqu'à l'apparition récente de méthodes de suivi haute fréquence ;

- Une connaissance insuffisante des processus dominants, ou une mauvaise hiérarchisation entre les processus. Pour contrer ce problème, Vadas *et al.* (2013) prônent une meilleure intégration entre expérimentation et modélisation. La difficulté à hiérarchiser les processus peut aussi provenir du fait que beaucoup de modèles bassin versant ont été construits par couplage de modèles développés pour des échelles plus fines (Radcliffe *et al.*, 2009). Or un processus important à une échelle fine ne l'est pas forcément à l'échelle du bassin versant dans son ensemble, comme l'expliquent Haygarth *et al.* (2005) ;

- Une mauvaise structure des modèles, en lien avec l'approche réductionniste dénoncée ci-dessus. Une conséquence de l'intégration de plusieurs modèles établis à une échelle fine est que le nombre de paramètres, déjà élevé dans chaque modèle élémentaire, augmente d'autant plus que le niveau spatial s'étend (puisque l'hétérogénéité du milieu augmente aussi). La surparamétrisation des modèles conduit à des problèmes d'équifinalité, i.e. quand plusieurs combinaisons de paramètres conduisent à des résultats de simulation satisfaisants (Beven, 2006). En conséquence, d'après Kirchner (2006), "Such models are often good mathematical marionettes ; they often can dance to the tune of the calibration data". Deux réponses ont été apportées à ce problème de surparamétrisation des modèles et d'équifinalité : i) construire des modèles parcimonieux, permettant de capturer les processus les plus importants (Radcliffe *et al.*, 2009 ; Hahn *et al.*, 2013) et ii) procéder à des analyses de sensibilité et d'incertitude dans des approches stochastiques (Beven, 2006) ;

- Des méthodes de calibration/évaluation inadaptées, en lien avec un manque d'évaluation de l'information contenue dans les données (Beven et Smith, 2015). En effet, les modèles phosphore sont souvent calibrés sur des données de prélèvements ponctuels journaliers ou hebdomadaires, alors que la dynamique du phosphore dans des bassins versants de petite taille (< 10 km^2) connaît de fortes variations infra journalières notamment en crue. La valeur de flux ou de concentration « observée » suite à un échantillonnage ponctuel peut donc être très éloignée de la « vraie » valeur moyenne de cette journée (que le modèle doit simuler). Les statistiques d'évaluation de modèles classiques, telles que le critère de Nash-Sutcliffe, vont être très pénalisées par l'incertitude sur les données pour les valeurs les plus élevées, qui sont aussi les plus incertaines en l'absence d'un échantillonnage très haute fréquence. D'autres sources d'incertitudes sur les données, telles que les temps de stockage des échantillons et l'incertitude sur la mesure elle-même, doivent être prises en compte et propagées dans les modèles (Jarvie *et al.*, 2002) ;

Si la liste des raisons de l'échec des modèles actuels est bien connue, et que les bonnes pratiques de modélisation ont été identifiées (Radcliffe *et al.*, 2009 ; Vadas *et al.*, 2013 ;

Beven et Smith, 2015 ; Wellen *et al.*, 2015), les exemples de mise en application sont encore rares.

1.4 Objectif général

L'objectif de la thèse est d'identifier et de quantifier les mécanismes à l'origine des transferts de phosphore dissous dans un bassin agricole sur socle, par une démarche intégrant analyse d'observations multi-échelle et modélisation. Cet objectif général se traduit en trois questions de recherche principales :

- Question 1 : Les mécanismes à l'origine du transfert des formes dissoutes et particulaires du phosphore sont-ils communs ou distincts ? Y a-t-il une saisonnalité dans le couplage/découplage des transferts de phosphore dissous et particulaire ? Dans quelle mesure la variabilité du signal peut-elle être reliée aux pratiques agricoles ou à des processus hydrologiques et biogéochimiques ?
- Question 2 : Quel est le rôle de la nappe dans le transfert de phosphore dissous ? Agit-elle uniquement sur le transfert en provoquant une connexion hydrologique entre les sols et la rivière, ou agit-elle aussi sur la solubilisation du phosphore dans les sols ?
- Question 3 : Comment raisonner la complexité d'un modèle en fonction de la quantité d'information contenue dans les données ? Comment quantifier l'incertitude des données et la propager dans les prédictions d'un modèle ?

1.5 Enjeux et démarche

L'identification des mécanismes à l'origine des transferts de phosphore est un préalable nécessaire à la mise en place d'actions pour réduire ces transferts. Plus précisément, il s'agit d'identifier les sources au sein des bassins versants, les mécanismes de mobilisation, les voies de transfert et leurs facteurs de contrôle. Ces questions représentent un enjeu régional pour la qualité de l'eau en Bretagne puisqu'au commencement de cette thèse (juin 2013), il existait très peu d'études scientifiques sur le phosphore conduites dans cette région avec une approche bassin versant. Ce manque de connaissance sur le phosphore en Bretagne peut s'expliquer par l'accent mis sur l'élément azote, du fait des problèmes d'algues vertes dans cette région côtière. Pourtant, en Bretagne, 80% de l'alimentation en eau potable provient des eaux de surface (où le phosphore est souvent considéré limitant) et des lieux de baignade en eau douce sont régulièrement fermés à la baignade en raison de la prolifération de cyanobactéries en été. Au-delà de l'enjeu régional, le contexte agro-pédo-climatique des bassins versants étudiés dans cette thèse contraste avec ceux étudiés dans la littérature internationale. En effet, rares sont les exemples d'études sur des petits bassins versants ($< 10 km^2$) cultivées en terres arables et avec des densités animales élevées, et donc avec des taux de phosphore dans le sol si élevés. Cette thèse cherche donc à répondre à un enjeu global, d'autres régions du globe présentant des caractéristiques agro-pédo-climatiques similaires. Le travail de recherche se concentre sur les formes solubles du phosphore, pour des raisons d'enjeu et des raisons pratiques :

- Les formes solubles du phosphore sont généralement plus biodisponibles pour l'eutrophisation que les formes particulaires, elles représentent un risque environnemental plus élevé ;
- Les observatoires de recherche qui ont servi de support à cette thèse ont été l'objet de nombreux travaux sur les solutés et assez peu sur les matières en suspension. J'ai donc préféré travailler sur le phosphore soluble afin de profiter de la connaissance existant sur les solutés et travailler en interaction avec d'autres projets en cours. Un travail sur les formes particulaires du phosphore devrait s'appuyer sur une étude détaillé sur les matières en suspension (traçage, etc) ;

La démarche adoptée consiste en l'analyse de données d'observation à plusieurs échelles de temps (année, saison, crue) et d'espace (bassins versants dans leur ensemble, versants isolés). La modélisation est utilisée comme outil de validation des hypothèses formulées suite à l'analyse des données. Cette démarche nécessite l'acquisition de données d'observation riches. C'est pour cette raison que j'ai choisi de travailler en priorité sur le bassin de versant de Kervidy-Naizin, site de l'ORE AgrHyS. Dans ce bassins versant, la concentration en phosphore était déjà suivie depuis 6 ans au commencement de la thèse. Pendant la durée de cette thèse, le bassin versant de Kervidy-Naizin a été un site d'étude central pour trois projets de recherche portant respectivement sur l'azote (ANR ESCAPADE), le carbone (ANR MOSAIC) et le phosphore (Trans-P). Cette thèse s'inscrit dans le projet Trans-P mais a été rendue plus riche grâce aux réflexions communes menées avec les autres projets, et a bénéficié de dispositif expérimentaux communs aux 3 projets. Les stratégies de gestion n'ont pas été testées, puisque les sites d'acquisitions de données à disposition sont des lieux d'observation et non d'expérimentation, que les modèles n'ont pas été conçus pour tester des scénarios de gestion ; cependant, des pistes pour la gestion seront formulées en fin de mémoire. Cette thèse est en effet financée par l'agence de l'eau Loire Bretagne, et porte dès lors des enjeux finalisés.

1.6 Plan du mémoire

La suite du mémoire est organisée en cinq chapitres :

- Le chapitre 2, **Matériels et méthodes** présente le site d'étude et le dispositif expérimental utilisé ;
- Le chapitre 3, **Dynamique d'exportation des formes particulaires et dissoutes** porte sur l'étude d'une chronique de qualité de l'eau dans un petit bassin versant agricole à dominance de terres arables pour étudier la saisonnalité des couplages/découplages entre les formes dissoutes et particulaires du phosphore. Le rôle des battements de nappe dans les zones humides ripariennes est exploré ;
- Le chapitre 4, **Identification de motifs saisonniers de crue** propose une méthodologie innovante pour analyser la dynamique du phosphore en crue. Il pose par ailleurs la question de la généralisation des résultats du chapitre 3 à un bassin versant herbager ;

- Le chapitre 5, **Rôle de la nappe dans le transfert de phosphore dissous** a pour objectif de confirmer et préciser les hypothèses émises dans les chapitres 3 et 4 au sujet du rôle de la nappe dans les transferts de phosphore dissous en provenance des zones humides. La méthode utilisée consiste en un suivi in situ de la solution de sol, mis en lien avec la qualité de l'eau dans la rivière ;

- Le chapitre 6, **Modélisation et analyse d'incertitude** présente un modèle de bassin versant intégrant la connaissance sur les processus principaux identifiés dans les chapitres 3 à 5. Un effort particulier a été porté à l'évaluation de l'incertitude dans les données et à la propagation de cette incertitude dans le modèle ;

- Le chapitre 7, **Conclusion générale** résume les principaux résultats de la thèse, en tire des enseignements pour la gestion, et propose des pistes de recherche pour tendre vers une vision intégrée des cycles du carbone, de l'azote et du phosphore ;

1.7 Le projet Trans-P

Ce travail de thèse s'est inscrit dans le projet de recherché Trans-P « Transfert du phosphore des terres agricoles au cours d'eau : stocks et flux, de l'observation à la modélisation ». Ce projet, porté par Agrocampus Ouest, l'INRA, le CNRS de Rennes et l'université de Tours, est financé par l'agence de l'eau Loire Bretagne sur la période 2013 – 2016. La motivation initiale de Trans-P a été le constat du peu de travaux menés sur les transferts de phosphore en France, notamment en Bretagne. Avant Trans-P, les travaux scientifiques les plus significatifs en France avaient porté sur les bassins de la Seine, ou des bassins versants alpins, c'est-à-dire des contextes agro-pédoclimatiques très différents de la Bretagne. Il y avait donc un déséquilibre de connaissance par rapport aux transferts d'azote ou de carbone, mieux documentés. Or, pour atteindre les objectifs de la directive cadre sur l'eau en matière de limitation de l'eutrophisation en eaux douces, il est nécessaire d'agir sur le phosphore, et donc de comprendre les mécanismes sous-jacents à son transfert vers les milieux aquatiques. Par ailleurs, la disposition 3B-1 du SDAGE Loire-Bretagne prévoit des actions visant à diminuer les transferts de phosphore à l'amont de 14 retenues prioritaires, dont 10 sont situées en Bretagne. Là encore, il est nécessaire d'évaluer les risques en étant capable d'estimer des stocks, des flux ainsi que leur variabilité temporelle et spatiale. Le projet trans-P est structuré en 3 volets :

Volet 1 : La variabilité et la distribution spatiale des stocks et pools de phosphore des sols, du petit bassin versant et à l'échelle régionale (Bretagne)

Ce volet vise à évaluer la composante « source » du « phosphorus transfer continuum ». Le travail combine deux approches complémentaires, attachées à deux échelles différentes. A l'échelle de la Bretagne, des bases de données régionales (base de données d'analyse de terre, réseau de mesure de la qualité des sols, sol de Bretagne) existent et contiennent des informations valorisables pour mieux connaître la variabilité régionale et l'évolution de la teneur en phosphore des sols agricoles. Au sein de l'ORE AgrHys (Chapitre 2), il a été possible de mettre en œuvre un échantillonnage plus dense et plus détaillé, dans le but

d'affiner les connaissances sur les facteurs de contrôle de la variabilité spatiale des teneurs en phosphore des sols.

Volet 2. La variabilité temporelle et spatiale des concentrations et des flux de phosphore, l'incertitude en relation avec la fréquence d'échantillonnage

Ce volet vise à quantifier les flux en sortie de bassins versants à partir de chroniques basse à moyenne fréquence contenues dans des bases de données existantes en Bretagne. Les méthodes développées doivent permettre d'extraire de l'information de ces données, en particulier être capable de quantifier les flux au plus précis (avec une incertitude associée), d'évaluer l'évolution temporelle de ces flux, leur variabilité spatiale, et d'extraire des indicateurs permettant d'apprécier la part des émissions d'origine diffuse et ponctuelle.

Volet 3. Modélisation des transferts de P, de l'échelle du bassin versant élémentaire à celle des retenues et de la région

Le présent travail de thèse s'inscrit dans ce volet. Il s'agit d'identifier les processus dominant, puis de les intégrer dans un modèle de transfert de phosphore.

Chapitre 2

Matériels et méthodes

2.1 L'ORE AgrHys et le bassin versant de Kervidy-Naizin

Le bassin versant de Kervidy-Naizin est situé au cœur de la région Bretagne, dans le Morbihan, à 20 km de la ville de Pontivy (Figure 2.1). Les premiers travaux scientifiques sur ce site remontent à 1971, avec l'installation par le CEMAGREF (aujourd'hui IRSTEA) d'une station de mesure du débit et d'un suivi de la qualité de l'eau au lieu-dit Stimoës. Le bassin versant étudié faisait alors 12 km^2, et avait pour but d'observer l'évolution de la qualité de l'eau en réponse au remembrement agricole (1971 – 1976).

Suite à l'installation d'une usine de transformation alimentaire, puis d'un étang à but récréatif en 1991, la station de suivi Stimoës a été progressivement abandonnée au profit d'un sous bassin versant purement agricole. Ce sous bassin versant de 5 km^2, appelé Kervidy-Naizin, a fait l'objet d'un suivi du débit par l'INRA depuis 1993 et d'un suivi de la qualité de l'eau depuis 2000, date de l'abandon définitif de la station de Stimoës. Aujourd'hui, le bassin versant de Kervidy-Naizin est l'un des deux sites de l'ORE AgrHys, avec celui des bassins versant de Kerbernez (Finistère). Il fait également partie du réseau des bassins versants RBV, consortium national qui fédère la recherche française sur les bassins versants.

2.1.1 Milieu physique

Kervidy-Naizin est un bassin versant d'ordre 2 (Strahler, 1952). Il est drainé par le Coët Dan, affluent de l'Evel qui est lui-même un affluent du Blavet. Son point le plus bas est à 93 m au-dessus du niveau de la mer et son point le plus haut est à 135 m ; les pentes des versants sont inférieures à 5%. Le socle géologique du bassin de Kervidy-Naizin est constitué de schistes briovériens (Protérozoïque supérieur) fissurés et fracturés. La composition minéralogique du schiste inclut, en proportion décroissante : du quartz, de la muscovite, des chlorites, des feldspaths (Pauwels *et al.*, 1998). Au-dessus du socle considéré imperméable, une couche d'altérite aux propriétés hydriques proches de celles du sol s'étend sur une profondeur variant entre quelques mètres en bas de versant jusque 30 mètres en haut de versant. La conductivité hydraulique et la porosité totale de l'altérite varient entre 8.10^{-6} et 5.10^{-5} m s^{-1} et entre 0.05 et 0.2 m^3 m^{-3}, respectivement (Molenat et Gascuel-Odoux, 2002). La couche d'altérite abrite une nappe superficielle qui fluctue

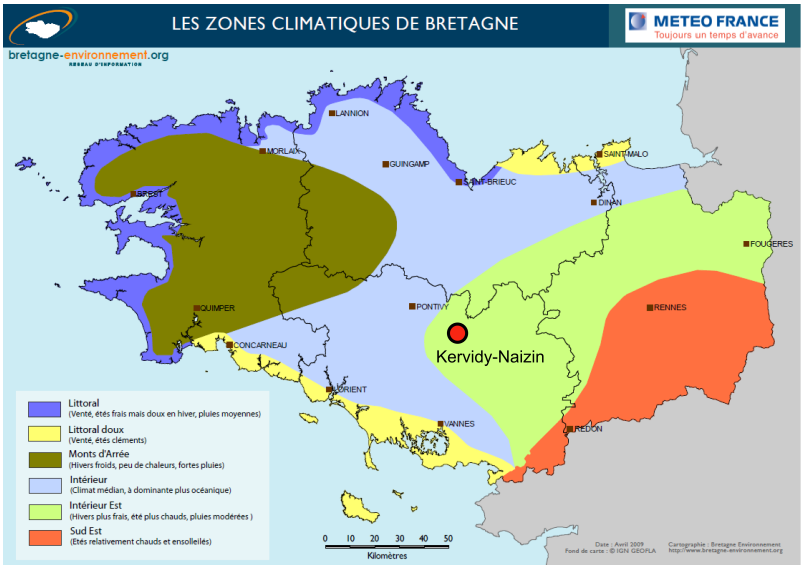

FIGURE 2.1 – Localisation du bassin versant de Kervidy-Naizin en Bretagne. Données Météo France mises en forme par Bretagne Environnement.

saisonnièrement entre 0 et 2 m en bas de versant et 2 et $>$ 8 m en haut de versant. Les sols de Kervidy-Naizin, développés sur un matériau limoneux issu de l'altération du schiste et de dépôts quarternaires, présentent un faciès limoneux à limoneux-argileux. Ils contiennent un grand nombre de phases minérales secondaires incluant illite, smectite, kaolinite et des oxydes de fer et oxy-hydroxydes de fer variés, et des oxydes de manganèse. Leur profondeur varie de 35 cm à 5 m, ils sont acides (pH de 5 à 7 en surface) et riches en matière organique (3 à 7 %). Les sols de Kervidy-Naizin s'organisent en fonction de la topographie : en haut de versants dominent des Luvisols bien drainés tandis que dans les bas de versants se trouvent des Luvisols-redoxisols présentant des traits hydromorphiques (Figure 2.2).

2.1.2 Climat

Le climat est tempéré océanique, avec des précipitations et un débit spécifique atteignant en moyenne respectivement 854 $\pm$ 179 mm et 290 $\pm$ 106 mm entre 2000 et 2014. La température moyenne annuelle est de 11.2 $\pm$ 0.6 $^{\circ}$ C et le nombre de jours où la température moyenne est négative est de onze en moyenne ; il neige très rarement sur le bassin versant. La période la plus humide s'étend d'octobre à février ; s'il pleut régulièrement tout au long de l'année, l'évapotranspiration élevée en été conduit au tarissement du ruisseau quasiment chaque année d'août à octobre. Les mois les plus chauds sont juillet et août (Figure 2.3).

2.1.3 Usage et occupation des sols

Le bassin versant de Kervidy-Naizin est le lieu d'une agriculture intensive où dominent les productions animales hors-sol (bovins lait, porcs). La densité animale estimée est de 13 UGB (unités gros bovin) ha^{-1}, soit un surplus d'azote de 36 kgN ha^{-1} et un surplus de

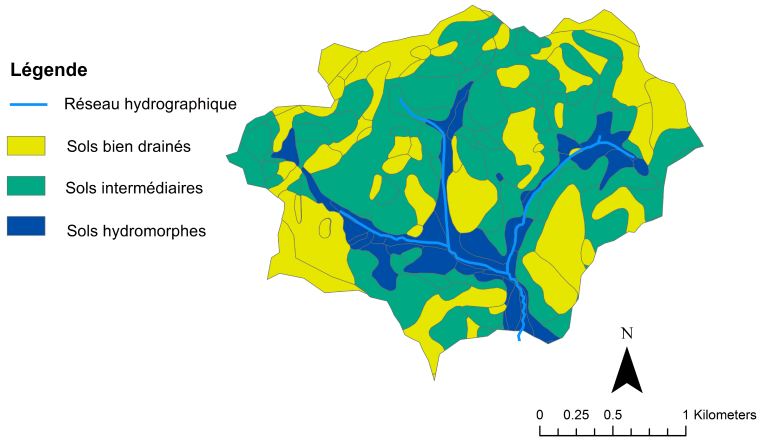

FIGURE 2.2 – Classes d'hydromorphie sur le bassin de Kervidy-Naizin.

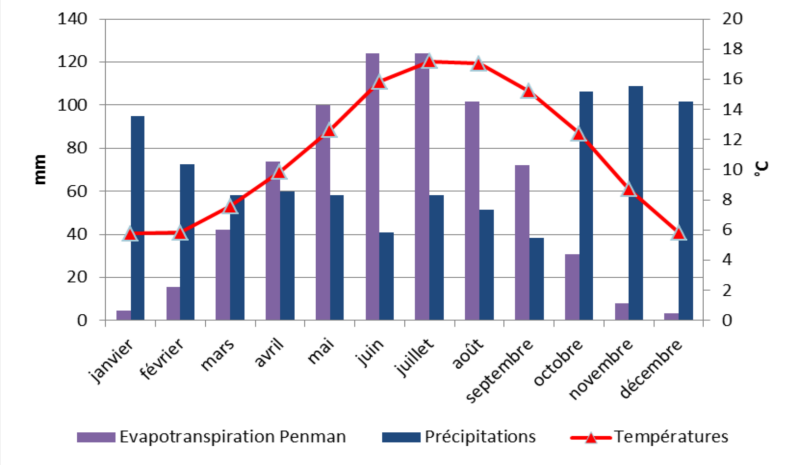

FIGURE 2.3 – Diagramme ombrothermique du site de Kervidy-Naizin données 2000 – 2014

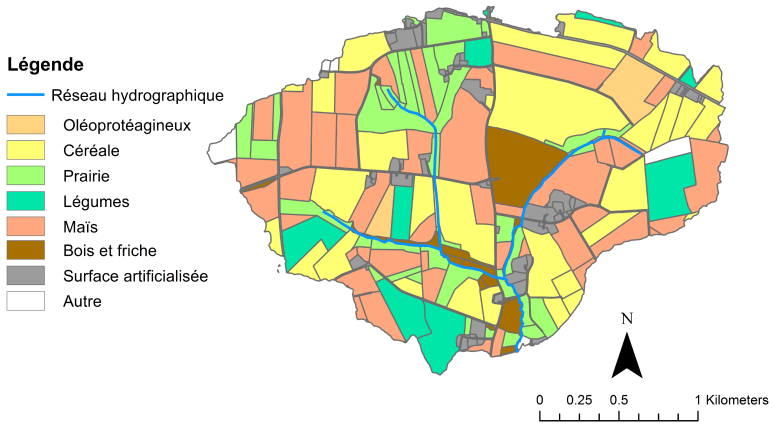

FIGURE 2.4 – Occupation du sol en 2013

phosphore de 12 kgP ha^{-1} en 2013. L'usage des sols était à 85% agricole en 2013, dont 35% de céréales, 36% de maïs, 16% de prairies, 10% de légumes de plein champ et 3% de colza (Figure 2.4 et Figure 2.5).

2.2 Dispositif expérimental

2.2.1 Instrumentation pour le suivi long terme

Le suivi long terme sur le bassin versant de Kervidy-Naizin comporte des mesures à l'exutoire, le long de deux transects et au niveau de la station météo du Toullo (Figure 2.6).

A l'exutoire, le débit est suivi à un pas de temps de 1 min au niveau d'une station de jaugeage située à l'aval d'un pont, dans une zone peu pentue. La station comporte un seuil rectangulaire à deux largeurs (Figure 2.7), la hauteur d'eau est mesurée dans un bac tranquilisateur par un codeur à flotteur (Thalimèdes OTT, précision constructeur : 1mm). La courbe de tarage a été établie par Carluer (1998). L'exutoire est aussi le lieu d'un échantillonnage manuel journalier à approximativement la même heure chaque jour (16 :00 – 18 :00) depuis 2000. Les éléments mesurés quotidiennement sont les anions majeurs (nitrate, sulfate, chlorure mesurés par chromatographie ionique DIONEX DX 100) et le carbone organique dissous (mesuré par un analyseur de carbone Shimadzu TOC 5050A). La fréquence d'échantillonnage pour le phosphore réactif filtré (SRP), le phosphore total (TP) et les matières en suspension (MES) est passée de tous les 6 jours entre 2007 et 2013 à journalière entre 2013 et 2015. Les échantillons prélevés pour le SRP sont filtrés immédiatement sur site (filtres en acétate de cellulose < 0.45 μm), puis analysé par spectrométrie après réaction avec le molybdate d'ammonium. Les échantillons prélevés pour le TP ne sont pas filtrés, ils sont digérés par réaction avec le potassium peroxydisulfate puis dosés comme le SRP. Les MES sont mesurées par pesée après filtration (< 0.45 μm). En

FIGURE 2.5 – Vue aérienne du paysage de Kervidy-Naizin (air papillon 2013)

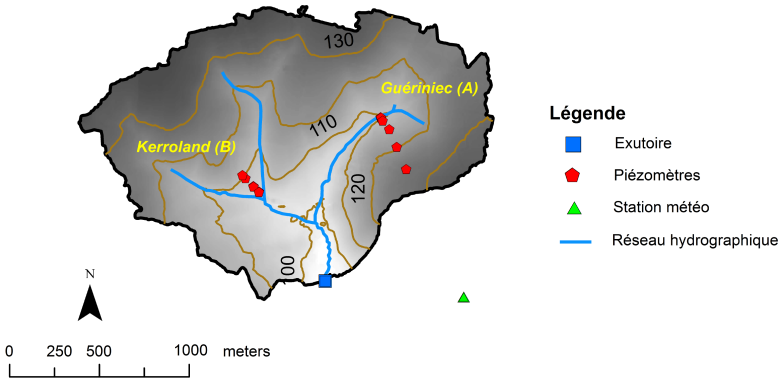

FIGURE 2.6 – Localisation des instruments de mesure pour le suivi long-terme

FIGURE 2.7 – Seuil à l'exutoire de Kervidy-Naizin.

plus des prélèvements manuels, des capteurs mesurent la turbidité, la température et la conductivité à un pas de temps de 10 min et un spectromètre laser permet un suivi indirect des nitrates et du carbone organique dissous à un pas de temps de 20 min. En l'absence d'un suivi haute fréquence continu pour le phosphore, des échantillonneurs automatiques sont utilisés pour prélever des échantillons en crue : environ 8 crues sont ainsi couvertes chaque année, avec 7 – 24 échantillons analysés (SRP, TP, MES) à chaque fois.

Actuellement, un réseau de 10 piézomètres localisés le long de deux transects (Guériniec appelé A dans cette thèse, et Kerroland appelé B) permet de mesurer la hauteur de nappe ainsi que la chimie de l'eau souterraine (Figure 2.6). Depuis 2009, les instruments utilisés pour mesurer les niveaux de nappe sont des capteurs de pression (Orpheus OTT, précision constructeur : 2 mm) qui fonctionnent au rythme de une mesure toutes les 15 minutes ; ces appareils mesurent aussi la température à la même fréquence. La chimie de l'eau de nappe est analysée environ quatre fois par an après prélèvement manuel ; les éléments mesurés sont les mêmes qu'à l'exutoire sauf le phosphore.

Le suivi météorologique est assuré par une station Cimel Enerco 516i (Figure 2.8) localisée à 1,1 km de l'exutoire à l'est du bassin versant. Les paramètres mesurés toutes les heures sont : la pluviométrie, les températures du sol à 10 et 50 cm de profondeur et de l'air à 10 et 50 cm de hauteur, l'humidité de l'air, la vitesse du vent, le rayonnement global, la durée d'insolation, ce qui permet le calcul de l'évapotranspiration potentielle par la formule de Penman.

2.2.2 Instrumentation pour le suivi des zones humides

En plus du suivi long terme, cette thèse utilise des données de suivi dans la solution du sol, dans les eaux de ruissellement et dans les eaux de drains collectées dans des zones

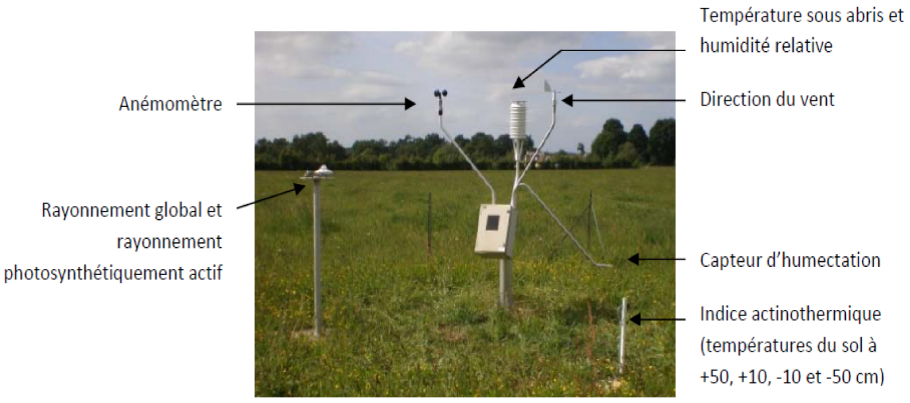

FIGURE 2.8 – Désignation des instruments de mesure à la station météorologique au lieu-dit le Toullo (thèse Alice Aubert)

ciblées du bassin versant. Ce suivi a eu lieu au cours des années hydrologiques 2013 – 2014 et 2014 – 2015 grâce à une collaboration avec le projet ANR MOSAIC portant sur la dynamique de la matière organique dans les sols. Le suivi de la solution de sol utilise des pièges à eau (Figure 2.9) et des mini-piézomètres (Figure 2.10). Les pièges à eau ont été placés à deux profondeurs (10 – 15 cm et 50 – 55 cm) en triplicat en deux sites dans la zone d'interception de la nappe avec le sol dans les bas-fonds de Guériniec et Kerroland. Plus de détails sont donnés dans le chapitre 5.

Des mini-piézomètres ont été placés à 5 cm de profondeur en trois sites dans la zone d'interception de la nappe avec le sol à Guériniec : deux dans la bande enherbée et une dans la parcelle cultivée (triplicat pour chaque site). Le but a été de comparer l'effet de l'occupation du sol sur la mobilité du phosphore dissous de part et d'autre de la bande enherbée. Pour quantifier approximativement les apports de sédiment et de phosphore de la parcelle cultivée vers les bas-fonds occupés par une bande enherbée, nous avons aussi installé des dispositifs de collecte des eaux de ruissellement. Ces dispositifs ont été placés en triplicat à l'interface entre la parcelle de Guériniec et la bande enherbée située en contrebas ; ils comportent un collecteur fabriqué avec une gouttière en PVC de 85 cm de large relié par un tuyau à un réservoir de 80l enterré. Au cours de l'année hydrologique 2013 – 2014, où la parcelle suivie était cultivée en orge d'hiver, 7 épisodes de pluie ont provoqué un ruissellement intercepté par au moins une des gouttières.

Enfin, deux drains ont été suivis ponctuellement au cours de l'année hydrologique 2013 – 2014 afin de comparer la dynamique saisonnière des concentrations entre des bas-fonds drainés et des bas-fonds non-drainés. Les deux drains suivis étaient localisés respectivement à proximité de Guériniec et de Kerroland.

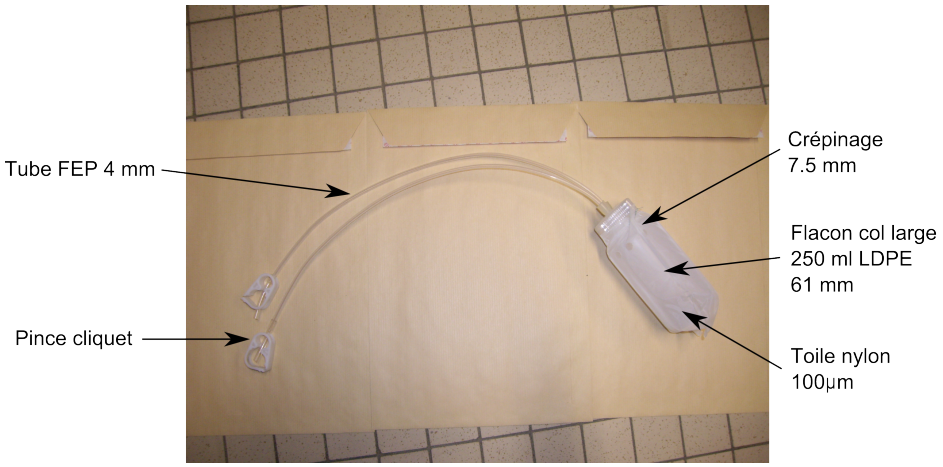

FIGURE 2.9 – Photographie d'un piège à eau avant sa mise en place (Guillaume Humbert)

FIGURE 2.10 – Haut : bande enherbée de Guériniec ; piézomètres et pièges à eau en place ; piège à eau en place. Bas : prélèvement dans un piège à eau ; mini-piézomètre à l'interface entre la parcelle et la bande enherbée de Guériniec ; dispositif de collecte des eaux de ruissèlement.

Chapitre 3

Dynamique d'exportation des formes particulaires et dissoutes du phosphore

Ce chapitre s'appuie sur un article publié dans Hydrological Processes.

Dupas R, Gascuel-Odoux C, Gilliet N, Grimaldi C, Gruau G. Distinct export dynamics for dissolved and particulate phosphorus reveal independent transport mechanisms in an arable headwater catchment. Hydrological Processes 2015 ; 29 : 3162 – 3178.

Il repose sur l'analyse d'une chronique de chimie de l'eau de 6 ans dans le bassin versant de Kervidy-Naizin, constituée antérieurement à cette thèse. Des analyses complémentaires sont présentées à la suite de cet article ; elles présentent des perspectives pour une analyse couplée Carbone - Phosphore.

Ce chapitre apporte des éléments de réponse à la question 1, rappelée ici :

Question 1 : Les mécanismes à l'origine du transfert des formes dissoutes et particulaires du phosphore sont-ils communs ou distincts ? Y a-t-il une saisonnalité dans le couplage/découplage des transferts de phosphore dissous et particulaire ? Dans quelle mesure la variabilité du signal peut-elle être reliée aux pratiques agricoles ou à des processus hydrologiques et biogéochimiques ?

3.1 Distinct export dynamics for dissolved and particulate phosphorus reveal independent transport mechanisms in an arable headwater catchment

Résumé

Cet article porte sur l'étude des concentrations en phosphore particulaire (PP) et en phosphore réactif soluble (SRP) à l'exutoire d'un petit (5 km²) bassin versant agricole intensif, pour identifier la variabilité saisonnière des sources et des voies de transfert de ces deux formes de phosphore. La forme et le sens des hystérèses débit-concentration en crue sont mis en relation avec l'état du bassin versant pendant quatre saisons définies selon des critères hydrologiques. A l'échelle de la crue comme à l'échelle de l'année, les dynamiques d'exportation du PP et du SRP sont différentes, ce qui suggère une absence de couplage entre les deux formes de phosphore. Pendant la plupart des évènements de crue, les hystérèses pour le PP sont de sens horaire, signe de la mobilisation d'une source situé dans ou proche du cours d'eau. A l'inverse, les hystérèses pour le SRP sont antihoraires, ce qui suggère que le SRP est exporté au cours d'eau via des transferts de subsurface. La montée de nappe dans les sols de zone humide riparienne est la cause la plus probable de ce transfert, par la connexion hydrologique qu'elle crée entre le cours d'eau et les horizons de surface riches en P. Les concentrations en SRP sont les plus élevées quand la contribution relative de la nappe profonde de versant est basse par rapport à la nappe de la zone humide riparienne. Donc il semble que les sols non fertilisés des zones ripariennes sont la source de SRP dans le bassin versant. Ce modèle conceptuel des transferts de phosphore avec des mécanismes différent pour PP et SRP apparaît valable pour la plus grande partie de l'année, à l'exception de crues de printemps où les exportations de PP et SRP sont synchrones du fait d'un mécanisme de transfert commun : le ruissellement et l'érosion en provenance des versants.

Abstract

This paper investigates particulate phosphorus (PP) and soluble reactive phosphorus (SRP) concentrations at the outlet of a small (5 km²) intensively farmed catchment to identify seasonal variability of sources and transport pathways for these two phosphorus forms. The shape and direction of discharge-concentration hystereses during floods were related to the hydrological conditions in the catchment during four hydrological periods. Both during flood events and on an annual basis, contrasting export dynamics highlighted a strong decoupling between SRP and PP export. During most flood events, discharge-concentration hystereses for PP were clockwise, indicating mobilisation of a source located within or near the stream channel. Seasonal variability of PP export was linked to the availability of stream sediment and the export capacity of the stream. In contrast, hysteresis shapes for SRP were anticlockwise, which suggests that SRP was transferred to the stream via subsurface flow. Groundwater rise in wetland soils was likely the cause of this transfer, through the hydrological connectivity it created between the stream and P-rich soil horizons. SRP concentrations were highest when the relative contribution of deep groundwater from the upland domain was low compared to wetland groundwater. Hence,

soils from non-fertilized riparian wetlands seemed to be the main source of SRP in the catchment. This conceptual model of P transfer with distinct hydrological controls for PP and SRP was valid throughout the year, except during spring storm events, during which PP and SRP exports were synchronised as a consequence of overland flow and erosion on hillslopes.

3.1.1 Introduction

Phosphorus (P) availability controls eutrophication in freshwater ecosystems, since P is generally the nutrient that limits algal development (Schindler *et al.*, 2008 ; Smith and Schindler, 2009). Most source apportionment studies conducted in Western countries have documented a general decrease in P point-source emissions in the last two decades and concluded on the need to redirect research and management efforts towards diffuse P emissions (Nemery *et al.*, 2005 ; Van Drecht *et al.*, 2009 ; Grizzetti *et al.*, 2012 ; Dupas *et al.*, 2015). The contribution of diffuse P emission can be preeminent in intensively livestock-farmed catchments, as a result of high applications rates of P-rich animal waste and subsequent enrichment of soils (Heckrath *et al.*, 1995, Ringeval *et al.*, 2014).

Cost-effective alleviation of diffuse P emissions implies identifying the spatial origin of P sources within landscapes, the dominant transport pathways and the temporal variability in their activation (Schoumans *et al.*, 2014). Areas of the landscape that contribute to diffuse P emission are called critical source areas, i.e. hydrologically active areas coinciding with P-enriched soils (Heathwaite *et al.*, 2005). The hydrological pathways that are often reported to contribute to diffuse P export include primarily overland flow and erosion, but also subsurface flow and artificial drainage (Haygarth *et al.*, 1998 ; Heathwaite and Dils, 2000 ; Simard *et al.*, 2000 ; van der Salm *et al.*, 2011). Several methods have been developed to investigate the respective contribution of these different transport pathways, including hillslope monitoring (Heathwaite and Dils, 2000), mixing models (Jarvie *et al.*, 2002 ; Jarvie *et al.*, 2011 ; Mellander *et al.*, 2012a), seasonal interpretation of discharge-concentration hysteresis during flood events (House and Warwick, 1998 ; Bowes *et al.*, 2005 ; Stutter *et al.*, 2008) or a combination of methods (e.g. Siwek *et al.*, 2013).

Floods in rural catchments generally coincide with increasing concentrations of dissolved and particulate P forms as a result of increased hydrological connectivity between hillslopes and streams, remobilisation of streambed sediments and bank erosion (Evans and Johnes, 2004 ; Evans *et al.*, 2004 ; Sharpley *et al.*, 2008). When plotting the change in concentration *versus* discharge during a flood event, hystereses are observed when a time lag exists between the concentration peak and discharge peak. The size and direction of discharge-concentration hystereses can be used to infer the spatial origin of the source and the dominant transport pathways (Williams, 1989 ; Lefrancois *et al.*, 2007). Clockwise hystereses in discharge-concentration plots indicate rapid connection between the stream and a source. The source availability decreases during the flood, either because of its depletion or because the energy of the flood is highest during flow rise and decreases afterwards. Anticlockwise hystereses correspond to a source which is progressively connected to the river during the flood so that its export predominantly occurs towards the end of the flood.

Most research studies investigating P discharge-concentration hystereses in medium-size catchments have shown predominance of clockwise hystereses, and have concluded that

resuspension of streambed sediments controls P export (Bowes *et al.*, 2003 ; 2005 ; Ide *et al.*, 2008 ; Stutter *et al.*, 2008). Observations in nested catchments give contrasting results : Bowes *et al.* (2003 ; 2005) observed anticlockwise hysteresis in a headwater catchment and clockwise hysteresis in a downstream catchment. They concluded that a land-to-river export dynamic was apparent in the headwater catchment, whilst it was eclipsed by in-channel processes in the downstream catchment. Haygarth *et al.* (2005) and Stutter *et al.* (2008) observed clockwise hysteresis in both headwater and downstream catchments, but less pronounced in the latter, probably due to lower flood energy. In addition, Bowes *et al.* (2005) and Ide *et al.* (2008) showed that the amplitude of P concentration peak was a function of the rate of change in discharge during the rising limb of the hydrograph, i.e. a proxy of the flood's energy. During a succession of storms, it is common to observe that clockwise hysteresis becomes less pronounced due to the progressive depletion of in-channel sources (Jordan *et al.*, 2005 ; Bowes *et al.*, 2008 ; Stutter *et al.*, 2008).

In many cases, the same hysteresis direction (clockwise or anticlockwise) is observed for both particulate and dissolved P forms. This coupling suggests that the transport mechanisms for both P forms are linked in space and time. However, examples of temporal decoupling between particulate and dissolved P forms also exist as documented in the Mercube, France (Jordan-Meille and Dorioz, 2004), the Kleine Aa, Switzerland (Pacini and Gachter, 1999 ; Lazzarotto *et al.*, 2005), the Corbeira, Spain (Rodriguez-Blanco *et al.*, 2013), two headwater catchments in Devon, England (Haygarth *et al.*, 2012) and one sub-catchment of the Eden River, England (Outram *et al.*, 2014). In these six catchments, particulate P (PP) is exported towards the beginning of floods, whilst soluble reactive phosphorus (SRP) exportations are delayed towards the end of floods, when PP and suspended sediment (SS) concentrations have dropped. These six catchments are dominated by forest and/or grassland, like other catchments where SRP transfer via subsurface pathways has been documented (e.g. Haygarth *et al.*, 1998). According to Dorioz *et al.* (2006), the same decoupling effect between SRP and PP could occur in arable catchments, provided that soils are enriched in P and that vegetated buffer strips limit erosion by trapping particles.

This paper investigates the concentration dynamics of SRP, PP and SS in a stream draining such an arable, intensively farmed catchment with the aims of i) elucidating relations between SRP and PP transport mechanisms and water dynamics, with particular attention paid to groundwater level fluctuations, ii) evaluating the role of seasonal hydroclimatic variations on these relationships, and iii) locating the spatial origin of SRP and PP sources. The method includes seasonal analysis of baseflow and flood concentrations of SRP, PP and SS and statistical analysis of the hydroclimatic drivers that cause the coupling/decoupling in the export of SRP and PP. The selected catchment (Kervidy-Naizin, France) is particularly suitable for this purpose as it benefits from a 6-year monitoring of SRP, PP and SS concentrations at its outlet, including data recovered both during baseflow and storm periods. This monitoring of P and SS concentrations can be combined with high-frequency measurements of rainfall, water table depth and stream discharge.

3.1.2 Materials and methods

Site description

The Kervidy-Naizin catchment is a small (5 km^2) agricultural catchment located in central Brittany, western France (48 ° N, 3 ° W). It belongs to the AgrHyS environmental research observatory (http ://www6.inra.fr /_agrhys_eng) set up in 1999 to monitor and understand the long-term effects of intensive agriculture and climate change on water quality. Numerous studies in the fields of hydrology and biogeochemistry have been carried out in this catchment, resulting in a detailed knowledge of the processes controlling water chemistry (e.g. Molenat *et al.*, 2002 ; Molenat *et al.*, 2008 ; Morel *et al.*, 2009 ; Lambert *et al.*, 2011 ; 2013 ; Aubert *et al.*, 2014). The catchment (Figure 3.1) is drained by a stream of second Strahler order, which generally dries up in the summer. The climate is temperate oceanic, with annual cumulative precipitation and specific discharge averaging 849±119 mm and 296±62 mm, respectively, from 2006 – 2013. Mean annual temperature was 10.2±0.5 ° C and mean daily temperature was below 0 ° C on average eleven days each year. Further description of the climate and hydrological variability is provided in the Supplementary Information (Figure 3.10, 3.11 and 3.12). Elevation ranges from 93 – 135 m above sea level. Topography is gentle, with maximum slopes not exceeding 5%. The bedrock consists of impervious, locally fractured Brioverian schists and is capped by several meters of unconsolidated weathered material and silty, loamy soils. The hydrological behaviour is dominated by the development of a water table whose dynamic varies seasonally along the hillslope. In the upland domain, consisting of well-drained soils, the water table remains below the soil surface throughout the year, varying in depth from 1 – 5 m. In the wetland domain, developed near the stream and consisting of hydromorphic soils, the water table is shallower, remaining near the soil surface generally from October to April/May each year. The seasonal fluctuation of the water-table in this catchment has been described as a succession of three hydrological periods (Aubert *et al.*, 2013a ; Lambert *et al.*, 2013) : Period A : progressive rewetting of the wetland soils after the dry summer season ; Period B : rise of the water table in the upland domain leading to prolonged waterlogging of wetland soils and to the development of a marked groundwater hydraulic gradient between upland and wetland domains ; and Period C : progressive drawdown of the water table leading to the progressive drying of the stream.

The land use is mostly agriculture, essentially arable crops and confined animal production. A detailed study conducted in 2010 led to the following land use subdivisions : 20% cereal crops, 30% corn, 20% grassland and 30% other land uses (wooded plots, buildings, gardens, roads). Animal density was estimated as high as 13 livestock units per ha in 2010. No point source emissions were recorded. Soil extractable P (Olsen method, ISO 11263) and total P (ISO 22036) ranged from 13 – 118 mg P kg^{-1} (extractable P) and from 567 – 1920 mg P kg^{-1} (total P) in arable fields and from 4 – 127 mg P kg^{-1} (extractable P) and from 292 – 2068 mg P kg^{-1} (total P) in grassland. Such high soil P statuses are frequent in the Brittany region (Lemercier *et al.*, 2008).

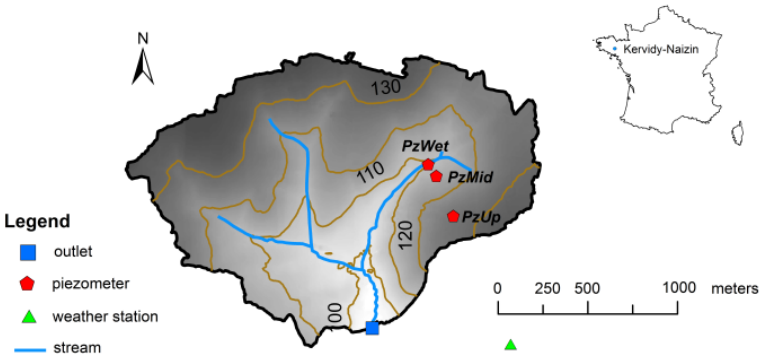

FIGURE 3.1 – Map of the Kervidy–Naizin catchment

Hydrological and chemical monitoring

Hourly rainfall data were recorded at the Toullo weather station, ca 1.1 km East of the catchment outlet (Figure 3.1). Stream discharge was determined every minute with an automatic gauge station at the outlet of the catchment and turbidity was monitored at 10 min intervals (APC-TU, Ponselle). Water table level was recorded at 15 min intervals using ten piezometers located along two transects stretching from the upland to the wetland domains. The analysis focused on three piezometers along one transect (Figure 3.1) referred to as PzWet, PzMid and PzUp.

The data set used here includes six hydrological years, from 1 September 2007 to 30 September 2013. Measured parameters included soluble reactive phosphorus (SRP), total phosphorus (TP) and suspended solids (SS). Two complementary monitoring strategies were used : infrequent regular sampling and high-frequency sampling of flood events. The regular sampling consisted of grab samples collected manually every 6 days at a fixed time, both during floods and baseflow periods. The 6-day sampling frequency reduced the effect of weekly trends (weekday/weekend), but the fixed time may be affected by diurnal cycles. For each sample, one aliquot was filtered directly on-site for SRP analysis (0.45 μm cellulose acetate filter), another aliquot being kept unfiltered for TP and SS determination. Both samples were then stored at 4 $^\circ$ C until analysis within a fortnight. An automatic sampler (ISCO 6712 Full-Size Portable Sampler) was placed in the shade at the outlet and collected water samples during storm events, at a frequency of one sample every 30 min for 12 hours. In total, 52 flood events were monitored during the 6 years of study, and an average of 12 samples among the 24 samples collected during each flood were selected for analysis of SRP, TP and SS. Only flood samples representing good coverage of the event (based on visual verification of discharge and turbidity data) were analysed. Hence, the data set used in this paper included 351 data points from the regular manual sampling and 650 data points from the automatic flood sampling.

SRP was determined colorimetrically by reaction with ammonium molybdate on filtered samples (ISO 15681). Precision of SRP measurement was ± 4 μg l^{-1}. TP was determined

with the same method, after digestion of the unfiltered samples with potassium peroxydisulfate. PP was approximated by subtracting SRP from TP. This approximation is acceptable because SRP represents 80% of total dissolved phosphorus (TDP) in this catchment, as shown by SRP, TDP and PP concentration measurements of 25 representative samples collected both during flood and baseflow periods and during all three periods (A, B and C). We ensured that storage of filtrates for a fortnight had little effect on SRP concentration by comparing samples analysed 24 h and 2 weeks after filtration (negative paired t-test $p<0.05$, $R^2=0.96$, $n=16$). SS concentration was determined by filtration through a glass-fibre filter, which was then dried at 105and weighed (EN 872 :2005). Specific turbidity was calculated for each data point as the turbidity-to-SS concentration ratio. It was used as an indicator of particle-size distribution, assuming that high specific turbidity indicates small particle size (Gippel, 1995 ; Landers and Sturm, 2013).

Data analysis

Functional division of the year into hydrological periods Two arguments justify the need for a functional division of the year into hydrological periods rather than the traditional monthly or quarterly aggregations. First, inter-annual variability in hydroclimatic conditions for a given month or quarter could differ greatly among years. For instance, discharge and water table level in November had typical "summer" features in some years and "winter" features in others (see Supporting Information, Figures 3.11 and 3.12). Second, grouping data points into functional periods was a useful means to relate observed features of P concentration data to the hydroclimatic conditions in each period. Therefore, data from both regular and automatic sampling of floods were analysed in the three hydrological periods A, B and C. The definition of hydrological periods was based on observation of daily water table level and on the difference between rainfall and potential evapotranspiration (PET) (Penman-Monteith). Consequently, the starting and ending dates of each period varied by year depending on the climate (Table 3.1). Transition from period A to period B began when the hydraulic gradient between PzMid and PzUp became higher than, and for the rest of the hydrological year never redescended below, that between PzWet and PzMid, indicating an increasing contribution of upslope groundwater compared to wetland groundwater. Transition from period B to period C began when daily PET became higher than daily rainfall, which corresponded to drawdown of the water table in the upland domain. We subdivided period B into two sub-periods, B1 and B2, to investigate whether the dynamics of flood-induced P export during the beginning of the winter differed from those during late winter. To this end, B2 arbitrarily began two months after the start of B.

Seasonal analysis of baseflow P and SS concentrations The method consisted of plotting the distribution of baseflow SRP, PP and SS concentrations for each period (A, B1, B2 and C). Data from the regular 6 daily samples were used after excluding data points sampled during floods and the following 24 h. The occurrence of floods was detected automatically from 10-min-frequency discharge data. The flood detection algorithm, written for the R software (R Development Core Team, 2012), considered that floods start when a 1% increase in discharge was observed in 10 min and ended when the discharge remained

Hydrological year	Period A	Period B1	Period B2	Period C
2007 – 2008	16 November	4 January	4 March	3 June
2008 – 2009	4 September	2 November	2 January	7 March
2009 – 2010	6 October 8	November	8 January	5 April
2010 – 2011	29 September	10 November	10 January	3 March
2011 – 2012	26 October	11 December	11 February	12 May
2012 – 2013	22 September	16 October	16 December	15 April

TABLE 3.1 – Starting dates of periods A, B1, B2 and C for the hydrological years 2007 – 2008 to 2012 – 2013

stable for three 10-min intervals in a row after a descending phase was detected. Discharge peaks had to be at least 10% higher than baseflow and higher than 20 l s^{-1} for an event to be considered as a flood. The above-mentioned criteria enabled rather small flood events to be detected, which was crucial, because even small variations in discharge could result in large changes in stream P concentrations. The final data set of baseflow samples consisted of 251 of the 351 points in the regular database, with 36 in period A, 46 in period B1, 73 in period B2 and 96 in period C.

Seasonal analysis of flood dynamics The dynamics of the 52 floods were described in terms of amplitudes, i.e. concentration peaks of SRP, PP and SS, and considering the shape and direction of the flood's discharge-concentration hysteresis. For this, we used the β parameter estimated by the 'pollutogram' approach by Rossi *et al.* (2005). The β parameter estimates whether the mass flux of a determinant is exported towards the beginning of a flood or instead towards its end, i.e. whether discharge-concentration hystereses are clockwise or anticlockwise. It is obtained by fitting the relationship $F(x) = x^{\beta}$, where $F(x)$ is the fraction of the total flux of a determinant exported during a flood and x is the fraction of the total cumulative water flow of the flood. $\beta < 1$ indicates that mass flux is exported towards the beginning of the flood (i.e. clockwise hysteresis), whilst $\beta > 1$ indicates that it is exported towards the end of the flood (i.e. anticlockwise hysteresis) (Stutter *et al.*, 2008). We chose to use the 'pollutogram' approach rather than the Hysteresis Index (Lawler *et al.*, 2006) because the latter requires floods to be covered at least beyond the mid-discharge point on the recession tail, which was not always the case with our sampling strategy. As a descriptor of hysteresis shape and direction, β can indicate the spatial origin and dominant transfer pathways of a determinant. Because the shape of a hysteresis can have several possible explanations, hydroclimatic metrics measured concomitantly with stream water quality (e.g. rainfall intensity, antecedent discharge and groundwater level) may help to clarify the underlying hydrological processes. As for baseflow data points, the variables describing dynamics of 52 floods were plotted for each period. The flood data set consisted of 5 floods in period A, 18 floods in period B1, 25 floods in period B2 and 4 floods in period C.

Multivariate analysis of floods Flood description variables (i.e. SRP, PP and SS peak concentrations; β SRP/PP/SS) were statistically analysed in relation to variables

Variable type	Variable name	Unit	Description
Flood hydrograph data	dQ/dt	l s^{-2}	Mean rate of change in discharge during flow rise
.	Qmax	l s^{-1}	Maximum discharge
Flood hydrograph data	rain_6h	mm	Cumulative rainfall during the 6 h preceding the start of the flood
Flood hydrograph data	Q_7d	l s^{-1}	Mean discharge during the 7 days preceding the start of the flood
Flood hydrograph data	Pz_1d_Wet /Mid/Up	m	Mean water-table level in the wetland/midslope/upland domains during the day preceding the start of the flood
.	Pz_max_Wet /Mid/Up	m	Maximum water-table level during the flood in the wetland/midslope/upland domain
.	var_Pz_Wet /Mid/Up	m	Water table variation during the flood in the wetland/midslope/upland domains
Flood hydrograph data	interflood_time	day	Days since the previous flood

TABLE 3.2 – Hydroclimatic variables used in the multivariate analysis of floods

characterising flood hydrological characteristics and their hydroclimatic context. Variables characterising flood events included peak discharge, mean rate of change in discharge during flow rise, maximum water-table height and water-table depth variations within the wetland, midslope and upslope domains. The variables characterising the hydroclimatic context included antecedent rainfall, antecedent discharge, antecedent water table level, and the number of days since the previous flood (Table 3.2). The multivariate analysis aimed to relate seasonal variability in flood characteristics to hydroclimatic conditions to infer seasonal variability in spatial origins and dominant transport pathways. We used principal component analysis (PCA) as a means to visualize variables and their correlations in a parameter space with a reduced number of dimensions.

3.1.3 Results

Considering data from the regular sampling only, mean discharge-weighted concentrations during the study period were 25 μg l^{-1}, 66 μg l^{-1} and 11.7 mg l^{-1} for SRP, TP and SS, respectively. Mean annual specific P load estimated with the discharge-weighted concentration method (Phillips *et al.*, 1999 ; Moatar *et al.*, 2013) was 19.4 kg km^{-2}, of which 38%

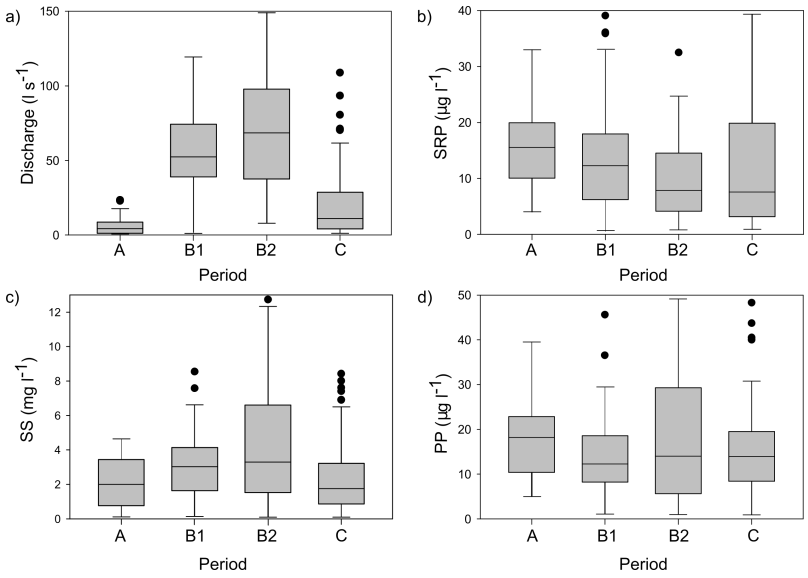

FIGURE 3.2 – Seasonal distribution of baseflow (a) discharge, (b) soluble reactive phosphorus (SRP), (c) suspended sediment (SS) and (d) particulate phosphorus (PP). The middle bar represents the median, the lower bar limits the 1st quartile (q0.25) and the upper bar limits the 3rd quartile (q0.75). The lower and upper lines are, respectively, the 1st quartile minus 1.5 times the interquartile range and the 3rd quartile plus 1.5 times the interquartile range

was SRP.

Seasonal analysis of baseflow P and SS concentrations

We found a significant effect of hydrological period on baseflow SRP and SS concentrations but not on PP concentrations (Kruskal-Wallis test, $p<0.05$). The seasonal distribution of baseflow SS and PP concentrations differed from that of SRP (Figure 3.2). The highest concentrations of SS were observed during B2, i.e. when the highest discharge values were recorded. Although no significant seasonal effect was visible for PP, a substantial number of high values were observed during B2, similarly to SS, and also during A. This seasonal evolution suggests that two different sources of PP were successively mobilised and exhausted, or that the same source was successively exhausted (between A and B1), replenished (between B1 and B2), and then exhausted again (between B2 and C). Concerning SRP, baseflow concentrations were the highest during A, i.e. during a period of low flow and low water table in the upland domain, and decreased during B1 and B2. This seasonal evolution suggests that SRP originated from a single source whose availability decreased during the winter. A substantial number of high values were observed again in period C, which indicates that a mechanism producing SRP was activated at this time of the year.

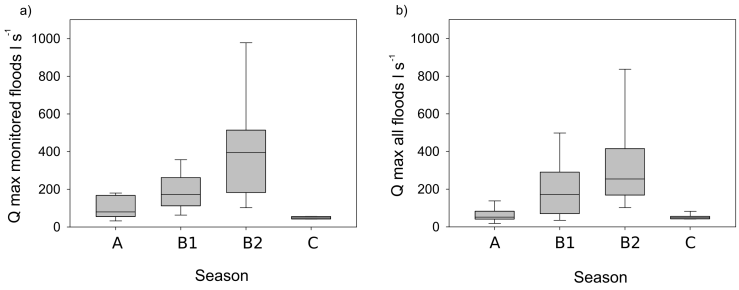

FIGURE 3.3 – Seasonal distribution of maximum discharge of (a) the 52 monitored floods and (b) all 309 floods

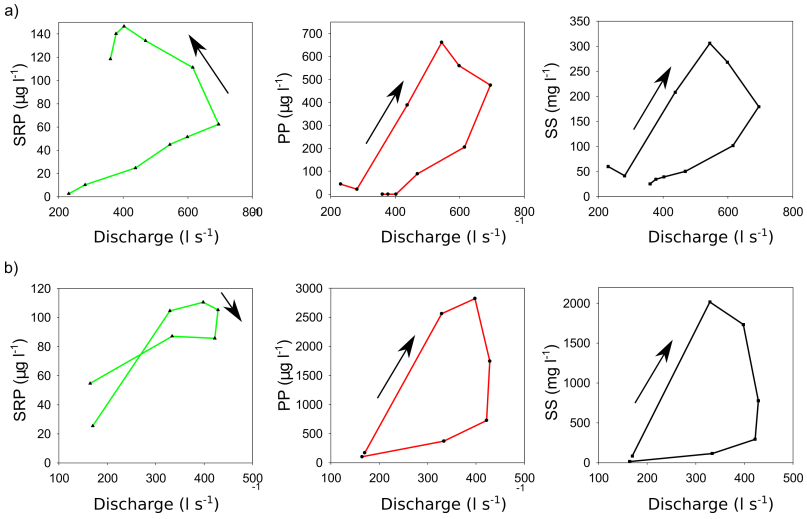

FIGURE 3.4 – Examples of discharge-concentration hysteresis patterns for (a) flood pattern 1 (01.29.2013) and (b) flood pattern 2 (05.30.2008). SRP, soluble reactive phosphorus ; PP, particulate phosphorus ; SS, suspended sediment

Seasonal analysis of flood dynamics

The seasonal distribution of maximum discharge values obtained for the 52 monitored floods was similar to that defined by the entire population of 309 floods that occurred during the study period (Figure 3.3). Hence, we considered that the 52 floods monitored were representative of the entire population of floods in the catchment.

We identified two main flood patterns among the 52 monitored floods observed during the study period (Figure 3.4). Pattern 1 was the most commonly observed (Figure 3.4a) : PP and SS concentrations peaked before maximum discharge (clockwise hysteresis), whilst SRP concentrations peaked after maximum discharge (anticlockwise hysteresis). Pattern 2 (Figure 3.4b) was characterised by synchronised SS, PP and SRP peaks during flow rise or at the time of maximum discharge (clockwise or no hysteresis). Eighty percent of discharge-SS and 71% of discharge-PP plots exhibited clockwise hysteresis, i.e. $\beta < 1$. Conversely, 77% of discharge-SRP plots exhibited anticlockwise hysteresis, i.e. $\beta > 1$. These results indicate a decoupling of the PP and SRP dynamics during most of the floods, PP (along with SS) being generally exported towards the beginning of the floods, whilst SRP was mainly exported towards the end of the floods, as illustrated by pattern 1.

In the following, we present the seasonal variability of flood patterns, as described by i) their concentration peaks (SRPmax, PPmax, SSmax) and ii) their hysteresis shapes/directions (β SRP, β PP, β SS). The seasonal distribution of concentration peaks during floods differed between PP and SS on the one hand and SRP on the other (Figure 3.5a). The highest concentration peaks for PP and SS were observed during A, i.e. when the stream started to flow again after the dry season, and during B2, i.e. when the highest discharge peaks were recorded. The highest concentration peaks for SRP were recorded during A and C, i.e. during periods of low flow and low water table in the upland domain. This seasonal distribution of concentration peaks during floods was similar to that of baseflow concentrations (Figure 3.2). This may suggest that the same pools were mobilised and depleted during baseflow and during flood events ; only the intensity of export increased during floods.

The seasonal distribution of β SRP/β PP/ β SS (Figure 3.5b) allows the periods when floods more closely resemble pattern 1 or 2 to be identified. Pattern 1 was dominant during A, B1 and B2, with β PP and $\beta SS < 1$ and $\beta SRP > 1$ for most of the floods occurring in these periods (81%, 73% and 81%, respectively). During these three periods, the different hysteretic behaviour of PP and SS concentrations on the one hand and of SRP concentration on the other hand was corroborated by inter-correlation analyses of concentrations during floods (Figure 3.6). Indeed, PP and SS concentrations were significantly correlated (Figure 3.6a) whereas SRP and PP concentrations were generally not correlated (Figure 3.6b). Pattern 2 was more common during C, as β SRP, β PP and β SS were 1 for half of the events. Furthermore, SRP was significantly correlated with PP in C (Figure 3.2b), which indicates synchronised export of SRP and PP during floods at this time of the year.

Although analysis of correlations indicates that PP export was synchronised with SS throughout the year, some floods during A exported PP later than SS ($\beta PP > \beta SS$). During B1 and B2, $\beta PP > \beta SS$ for 77% of the events, i.e. the amplitude of the PP hysteresis was generally not as large as that of SS. Differences in the dynamics of PP and SS export are related to differences in the P content of exported particles. Particles' P content during a flood was generally positively correlated with specific turbidity (Figure 3.6). Such

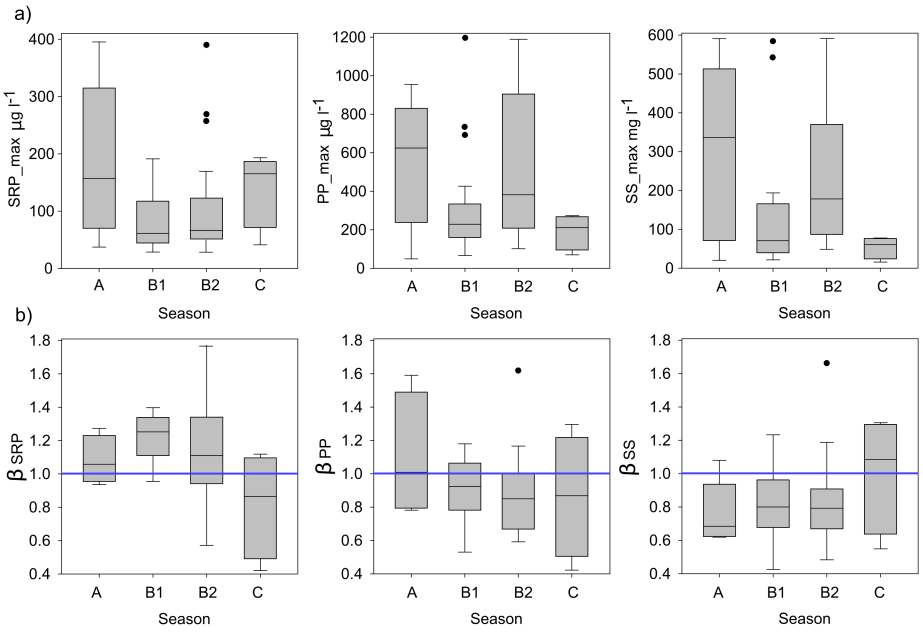

FIGURE 3.5 – Seasonal distribution of (a) peak concentration and (b) β for soluble reactive phosphorus (SRP), particulate phosphorus (PP) and suspended sediment (SS) during floods. Three outliers of peak PP and SS concentrations during period B2 are not visible with the scale used. The middle bar represents the median, the lower limit the 1st quartile (q0.25) and the upper limit the 3rd quartile (q0.75). The lower and upper lines are, respectively, the 1st quartile minus 1.5 times the interquartile range and the 3rd quartile plus 1.5 times the interquartile range. The horizontal line represents $\beta = 1$

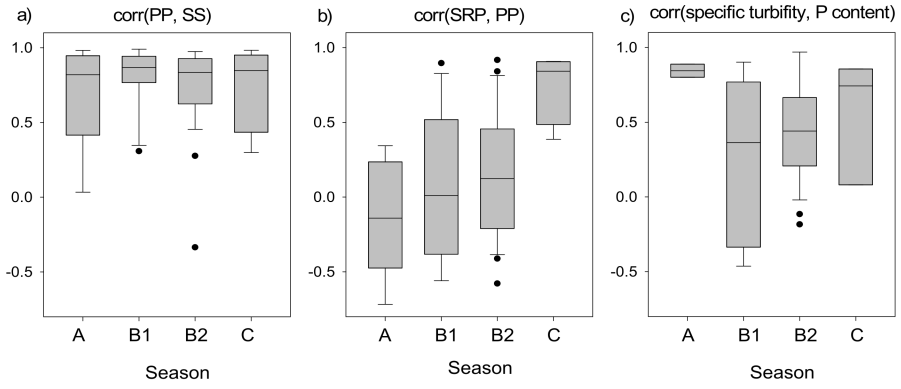

FIGURE 3.6 – Pearson correlation coefficients for all data points of each flood, calculated between (a) particulate phosphorus (PP) and suspended sediment (SS), (b) PP and soluble reactive phosphorus (SRP) and (c) specific turbidity and particle P content. The middle bar represents the median, the lower limit the 1st quartile (q0.25) and the upper limit the 3rd quartile (q0.75). The lower and upper lines are, respectively, the 1st quartile minus 1.5 times the interquartile range and the 3rd quartile plus 1.5 times the interquartile range

a correlation indicates that changes in particles' P content during floods were linked to particle-size sorting, as specific turbidity depends on particle size (Gippel, 1995 ; Landers and Sturm, 2013). Because the correlation between particles' P content and specific turbidity was higher during periods A and C than periods B1 and B2, it seems that particle-size sorting controlled the change in particles' P content during floods of A and C, whilst another mechanism controlled the change in particles' P content during floods of B1 and B2. Soluble reactive phosphorus represented 3 – 56% of TP load during monitored floods (26% in average). The lowest mean percentage of SRP in TP load was observed in B2 (21%) and the highest in C (41%) (Figure 3.7).

Multivariate analysis of floods

Correlations of hydroclimatic variables with SRP/PP/SS concentration peaks highlighted different hydroclimatic controls for PP and SS on the one hand and SRP on the other (Table 3.3). We considered Pearson correlation coefficients above 0.5 'strong', those above 0.25 'moderate' and those below 0.25 but significantly different from zero 'weak'. Maximum PP and SS concentrations were positively and stongly correlated with rate of change in discharge during flow rise (dQ/dt) and maximum discharge (Qmax), i.e. variables describing the 'energy' of the flood. Maximum PP and SS concentrations were also moderately correlated with maximum water-table level in the wetland domain and at the border between wetland and hillslope (Pz_max_Wet, Pz_max_Mid). In contrast, maximum SRP concentrations were only weakly to moderately correlated with the latter variables. The strongest correlation for maximum SRP concentration was observed with the variable describing variation in the water table at the border between wetland and hillslope (var_Pz_Mid). This suggests that high SRP concentration peaks were associated with large fluctuations of the

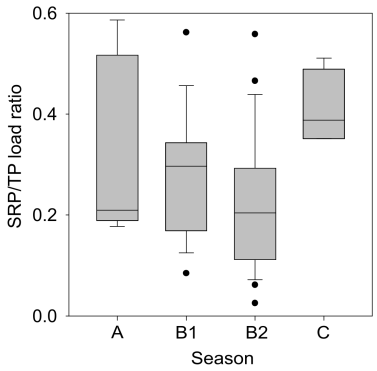

FIGURE 3.7 – Seasonal distribution of the soluble reactive phosphorus (SRP) / total phosphorus (TP) load ratio during all floods. The middle bar represents the median, the lower limit the 1st quartile (q0.25) and the upper limit the 3rd quartile (q0.75). The lower and upper lines are, respectively, the 1st quartile minus 1.5 times the interquartile range and the 3rd quartile plus 1.5 times the interquartile range

water table at this point in the catchment. Finally, maximum SRP concentration was negatively correlated with antecedent water-table level in the upland domain (Pz_1d_Up), which indicates that the highest SRP peaks occurred when the relative contribution of upland groundwater was low compared to that of wetland groundwater.

Correlations of hydroclimatic variables with $\beta SRP/PP/SS$ highlighted that flood dynamics were not governed by the same hydroclimatic characteristics for SS and PP on the one hand and SRP on the other (Table 3.4). βPP and βSS were negatively (but moderately) correlated with the flood 'energy' variable (Qmax, dQ/dt), which means that during the most energetic floods, PP and SS were exported towards the very beginning of the flood. βPP and βSS were also negatively and weakly to moderately correlated with antecedent discharge (Q_7d) and water table (Pz_1d_Wet/Up). Such antecedent flow conditions are favourable for sediment accumulation in the stream channel. Conversely, βPP and βSS were moderately positively correlated with rainfall intensity during 6 h before the flood (rain_6h), i.e. peak concentration was closer to peak discharge when the rainfall causing the flood was intense. Variability in βSRP was not related to any of the hydroclimatic variables tested ; all p values exceeded 0.1.

In the PCA for both seasonal and multivariate analysis of floods, only hydroclimatic variables contributed to construction of the axes (Figure 3.8). The first three axes of the PCA explain 87% of the variability in hydroclimatic conditions during floods. Axis 1, which represents 54% of the variability in hydroclimatic conditions, distinguishes the floods depending on antecedent discharge (Q_7d), antecedent water-table level (PZ_1d_wetland/upslope) and flood magnitude (Qmax, max_Pz_Wet). Nearly 58% of the variability of hydroclimatic conditions among hydrological periods A/B1/B2/C is explained by axis 1 (ANOVA $p<0.01$) : axis 1 distinguishes periods B1/B2 from period C (Figure 3.8b). Axis 2, which represents 22% of the variability in hydroclimatic conditions, is significantly correlated with antecedent discharge (Q_7d), antecedent water-table level (PZ_1d_upslope), rate of change in discharge during flow rise (dQ/dt) and flood magnitude (Qmax). Axis 2 does

.	dQ/dt	Qmax	rain_6h	Q_7d	Pz_1d_Wet	Pz_max_Wet	var_Pz_Wet
PP max	0.82***	0.59***	-0.01	0.07	0.23*	0.43***	-0.03
SS max	0.77***	0.53***	-0.06	0.01	0.2	0.42***	0.01
SRP max	0.33**	0.26*	0.09	-0.13	-0.13	0.01	-0.07

.	Pz_1d_Mid	Pz_max_Mid	var_Pz_Mid	Pz_1d_Up	Pz_max_Up	var_Pz_Up	interflood_time
PP max	0.12	0.29*	0.33**	0.13	0.17	0.04	-0.06
SS max	0.1	0.23*	0.3**	0.1	0.15	0.08	-0.09
SRP max	-0.11	0.25*	0.51***	-0.25*	-0.19	0.01	0.15

TABLE 3.3 – Pearson correlation coefficients between particulate phosphorus (PP), suspended sediment (SS) and soluble reactive phosphorus (SRP) peak concentrations and hydrological variables (see Table 3.2 for definitions)

.	dQ/dt	Qmax	rain_6h	Q_7d	Pz_1d_Wet	Pz_max_Wet	var_Pz_Wet
βPP	-0.30**	-0.26*	0.25*	-0.26*	-0.23	-0.13	0.01
βSS	-0.36**	-0.30**	0.38***	-0.3**	-0.24*	-0.28*	0.05
βSRP	-0.04	0.09	-0.07	0.11	0.15	0.22	0.03

.	Pz_1d_Mid	Pz_max_Mid	var_Pz_Mid	Pz_1d_Up	Pz_max_Up	var_Pz_Up	interflood_time
βPP	-0.12	-0.08	0.04	-0.32**	-0.30**	0.04	0.05
βSS	-0.1	-0.24*	-0.17	-0.30**	-0.30**	0.07	0.03
βSRP	0.2	0.19	-0.02	0.15	0.16	0.04	-0.02

TABLE 3.4 – Pearson correlation coefficients between β particulate phosphorus (PP), β suspended sediment (SS) and β soluble reactive phosphorus (SRP) and hydrological variables (see Table 3.2 for definitions)

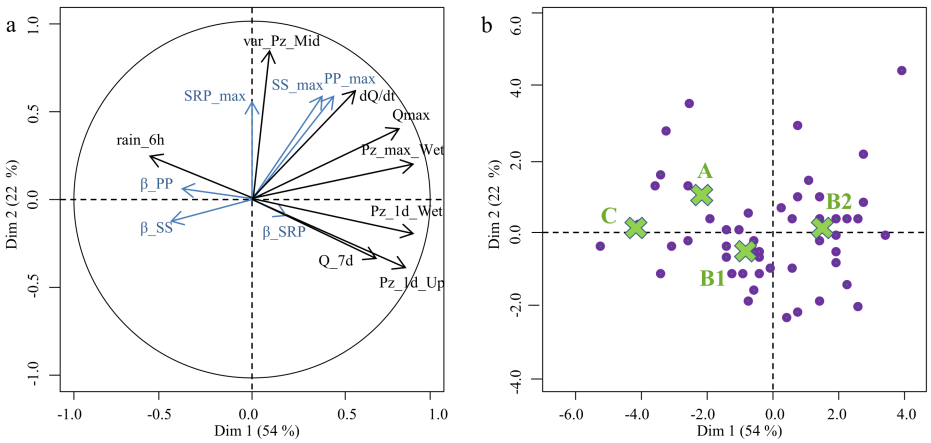

FIGURE 3.8 – Principal component analysis (a) variable map and (b) individual map. Only hydrological variables (black) contributed to construction of the axes. Flood description variables (blue) are illustrative variables. Points A, B1, B2, C in the individual map represent centroids of the hydrological periods

not distinguish hydrological periods A/B1/B2/C (ANOVA $p<0.05$). Axis 3, representing 11% of the variability in hydroclimatic conditions, is significantly correlated with rainfall intensity (rain_6h), rate of change in discharge (dQ/dt) and water-table fluctuation ($p<0.01$). Axis 3 distinguishes hydrological period A from C (ANOVA $p<0.05$), as floods during A are associated with larger fluctuations in the water table (var_Pz_Mid) than during C, whilst floods during C are associated with higher rainfall intensity (rain_6h) and higher rate of change in discharge (dQ/dt).

3.1.4 Discussion

A catchment with low P loads and concentrations despite a high soil P status

The mean annual specific total P load estimated in the Kervidy-Naizin catchment (19.4 kg km^{-2}) was in the lower range of load values reported in 79 catchments in France (10 – 140 kg km^{-2} ; Dupas *et al.*, 2015) and 62 catchments in Europe (10 – 600 kg km^{-2}, Kronvang *et al.*, 2007). Accordingly, recorded concentrations were below the threshold defining 'good ecological status' according to the European Water Framework directive ($Q90SRP < 163$ μg l^{-1} $Q90TP < 200$ μg l^{-1}). Such an apparent contradiction between high soil P statuses and low P loads and concentrations in the river has already been highlighted by several authors (e.g. Jordan *et al.*, 2012 ; Mellander *et al.*, 2012b ; Shore *et al.* 2014), probably due to river P concentrations and loads being more directly related to catchments' transport potential than to source risk. The 38% SRP was in the higher range of values reported in France (20 – 53%), which agrees with the finding of Dupas *et al.* (2015) that low-order catchments have higher percentages of dissolved P than large river networks. The discharge-weighted concentration method may lead to a systematic bias in TP and SRP load calculation of up to -60%, as Moatar *et al.* (2013) highlighted with data from large watersheds (>1000 km²) and infrequent sampling. However, Johnes *et al.*

(2007) and Cassidy and Jordan (2011) found that this method was the most appropriate for calculating P loads when weekly data are available because, despite high imprecision, bias is usually low. Because the regular sampling was relatively frequent and included 100 out of 251 points recovered during floods or the following 24 h, we assumed that estimated loads in the Kervidy-Naizin catchment were close to the true values.

Decoupling of SRP and PP dynamics

Both on an annual basis and during flood events, contrasting dynamics indicate a strong temporal decoupling of SRP and PP. This decoupling suggests that the standard hypothesis for arable catchments that erosion and surface transfer from agricultural fields control PP export, which in turn controls SRP in the stream, is not valid in the Kervidy-Naizin catchment. Instead, our data suggest that SRP is exported independently from PP and originates from a different source during most of year. To our knowledge, such a decoupling between SRP and PP has only been documented in forest and grassland catchments (Jordan-Meille and Dorioz, 2004 ; Lazzarotto *et al.*, 2005 ; Haygarth *et al.*, 2012 ; Rodriguez-Blanco *et al.*, 2013 ; Outram *et al.*, 2014) but not yet in arable catchments. Only spring storm events exhibited synchronised export of PP and SRP, which indicates that erosion and overland flow can control PP and SRP at this time of the year (Le Bissonnais *et al.*, 2002). Because manure and slurry were generally applied in spring, incidental losses are likely to have occurred at this time of the year.

Seasonal variability in hydrological controls on PP and SS dynamics

Discharge-concentration hystereses during floods were generally clockwise for both PP and SS. This type of hysteresis indicates that the availability of a sediment stock decreased during floods, either because the stock was depleted or because the export capacity of the floods was higher during the rising limb than during the falling limb of the hydrograph (McDowell and Sharpley, 2002 ; Seeger *et al.*, 2004 ; Lefrancois *et al.*, 2007). In the Kervidy-Naizin catchment, seasonal change in flood characteristics showed that the export of PP and SS was controlled by the export capacity of floods and availability of stream sediments. The same type of hysteresis and seasonal change has been observed in other catchments where mobilisation of in-channel sediments dominates P export (Bowes *et al.*, 2005 ; Haygarth *et al.*, 2005 ; Stutter *et al.*, 2008). Although in-channel sediments were likely to be the main source of particles exported during floods, Vongvixay *et al.* (2010) highlighted that contribution from hillslope erosion was significant in the P budget of the Kervidy-Naizin catchment, especially because particles originating from agricultural fields were richer in P than those originating from stream sediments or river banks.

To identify the spatial origin of PP and SS sources, we assumed that early PP and SS peaks (low β values) indicate a large contribution of in-channel sources and that PP and SS peaks close to the discharge peak indicate sources located further away from the stream (higher β values, close to 1). Furthermore, we assumed that strong correlation between particles' P content and specific turbidity means that size sorting from a single sediment source controlled the change in particles' P content during a flood (Gippel, 1995 ; Landers and Sturm, 2013). Conversely, low correlation between particles' P content and specific turbidity indicates that several sources may have contributed to the export of PP and

SS during a flood. The lowest βSS values were observed during period A, together with good correlation between particles' P content and specific turbidity. This suggests a large contribution of in-channel sources. Indeed, availability of in-channel sediments is likely to have been high when the stream started to flow again after the dry season, and the probability of sediment delivery from hillslopes was low at this time of the year because hillslopes were hydrologically disconnected from the stream (Vongvixay *et al.*, 2010). Such observation of within-channel sources of SS and PP being preponderant is common in catchments from the temperate zone (Bowes *et al.*, 2005 ; Kronvang *et al.*, 2012 ; 2013 ; Lu *et al.*, 2014). Unexpectedly, βPP in period A sometimes exceeded 1, unlike βSS. A possible explanation is that the stream network was not entirely connected during this period. Thus, successive floods during period A connected new portions of the stream network, causing export of new, P-rich sediment pools. βSS values increased during periods B1 and B2, and particles' P content was weakly correlated with specific turbidity. This suggests a larger contribution of hillslope erosion to PP and SS export, linked to decreased sediment availability in the stream channel and increased connectivity between the stream and hillslopes. During period C, βSS values exceeded 1 and particles' P content was again strongly correlated with specific turbidity. This suggests that hillslopes were the main source of SS. Soil sealing (i.e. formation of a thin layer of compacted soil caused by rain impact) following seedbed preparation for spring crops, was the most probable cause of hillslope erosion in spring (Le Bissonnais *et al.*, 2002).

Seasonal variability in hydrological controls on SRP dynamics

Discharge-concentration hystereses during floods were generally anticlockwise for SRP. This type of hysteresis is often interpreted as indicating subsurface flow pathways (e.g. Morel *et al.*, 2009), the time lag between discharge and concentration response resulting from the time necessary for the groundwater table to reach shallow soil horizons in the wetland domain. An alternative explanation could be that SRP was sorbed to SS during the initial stage of the events and could only increase when SS has dropped (Lazzarrotto *et al.*, 2005). However, further analyses of hydroclimatic variables tend to confirm the influence of water-table fluctuations on SRP export. The multivariate analysis of floods revealed that dynamics of SRP export were controlled by the amplitude of water-table fluctuation and by the relative position of the groundwater level between the wetland and the upland domain. Specifically, water-table fluctuation observed at the border between the hillslope and wetland domain had the highest correlation with peak SRP concentration (Table 3). The border between the wetland domain, usually planted with a buffer strip, and the hillslope domain, usually cultivated, was likely to be a critical ecotone for SRP transfer in the Kervidy-Naizin catchment because i) water-table fluctuation at this point could reach the soil surface during floods in period A and remained near the soil surface during period B (i.e. it was a hydrologically active zone) and ii) it corresponded to cultivated plots or to the field side of a buffer strip (i.e. potentially P-enriched soils). Hence, riparian soils, even when occupied by a vegetated buffer strip, were probably the main source of SRP. Further investigation would be necessary to determine whether this area is a source of SRP only because groundwater is reaching the shallow soil horizon or because soils were enriched in P. Several authors have drawn attention to the fact that vegetated buffer strips are only temporary sinks for P and that their aging might turn them into P sources (Dorioz *et al.*,

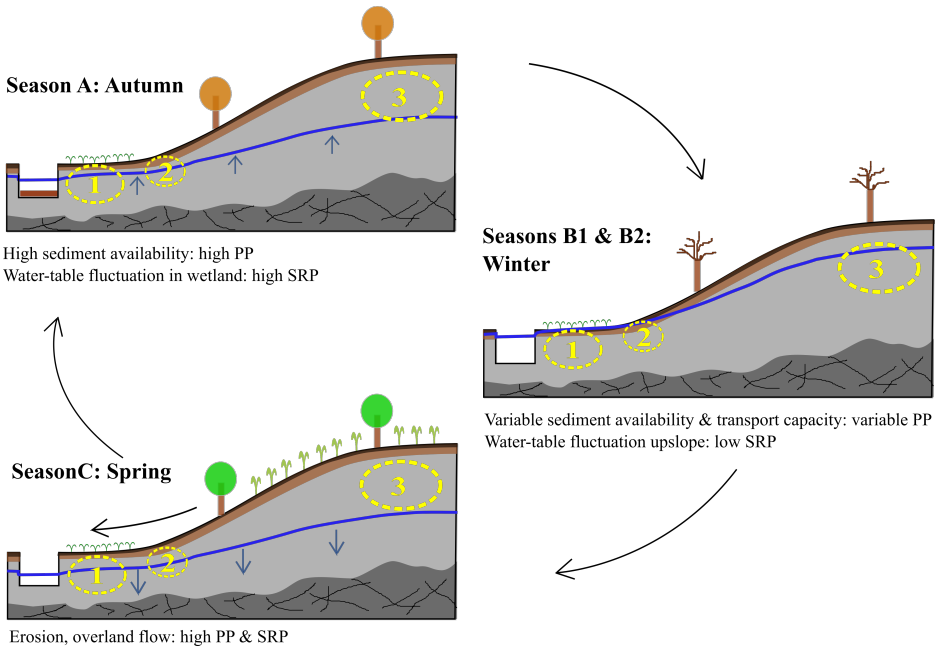

FIGURE 3.9 – Conceptual model of soluble reactive phosphorus (SRP) and particulate phosphorus (PP) export in an agricultural headwater catchment during three periods of the year. SRP concentrations are determined by the relative contributions of three compartments : (1) wetland soils, (2) midslope groundwater and (3) upland groundwater. PP concentrations are determined by sediment availability and stream export capacity

2006 ; Stutter *et al.*, 2009 ; Roberts *et al.*, 2012). However, the mechanisms leading to P delivery from vegetated buffer strips remain unclear : Stutter *et al.* (2009) demonstrated that increased biological activity could release SRP in soil that was not saturated in P. In the Kervidy-Naizin catchment, vegetated buffer strips coincide with riparian wetlands, i.e. soils that are periodically saturated with water. Hence, changes in the redox and pH status of wetland soils as a result of periodic waterlogging could increase SRP extractability in this area of the catchment (Obour *et al.*, 2011 ; Scalenghe *et al.*, 2012). To further investigate the biogeochemical processes involved in the production/depletion of mobile P in wetland soils, we plan to monitor soil pore water in valley-bottom areas of the Kervidy-Naizin catchment with a protocol similar to that of Lambert *et al.* (2013).

Comparing SRP with other elements used as tracers provides a useful means to further constrain the spatial location of sources and transfer pathways. In the Mercube catchment, Jordan-Meille and Dorioz (2004) observed that the delayed export of SRP during floods was synchronised with that of chloride and nitrate, which they interpreted as indicating transfer via subsurface flow. In-situ experiments with dye and bromide as tracers in the Kleine Aa catchment led to the conclusion that P transfer through soil macropores and artificial drainage systems could explain the delayed export of SRP (Gachter *et al.*, 1998). In the Kervidy-Naizin catchment, the dynamics of SRP export were similar to those of dissolved organic carbon (DOC), whose production and transfer mechanisms are well known

(Morel *et al.*, 2009 ; Lambert *et al.*, 2011 ; 2013). The similarity with DOC export dynamics supports the idea that SRP originates for a large part from riparian wetland soils and echoes recent findings that organic and inorganic P released from the soil microbial biomass might represent a significant pool of mobile P in riparian buffer strips (Turner and Haygarth, 2001 ; Turner *et al.*, 2003 ; Blackwell *et al.*, 2010 ; Roberts *et al.*, 2013). Indeed, Lambert *et al.* (2013) identified microbial biomass as an important source of DOC during periods A and C in the Kervidy-Naizin catchment. On an annual basis, the decrease in SRP concentration also coincides with the evolution of DOC concentrations in Kervidy-Naizin (Aubert *et al.*, 2013b) and other catchments (Hornberger *et al.*, 1994 ; Dawson *et al.*, 2008). Decrease in flood and baseflow SRP concentrations between periods A and B could be due to the depletion of a pool of mobile P in the wetland domain and/or dilution by deep groundwater with low P concentration from the upland domain (Figure 3.9). During periods A to B2, variation in stream SRP could not be directly related to the calendar of agricultural practices in the catchment. This substantiates the thesis of Haygarth *et al.* (2012) that no clear temporal relation can generally be identified between addition of fertiliser and stream P concentration, and that P losses are instead determined by the long-term history of P inputs and hydrological processes (Haygarth *et al.*, 2014).

Finally, baseflow SRP concentrations increased again at the end of period C (i.e. spring), although P-rich soil horizons became progressively disconnected from the stream at this period of the year. Several hypotheses can explain high SRP concentration during baseflow in period C in the absence of point sources, e.g. : i) release of SRP from streambed sediments ; ii) reducing conditions causing the solubilisation of redox-sensitive minerals, such as iron (Fe), in soils and iii) net mineralisation of soil organic P. The spring period also displayed specific features during floods : peak SRP concentrations were no longer controlled by water-table dynamics but rather by rainfall intensity. Concomitantly, flood SRP dynamics was synchronized with PP, suggesting common spatial origin and transport mechanisms. Thus the main transport mechanism of SRP and PP during spring storms must have been overland flow and soil erosion caused by soil sealing. Such surface transport may have caused incidental losses of recently applied manure.

3.1.5 Conclusion

This paper reports on the export dynamics of PP and SRP in a headwater, agricultural catchment using infrequent regular sampling combined with high-frequency monitoring of floods. Strong decoupling was observed between PP and SRP export dynamics both on an annual basis and during most of the floods. This decoupling suggests that PP and SRP had different spatial origins and/or followed different transport pathways for the most part of the year. Additionally, different hydroclimatic features controlled SRP and PP export. PP export was controlled by flood export capacity and sediment availability, whilst SRP dynamics was controlled by water-table fluctuation in the wetland domain. The spatial origin and transport mechanisms of PP vary throughout the year : in the beginning of the hydrological year (October to November), PP export originated from in-channel sediments and/or bank erosion, whilst PP export in spring (May to July) came from erosion on hillslopes. Winter floods represent a mixture of both origins. Soluble reactive P concentrations were the highest in the beginning of the hydrological year, when the catchment

became wetter and the water table fluctuated in the wetland domain. As winter progressed, SRP concentration decreased during floods and baseflow periods, due to depletion of the wetland P pool and/or dilution by deep groundwater with low P concentration from the upland domain. In the last months before the stream dried out in summer, SRP concentration increased during baseflow periods, even though P-rich soils were being progressively disconnected from the stream. The possible mechanisms causing the release of SRP could thus involve in-stream processes, reduction of Fe oxide-hydroxides in wetland soils or net mineralisation of soil organic P. At the same time, SRP and PP export during spring floods were synchronised and caused by erosion and overland flow. All in all, variation in stream SRP could not be directly related to the calendar of agricultural practices in the catchment, except for some spring floods which may have caused incidental losses of recently applied manure. Therefore, management recommendations in our study catchment include erosion-control measures and restrictions on fertilisation to avoid P enrichment of wetlands, which are high-risk areas due to their high hydrological connectivity with streams.

Acknowledgments

This work was funded by the 'Agence de l'Eau Loire Bretagne' via the 'Trans-P' project. Long-term monitoring in the Kervidy-Naizin catchment is supported by 'ORE AghrHyS'. Jean-Paul Guillard performed the manual sampling, and Nicolas Gilliet was in charge of the automatic sampling. Laurence Carteaux, Yannick Fauvel and Armelle Racapé performed the chemical analyses. We also thank Michelle and Michael Corson for their advice in writing this paper and correcting its English style.

The authors declare that there are no conflicts of interest.

References

Aubert AH, Gascuel-Odoux C, Gruau G, Akkal N, Faucheux M, Fauvel Y, Grimaldi C, Hamon Y, Jaffrézic A, Lecoz-Boutnik M, Molénat J, Petitjean P, Ruiz L, Merot P. 2013a. Solute transport dynamics in small, shallow groundwater-dominated agricultural catchments : insights from a high-frequency, multisolute 10 yr-long monitoring study. Hydrology and Earth System Sciences 17(4) : 1379-1391. DOI : 10.5194/hess-17-1379-2013

Aubert AH, Gascuel-Odoux C, Merot P. 2013b. Annual hysteresis of water quality : A method to analyse the effect of intra- and inter-annual climatic conditions. Journal of Hydrology 478 : 29-39. DOI : 10.1016/j.jhydrol.2012.11.027.

Aubert AH, Kirchner JW, Gascuel-Odoux C, Faucheux M, Gruau G, Merot P. 2014. Fractal water quality fluctuations spanning the periodic table in an intensively farmed watershed. Environmental Science Technology 48(2) : 930-937. DOI : 10.1021/es403723r.

Blackwell MSA, Brookes RC, de la Fuente-Martinez N, Gordon H, Murray PJ, Snars KE, Williams JK, Bol R, Haygart PM. 2010. Phosphorus solubilization and potential transfer to surface waters from the soil microbial biomass following drying-rewetting and freezing-thawings. In : Sparks, D.L. (Ed.), Advances in Agronomy, Vol 106. Advances in Agronomy Elsevier Academic Press Inc, San Diego, pp. 1-35. DOI : 10.1016/s0065-2113(10)06001-3.

Bowes MJ, House WA, Hodgkinson RA. 2003. Phosphorus dynamics along a river

continuum. Science of the Total Environment 313(1-3) : 199-212. DOI : 10.1016/s0048-9697(03)00260-2.

Bowes MJ, House WA, Hodgkinson RA, Leach DV. 2005. Phosphorus-discharge hysteresis during storm events along a river catchment : the River Swale, UK. Water Research 39(5) : 751-762. DOI : 10.1016/j.watres.2004.11.027.

Bowes MJ, Smith JT, Jarvie HP, Neal C. 2008. Modelling of phosphorus inputs to rivers from diffuse and point sources. Science of the Total Environment 395(2-3) : 125-138. DOI : 10.1016/j.scitotenv.2008.01.054.

Cassidy R, Jordan P. 2011. Limitations of instantaneous water quality sampling in surface-water catchments : Comparison with near-continuous phosphorus time-series data. Journal of Hydrology 405 : 182-193. DOI : 10.1016/j.jhydrol.2011.05.020.

Dawson JJC, Soulsby C, Tetzlaff D, Hrachowitz M, Dunn SM, Malcolm IA. 2008. Influence of hydrology and seasonality on DOC exports from three contrasting upland catchments. Biogeochemistry 90(1) : 93-113. DOI : 10.1007/s10533-008-9234-3.

Dorioz JM, Wang D, Poulenard J, Trevisan D. 2006. The effect of grass buffer strips on phosphorus dynamics - A critical review and synthesis as a basis for application in agricultural landscapes in France. Agriculture Ecosystems Environment 117(1) : 4-21. DOI : 10.1016/j.agee.2006.03.029.

Dupas R, Delmas M, Dorioz JM, Garnier J, Moatar F, Gascuel-Odoux C. 2015. Assessing the impact of agricultural pressures on N and P loads and eutrophication risk. Ecological Indicators 48 : 396-407. DOI :10.1016/j.ecolind.2014.08.007

Evans DJ, Johnes P. 2004. Physico-chemical controls on phosphorus cycling in two lowland streams. Part 1 - the water column. Science of the Total Environment 329(1-3) : 145-163. DOI : 10.1016/j.scitotenv.2004.02.016.

Evans DJ, Johnes PJ, Lawrence DS. 2004. Physico-chemical controls on phosphorus cycling in two lowland streams. Part 2 - The sediment phase. Science of the Total Environment 329(1-3) : 165-182. DOI : 10.1016/j.scitotenv.2004.02.023.

Gachter R, Ngatiah JM, Stamm C. 1998. Transport of phosphate from soil to surface waters by preferential flow. Environmental Science Technology 32(13) : 1865-1869. DOI : 10.1021/es9707825.

Gippel CJ. 1995. Potential of turbidity monitoring for measuring the transport of suspended-solids in streams. Hydrological Processes 9(1) : 83-97. DOI : 10.1002/hyp.3360090108.

Grizzetti B, Bouraoui F, Aloe A. 2012. Changes of nitrogen and phosphorus loads to European seas. Global Change Biology 18(2) : 769-782. DOI : 10.1111/j.1365-2486.2011.02576.x.

Haygarth PM, Hepworth L, Jarvis SC. 1998. Forms of phosphorus transfer in hydrological pathways from soil under grazed grassland. European Journal of Soil Science 49(1) : 65-72. DOI : 10.1046/j.1365-2389.1998.00131.x.

Haygarth PM, Jarvie HP, Powers SM, Sharpley AN, Elser JJ, Shen JB, Peterson HM, Chan NI, Howden NJK, Burt T, Worral F, Zhang FS, Liu XJ. 2014. Sustainable Phosphorus Management and the Need for a Long-Term Perspective : The Legacy Hypothesis. Environmental Science Technology 48 : 8417-8419. DOI : 10.1021/es502852s.

Haygarth PM, Page TJC, Beven KJ, Freer J, Joynes A, Butler P, Wood GA, Owens PN. 2012. Scaling up the phosphorus signal from soil hillslopes to headwater catchments. Freshwater Biology 57 : 7-25. DOI : 10.1111/j.1365-2427.2012.02748.x.

Haygarth PM, Wood FL, Heathwaite AL, Butler PJ. 2005. Phosphorus dynamics ob-

served through increasing scales in a nested headwater-to-river channel study. Science of the Total Environment 344(1-3) : 83-106. DOI : 10.1016/j.scitotoenv.2005.02.007.

Heathwaite AL, Dils RM. 2000. Characterising phosphorus loss in surface and subsurface hydrological pathways. Science of the Total Environment 251 : 523-538. DOI : 10.1016/s0048-9697(00)00393-4.

Heathwaite AL, Quinn PF, Hewett CJM. 2005. Modelling and managing critical source areas of diffuse pollution from agricultural land using flow connectivity simulation. Journal of Hydrology 304(1-4) : 446-461. DOI : 10.1016/j.jhysrol.2004.07.043.

Heckrath G, Brookes PC, Poulton PR, Goulding KWT. 1995. Phosphorus leaching from soils containing different phosphorus concentrations in the Broadbalk experiment. Journal of Environmental Quality 24(5) : 904-910.

Hornberger GM, Bencala KE, McKnight DM. 1994. Hydrological controls on dissolved organic-carbon during snowmelt in the Snake river near Montezuma, Colorado. Biogeochemistry 25(3) : 147-165. DOI : 10.1007/bf00024390.

House WA, Warwick MS. 1998. Hysteresis of the solute concentration/discharge relationship in rivers during storms. Water Research 32(8) : 2279-2290. DOI : 10.1016/s0043-1354(97)00473-9.

Ide J, Haga H, Chiwa M, Otsuki K. 2008. Effects of antecedent rain history on particulate phosphorus loss from a small forested watershed of Japanese cypress (Chamaecyparis obtusa). Journal of Hydrology 352(3-4) : 322-335. DOI : 10.1016/j.jhydrol.2008.01.012.

Jarvie HP, Neal C, Williams RJ, Neal M, Wickham HD, Hill LK, Wade AJ, Warwick A, White J. 2002. Phosphorus sources, speciation and dynamics in the lowland eutrophic River Kennet, UK. Science of the Total Environment 282 : 175-203. DOI : 10.1016/s0048-9697(01)00951-2.

Jarvie HP, Neal C, Withers PJA, Baker DB, Richards RP, Sharpley AN. 2011. Quantifying phosphorus retention and release in rivers and watersheds using extended end-member mixing analysis (E-EMMA). Journal of Environmental Quality 40(2) : 492-504. DOI : 10.2134/jeq2010.0298.

Johnes PJ. 2007. Uncertainties in annual riverine phosphorus load estimation : Impact of load estimation methodology, sampling frequency, baseflow index and catchment population density. Journal of Hydrology 332 : 241-258. DOI : 10.1016/j.jhydrol.2006.07.006

Jordan-Meille L, Dorioz JM. 2004. Soluble phosphorus dynamics in an agricultural watershed. Agronomie, 24(5) : 237-248. DOI : 10.1051/agro :2004021.

Jordan P, Arnscheidt J, McGrogan H, McCormick S. 2005. High-resolution phosphorus transfers at the catchment scale : the hidden importance of non-storm transfers. Hydrology and Earth System Sciences 9(6) : 685-691.

Jordan P, Melland AR, Mellander PE, Shortle G, Wall D. 2012. The seasonality of phosphorus transfers from land to water : implications for trophic impacts and policy evaluation. Science of the Total Environment 434 : 101-9. DOI : 10.1016/j.scitotenv.2011.12.070.

Kronvang B, Andersen HE, Larsen SE, Audet J. 2013. Importance of bank erosion for sediment input, storage and export at the catchment scale. Journal of Soils and Sediments 13(1) : 230-241. DOI : 10.1007/s11368-012-0597-7.

Kronvang B, Audet J, Baattrup-Pedersen A, Jensen HS, Larsen SE. 2012. Phosphorus Load to Surface Water from Bank Erosion in a Danish Lowland River Basin. Journal of Environmental Quality 41(2) : 304-313. DOI : 10.2134/jeq2010.0434.

Kronvang B, Vagstad N, Behrendt H, Bogestrand J, Larsen SE. 2007. Phosphorus losses at the catchment scale within Europe : an overview. Soil Use and Management 23 : 104-116. DOI : 10.1111/j.1475-2743.2007.00113.x.

Lambert T, Pierson-Wickmann AC, Gruau G, Jaffrezic A, Petitjean P, Thibault JN, Jeanneau L. 2013. Hydrologically driven seasonal changes in the sources and production mechanisms of dissolved organic carbon in a small lowland catchment. Water Resources Research 49(9) : 5792-5803. DOI : 10.1002/wrcr.20466.

Lambert T, Pierson-Wickmann AC, Gruau G, Thibault JN, Jaffrezic A. 2011. Carbon isotopes as tracers of dissolved organic carbon sources and water pathways in headwater catchments. Journal of Hydrology 402(3-4) : 228-238. DOI : 10.1016/j.jhydrol.2011.03.014.

Landers MN, Sturm T. 2013. Hysteresis in suspended sediment to turbidity relations due to changing particle size distributions. Water Resources Research 49(9) : 5487-5500. DOI : 10.1002/wrcr.20394.

Lawler DM, Petts GE, Foster IDL, Harper S. 2006. Turbidity dynamics during spring storm events in an urban headwater river system : The Upper Tame, West Midlands, UK. Science of the Total Environment 360 : 109-126. DOI : 10.1016/j.scitotenv.2005.08.032.

Lazzarotto P, Prasuhn V, Butscher E, Crespi C, Flühler H, Stamm C. 2005. Phosphorus export dynamics from two Swiss grassland catchments. Journal of Hydrology 304(1-4) : 139-150. DOI : 10.1016/j.jhydrol.2004.07.027.

Le Bissonnais Y, Cros-Cayot S, Gascuel-Odoux C. 2002. Topographic dependence of aggregate stability, overland flow and sediment transport. Agronomie 22 : 489-501. DOI : 10.1051/agro :2002024.

Lefrancois J, Grimaldi C, Gascuel-Odoux C, Gilliet N. 2007. Suspended sediment and discharge relationships to identify bank degradation as a main sediment source on small agricultural catchments. Hydrological Processes 21(21) : 2923-2933. DOI : 10.1002/hyp.6509.

Lemercier B, Gaudin L, Walter C, Aurousseau P, Arrouays D, Schvartz C, Saby NPA, Follain S, Abrassart J. 2008. Soil phosphorus monitoring at the regional level by means of a soil test database. Soil Use and Management 24(2) : 131-138. DOI : 10.1111/j.1475-2743.2008.00146.x.

Lu S, Kronvang B, Audet J, Trolle D, Andersen HE, Thodsen H, van Griensven A. 2014. Modelling sediment and total phosphorus export from a lowland catchment : comparing sediment routing methods. Hydrological Processes. DOI : 10.1002/hyp.10149.

McDowell RW, Sharpley AN. 2002. The effect of antecedent moisture conditions on sediment and phosphorus loss during overland flow : Mahantango Creek catchment, Pennsylvania, USA. Hydrological Processes 16(15) : 3037-3050. DOI : 10.1002/hyp.1087.

Mellander PE, Jordan P, Wall DP, Melland AR, Meehan R, Kelly C. 2012b. Delivery and impact bypass in a karst aquifer with high phosphorus source and pathway potential. Water Research 46 : 2225-2236. DOI : 10.1016/j.watres.2012.01.048

Mellander P-E, Melland AR, Jordan P, Wall DP, Murphy PNC, Shortle G. 2012a. Quantifying nutrient transfer pathways in agricultural catchments using high temporal resolution data. Environmental Science Policy 24 : 44-57. DOI : 10.1016/j.envsci.2012.06.004.

Moatar F, Meybeck M, Raymond S, Birgand F, Curie F. 2013. River flux uncertainties predicted by hydrological variability and riverine material behaviour. Hydrological Processes 27(25) : 3535-3546. DOI : 10.1002/hyp.9464.

Molenat J, Durand P, Gascuel-Odoux C, Davy P, Gruau G. 2002. Mechanisms of nitrate

transfer from soil to stream in an agricultural watershed of French Brittany. Water Air and Soil Pollution 133(1-4) : 161-183. DOI : 10.1023/a :1012903626192.

Molenat J, Gascuel-Odoux C, Davy P, Durand P. 2005. How to model shallow water-table depth variations : the case of the Kervidy-Naizin catchment, France. Hydrological Processes 19(4) : 901-920. DOI : 10.1002/hyp.5546.

Morel B, Durand P, Jaffrezic A, Gruau G, Molenat J. 2009. Sources of dissolved organic carbon during stormflow in a headwater agricultural catchment. Hydrological Processes 23(20) : 2888-2901. DOI : 10.1002/hyp.7379.

Nemery J, Garnier J, Morel C. 2005. Phosphorus budget in the Marne Watershed (France) : urban vs. diffuse sources, dissolved vs. particulate forms. Biogeochemistry 72(1) : 35-66. DOI : 10.1007/s10533-004-0078-1.

Obour AK, Silveira ML, Vendramini JMB, Sollenberger LE, O'Connor GA. 2011. Fluctuating water table effect on phosphorus release and availability from a Florida Spodosol. Nutrient Cycling in Agroecosystems 91(2) : 207-217. DOI : 10.1007/s10705-011-9456-y.

Outram FN, Lloyd CEM, Jonczyk J, Benskin CMH, Grant F, Perks MT, Deasy C, Burke SP, Collins AL, Freer J, Haygarth PM, Hiscock KM, Johnes PJ, Lovett AL. 2014. High-frequency monitoring of nitrogen and phosphorus response in three rural catchments to the end of the 2011-2012 drought in England. Hydrology and Earth System Sciences 18 : 3429-3448. DOI : 10.5194/hess-18-3429-2014.

Pacini N, Gachter R. 1999. Speciation of riverine particulate phosphorus during rain events. Biogeochemistry 47(1) : 87-109. DOI : 10.1023/a :1006153302488.

Phillips JM, Webb BW, Walling DE, Leeks GJL. 1999. Estimating the suspended sediment loads of rivers in the LOIS study area using infrequent samples. Hydrological Processes 13 : 1035-1050.

R Development Core Team (2012). R : A language and environment for statistical computing. R Foundation for Statistical Computing, Vienna, Austria. ISBN 3-900051-07-0, URL http ://www.R-project.org/.

Ringeval B, Nowak B, Nesme T, Delmas M, Pellerin S. 2014. Contribution of anthropogenic phosphorus to agricultural soil fertility and food production. Global Biogeochemical Cycles 28 : 743-756. DOI : 10.1002/2014gb004842.

Roberts WM, Matthews RA, Blackwell MSA, Peukert S, Collins AL, Stutter MI, Haygarth PM. 2013. Microbial biomass phosphorus contributions to phosphorus solubility in riparian vegetated buffer strip soils. Biology and Fertility of Soils 49(8) : 1237-1241. DOI : 10.1007/s00374-013-0802-x.

Roberts WM, Stutter MI, Haygarth PM. 2012. Phosphorus Retention and Remobilization in Vegetated Buffer Strips : A Review. Journal of Environmental Quality 41(2) : 389-399. DOI : 10.2134/jeq2010.0543.

Rodriguez-Blanco ML, Taboada-Castro MM, Taboada-Castro MT. 2013. Phosphorus transport into a stream draining from a mixed land use catchment in Galicia (NW Spain) : Significance of runoff events. Journal of Hydrology 481 : 12-21. DOI : 10.1016/j.jhydrol.2012.11.046.

Rossi L, Krejci V, Rauch W, Kreikenbaum S, Fankhauser R, Gujer W. 2005. Stochastic modeling of total suspended solids (TSS) in urban areas during rain events. Water Research 39(17) : 4188-4196. DOI : 10.1016/j.watres.2005.07.041.

Scalenghe R, Edwards AC, Barberis E, Ajmone-Marsan F. 2012. Are agricultural soils under a continental temperate climate susceptible to episodic reducing conditions and

increased leaching of phosphorus ? Journal of Environmental Management 97 : 141-147. DOI : 10.1016/j.jenvman.2011.11.015.

Schindler DW, Hecky RE, Findlay DL, Stainton MP, Parker BT, Paterson MJ, Beaty KG, Lyng M, Kasian SEM. 2008. Eutrophication of lakes cannot be controlled by reducing nitrogen input : Results of a 37-year whole-ecosystem experiment. Proceedings of the National Academy of Sciences of the United States of America 105(32) : 11254-11258. DOI : 10.1073/pnas.0805108105.

Schoumans OF, Chardon WJ, Bechmann ME, Gascuel-Odoux C, Hofman G, Kronvang B, Rubaek GH, Ulen B, Dorioz JM. 2014. Mitigation options to reduce phosphorus losses from the agricultural sector and improve surface water quality : A review. Science of the Total Environment 468 : 1255-1266. DOI : 10.1016/j.scitotenv.2013.08.061. Seeger M, Errea MP, Begueria S, Arnaez J, Marti C, Garcia-Ruiz JM. 2004. Catchment soil moisture and rainfall characteristics as determinant factors for discharge/suspended sediment hysteretic loops in a small headwater catchment in the Spanish pyrenees. Journal of Hydrology 288(3-4) : 299-311. DOI : 10.1016/j.jhydrol.2003.10.012.

Sharpley AN, Kleinman PJ, Heathwaite PJ, Gburek WJ, Folmar GJ, Schmidt JP. 2008. Phosphorus loss from an agricultural watershed as a function of storm size. Journal of Environmental Quality 37(2) : 362-8. DOI : 10.2134/jeq2007.0366.

Shore M, Jordan P, Mellander P-E, Kelly-Quinn M, Wall DP, Murphy PNC, Melland AR. 2014. Evaluating the critical source area concept of phosphorus loss from soils to water-bodies in agricultural catchments. Science of the Total Environment 490 :405–415. DOI : 10.1016/j.scitotenv.2014.04.122

Simard RR, Beauchemin S, Haygarth PM. 2000. Potential for preferential pathways of phosphorus transport. Journal of Environmental Quality 29(1) : 97-105. Siwek J, Siwek JP, Zelazny M. 2013. Environmental and land use factors affecting phosphate hysteresis patterns of stream water during flood events (Carpathian Foothills, Poland). Hydrological Processes 27(25) : 3674-3684. DOI : 10.1002/hyp.9484.

Smith VH, Schindler DW. 2009. Eutrophication science : where do we go from here ? Trends in Ecology Evolution 24(4) : 201-207. DOI : 10.1016/j.tree.2008.11.009.

Stutter MI, Langan SJ, Cooper RJ. 2008. Spatial contributions of diffuse inputs and within-channel processes to the form of stream water phosphorus over storm events. Journal of Hydrology 350(3-4) : 203-214. DOI : 10.1016/j.jhydrol.2007.10.045.

Stutter MI, Langan SJ, Lumsdon DG. 2009. Vegetated Buffer Strips Can Lead to Increased Release of Phosphorus to Waters : A Biogeochemical Assessment of the Mechanisms. Environmental Science Technology 43(6) : 1858-1863. DOI : 10.1021/es8030193.

Turner BL, Driessen JP, Haygarth PM, McKelvie ID. 2003. Potential contribution of lysed bacterial cells to phosphorus solubilisation in two rewetted Australian pasture soils. Soil Biology Biochemistry 35(1) : 187-189. DOI : 10.1016/s0038-0717(02)00244-4.

Turner BL, Haygarth PM. 2001. Biogeochemistry - Phosphorus solubilization in rewetted soils. Nature 411(6835) : 258-258. DOI : 10.1038/35077146.

van der Salm C, Dupas R, Grant R, Heckrath G, Iversen BV, Kronvang B, Levi C, Ribaek GH, Schoumans OF. 2011. Predicting Phosphorus Losses with the PLEASE Model on a Local Scale in Denmark and the Netherlands. Journal of Environmental Quality 40(5) : 1617-1626. DOI : 10.2134/jeq2010.0548.

Van Drecht G, Bouwman AF, Harrison J, Knoop JM. 2009. Global nitrogen and phos-

phate in urban wastewater for the period 1970 to 2050. Global Biogeochemical Cycles 23. DOI : 10.1029/2009gb003458.

Vongvixay A, Grimaldi C, Gascuel-Odoux C, Laguinie P, Faucheux M, Gilliet N, Mayet M. 2010. Analysis of suspended sediment concentration and discharge relations to identify particle origins in small agricultural watersheds. In : Banasik, K., Horowitz, A.J., Owens, P.N., Stone, M., Walling, D.E. (Eds.), Sediment Dynamics for a Changing Future. IAHS Publication pp. 76-83.

Williams GP. 1989. Sediment concentration versus water discharge during single hydrologic events in rivers. Journal of Hydrology 111 :89–106. DOI : 10.1016/0022-1694(89)90254-0.

3.1.6 Supplementary materials

Figure 3.10 to 3.12 provide supplementary information about the monthly distribution of climate and hydrological variables, together with their inter-annual variability.

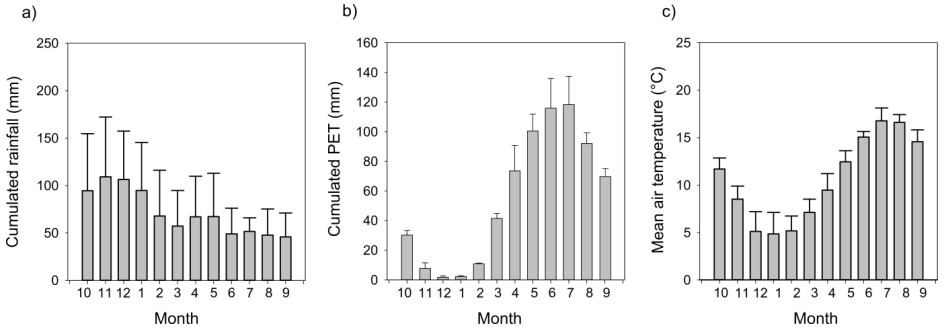

FIGURE 3.10 – Annual distribution (2007-2013) of monthly cumulated rainfall (a), cumulated Penman Potential Evapotranspiration (b) and mean air temperature (c). Error bars represent standard deviation.

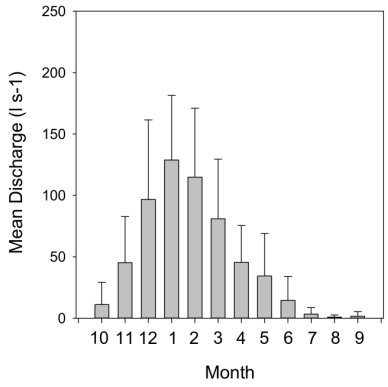

FIGURE 3.11 – Annual distribution (2007-2013) of mean monthly discharge. Error bars represent standard deviation.

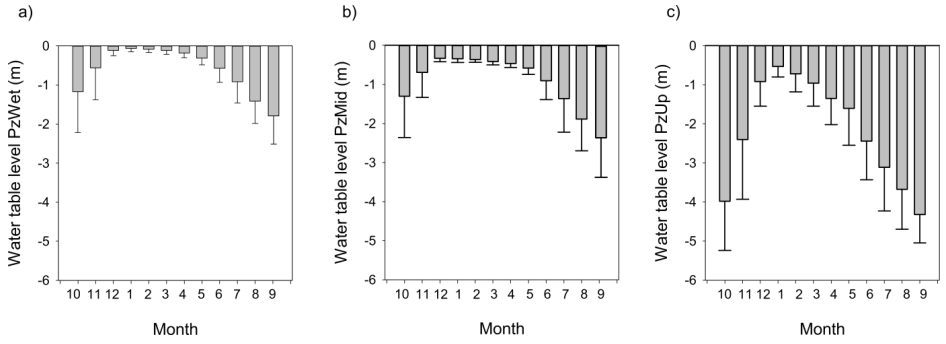

FIGURE 3.12 – Annual distribution (2007-2013) of mean monthly water table level in the wetland (a), midslope (b) and upslope (c) domains. Error bars represent standard deviation.

Figure 3.13 shows the result of a test to check whether SRP concentration was stable when storing filtrates at 4 ° C during 4h, 26h, 1 week, 2 weeks and 3 weeks. Although there seems to be a decrease in measured concentration after 2 weeks, we considered that it was acceptable given the precision of analyses. 2 weeks was the upper limit of filtrates time of storage for this study.

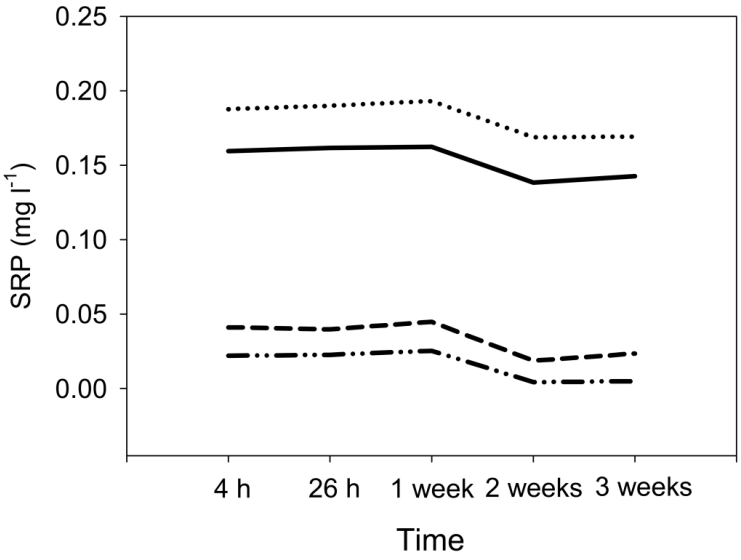

FIGURE 3.13 – Evolution of SRP concentration after keeping filtered water samples ($<$ 0.45 μm) at 4 $^\circ$ C.

3.2 Lien avec les dynamiques de l'azote et du carbone organique dissous

Les figures 3.14 et 3.15 représentent respectivement les dynamiques saisonnières et en crue pour le nitrate (NO_3^-), le carbone organique dissous (DOC) et le phosphore dissous (SRP), pour une année moyenne. La manière de représenter les séries temporelles annuelles est inspirée de Aubert *et al.* (2013). On remarque, comment mentionné dans ce chapitre, que la dynamique du SRP est très proche de celle du DOC, mais opposée à celle du NO_3^-. Pour le SRP comme pour le DOC, les périodes de plus hautes concentrations correspondent à des périodes de forte contribution des zones ripariennes par rapport à la nappe de haut de versant (automne et printemps). A l'inverse, la période de plus hautes concentrations pour le NO_3^- est l'hiver, lorsque la nappe de haut de versnt contribue le plus à l'écoulement. A l'exception des crues d'automne, pour lesquelles on observe un flush à la fois de NO_3^-, de DOC et de SRP, la dynamique en crue pour le SRP et le DOC est opposée à celle du NO_3^- (concentration *versus* dilution).

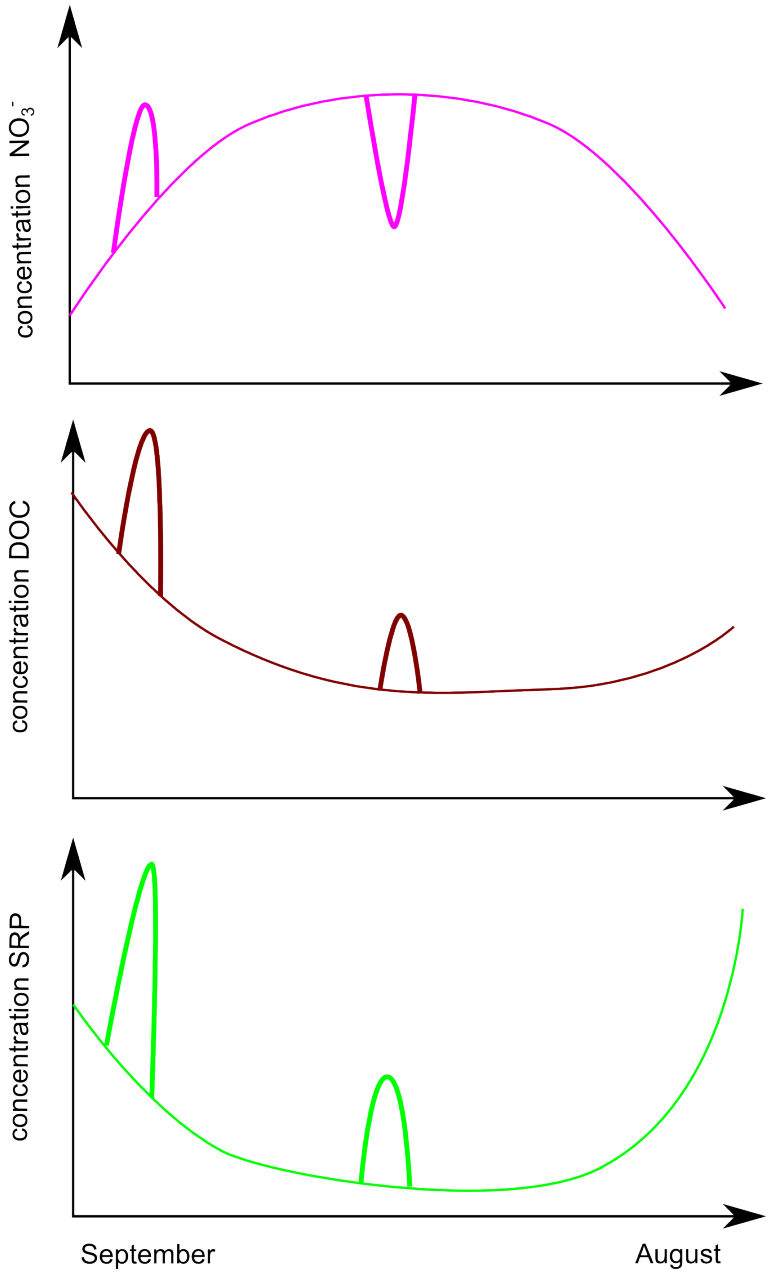

FIGURE 3.14 – Seasonal dynamics of Soluble Reactive Phosphorus (SRP), Dissolved Organic Carbon (DOC) and nitrate (NO_3^-).

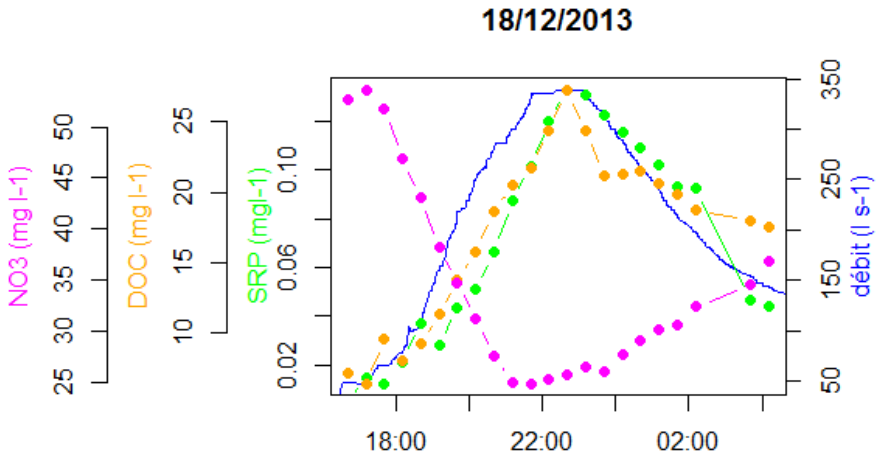

FIGURE 3.15 – Storm dynamics of Soluble Reactive Phosphorus (SRP), Dissolved Organic Carbon (DOC) and nitrate (NO_3^-).

3.3 Conclusion du chapitre

Si des dynamiques d'exportation différentes pour le phosphore particulaire (PP) et dissous (SRP) avaient été mises en évidence par plusieurs études dans des bassins versants herbagers, ce chapitre a montré que cette non-synchronisation a aussi lieu dans un bassin versant à dominance de terres arables. Nos résultats contrastent avec la vision traditionnelle des transferts de P dans les paysages à dominance de terres arables, selon laquelle le P serait majoritairement transféré sous forme particulaire pendant les crues, et que le phosphore dissous proviendrait de la solubilisation du PP atteignant le cours d'eau. La question de la synchronisation/non-synchronisation des transferts du PP et du SRP a aussi été abordée sous l'angle d'une analyse fréquentielle dans cette thèse. Cependant, la méthode d'analyse spectrale mise en œuvre, grâce à un séjour de deux jours à l'ETH Zürich avec James Kirchner, n'a pas abouti à des résultats exploitables du fait de la trop faible fréquence des données et d'un bruit de mesure trop important.

Les zones riparienes semblent jouer un rôle déterminant dans les mécanismes à l'origine du transfert de PP et SRP, à deux titres. Premièrement, elles sont occupées par des bandes enherbées qui limitent les transferts directs de P particulaire et dissous mobilisé dans les versants. Seuls certains orages printaniers de forte intensité, à une période de l'année où l'état structural du sol est dégradé et où ont lieu les épandages, posent un risque de transfert des parcelles cultivées au cours d'eau. Deuxièmement, les zones riparienes sont des zones de fluctuations de nappe, ce qui crée une connexion hydrologique entre sol et cours d'eau lors des crues. Il semble qu'un pool de P mobile soit présent dans les zones riparienes à l'automne, puis que ce pool soit exporté par transfert de sub-surface au cours de l'hiver jusqu'à son épuisement progressif.

Ce chapitre pose la question de la généralisation des mécanismes mis en évidence à d'autres types de bassins versants. Il pose aussi la question des méthodes adaptées pour analyser des séries temporelles de crue quand la quantité de données est élevée. Le chapitre 4 propose donc d'appliquer une méthode de clustering originale aux données de crue de Kervidy-Naizin, mais aussi du bassin versant herbager du Moulinet, afin d'identifier la distribution saisonnières de motifs et d'en produire une interprétation dans ces deux bassins contrastés. Pour confirmer les hypothèses formulées dans ce chapitre, issues d'une analyse statistique de données de qualité d'eau à l'exutoire du bassin versant, il est nécessaire de changer d'échelle d'observation pour étudier les mécanismes au sein des zones humides. C'est ce que propose le chapitre 5 où, en suivant la concentration dans la solution du sol dans les zones humides pendant une année hydrologique, nous avons cherché à répondre aux questions suivantes : y a-t-il effectivement présence d'un pool de phosphore mobile dans les sols à l'automne ? Y a-t-il transmission du signal entre la mobilisation dans les zones humides et la concentration dans le cours d'eau ? Les fluctuations de nappe contrôlent-elles uniquement le transfert de P ou agissent-elles aussi sur les mécanismes biogéochimiques à l'origine de la solubilisation du P ?

Chapitre 4

Identification de motifs saisonniers de crue

Ce chapitre s'appuie sur un article publié dans Water Resources Research.

Dupas R, Tavenard R, Fovet O, Gilliet N, Grimaldi C, Gascuel-Odoux C. Identifying seasonal patterns of phosphorus storm dynamics with Dynamic Time Warping. Water Resour. Res. 2015 ; 51

Il repose sur une méthode originale d'analyse des crues, développée grâce à une collaboration avec Romain Tavenard (IRISA, Université de Rennes 2), et appliquée sur les bassins de Kervidy-Naizin et du Moulinet.

Ce chapitre apporte des éléments de réponse à la question 1, rappelée ici :

Question 1 : Les mécanismes à l'origine du transfert des formes dissoutes et particulaires du phosphore sont-ils communs ou distincts ? Y a-t-il une saisonnalité dans le couplage/découplage des transferts de phosphore dissous et particulaire ? Dans quelle mesure la variabilité du signal peut-elle être reliée aux pratiques agricoles ou à des processus hydrologiques et biogéochimiques ?

4.1 Identifying seasonal patterns of phosphorus storm dynamics with Dynamic Time Warping

Résumé

Le transfert de phosphore (P) en crue représente une part importante du flux annuel dans les cours d'eau, et contribue à l'eutrophisation des masses d'eau aval. Pour améliorer les connaissances sur la dynamique du P en crue, il est nécessaire de mettre au point des méthodes d'analyse automatiques ou semi-automatiques afin d'extraire de l'information à partir de bases de données de plus en plus grandes. Dans ce chapitre, des motifs saisonniers de dynamique du phosphore en crue sont identifiés dans deux bassins versants contrastés (arable et herbager) grâce à Dynamic Time Warping (DTW) combiné à la méthode de clustering k-means. DTW est utilisé pour réaligner des séries temporelles de débit (hydrogramme) quand ces dernières ont des longueurs différentes ou des différences de phase. La même déformation temporelle est appliquée sur les séries temporelles P, et un algorithme k-means est appliqué sur ces dernières. Dans le bassin versant à dominance de terres arables, le motif de crue le plus fréquent en automne et en hiver montre des dynamique d'exportation différentes pour le P particulaire et le P dissous, ce qui suggère des mécanismes de transfert indépendants. A l'inverse, le motif de crue le plus fréquent au printemps montre une synchronisation du P particulaire et du P dissous. Dans le bassin versant herbager, l'occurrence des crues avec synchronisation de l'export de P particulaire et dissous ne présente pas de saisonnalité, mais est plutôt lié à l'amplitude de la crue. Les différences de distribution saisonnière entre les motifs de crue identifiés dans les deux bassins versants sont interprétées en termes de sources et de voies de transfert. L'algorithme de clustering après transformation DTW s'est avéré utile pour identifier les motifs les plus fréquents mais aussi pour isoler des motifs rares. Cette méthode ouvre de nouvelles possibilités pour l'interprétation des données hautes-fréquence et multi-paramètres qui sont actuellement acquises dans le monde entier.

Abstract

Phosphorus (P) transfer during storm events represents a significant part of annual P loads in streams and contributes to eutrophication in downstream water bodies. To improve understanding of P storm dynamics, automated or semi-automated methods are needed to extract meaningful information from ever-growing water quality measurement datasets. In this paper, seasonal patterns of P storm dynamics are identified in two contrasting watersheds (arable and grassland) through Dynamic Time Warping (DTW) combined with k-means clustering. DTW was used to align discharge time series of different lengths and with differences in phase, which allowed robust application of a k-means clustering algorithm on rescaled P time series. In the arable watershed, the main storm pattern identified from autumn to winter displayed distinct export dynamics for particulate and dissolved P, which suggests independent transport mechanisms for both P forms. Conversely, the main storm pattern identified in spring displayed synchronized export of particulate and dissolved P. In the grassland watershed, the occurrence of synchronized export of dissolved and particulate P forms was not related to the season, but rather to the amplitude of storm events. Differences between the seasonal distributions of the patterns identified for

the two watersheds were interpreted in terms of P sources and transport pathways. The DTW-based clustering algorithm used in this study proved useful for identifying common patterns in water quality time series and for isolating unusual events. It will open new possibilities for interpreting the high-frequency and multi-parameter water quality time series that are currently acquired worldwide.

4.1.1 Introduction

Storm-induced changes in stream flow and chemistry have been a major research topic in hydrology for years. The concentration of certain elements, such as phosphorus (P), can increase by one to several orders of magnitude during storms (Heathwaite and Dils, 2000 ; Sharpley *et al.*, 2008). Combined with the increase in discharge (Q), P export rates during storm events surpass those in baseflow conditions ; so, storm events can represent a large part of the annual P load in rural watersheds (Gburek and Sharpley, 1998 ; Pionke *et al.*, 1999 ; Melland *et al.*, 2012 ; Rodriguez-Blanco *et al.*, 2013a, 2013b). Another reason that scientists focus on storm events is that dynamics of P concentrations during storms can be analyzed to infer spatial origins of sources and dominant transport pathways. Early concentration peaks, relative to the discharge peak, indicate mobilization of a P source located within or close to the stream channel (supply limitation), whereas late concentration peaks are often interpreted as resulting from mobilization of a P source on hillslopes (transport limitation) (Haygarth *et al.*, 2005 ; Stutter *et al.*, 2008 ; Dupas *et al.*, 2015a ; Perks *et al.*, 2015). Discharge-concentration hysteresis plots are often used to better visualize time lags between discharge and concentration peaks during storm events (Williams, 1989 ; Bowes *et al.*, 2005, 2015 ; Cerro *et al.*, 2014 ; Outram *et al.*, 2014 ; Bieroza and Heathwaite, 2015 ; Ramos *et al.*, 2015 ;).

To refine load estimations and infer transport mechanisms, researchers have developed methods to interpret water quality time series during storm events. When few storm events are studied at a time, end-member mixing analysis (Soulsby *et al.*, 2003 ; Jarvie *et al.*, 2011 ; Delsman *et al.*, 2013 ; Lambert *et al.*, 2014 ;) and loadograph recession analysis (Mellander *et al.*, 2012, 2013, 2015) are useful techniques to trace the origin of one or several elements of interest. When a large number of monitored storm events is available and several water quality parameters are measured, statistical descriptor variables and clustering techniques can be valuable for interpreting the data (e.g. perform seasonal and interannual analyses, compare watersheds). The "hysteresis index" (Lawler *et al.*, 2006), the "pollutogram factor" (Rossi *et al.*, 2005 ; Stutter *et al.*, 2008) and the semiquantitative index of Butturini *et al.* (2008) are three examples of descriptor variables used to quantify the magnitude and direction of hysteresis loops in discharge-concentration plots. Such descriptor variables can be used to cluster storm events, or alternatively, time series can be direct input into clustering algorithms (Aubert *et al.*, 2013a). Clustering algorithms create groups, called clusters, with minimum within-cluster variance and maximum between-cluster variance. Existing clustering techniques include k-means, hierarchical clustering, interval clustering and self-organizing maps (Astel *et al.*, 2007 ; Fytilis and Rizzo, 2013 ; Toth, 2013 ; Wong and Hu, 2013). The need for such automated data analysis methods is increasing along with the worldwide development of high-frequency and multi-parameter water quality measurement instruments (Jordan *et al.*, 2007 ; Rozemeijer *et al.*, 2010 ; Wade *et al.*, 2012 ; Bowes *et al.*,

2015). Clustering techniques have proven useful for identifying seasonal storm patterns and thus for increasing knowledge about seasonal variability in storm export mechanisms (e.g. Aubert *et al.* (2013a), Bende-Michl *et al.* (2013)).

Clustering techniques usually require calculating a distance between pairs of comparable points in several time series. For this reason, direct clustering (without using hysteresis-descriptor variables) of high frequency storm concentration time series is usually irrelevant because their length (number of measurement points) may differ and/or measurement points may have different positions relative to the hydrograph (flow rise and recession) ; hence, it is difficult to calculate a distance between pairs of comparable points. While existing hysteresis-descriptors have proven useful in describing the variation in concentrations relative to the variation in discharge, they cannot describe complex patterns such as storm events with two concentration peaks (Rodriguez-Blanco *et al.*, 2013a). The aim of this study was to develop a clustering method that overcomes these two limits and test its ability to compare seasonal variability of P storm dynamics in two headwater watersheds. Both watersheds are ca. 5 km^2, have similar climate and geology, but differ in land use and P pressure intensity. The clustering method used relies on Dynamic Time Warping (DTW), an algorithm that aligns time series that may have different lengths and/or local distortions (Sakoe and Chiba, 1978). The intended benefit of using DTW was to enable comparison of storm event time series with differences in the position of the discharge peak and/or differences in durations/slopes of the rising and recession limbs of hydrographs. DTW is used here in combination with the classic Euclidian distance in a k-means clustering framework. This study is part of a wider investigation into P transport mechanisms in agricultural watersheds in western France.

4.1.2 Materials and Methods

Study sites

The two study watersheds, Kervidy-Naizin and Moulinet, are located in agricultural areas in western France (respectively 48 ° N, 3 ° W and 48 ° N, 1 ° W, Figure 4.1). The Kervidy-Naizin watershed belongs to the AgrHyS environmental research observatory (http ://www6.inra.fr/ore _agrhys_eng), which studies the impact of agriculture and climate change on water quality (Molenat *et al.*, 2008 ; Salmon-Monviola *et al.*, 2013 ; Aubert *et al.*, 2013b ; Lambert *et al.*, 2014). The Moulinet watershed belongs to the PFC environmental research observatory (https ://www6.inra.fr /ore-pfc), which studies both sediment and solute transfers and their impacts on aquatic ecosystems (Lefrancois *et al.*, 2007 ; Vongvixay *et al.*, 2010 ; Gascuel-Odoux *et al.*, 2011). The two watersheds share most of their physical characteristics, as described elsewhere (e.g. Dupas *et al.* (2015a) for Kervidy-Naizin and Lefrancois *et al.* (2007) for Moulinet). Briefly, both are second Strahler order watersheds, are ca. 5 km^2 in size, with a temperate oceanic climate. During the study period (2007 – 2014), means ± standard deviations of annual rainfall, temperature and discharge in Kervidy-Naizin were 924±178 mm, 10.8±0.6 ° C and 344±168 mm, respectively, while those in Moulinet were 862±131 mm, 11.2±0.5 ° C and 352±91 mm, respectively. The stream in Kervidy-Naizin is usually dry from August to October every year, while that in Moulinet flows all year. The topography in both watersheds is gentle, with slopes not exceeding 5%. Bedrock consists of impervious Brioverian schists capped by several me-

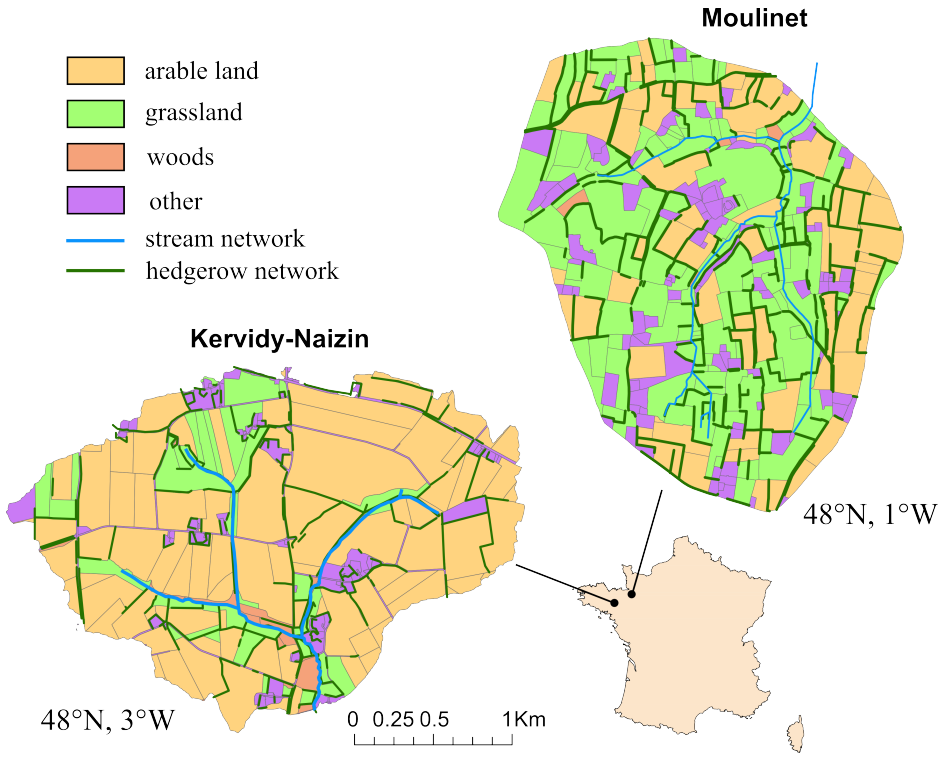

FIGURE 4.1 – Land use in the Kervidy-Naizin (2013 survey) and Moulinet watersheds (2008 survey).

ters of unconsolidated weathered material and loamy soils. Soils are naturally well-drained in the upland domain but hydromorphic in riparian wetlands, since the water table reaches the soil surface ca. 6 months per year (Molenat at al., 2008). Artificial drainage represents <10% of the surface area in both watersheds but is generally ineffective at lowering the water table in the wetland area because the drains are in disrepair.

Kervidy-Naizin and Moulinet differ in land use, landscape structures and P pressure intensity (P surplus and soil P content). Agricultural activities in the Kervidy-Naizin watershed are dominated by intensive indoor animal production (dairy and pig farming). Agricultural land use consists of 85% arable crops (mainly cereals and maize) and 15% grassland. Hedgerow density is low (46 m ha^{-1}), but the stream network is protected by a row of trees and there is no presence of cattle near the stream network (Benhamou *et al.*, 2013). Estimated soil P surplus was 13.1 kg P ha^{-1} yr^{-1} (Dupas *et al.*, 2015b), and soil extractable P (Olsen method, ISO 11263) in 2013 was 62±28 mg P kg^{-1} (n = 86 samples).

Agriculture in Moulinet is dominated by moderately intensive dairy production. Agricultural land use consists of 40% arable crops (mainly cereals and maize) and 60% grassland. Hedgerow density is relatively high (76 m ha^{-1}), which is characteristic of a "bocage" landscape. However, stream banks are degraded by cattle trampling, and the tree row along the stream network is discontinuous (Lefrancois *et al.*, 2007 ; Gascuel-Odoux *et al.*, 2011). Estimated soil P surplus was 8.1 kg P ha^{-1} yr^{-1}, and soil extractable P in 2008 was 37±7 mg

P kg^{-1} (n = 6). Although the amount of soil data in the Moulinet watershed was lower than that of Kervidy-Naizin, the difference in soil P content between the two areas is confirmed by the national P map of French topsoils (Delmas *et al.*, 2015).

In both watersheds, manure and slurry spreading is prohibited from July to January (or March for maize).

Stream monitoring

Stream discharge was determined at the outlet of each watershed with an automatic gauging station, every minute in Kervidy-Naizin and every 10 minutes in Moulinet. To obtain consistent 10-minute frequencies, the one-minute measurements in Kervidy-Naizin were sub-sampled every 10 minutes.

To record both long-term and within-storm dynamics of P concentrations, two monitoring strategies complemented each other from 2007 to 2014 : regular sampling every 6 days (manual in Kervidy-Naizin ; automatic in Moulinet) at approximately the same time (17 :00 local time), and high-frequency sampling during storm events with autosamplers (ISCO 6712 Full-Size Portable Sampler). The autosamplers were placed in the shade at the outlet and collected samples when the stream level reached a threshold (adjusted depending on baseflow discharge level), at a frequency of one sample every 30 minutes for 12 hours. In total, 54 storm events were remotely monitored in Kervidy-Naizin (Figure 4.2) and 58 in Moulinet (Figure 4.3), with 7 – 24 samples analyzed per storm. Only storm samples with good coverage of the event and with only one discharge peak (based on visual verification of discharge and turbidity data) were sent, within one week, for analysis. For each sample collected, one aliquot was filtered directly on-site for soluble reactive P (SRP) analysis (0.45 μm cellulose acetate filter) and another aliquot remained unfiltered for total P (TP) analysis. SRP was determined colorimetrically by reaction with ammonium molybdate. Precision of SRP measurement was ± 4 $\mu g\ l^{-1}$. TP was determined with the same method, after digestion of the unfiltered samples with potassium peroxydisulfate. Particulate phosphorus (PP) was approximated by subtracting SRP from TP, because analyses have shown that 80% of total dissolved P consisted of SRP (Dupas *et al.*, 2015a).

Clustering method

We used a two-step approach to perform storm clustering. The first step consisted of realigning all storm time series so that their discharges temporally matched. Temporal realignment overcame three difficulties that may arise when comparing storm-event data : time series may have i) different starting times due to the discharge threshold at which the autosamplers were triggered, since it was regularly re-adjusted according to baseflow discharge level, ii) different lengths due to analysis of 7-24 samples, and iii) differences in phase that yield different positions of the discharge peak and of concentration data points relative to the hydrograph. To align time series, we used the DTW algorithm. DTW was originally developed for speech recognition (Sakoe and Chiba, 1978) to measure the similarity between pairs of time series. Given two time series, $S = S_1, \ldots, S_i, \ldots, S_{N_S}$ and $R = R_1, \ldots, R_j, \ldots, R_{N_R}$, DTW finds an optimal alignment that allows for both global phase correction and local distortions (stretched and compressed sections). To do so, all local (squared) distances between pairs of points in the time series are stored in a matrix,

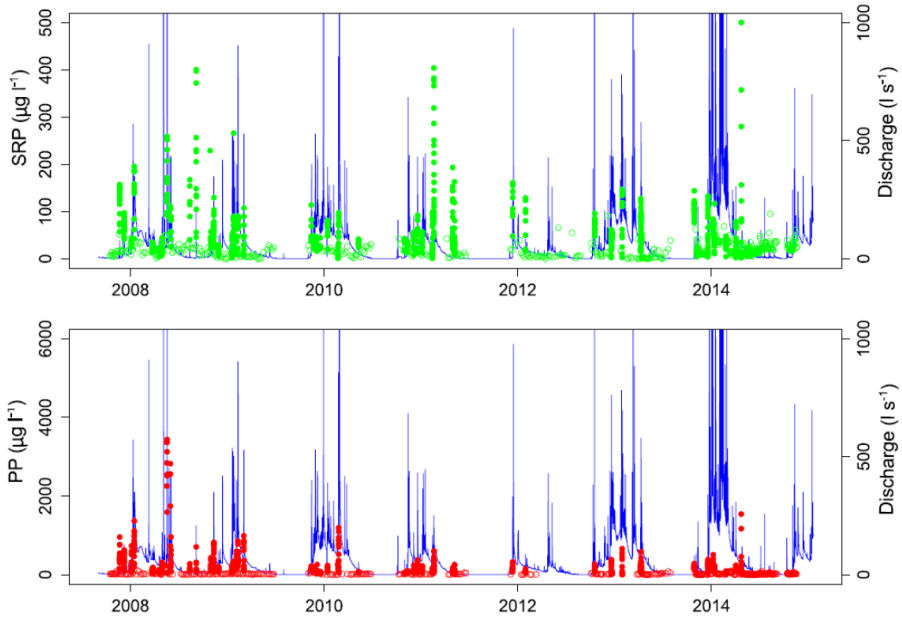

FIGURE 4.2 – Discharge and phosphorus time series in the Kervidy-Naizin watershed (SRP : Soluble Reactive Phosphorus ; PP : Particulate Phosphorus). Time resolution for discharge is 10 minutes. Open circles represent baseflow samples (every 6 days), and filled circles represent storm events monitored at high frequency (every 30 minutes).

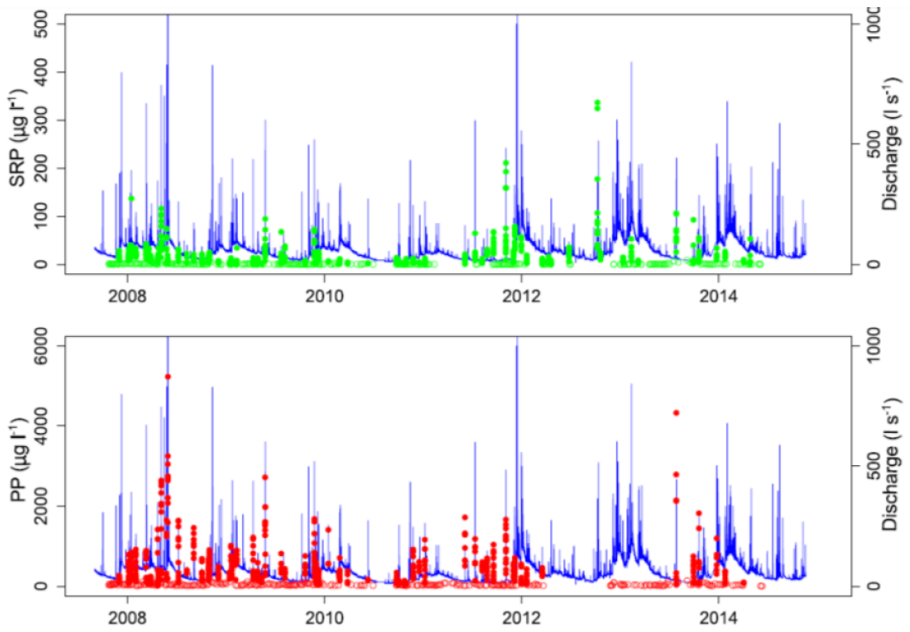

FIGURE 4.3 – Discharge and phosphorus time series in the Moulinet watershed (SRP : Soluble Reactive Phosphorus ; PP : Particulate Phosphorus). Time resolution for discharge is 10 minutes. Open circles represent baseflow samples (every 6 days), and filled circles represent storm events monitored at high frequency (every 30 minutes).

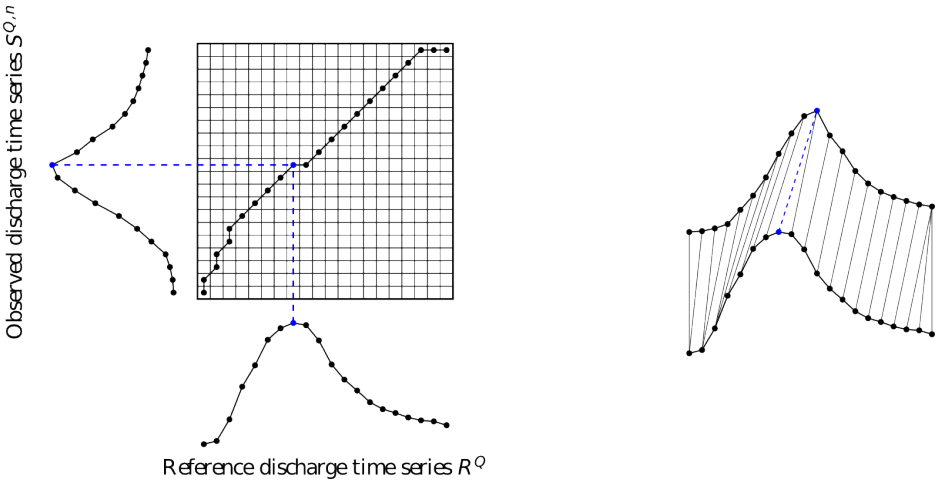

FIGURE 4.4 – Time series alignment with Dynamic Time Warping : optimal path and corresponding point-wise alignment. Discharge time series are subsampled for the sake of clarity in the figure.

and the DTW algorithm finds the matrix path W^*, called "matching path", that minimizes the cumulative squared distance (Figure 4.4, left) :

$W^*(S,R) = \underset{W \in P}{\operatorname{argmin}} \sum_{(i,j)\in W} d(S_i, R_j)^2$

The set P of admissible paths is restricted to those fulfilling the following conditions :

- boundary conditions (the first and last elements of time series S and R have to be matched together) ;
- monotonicity condition (temporal ordering in time series must be respected) ;
- continuity condition (each element in one of the two time series must be matched to at least one element in the other time series).

This matching path can be viewed as the optimal way to perform point-wise alignment of time series (Figure 4.4, right).

We used the matching path obtained to align each discharge time series $S^{Q,n}$ to the same reference discharge time series R^Q. The reference discharge time series used in this study (Figure 4.4) was chosen in the database as a storm event with full coverage of flow rise and flow recession phases. Alternatively, one could choose a synthetic idealized storm hydrograph. As stated above, the continuity condition imposed on admissible paths results in each element of reference time series R^Q being matched with at least one element in $S^{Q,n}$. Let us denote $f_{W_Q^*}$ the function that, given a time series $S^{Q,n}$, a matching path W_{Q^*} and a time index $j \in (1, N_R)$, returns the (non-empty) set of elements in $S^{Q,n}$ that were matched with R_{jQ} in W_{Q^*} :

$f_{W_{Q^*}}(S^{Q,n}, j) = \{S_i^{Q,n} \text{ such that } (i,j) \in W_{Q^*}\}$

In a regularization step, we temporally rescaled all the time series for the concentration parameters (here PP and SRP) for each storm using information from the DTW alignment

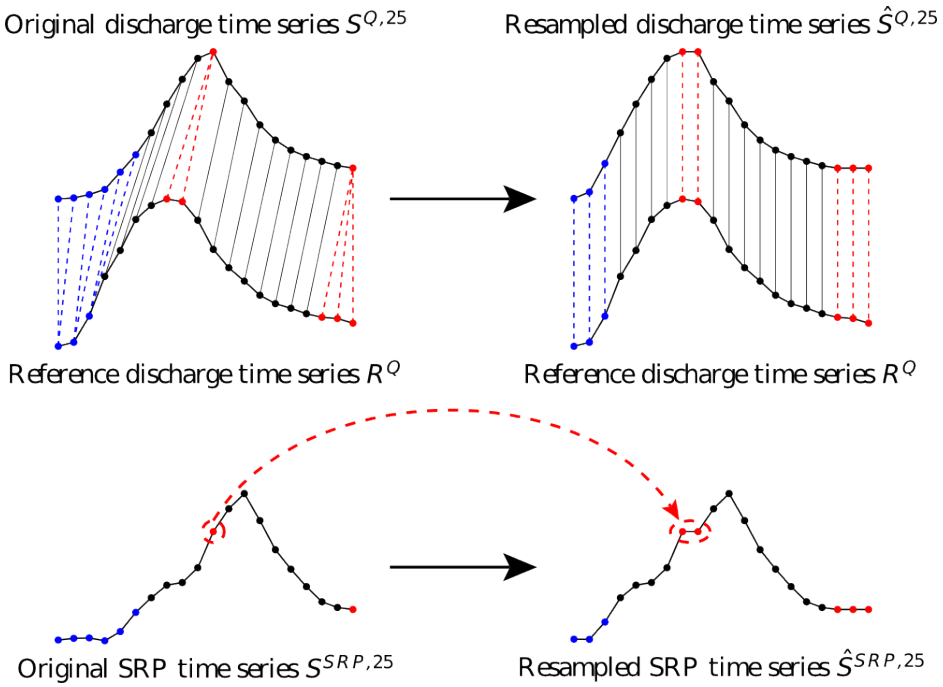

FIGURE 4.5 – Regularization step : Resampling of water quality time series based on the Dynamic Time Warping alignment path (example of soluble reactive phosphorus (SRP) during storm 25).

computed from discharge information (Figure 4.5). Given a time series $S^{p,n}$ for parameter p, we generated a regularized time series $\hat{S}^{p,n}$ of length N_R such that :

$\forall j \in (1, N_R), \hat{S}^{p,n}_j = average(f_{W_{Q^*}}(S^{p,n}, j))$

Note that in this formula, the matching path W_{Q^*} was computed from discharge information. In practice, this means that concentration parameters extracted, for example, at the time of maximum discharge that are matched to the reference discharge maximum (Figure 4.4, blue dot) are time-aligned for all storms in the dataset.

At this point, each time series was represented as a vector $\hat{S}^n$ of length $N_p * N_R$, where N_p is the number of water quality parameters considered in the study (all parameters were used together in the clustering process).

In the second step, a standard k-means algorithm was used to cluster rescaled time series. The k-means clustering algorithm aims to minimize intra-cluster variance V :

$V = \sum_{i=1}^{k} \sum_{\hat{S}^n \in C^i} \left|\left| \hat{S}^n - \mu^i \right|\right|^2$

where C^i is the i-th cluster of mean μ^i. Note that a Euclidean distance was used for clustering since time series had already been rescaled during the regularization step ; hence, no time-sensitive metric (such as DTW) was needed at this point. A single program written in the Python language performed the two successive steps : DTW alignment and k-means clustering.

Data preparation and program runs

In this study, parameters of interest were PP and SRP, because we were interested in the synchronization/desynchronization of their dynamics with each other and with the dynamics of discharge. Turbidity and suspended matter concentration data are available for both watersheds but were not included in the clustering because they are highly correlated with PP (Dupas *et al.*, 2015a), and we wanted to give equal weights to particulate and dissolved P forms. We focused analysis on storm events with a SRP concentration peak > 30 μg l^{-1} to ensure significant variation in concentration compared to baseflow conditions (18±18 μg l^{-1} in Kervidy-Naizin and 10±29 μg l^{-1} in Moulinet, Figure 4.2 and Figure 4.3, respectively). As a result, 48 out of 54 events were kept for analysis for Kervidy-Naizin and 20 out of 58 events for Moulinet. This pre-selection step biased the characteristics of storm events analyzed later by discarding many events, especially in the Moulinet watershed, where SRP concentrations were particularly low (Figure 4.3). This was necessary to ensure that variations in measured SRP concentrations during storm events were not due to measurement errors. Because we wanted to focus analysis on concentration dynamics rather than concentration values themselves, data were normalized between 0 and 1 for each event, with 0 = the antecedent concentration value measured in baseflow conditions and 1 = the highest recorded value during the storm event. Peak concentrations were analyzed separately. Because the data were normalized, it was crucial to eliminate storm events with insignificant variations in concentration, because measurement noise would be treated as actual concentration peaks. Two strategies for initializing the k-means clustering algorithm were tested, one using three randomly selected storm events, the other using three storms with meaningful patterns, identified in a previous study (Dupas *et al.*, 2015a) : i) synchronized SRP and PP peaks, ii) unsynchronized SRP and PP peaks and iii) "double SRP peak" storm events and single PP peak patterns. These patterns were considered to contain meaningful information because they can be interpreted in terms of P transport mechanisms. For both strategies, the number of clusters (k) was set to three. The success of each strategy was assessed based on its ability to identify clusters that resembled the three above-mentioned patterns. Storm events from both watersheds were clustered together to increase the number of time series in the clustering and to be able to compare the seasonal distribution of the same identified patterns in both watersheds. The clusters obtained were analyzed by season because a previous study with data from the Kervidy-Naizin (Dupas *et al.*, 2015a), which involved multivariate analysis of hydroclimatic variables, showed that storm characteristics depended greatly on the season.

Pattern identification

When initializing the clustering algorithm with three randomly selected storm events, the resulting clusters did not clearly identify the three patterns expected (Figure 4.6). For all three clusters, PP peaks during flow rise or at the time of maximum discharge and decreases quickly ; PP decreases more slowly during flow recession in cluster 2 than in clusters 1 and 3. For all three clusters, SRP increases more progressively than PP and remains high during flow recession ; SRP remains high longer in cluster 1 than in clusters 2 and 3.

Overall, initializing the clustering algorithm with random storm events revealed the

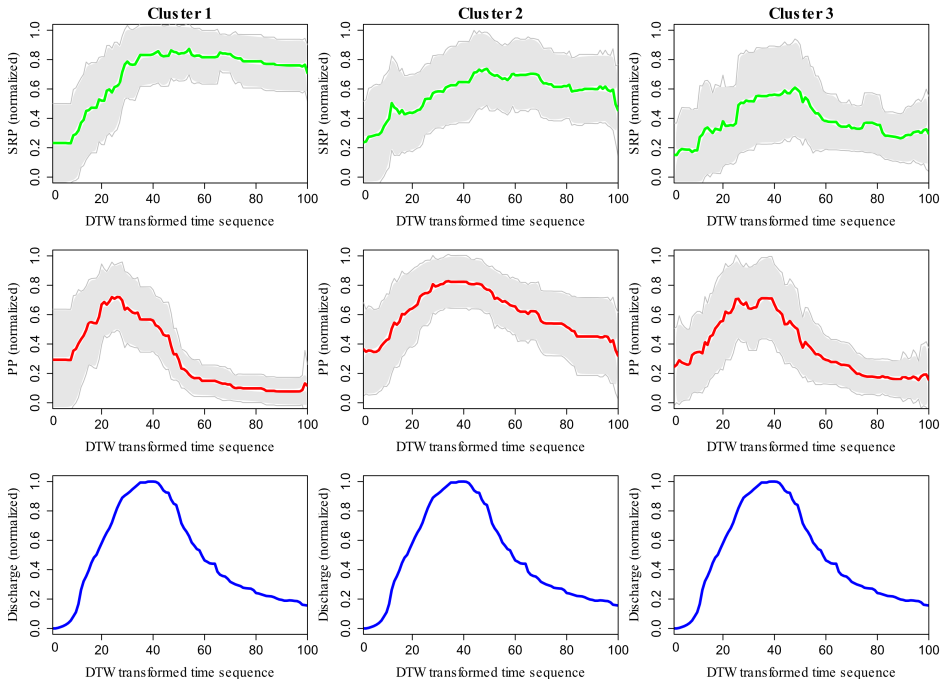

FIGURE 4.6 – Representation of the clusters obtained with Dynamic Time Warping (DTW) - k-means algorithm, random initialization. All data were normalized between 0 and 1. Time is represented as a DTW-transformed sequence of 100 points. Thick lines represent the mean of all the time series (Kervidy-Naizin and Moulinet) in a given cluster, and gray zones represent ± 1 standard deviation.

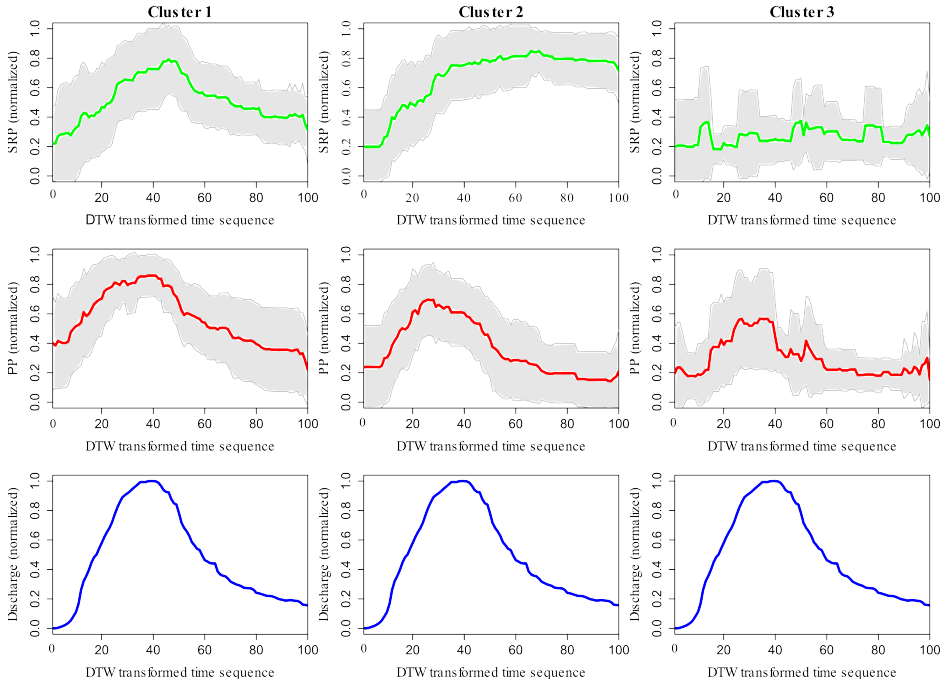

FIGURE 4.7 – Representation of the clusters obtained with Dynamic Time Warping (DTW) - k-means algorithm, initialization with three meaningful time series. All data were normalized between 0 and 1. Time is represented as a DTW-transformed sequence of 100 points. Thick lines represent the mean of all the time series (Kervidy-Naizin and Moulinet) in a given cluster, and gray zones represent ±1 standard deviation.

shape of the dominant storm pattern in each cluster, as identified in a previous study (i.e. clockwise hysteresis for PP and counterclockwise hysteresis for SRP, Dupas *et al.* (2015a)), with slight differences in the speed of PP and SRP rise and decrease between clusters. It did not identify other patterns of interest, such as storms with synchronized variations in PP and SRP or storms with a double peak of SRP.

When initializing the clustering algorithm with time series of three meaningful storm events, the three clusters identified corresponded to three very distinct storm patterns (Figure 4.7). For this reason, subsequent analyses focused on results from this second strategy.

Cluster 1 displays relatively synchronized variations in SRP, PP and discharge, i.e. no hysteresis pattern in a concentration-discharge plot. In the Kervidy-Naizin watershed, 14/48 storm events belong to cluster 1 (29%), whereas 16/20 events belong to this cluster in the Moulinet watershed (80%).

Cluster 2 displays unsynchronized variations in SRP, PP and discharge. PP has a sharp peak during flow rising (clockwise hysteresis) ; in contrast, SRP increases gradually and remains high during flow recession (counterclockwise hysteresis). In the Kervidy-Naizin watershed, 27/48 events belong to cluster 2 (56%), whereas 2/20 events belong to this cluster in the Moulinet watershed (10%). Cluster 3 does not display a clear pattern. It

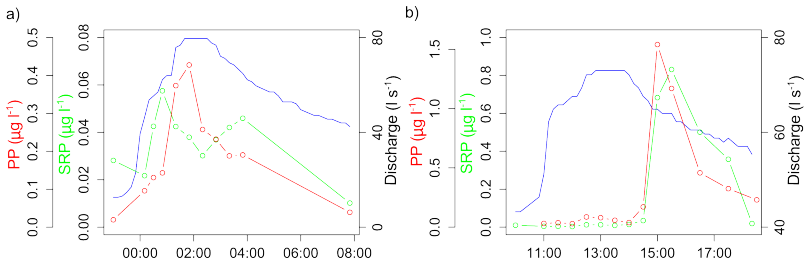

FIGURE 4.8 – Patterns of two storm events in cluster 3 for the Kervidy-Naizin watershed : a) double peak of soluble reactive phosphorus (SRP) (30 Oct 2008) and b) synchronized and delayed particulate phosphorus (PP) and SRP peaks (23 Apr 2014).

only comprised 7/48 events from the Kervidy-Naizin watershed (15%) and 2/20 events from the Moulinet watershed (10%), with a variety of shapes. Cluster 3 can be seen as a miscellaneous cluster with heterogeneous storm shapes. Among the storm events comprised in cluster 3, two present interesting pattern (Figure 4.8) : one with two SRP peaks and one with both PP and SRP peaks considerably delayed after the discharge peak.

Comparison of concentration values and seasonal distribution of patterns

In both watersheds, the storm events that were discarded because of SRP concentration peaks < 30 μg l^{-1} generally had low maximum discharges (Figure 4.9) and occurred throughout the year (Figure 4.10). In Kervidy-Naizin, maximum discharges for events in cluster 2 were significantly higher than those of events in other clusters ; in Moulinet, maximum discharges for events in cluster 1 were significantly higher than those of events in other clusters (Wilcoxon rank-sum test, $p < 0.05$). No significant difference in SRP or PP concentrations (Figure 4.9) or loads (result not shown) existed between clusters 1 and 2 in Kervidy-Naizin or Moulinet. SRP concentrations were higher in Kervidy-Naizin than in Moulinet, whereas the opposite occurred for PP (see also Figures 4.2 and 4.3)

Seasonal analysis revealed that each of the storm patterns identified after expert initialization had a different probability of occurrence depending on the quarter of the year, and that this seasonal distribution differed between Kervidy-Naizin and Moulinet (Figure 4.10). In Kervidy-Naizin, cluster 2, with unsynchronized export of PP and SRP, dominated from autumn to winter (September – February). Cluster 1, with synchronized export of PP and SRP, dominated in spring (March – May). Cluster 3, the heterogeneous cluster, was present all year, with the double SRP peak event occurring at the beginning of the hydrological year (October) and the events with synchronized and delayed PP and SRP peaks occurring in spring (April). In Moulinet, cluster 1 dominated all year, whereas cluster 2 occurred only in summer (June – August). Cluster 3 was present once in winter (September – November) and once in spring (March – May).

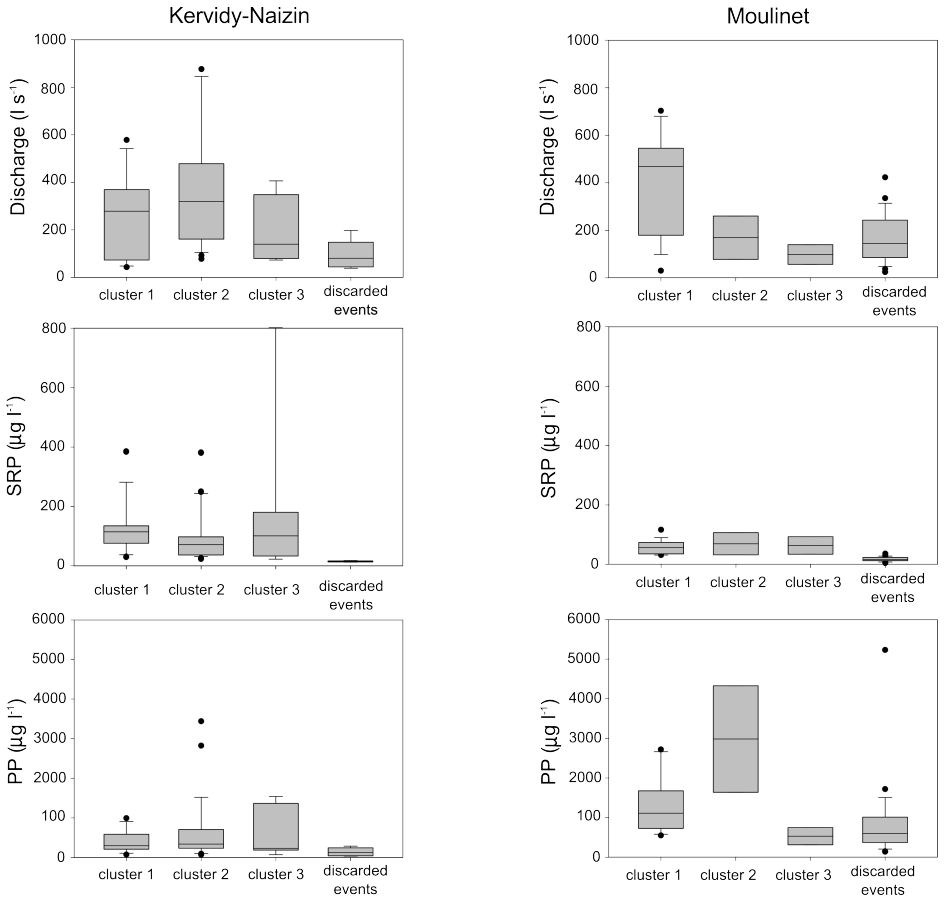

FIGURE 4.9 – Boxplots of peak discharge and maximum concentration of SRP (soluble reactive phosphorus) and PP (particulate phosphorus) of each cluster in each study watershed.

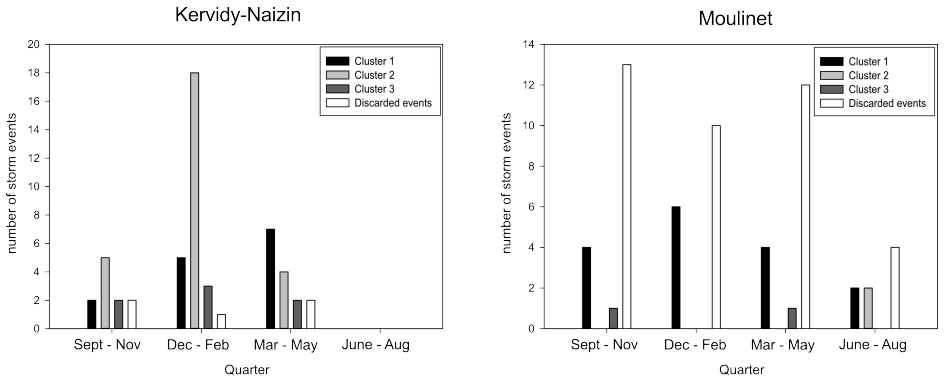

FIGURE 4.10 – Quarterly distribution of clusters in the Kervidy-Naizin and Moulinet watersheds.

4.1.3 Discussion

Hydrological interpretation

Synchronized export of PP and SRP is often interpreted as resulting from PP and SRP having the same spatial origin and following the same transport pathways. Conversely, distinct export dynamics between PP and SRP indicate independent transport mechanisms. Interpretation of time lags between concentration and discharge peaks can be used to infer transport mechanisms (Bowes *et al.*, 2005, 2015 ; Haygarth *et al.*, 2005 ; Stutter *et al.*, 2008 ; Outram *et al.*, 2014 ; Perks *et al.*, 2015).

In cluster 1, PP and SRP peaks are synchronized and are close to the discharge peak ; this type of pattern is often interpreted as mobilization of both dissolved and particulate P forms on hillslopes, followed by delivery by overland flow and erosion (Lefrancois *et al.*, 2007 ; Ramos *et al.*, 2015). Pattern 1 occurred all year in Moulinet regardless of the season (Figure 4.10), but mainly occurred during the largest storm events (Figure 4.9). However, since 66% of storm events were discarded from the Moulinet dataset because of low SRP concentrations, thus creating a bias toward large events, the actual percentage of storm events causing overland flow and erosion (i.e., in cluster 1) was lower than the 80% calculated. In contrast to Moulinet, pattern 1 occurred mainly in spring in Kervidy-Naizin (Figure 4.10), but did not necessarily require large storm events to occur (Figure 4.9). Thus, season seemed to control the occurrence of pattern 1 in Kervidy-Naizin, whereas storm size determined its occurrence in Moulinet. A probable explanation is that Kervidy-Naizin is an arable watershed in which seedbed preparation in spring, combined with high-intensity rainfall during spring storms (Dupas *et al.*, 2015a), can degrade the soil surface structure. As a consequence, erosion and overland flow can occur at this time of the year (Le Bissonnais *et al.*, 2002). Such surface transfer may also cause incidental losses of animal manure, which is frequently applied in spring. Conversely, the dominance of permanent grassland throughout the year in Moulinet makes this watershed less sensitive to the seasonality of agricultural practices than Kervidy-Naizin. Events in cluster 1 in Moulinet were the largest events, probably because they connect areas of the watershed located far from the stream, which contain more arable land and higher soil P content than riparian areas (Gascuel-Odoux *et al.*, 2007).

In cluster 2, PP and SRP peaks are unsynchronized. The PP peak present on the rising limb of the hydrograph probably resulted from mobilization of a P source located within or close to the stream channel (Bowes *et al.*, 2005 ; Haygarth *et al.*, 2005 ; Stutter *et al.*, 2008 ; Bieroza and Heathwaite, 2015). This export mechanism is preponderant for PP both in Kervidy-Naizin and Moulinet. In the cluster analysis of Moulinet storms, events with early PP concentration peaks are in the minority because we discarded the smallest storms by excluding events with SRP < 30 μg l^{-1}. Previous work on the Moulinet watershed has shown that erosion of the stream channel and remobilization of streambed sediment are major sources of suspended solids, including PP (Lefrancois *et al.*, 2007 ; Vongvixay *et al.*, 2010), as in many watersheds from the temperate zone (Bowes *et al.*, 2005 ; Kronvang *et al.*, 2012 ; Lu *et al.*, 2015). Unlike PP, SRP increased gradually and was followed by a plateau that lasted until the end of flow recession. Such dynamics are often interpreted as resulting from subsurface transfer of a source located in the riparian area (e.g. Morel *et al.* (2009) ; Cerro *et al.* (2014) ; Perks *et al.*, 2015 ; Ramos *et al.* (2015)). In the context of watersheds with

impervious bedrock, water table rise in riparian wetlands is the most probable mechanism causing SRP transfer via subsurface flow paths (Dupas *et al.*, 2015a). In Kervidy-Naizin, SRP dynamics during storm events are similar to those of dissolved organic carbon, which supports the idea that SRP is transferred from riparian wetlands via subsurface flowpaths (Aubert *et al.*, 2013b ; Lambert *et al.*, 2014 ; Dupas *et al.*, 2015a). Extensive monitoring of soil and soil-solution SRP concentrations in Kervidy-Naizin has shown that some riparian areas were highly enriched in P and that groundwater level dynamics controlled its solubilization and transfer (Dupas *et al.*, 2015c). This transfer mechanism of SRP dominated all year in Kervidy-Naizin, except for storm events in spring when it was overshadowed by incidental losses of recently applied animal manure. In Moulinet, the events that caused SRP to exceed 30 μg l^{-1} were only those causing overland flow and erosion, probably because soil P content in riparian areas was too low for groundwater fluctuation to cause subsurface transfer of SRP.

In cluster 3, the double SRP peak events (Figure 4.8) may have at least two interpretations. First, because this event occurred in Kervidy-Naizin at the start of the hydrological season, the first rainfall events of the hydrological year may have formed ponds in the dry stream channel. These ponds may have solubilized P from organic matter that accumulated in the stream channel during autumn leaf fall. Connection of these ponds by a storm event that fully rewetted the stream network may have caused the first peak. The mechanism causing the second peak was probably groundwater fluctuation in riparian areas, as in storm events belonging to cluster 2. Alternatively, resuspension of streambed sediments during flow rise could have caused immobilization of SRP by sorption on particles (Lazzarotto *et al.*, 2005), thus creating a hollow in the middle of the SRP peak. The event with synchronized and delayed export of PP and SRP (Figure 4.8) was accompanied by an ammonium concentration exceeding 17 mg l^{-1} (data not shown), while it usually remains below 0.01 mg l^{-1} in Kervidy-Naizin during baseflow. Such high levels of ammonium are the signature of incidental transfer of animal manure to the stream in spring, even during a small storm. Thus, this event may be an extreme example of cluster 1, for which the occurrence of overland flow and erosion coincides with high source risk.

Implications for management

These findings have implications for management. First, distinct export mechanisms for SRP and PP were demonstrated for most storm events ; hence, distinct management strategies should address both P forms. It would be useful to assess the bioavailability of PP to decide whether priority should be given to management strategies that target only SRP or both SRP and PP. During most storm events, PP originates from the stream channel ; therefore, measures to reduce bank erosion, such as implanting riparian vegetation, restoring channel shape and restricting cattle access to the stream, should reduce the PP load (Lefrancois *et al.*, 2007 ; Vongvixay *et al.*, 2010). Unlike PP, SRP originates mainly from riparian areas and is transferred to the stream because of the hydrological connectivity created by groundwater rise in these zones. Comparison between Kervidy-Naizin and Moulinet and in-situ measurement of pore-water SRP concentrations in riparian soils (Dupas *et al.*, 2015c), suggest that the amount of SRP transferred dependents greatly on soil P status in these hydrologically active areas. To keep/restore a low soil P status in riparian areas, which are usually already managed as unfertilized buffer strips, one could : i) mine P

from these zones by exporting biomass ; ii) prevent further P enrichment of these zones by reducing erosion in upslope arable fields ; or iii) increase immobilization, e.g. by using P-sorbing material in the most sensitive areas. Both catchments exhibit evidence of overland flow and erosion in upslope fields during a minority of events, which be accompanied by incidental losses of manure/slurry. Since degradation of soil structure is often the cause of soil erosion (Le Bissonnais *et al.*, 2002), conservation practices should be promoted. Better prediction of major rainfall events during the manure spreading season would reduce the risk of incidental losses to the stream or to riparian areas. Unlike other regions, direct P losses from upslope arable fields appear to be less importance than P remobilization in the riparian zone or in the stream channel itself. One probable reason is that slopes are moderately steep and riparian buffer strips have been installed along the entire stream network. The signal of mobilization in upslope fields is rarely transmitted to the stream ; however, this does not mean that efforts to reduce erosion and overland flow are ineffective (Haygarth *et al.*, 2012), because they would contribute to limit the enrichment of riparian zones where remobilization takes place.

Methodological limits and perspectives

With the recent development of high-frequency and multi-parameter water quality measurement techniques, the amount of data generated often exceeds the capacity of manual analysis (Jordan *et al.*, 2007 ; Rozemeijer *et al.*, 2010 ; Wade *et al.*, 2012 ; Kirchner and Neal, 2013). Hence, automated or semi-automated techniques are required to extract meaningful information and knowledge from the data. The DTW-based clustering method presented here has proven useful for identifying meaningful patterns in storm water quality time series with several parameters (Q, PP, SRP). The main advantage of DTW-based clustering is that it provides a synthetic view of P storm patterns in the two watersheds, which renders data analysis and interpretation of multiple time series easier than using visual description. After DTW-transformation, the time lags of discharge and concentration peaks can be compared even when hydrographs have different shapes. One improvement compared to previous storm-description approaches (Rossi *et al.*, 2005 ; Lawler *et al.*, 2006 ; Butturini *et al.*, 2008 ; Stutter *et al.*, 2008) is that DTW can isolate events with an unusual pattern in the same cluster (here, cluster 3). It did not, however, create a specific cluster for each type of unusual event, even when we increased the number of potential clusters in k-means (results not shown). If identifying exceptional events is an objective of a study, dedicated methods, such as statistical modeling of extreme values (Coles *et al.*, 2001), should be investigated instead of k-means.

In the present application, we interpreted seasonal distributions of clusters in terms of P transport mechanisms in two watersheds. The dataset used, i.e. 68 storm time series with two water quality parameters, was relatively modest compared to what would have been obtained with nearly-continuous measurement. Based on analysis of daily data in Kervidy-Naizin, Aubert *et al.*, (2013a) estimated that an average of 31 storm events with noticeable changes in stream chemistry occur yearly in the watershed. By extrapolating this value to seven years and two watersheds, over 400 storm events could have been monitored in the Kervidy-Naizin and Moulinet watersheds during the study period. Besides monitoring more events, nearly-continuous monitoring would enable exhaustive sampling of all storm events, which would prevent the risk of sampling bias in the dataset (Outram *et al.*, 2014).

In contrast, the monitoring strategy used in this study creates unavoidable sampling bias : for example, during a succession of storms, autosamplers will often trigger during the first one but miss those that follow. With more data and greater confidence that datasets are unbiased, further analysis with the DTW-based clustering method is possible, in addition to seasonal analysis of storm dynamics :

- Applying the clustering method to non-normalized data to obtain clusters that consider both concentrations values and their dynamics. In the present application, data were normalized because the Euclidean distance used in k-means is sensitive to concentration values, and we wanted to focus analysis on their dynamics relative to the hydrograph. The concentrations values were analyzed separately (Figure 4.9), which did not reveal significant differences between clusters. Variables used previously to describe storm dynamics (Rossi *et al.*, 2005 ; Lawler *et al.*, 2006 ; Butturini *et al.*, 2008 ; Stutter *et al.*, 2008) also require separate analysis of concentration values ;

- Comparing interannual pattern distributions to investigate effects of interannual climate variability (Aubert *et al.*, 2013a). Contrary to seasonal analysis, in which storm events can be grouped by quarter regardless of the year, studying each year separately would require monitoring many storm events in each combination of year quarter. One could also group different years according to climatic characteristics ;

- Increasing k in k-means to investigate the ability of the clustering method to create a specific cluster for each type of unusual pattern, because the unusual storm events would be present in larger number.

Because the DTW-based clustering method presented here involves a k-means algorithm, results were highly sensitive to initialization strategy. Initialization with randomly selected storm events resulted in cluster patterns that were not meaningful for inferring the seasonality of P transport mechanisms (Figure 4.6). In contrast, initialization with previously identified storm events (Figure 4.7) led to clusters with meaningful patterns. Hence, in this application of a semi-automated method, expertise and a hypothesis-driven approach was necessary to extract useful information and knowledge from data.

4.1.4 Conclusion

This paper describes a new method to identify patterns of P storm dynamics in two contrasting watersheds. The method consists of two steps :

- Using DTW to temporally realign discharge data onto a reference time series and rescaling P data with the same transformation ;

- Applying a k-means clustering algorithm to rescaled P data.

Meaningful patterns were identified when expert initialization was performed. Seasonal distribution of these patterns in two contrasting watersheds was analyzed to investigate the variability in P transport mechanisms. In the arable watershed, most analyzed storm events exhibited unsynchronized export of PP and SRP, suggesting independent origins and/or transport pathways. PP was seemingly mobilized through resuspension of streambed sediments and/or erosion of the stream channel. SRP was transferred via subsurface

flow paths. Indications of hillslope erosion and delivery of PP and SRP were only identified for a minority of events, mainly in spring, because of the combination of high source and transport risks during this time of the year. In the grassland watershed, events with subsurface transfer of SRP were less frequent, probably because of lower soil P content than in the arable watershed. Occurrence of hillslope erosion and synchronized delivery and PP and SRP was not related to seasonal risk factors, but rather to the amplitude of storm events. Beyond the study case, the DTW clustering method opens new possibilities for data interpretation in the context of the worldwide development of high-frequency and multiparameter measurement techniques.

Acknowledgements

Data of "ORE AgrHyS" can be downloaded from http ://www6.inra.fr/ ore_agrhys/Donnees. Data of "ORE PFC" can be requested from the corresponding author. The DTW-based clustering program has not been released. This work was funded by the "Agence de l'Eau Loire Bretagne" via the "Trans-P project". Long-term monitoring in the Kervidy-Naizin watershed is supported by "ORE AgrHyS". Long-term monitoring in the Moulinet watershed is supported by "ORE PFC". We would like to thank all those who helped with the field and lab work, particularly Jean-Paul Guillard and Laurence Carteaux.

References

Astel, A., S. Tsakouski, P. Barbieri, and V. Simeonov (2007), Comparison of self-organizing maps classification approach with cluster and principal components analysis for large environmental data sets, Water Res., 41(19), 4566-4578.10.1016/j.watres.2007.06.030

Aubert, A. H., R. Tavenard, R. Emonet, A. de Lavenne, S. Malinowski, T. Guyet, R. Quiniou, J. M. Odobez, P. Merot, and C. Gascuel-Odoux (2013a), Clustering flood events from water quality time series using Latent Dirichlet Allocation model, Water Resources Research, 49(12), 8187-8199.10.1002/2013wr014086

Aubert, A. H., *et al.* (2013b), Solute transport dynamics in small, shallow groundwater-dominated agricultural catchments : insights from a high-frequency, multisolute 10 yr-long monitoring study, Hydrology and Earth System Sciences, 17(4), 1379-1391. 10.5194/hess-17-1379-2013

Bende-Michl, U., K. Verburg, and H. P. Cresswell (2013), High-frequency nutrient monitoring to infer seasonal patterns in catchment source availability, mobilisation and delivery, Environmental monitoring and assessment, 185(11), 9191-9219.10.1007/s10661-013-3246-8

Benhamou, C., J. Salmon-Monviola, P. Durand, C. Grimaldi, and P. Merot (2013), Modeling the interaction between fields and a surrounding hedgerow network and its impact on water and nitrogen flows of a small watershed, Agricultural Water Management, 121, 62-72.10.1016/j.agwat.2013.01.004

Bieroza, M. Z., and A. L. Heathwaite (2015), Seasonal variation in phosphorus concentration-discharge hysteresis inferred from high-frequency in situ monitoring, Journal of Hydrology, 524, 333-347. 10.1016/j.jhydrol.2015.02.036

Bowes, M. J., W. A. House, R. A. Hodgkinson, and D. V. Leach (2005), Phosphorus-discharge hysteresis during storm events along a river catchment : the River Swale, UK,

Water Res., 39(5), 751-762.10.1016/j.watres.2004.11.027

Bowes, M. J., H. P. Jarvie, S. J. Halliday, R. A. Skeffington, A. J. Wade, M. Loewenthal, E. Gozzard, J. R. Newman, and E. J. Palmer-Felgate (2015), Characterising phosphorus and nitrate inputs to a rural river using high-frequency concentration-flow relationships, Science of the total environment, 511, 608-620.10.1016/j.scitotenv.2014.12.086

Butturini, A., M. Alvarez, S. Bernal, E. Vazquez, and F. Sabater (2008), Diversity and temporal sequences of forms of DOC and NO_3^- discharge responses in an intermittent stream : Predictable or random succession ?, Journal of Geophysical Research-Biogeosciences, 113(G3).10.1029/2008jg000721

Cerro, I., J. M. Sanchez-Perez, E. Ruiz-Romera, and I. Antiguedad (2014), Variability of particulate (SS, POC) and dissolved (DOC, NO3) matter during storm events in the Alegria agricultural watershed, Hydrological Processes, 28(5), 2855-2867.10.1002/hyp.9850

Coles, S., J. Bawa, L. Trenner, and P. Dorazio (2001), An introduction to statistical modeling of extreme values, London : Springer

Delmas, M., N. Saby, D. Arrouays, R. Dupas, B. Lemercier, S. Pellerin, and C. Gascuel-Odoux (2015), Explaining and mapping total phosphorus content in French topsoils, Soil Use and Management, 31(2), 259-269.

Delsman, J. R., G. Essink, K. J. Beven, and P. J. Stuyfzand (2013), Uncertainty estimation of end-member mixing using generalized likelihood uncertainty estimation (GLUE), applied in a lowland catchment, Water Resources Research, 49(8), 4792-4806.10.1002/wrcr.20341

Dupas, R., C. Gascuel-Odoux, N. Gilliet, C. Grimaldi, and G. Gruau (2015a), Distinct export dynamics for dissolved and particulate phosphorus reveal independent transport mechanisms in an arable headwater catchment, Hydrological Processes, 29(14), 3162-3178.10.1002/hyp.10432

Dupas, R., M. Delmas, J. M. Dorioz, J. Garnier, F. Moatar, and C. Gascuel-Odoux (2015b), Assessing the impact of agricultural pressures on N and P loads and eutrophication risk, Ecological Indicators, 48, 396–407.10.1016/j.ecolind.2014.08.007

Dupas, R., G. Gruau, S. Gu, G. Humbert, A. Jaffrezic, and C. Gascuel-Odoux (2015c), Groundwater control of biogeochemical processes causing phosphorus release from riparian wetlands, Water Research, 84. 10.1016/j.watres.2015.07.048

Fytilis, N., and D. M. Rizzo (2013), Coupling self-organizing maps with a Naive Bayesian classifier : Stream classification studies using multiple assessment data, Water Resources Research, 49(11), 7747-7762.10.1002/2012wr013422

Gascuel-Odoux, C., C. Grimaldi, N. Gilliet, Y. Fauvel, and J. M. Dorioz (2007), Intercomparison of suspended sediment and phosphorus fluxes and concentrations on two agricultural headwater catchments 6th International Phosphorus Workshop (IPW6), COST action 869 “Mitigation options for nutrient reduction in surface water and groundwaters”

Gascuel-Odoux, C., P. Aurousseau, T. Doray, H. Squividant, F. Macary, D. Uny, and C. Grimaldi (2011), Incorporating landscape features to obtain an object-oriented landscape drainage network representing the connectivity of surface flow pathways over rural catchments, Hydrological Processes, 25(23), 3625-3636.10.1002/hyp.8089

Gburek, W. J., and A. N. Sharpley (1998), Hydrologic controls on phosphorus loss from upland agricultural watersheds, Journal of Environmental Quality, 27(2), 267-277

Haygarth, P. M., T. J. C. Page, K. J. Beven, J. Freer, A. Joynes, P. Butler, G. A. Wood, and P. N. Owens (2012), Scaling up the phosphorus signal from soil hillslopes to

headwater catchments, Freshwater Biology, 57, 7-25. 10.1111/j.1365-2427.2012.02748.x

Haygarth, P. M., F. L. Wood, A. L. Heathwaite, and P. J. Butler (2005), Phosphorus dynamics observed through increasing scales in a nested headwater-to-river channel study, Science of the Total Environment, 344(1-3), 83-106.10.1016/j.scitotoenv.2005.02.007

Heathwaite, A. L., and R. M. Dils (2000), Characterising phosphorus loss in surface and subsurface hydrological pathways, Science of the Total Environment, 251, 523-538.10.1016/s0048-9697(00)00393-4

Jarvie, H. P., C. Neal, P. J. A. Withers, D. B. Baker, R. P. Richards, and A. N. Sharpley (2011), Quantifying Phosphorus Retention and Release in Rivers and Watersheds Using Extended End-Member Mixing Analysis (E-EMMA), Journal of Environmental Quality, 40(2), 492-504.10.2134/jeq2010.0298

Jordan, P., A. Arnscheidt, H. McGrogan, and S. McCormick (2007), Characterising phosphorus transfers in rural catchments using a continuous bank-side analyser, Hydrology and Earth System Sciences, 11(1), 372-381

Kirchner, J. W., and C. Neal (2013), Universal fractal scaling in stream chemistry and its implications for solute transport and water quality trend detection, Proceedings of the National Academy of Sciences of the United States of America, 110(30), 12213-12218.10.1073/pnas.1304328110

Kronvang, B., J. Audet, A. Baattrup-Pedersen, H. S. Jensen, and S. E. Larsen (2012), Phosphorus Load to Surface Water from Bank Erosion in a Danish Lowland River Basin, Journal of Environmental Quality, 41(2), 304-313.10.2134/jeq2010.0434

Lambert, T., A. C. Pierson-Wickmann, G. Gruau, A. Jaffrezic, P. Petitjean, J. N. Thibault, and L. Jeanneau (2014), DOC sources and DOC transport pathways in a small headwater catchment as revealed by carbon isotope fluctuation during storm events, Biogeosciences, 11(11), 3043-3056.10.5194/bg-11-3043-2014

Lawler, D. M., G. E. Petts, I. D. L. Foster, and S. Harper (2006), Turbidity dynamics during spring storm events in an urban headwater river system : The Upper Tame, West Midlands, UK, Science of the Total Environment, 360(1-3), 109-126.10.1016/j.scitotenv.2005.08.032

Lazzarotto, P., V. Prasuhn, E. Butscher, C. Crespi, H. Flühler, and C. Stamm (2005), Phosphorus export dynamics from two Swiss grassland catchments, Journal of Hydrology, 304(1-4), 139-150.10.1016/j.jhydrol.2004.07.027

Le Bissonnais, Y., S. Cros-Cayot, and C. Gascuel-Odoux (2002), Topographic dependence of aggregate stability, overland flow and sediment transport, Agronomie, 22(5), 489-501.10.1051/agro :2002024

Lefrancois, J., C. Grimaldi, C. Gascuel-Odoux, and N. Gilliet (2007), Suspended sediment and discharge relationships to identify bank degradation as a main sediment source on small agricultural catchments, Hydrological Processes, 21(21), 2923-2933.10.1002/hyp.6509

Lu, S. L., B. Kronvang, J. Audet, D. Trolle, H. E. Andersen, H. Thodsen, and A. van Griensven (2015), Modelling sediment and total phosphorus export from a lowland catchment : comparing sediment routing methods, Hydrological Processes, 29(2), 280-294.10.1002/hyp.10149

Melland, A. R., P. E. Mellander, P. N. C. Murphy, D. P. Wall, S. Mechan, O. Shine, G. Shortle, and P. Jordan (2012), Stream water quality in intensive cereal cropping catchments with regulated nutrient management, Environmental Science Policy, 24, 58-70.10.1016/j.envsci.2012.06.006

Mellander, P.-E., A. R. Melland, P. Jordan, D. P. Wall, P. N. C. Murphy, and G. Shortle

(2012), Quantifying nutrient transfer pathways in agricultural catchments using high temporal resolution data, Environmental Science Policy, 24, 44-57.10.1016/j.envsci.2012.06.004

Mellander, P. E., P. Jordan, M. Shore, A. R. Melland, and G. Shortle (2015), Flow paths and phosphorus transfer pathways in two agricultural streams with contrasting flow controls, Hydrological Processes.10.1002/hyp.10415

Mellander, P. E., P. Jordan, A. R. Melland, P. N. C. Murphy, D. P. Wall, S. Mechan, R. Meehan, C. Kelly, O. Shine, and G. Shortle (2013), Quantification of Phosphorus Transport from a Karstic Agricultural Watershed to Emerging Spring Water, Environ. Sci. Technol., 47(12), 6111-6119.10.1021/es304909y

Molenat, J., C. Gascuel-Odoux, L. Ruiz, and G. Gruau (2008), Role of water table dynamics on stream nitrate export and concentration. in agricultural headwater catchment (France), Journal of Hydrology, 348(3-4), 363-378.10.1016/j.jhydrol.2007.10.005

Morel, B., P. Durand, A. Jaffrezic, G. Gruau, and J. Molenat (2009), Sources of dissolved organic carbon during stormflow in a headwater agricultural catchment, Hydrological Processes, 23(20), 2888-2901.10.1002/hyp.7379

Outram, F. N., *et al.* (2014), High-frequency monitoring of nitrogen and phosphorus response in three rural catchments to the end of the 2011-2012 drought in England, Hydrology and Earth System Sciences, 18(9), 3429-3448.10.5194/hess-18-3429-2014

Perks, M. T., G. J. Owen, C. M. H. Benskin, J. Jonczyk, C. Deasy, S. Burke, S. M. Reaney, and P. M. Haygarth (2015), Dominant mechanisms for the delivery of fine sediment and phosphorus to fluvial networks draining grassland dominated headwater catchments, Science of the Total Environment, 523, 178-190. 10.1016/j.scitotenv.2015.03.008

Pionke, H. B., W. J. Gburek, R. R. Schnabel, A. N. Sharpley, and G. F. Elwinger (1999), Seasonal flow, nutrient concentrations and loading patterns in stream flow draining an agricultural hill-land watershed, Journal of Hydrology, 220(1-2), 62-73.10.1016/s0022-1694(99)00064-5

Ramos, T. B., *et al.* (2015), Sediment and nutrient dynamics during storm events in the Enxoe temporary river, southern Portugal, Catena, 127, 177-190.10.1016/j.catena.2015.01.001

Rodriguez-Blanco, M. L., M. M. Taboada-Castro, and M. T. Taboada-Castro (2013a), Phosphorus transport into a stream draining from a mixed land use catchment in Galicia (NW Spain) : Significance of runoff events, Journal of Hydrology, 481, 12-21.10.1016/j.jhydrol.2012.11.046

Rodriguez-Blanco, M. L., M. M. Taboada-Castro, J. J. Keizer, and M. T. Taboada-Castro (2013b), Phosphorus Loss from a Mixed Land Use Catchment in Northwest Spain, Journal of Environmental Quality, 42(4), 1151-1158.10.2134/jeq2012.0318

Rossi, L., V. Krejci, W. Rauch, S. Kreikenbaum, R. Fankhauser, and W. Gujer (2005), Stochastic modeling of total suspended solids (TSS) in urban areas during rain events, Water Res., 39(17), 4188-4196.10.1016/j.watres.2005.07.041

Rozemeijer, J. C., Y. Van der Velde, F. C. Van Geer, G. H. De Rooij, P. Torfs, and H. P. Broers (2010), Improving Load Estimates for NO3 and P in Surface Waters by Characterizing the Concentration Response to Rainfall Events, Environ. Sci. Technol., 44(16), 6305-6312.10.1021/es101252e

Sakoe, H., and S. Chiba (1978), Dynamic-programming algorithm optimization for spoken word recognition, Ieee Transactions on Acoustics Speech and Signal Processing, 26(1), 43-49.10.1109/tassp.1978.1163055

Salmon-Monviola, J., P. Moreau, C. Benhamou, P. Durand, P. Merot, F. Oehler, and

C. Gascuel-Odoux (2013), Effect of climate change and increased atmospheric CO2 on hydrological and nitrogen cycling in an intensive agricultural headwater catchment in western France, Climatic Change, 120(1-2), 433-447.10.1007/s10584-013-0828-y

Sharpley, A. N., P. J. Kleinman, A. L. Heathwaite, W. J. Gburek, G. J. Folmar, and J. P. Schmidt (2008), Phosphorus loss from an agricultural watershed as a function of storm size, J Environ Qual, 37(2), 362-368.10.2134/jeq2007.0366

Soulsby, C., J. Petry, M. J. Brewer, S. M. Dunn, B. Ott, and I. A. Malcolm (2003), Identifying and assessing uncertainty in hydrological pathways : a novel approach to end member mixing in a Scottish agricultural catchment, Journal of Hydrology, 274(1-4), 109-128.10.1016/s0022-1694(02)00398-0

Stutter, M. I., S. J. Langan, and R. J. Cooper (2008), Spatial contributions of diffuse inputs and within-channel processes to the form of stream water phosphorus over storm events, Journal of Hydrology, 350(3-4), 203-214.10.1016/j.jhydrol.2007.10.045

Toth, E. (2013), Catchment classification based on characterisation of streamflow and precipitation time series, Hydrology and Earth System Sciences, 17(3), 1149-1159.10.5194/hess-17-1149-2013

Vongvixay, A., C. Grimaldi, C. Gascuel-Odoux, P. Laguionie, M. Faucheux, N. Gilliet, and M. Mayet (2010), Analysis of suspended sediment concentration and discharge relations to identify particle origins in small agricultural watersheds, in Sediment Dynamics for a Changing Future, edited by K. Banasik, A. J. Horowitz, P. N. Owens, M. Stone and D. E. Walling, pp. 76-83.

Wade, A. J., *et al.* (2012), Hydrochemical processes in lowland rivers : insights from in situ, high-resolution monitoring, Hydrology and Earth System Sciences, 16(11), 4323-4342.10.5194/hess-16-4323-2012

Williams, G. P. (1989), Sediment concentration versus water discharge during single hydrologic events in rivers, Journal of Hydrology, 111(1-4), 89-106.10.1016/0022-1694(89)90254-0

Wong, H., and B. Q. Hu (2013), Application of interval clustering approach to water quality evaluation, Journal of Hydrology, 491, 1-12.10.1016/j.jhydrol.2013.03.009

4.1.5 Supplementary materials

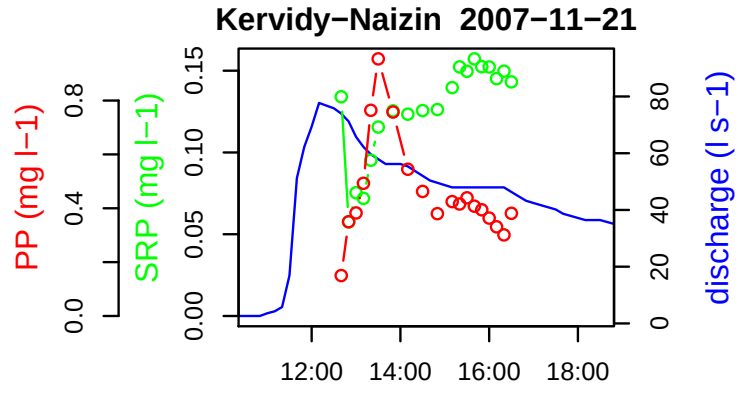
Kervidy−Naizin 2007−11−21
PP (mg l−1)
SRP (mg l−1)
discharge (l s−1)
0.0 0.4 0.8
0.00 0.05 0.10 0.15
0 20 40 60 80
12:00 14:00 16:00 18:00

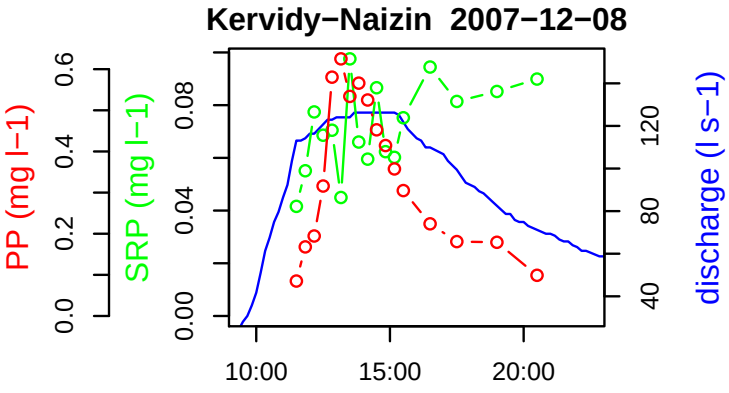
Kervidy−Naizin 2007−12−08
PP (mg l−1)
SRP (mg l−1)
discharge (l s−1)
0.0 0.2 0.4 0.6
0.00 0.04 0.08
40 80 120
10:00 15:00 20:00

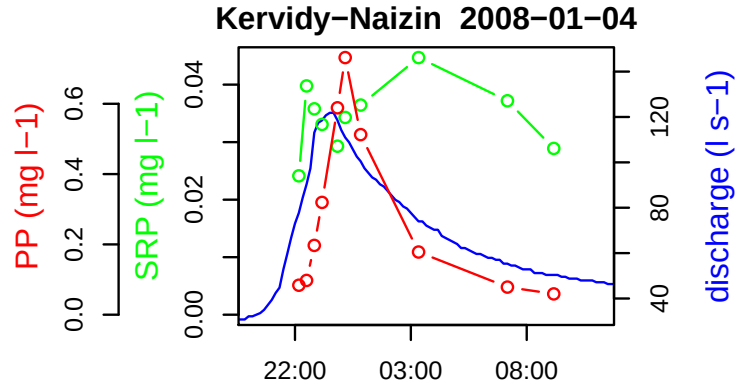
Kervidy−Naizin 2008−01−04
PP (mg l−1)
SRP (mg l−1)
discharge (l s−1)
0.0 0.2 0.4 0.6
0.00 0.02 0.04
40 80 120
22:00 03:00 08:00

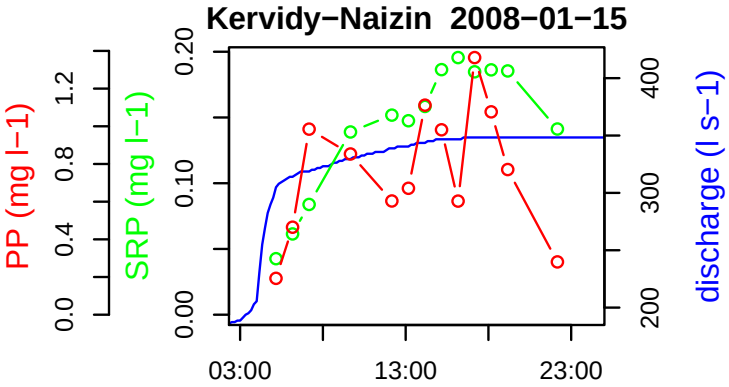
Kervidy−Naizin 2008−01−15
PP (mg l−1)
SRP (mg l−1)
discharge (l s−1)
0.0 0.4 0.8 1.2
0.00 0.10 0.20
200 300 400
03:00 13:00 23:00

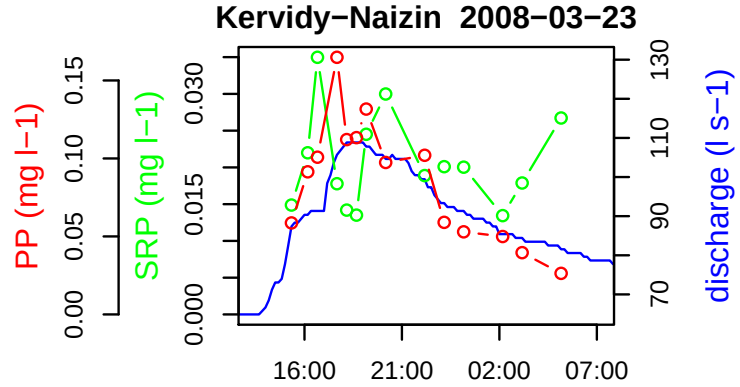
Kervidy−Naizin 2008−03−23
PP (mg l−1)
SRP (mg l−1)
discharge (l s−1)
0.00 0.05 0.10 0.15
0.000 0.015 0.030
70 90 110 130
16:00 21:00 02:00 07:00

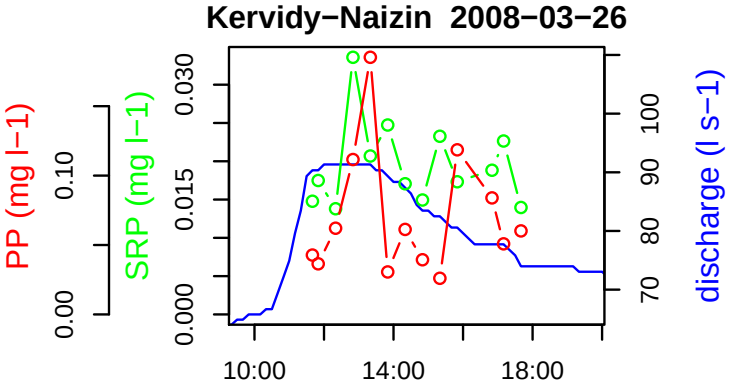
Kervidy−Naizin 2008−03−26
PP (mg l−1)
SRP (mg l−1)
discharge (l s−1)
0.00 0.10
0.000 0.015 0.030
70 80 90 100
10:00 14:00 18:00

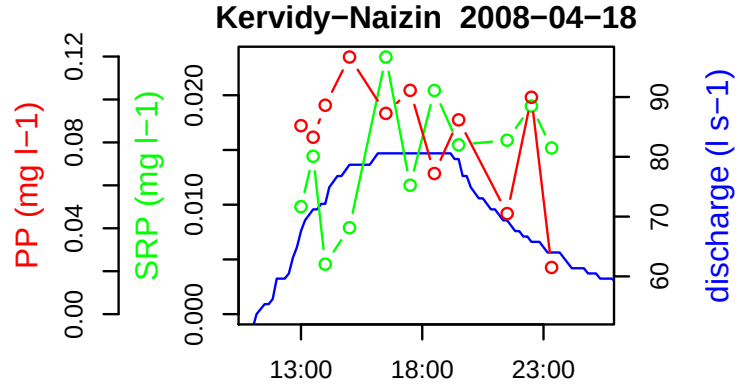
Kervidy−Naizin 2008−04−18
PP (mg l−1)
SRP (mg l−1)
discharge (l s−1)
0.00 0.04 0.08 0.12
0.000 0.010 0.020
60 70 80 90
13:00 18:00 23:00

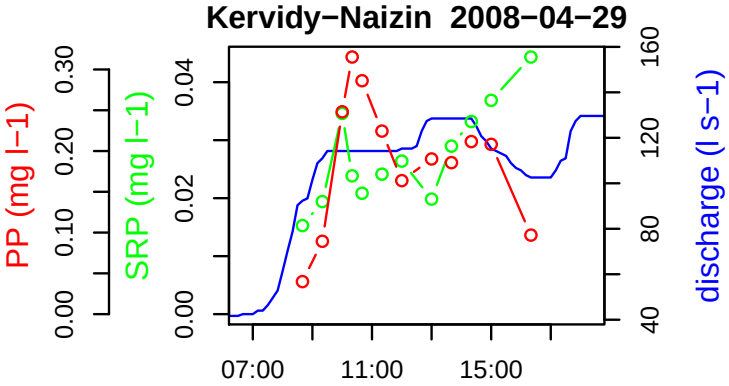
Kervidy−Naizin 2008−04−29
PP (mg l−1)
SRP (mg l−1)
discharge (l s−1)
0.00 0.10 0.20 0.30
0.00 0.02 0.04
40 80 120 160
07:00 11:00 15:00

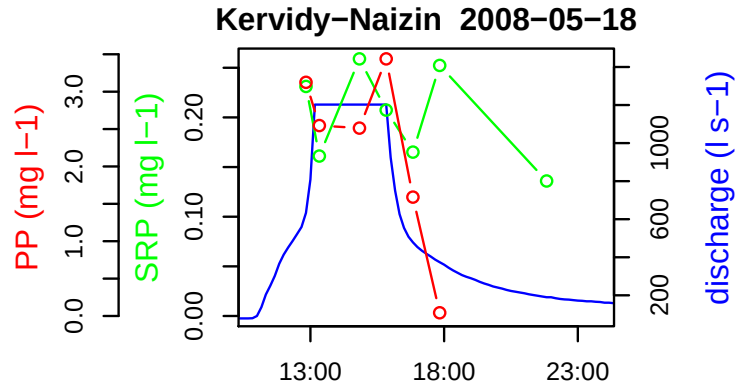
Kervidy−Naizin 2008−05−18
PP (mg l−1)
SRP (mg l−1)
discharge (l s−1)
0.0 1.0 2.0 3.0
0.00 0.10 0.20
200 600 1000
13:00 18:00 23:00

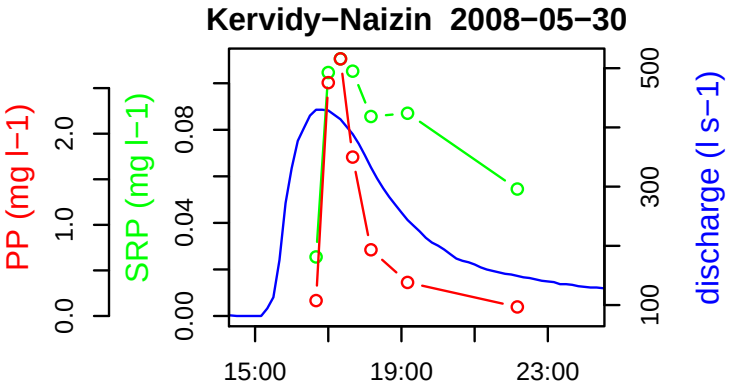
Kervidy−Naizin 2008−05−30
PP (mg l−1)
SRP (mg l−1)
discharge (l s−1)
0.0 1.0 2.0
0.00 0.04 0.08
100 300 500
15:00 19:00 23:00

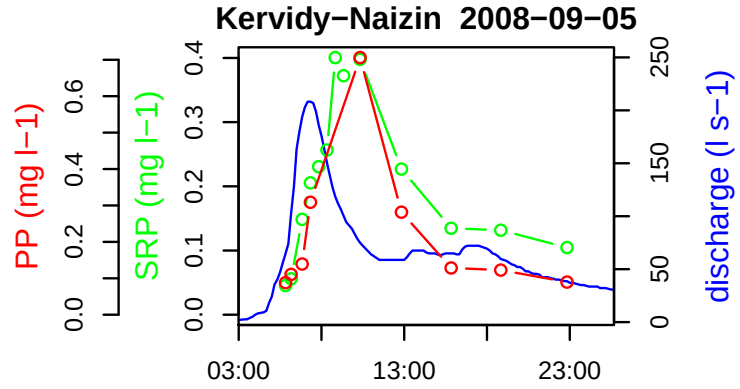
Kervidy−Naizin 2008−09−05
PP (mg l−1)
SRP (mg l−1)
discharge (l s−1)
0.0 0.2 0.4 0.6
0.0 0.1 0.2 0.3 0.4
0 50 150 250
03:00 13:00 23:00

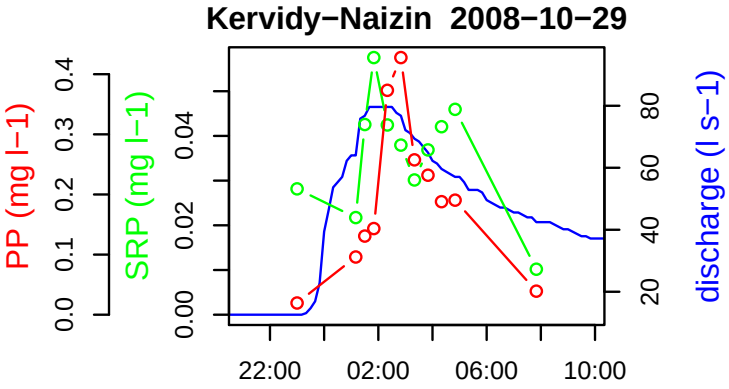
Kervidy−Naizin 2008−10−29
PP (mg l−1)
SRP (mg l−1)
discharge (l s−1)
0.0 0.1 0.2 0.3 0.4
0.00 0.02 0.04
20 40 60 80
22:00 02:00 06:00 10:00

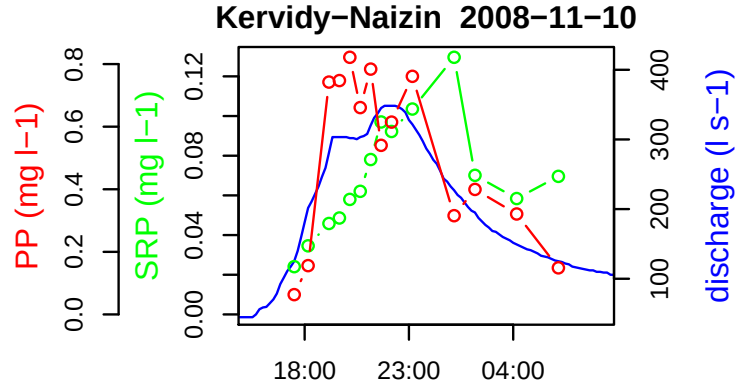
Kervidy−Naizin 2008−11−10
PP (mg l−1)
SRP (mg l−1)
discharge (l s−1)
0.0 0.2 0.4 0.6 0.8
0.00 0.04 0.08 0.12
100 200 300 400
18:00 23:00 04:00

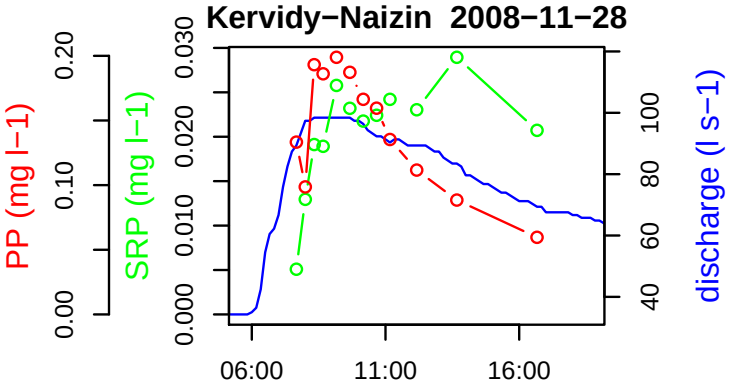
Kervidy−Naizin 2008−11−28
PP (mg l−1)
SRP (mg l−1)
discharge (l s−1)
0.00 0.10 0.20
0.000 0.010 0.020 0.030
40 60 80 100
06:00 11:00 16:00

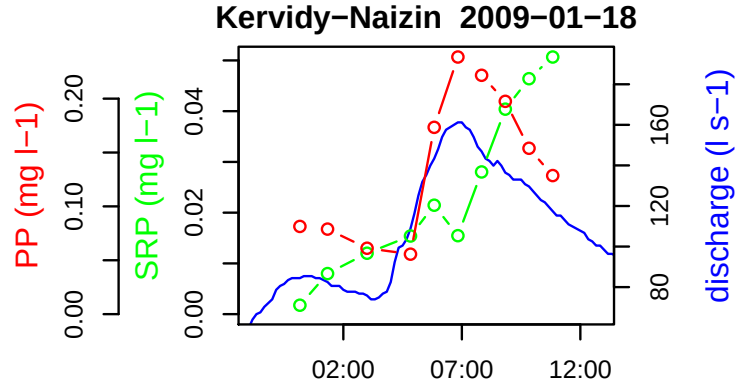
Kervidy−Naizin 2009−01−18
PP (mg l−1)
SRP (mg l−1)
discharge (l s−1)
0.00 0.10 0.20
0.00 0.02 0.04
80 120 160
02:00 07:00 12:00

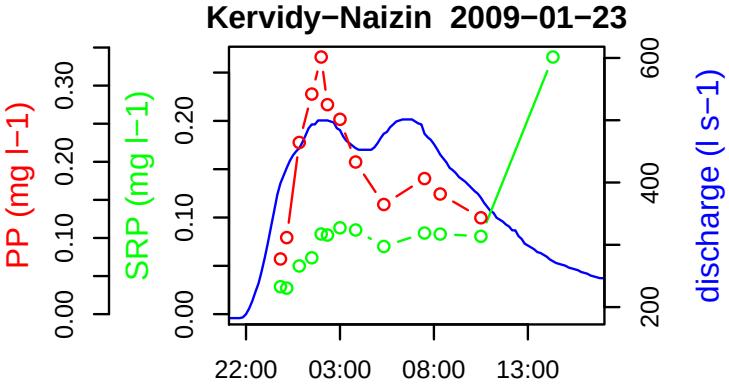
Kervidy−Naizin 2009−01−23
PP (mg l−1)
SRP (mg l−1)
discharge (l s−1)
0.00 0.10 0.20 0.30
0.00 0.10 0.20
200 400 600
22:00 03:00 08:00 13:00

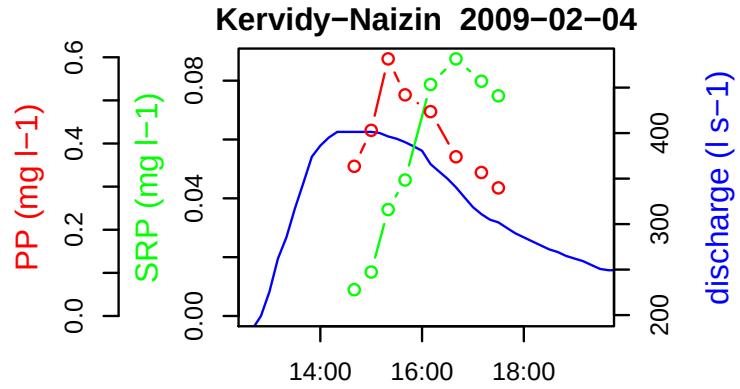
Kervidy−Naizin 2009−02−04
PP (mg l−1)
SRP (mg l−1)
discharge (l s−1)
14:00
16:00
18:00

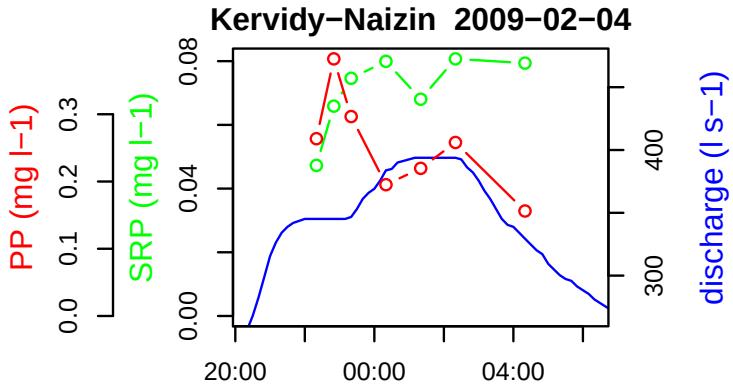
Kervidy−Naizin 2009−02−04
PP (mg l−1)
SRP (mg l−1)
discharge (l s−1)
20:00
00:00
04:00

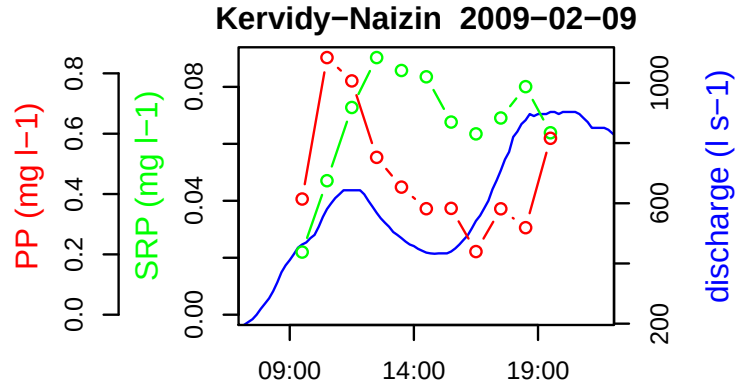
Kervidy−Naizin 2009−02−09
PP (mg l−1)
SRP (mg l−1)
discharge (l s−1)
09:00
14:00
19:00

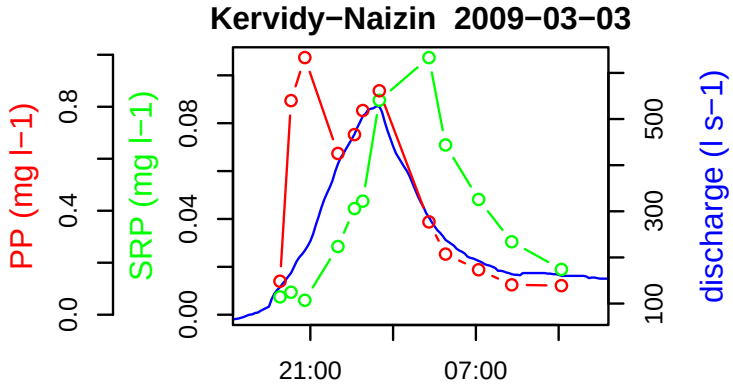
Kervidy−Naizin 2009−03−03
PP (mg l−1)
SRP (mg l−1)
discharge (l s−1)
21:00
07:00

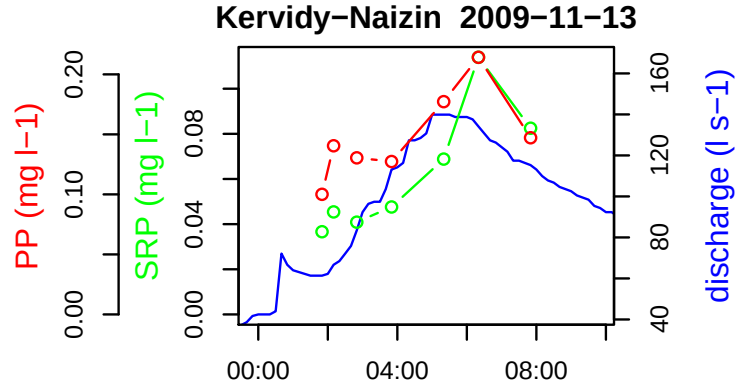
Kervidy−Naizin 2009−11−13
PP (mg l−1)
SRP (mg l−1)
discharge (l s−1)
00:00
04:00
08:00

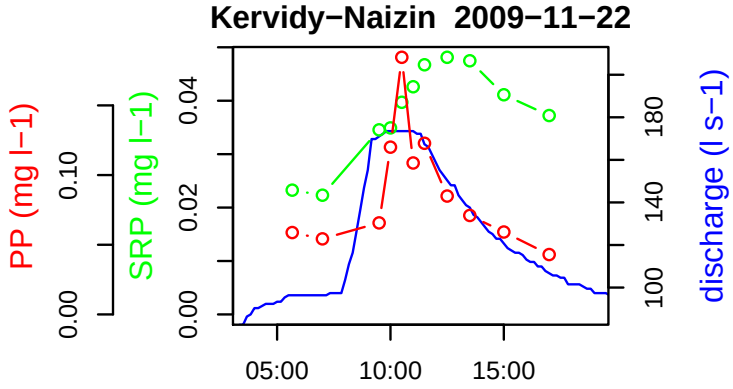
Kervidy−Naizin 2009−11−22
PP (mg l−1)
SRP (mg l−1)
discharge (l s−1)
05:00
10:00
15:00

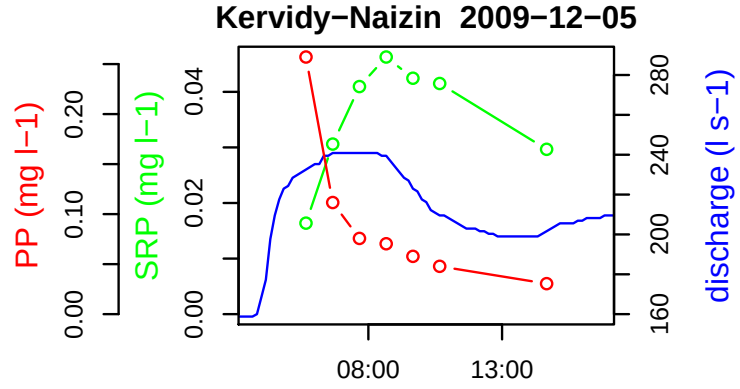
Kervidy−Naizin 2009−12−05
PP (mg l−1)
SRP (mg l−1)
discharge (l s−1)
08:00
13:00

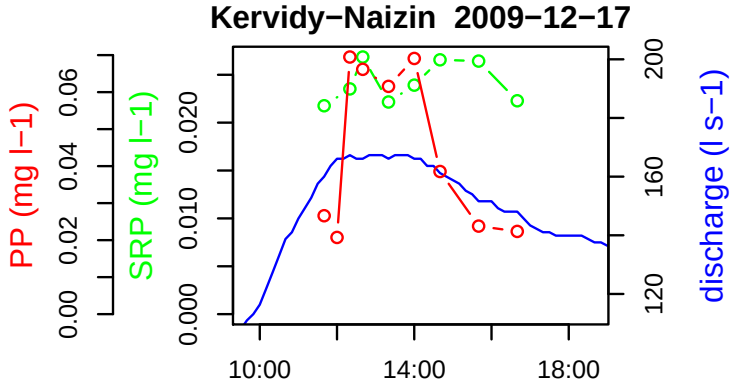
Kervidy−Naizin 2009−12−17
PP (mg l−1)
SRP (mg l−1)
discharge (l s−1)
10:00
14:00
18:00

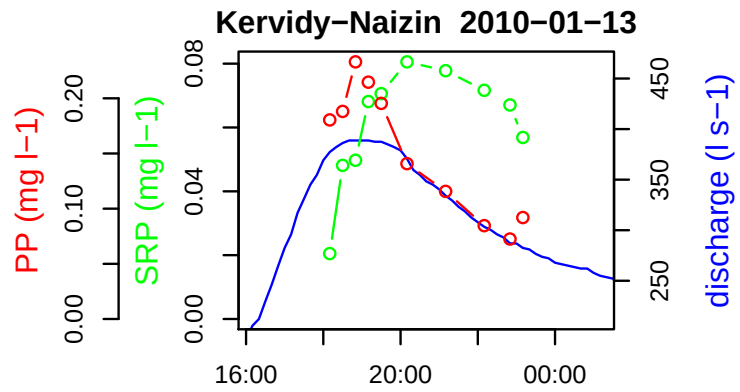
Kervidy−Naizin 2010−01−13
PP (mg l−1)
SRP (mg l−1)
discharge (l s−1)
16:00
20:00
00:00

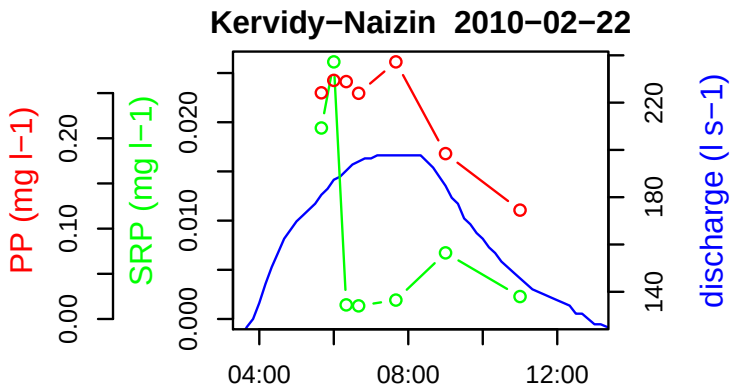
Kervidy−Naizin 2010−02−22
PP (mg l−1)
SRP (mg l−1)
discharge (l s−1)
04:00
08:00
12:00

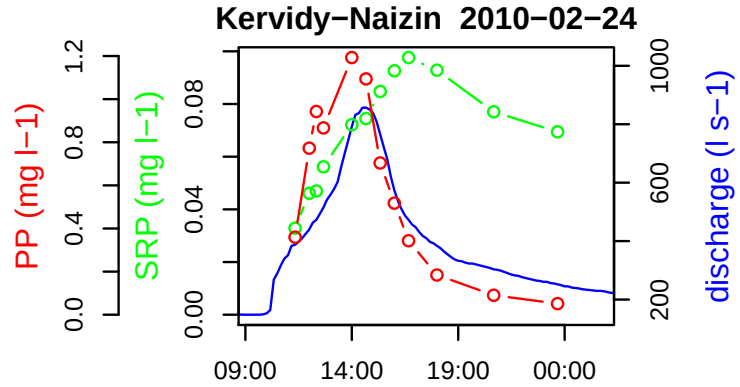
Kervidy−Naizin 2010−02−24
PP (mg l−1)
SRP (mg l−1)
discharge (l s−1)
09:00
14:00
19:00
00:00

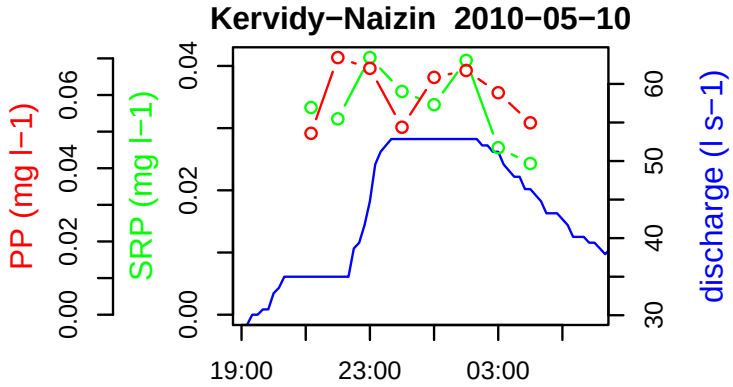
Kervidy−Naizin 2010−05−10
PP (mg l−1)
SRP (mg l−1)
discharge (l s−1)
19:00
23:00
03:00

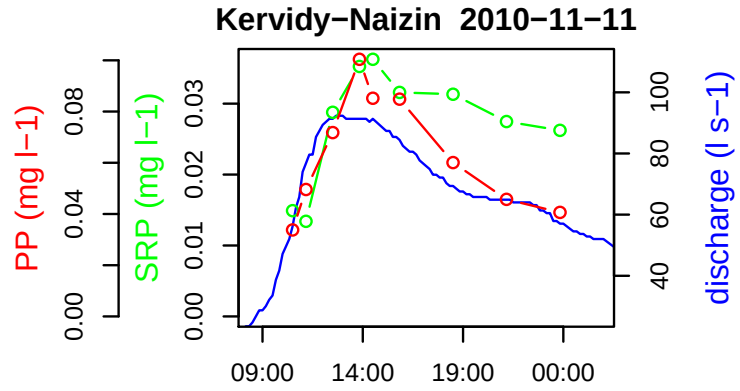
Kervidy−Naizin 2010−11−11
PP (mg l−1)
SRP (mg l−1)
discharge (l s−1)
09:00
14:00
19:00
00:00

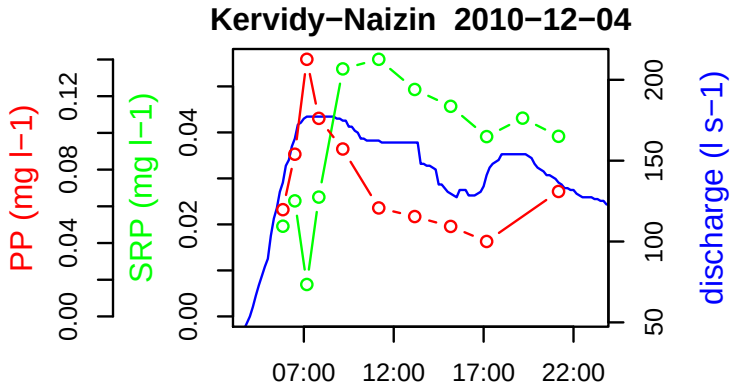
Kervidy−Naizin 2010−12−04
PP (mg l−1)
SRP (mg l−1)
discharge (l s−1)
07:00
12:00
17:00
22:00

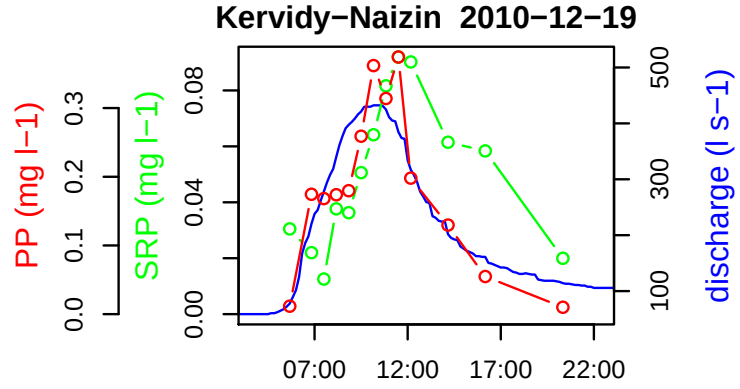
Kervidy−Naizin 2010−12−19
PP (mg l−1)
SRP (mg l−1)
discharge (l s−1)
07:00
12:00
17:00
22:00

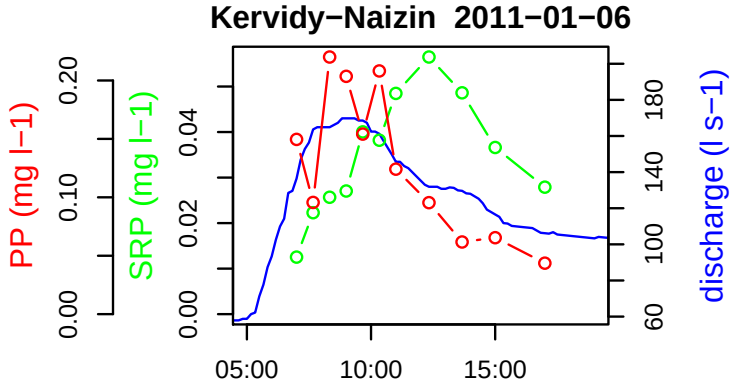
Kervidy−Naizin 2011−01−06
PP (mg l−1)
SRP (mg l−1)
discharge (l s−1)
05:00
10:00
15:00

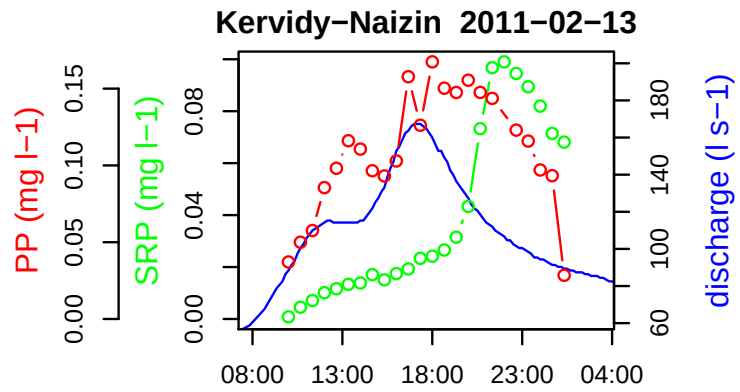
Kervidy−Naizin 2011−02−13
PP (mg l−1)
SRP (mg l−1)
discharge (l s−1)
0.00 0.05 0.10 0.15
0.00 0.04 0.08
60 100 140 180
08:00 13:00 18:00 23:00 04:00

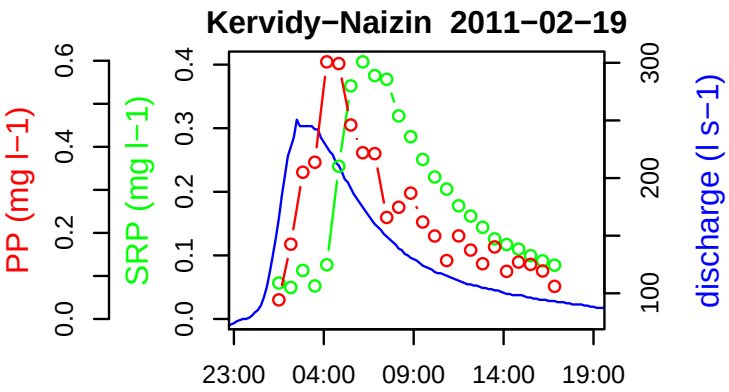
Kervidy−Naizin 2011−02−19
PP (mg l−1)
SRP (mg l−1)
discharge (l s−1)
0.0 0.2 0.4 0.6
0.0 0.1 0.2 0.3 0.4
100 200 300
23:00 04:00 09:00 14:00 19:00

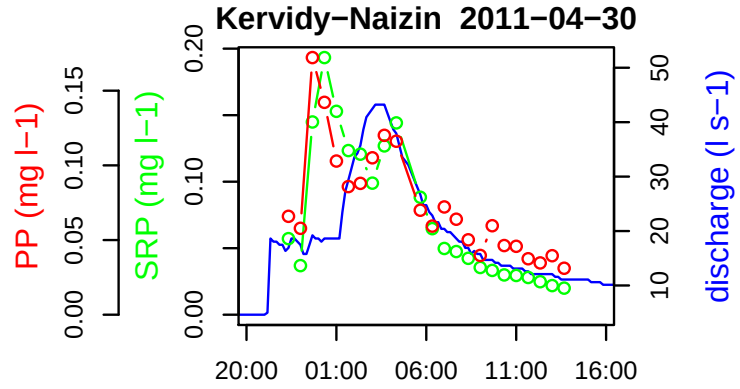
Kervidy−Naizin 2011−04−30
PP (mg l−1)
SRP (mg l−1)
discharge (l s−1)
0.00 0.05 0.10 0.15
0.00 0.10 0.20
10 20 30 40 50
20:00 01:00 06:00 11:00 16:00

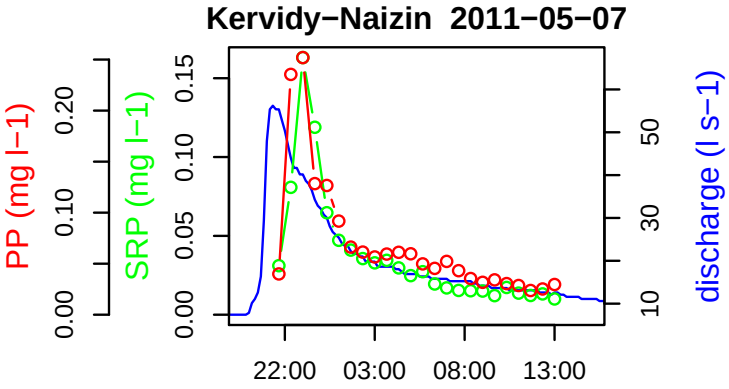
Kervidy−Naizin 2011−05−07
PP (mg l−1)
SRP (mg l−1)
discharge (l s−1)
0.00 0.10 0.20
0.00 0.05 0.10 0.15
10 30 50
22:00 03:00 08:00 13:00

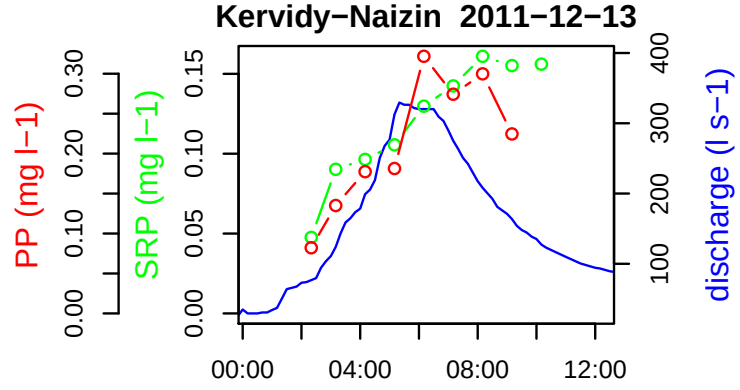
Kervidy−Naizin 2011−12−13
PP (mg l−1)
SRP (mg l−1)
discharge (l s−1)
0.00 0.10 0.20 0.30
0.00 0.05 0.10 0.15
100 200 300 400
00:00 04:00 08:00 12:00

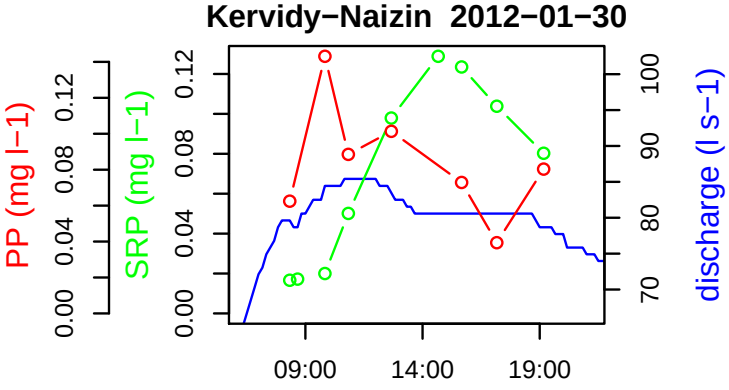
Kervidy−Naizin 2012−01−30
PP (mg l−1)
SRP (mg l−1)
discharge (l s−1)
0.00 0.04 0.08 0.12
0.00 0.04 0.08 0.12
70 80 90 100
09:00 14:00 19:00

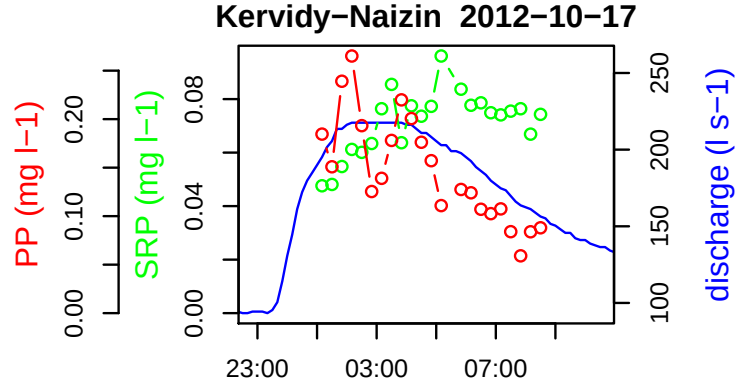
Kervidy−Naizin 2012−10−17
PP (mg l−1)
SRP (mg l−1)
discharge (l s−1)
0.00 0.10 0.20
0.00 0.04 0.08
100 150 200 250
23:00 03:00 07:00

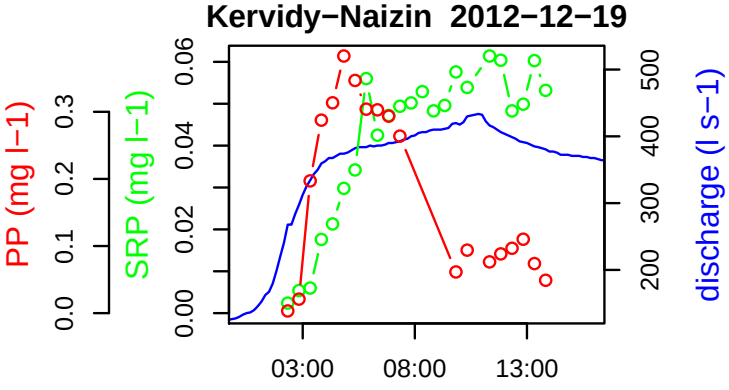
Kervidy−Naizin 2012−12−19
PP (mg l−1)
SRP (mg l−1)
discharge (l s−1)
0.0 0.1 0.2 0.3
0.00 0.02 0.04 0.06
200 300 400 500
03:00 08:00 13:00

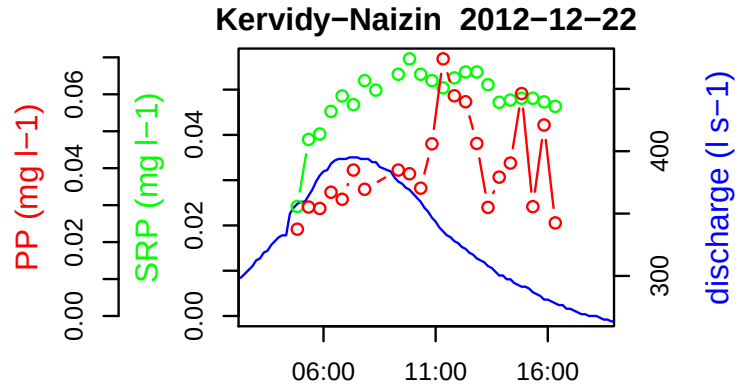
Kervidy−Naizin 2012−12−22
PP (mg l−1)
SRP (mg l−1)
discharge (l s−1)
0.00 0.02 0.04 0.06
0.00 0.02 0.04
300 400
06:00 11:00 16:00

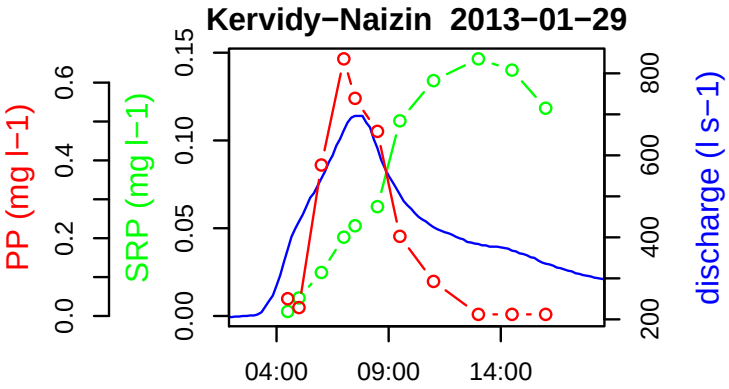
Kervidy−Naizin 2013−01−29
PP (mg l−1)
SRP (mg l−1)
discharge (l s−1)
0.0 0.2 0.4 0.6
0.00 0.05 0.10 0.15
200 400 600 800
04:00 09:00 14:00

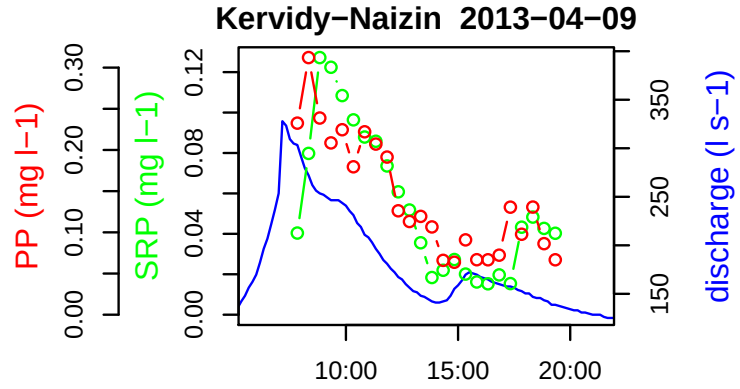
Kervidy−Naizin 2013−04−09
PP (mg l−1)
SRP (mg l−1)
discharge (l s−1)
0.00 0.10 0.20 0.30
0.00 0.04 0.08 0.12
150 250 350
10:00 15:00 20:00

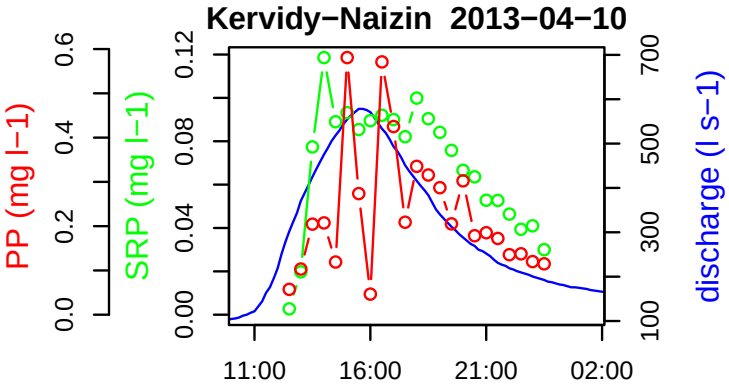
Kervidy−Naizin 2013−04−10
PP (mg l−1)
SRP (mg l−1)
discharge (l s−1)
0.0 0.2 0.4 0.6
0.00 0.04 0.08 0.12
100 300 500 700
11:00 16:00 21:00 02:00

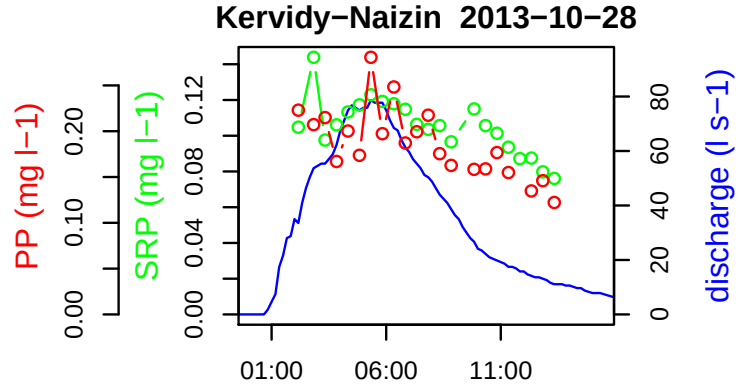
Kervidy−Naizin 2013−10−28
PP (mg l−1)
SRP (mg l−1)
discharge (l s−1)
0.00 0.10 0.20
0.00 0.04 0.08 0.12
0 20 40 60 80
01:00 06:00 11:00

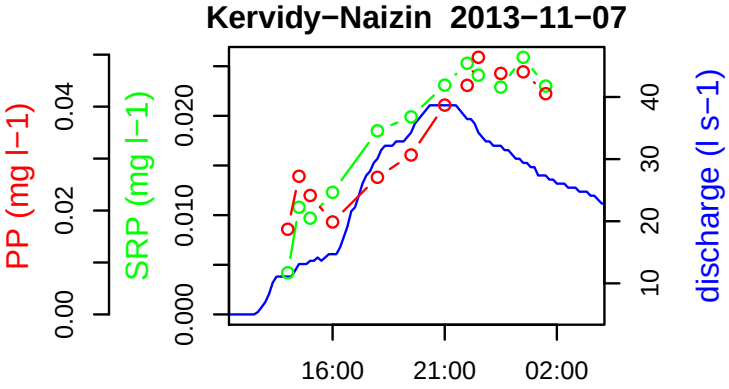
Kervidy−Naizin 2013−11−07
PP (mg l−1)
SRP (mg l−1)
discharge (l s−1)
0.00 0.02 0.04
0.000 0.010 0.020
10 20 30 40
16:00 21:00 02:00

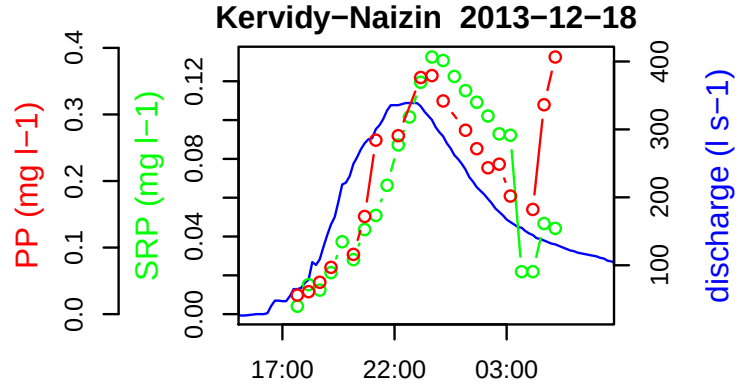
Kervidy−Naizin 2013−12−18
PP (mg l−1)
SRP (mg l−1)
discharge (l s−1)
0.0 0.1 0.2 0.3 0.4
0.00 0.04 0.08 0.12
100 200 300 400
17:00 22:00 03:00

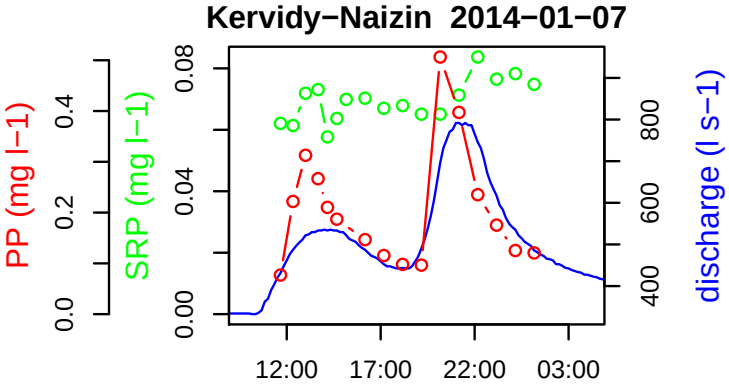
Kervidy−Naizin 2014−01−07
PP (mg l−1)
SRP (mg l−1)
discharge (l s−1)
0.0 0.2 0.4
0.00 0.04 0.08
400 600 800
12:00 17:00 22:00 03:00

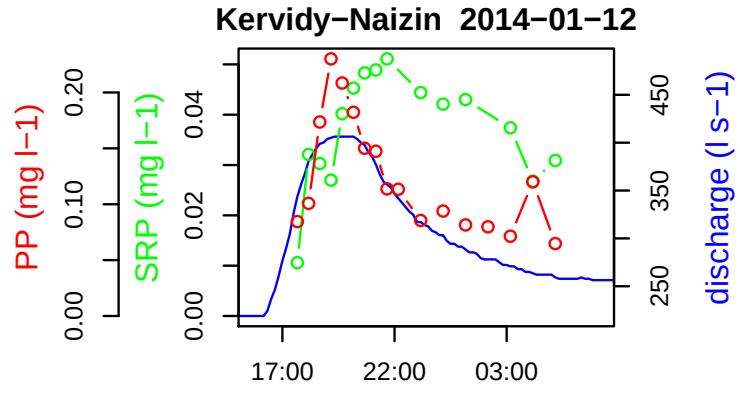
Kervidy−Naizin 2014−01−12
PP (mg l−1)
SRP (mg l−1)
discharge (l s−1)
0.00
0.10
0.20
0.00
0.02
0.04
250
350
450
17:00
22:00
03:00

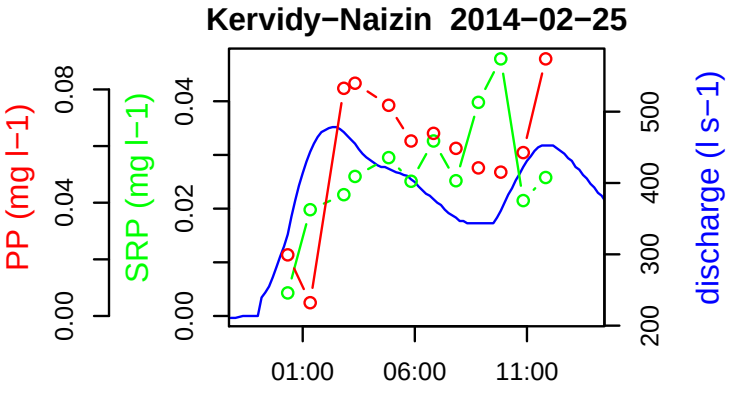
Kervidy−Naizin 2014−02−25
PP (mg l−1)
SRP (mg l−1)
discharge (l s−1)
0.00
0.04
0.08
0.00
0.02
0.04
200
300
400
500
01:00
06:00
11:00

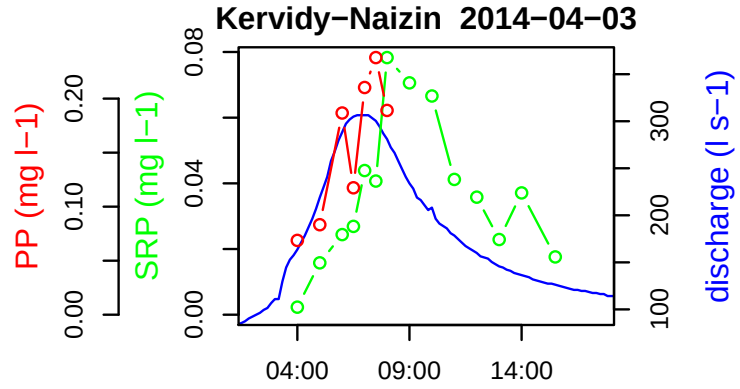
Kervidy−Naizin 2014−04−03
PP (mg l−1)
SRP (mg l−1)
discharge (l s−1)
0.00
0.10
0.20
0.00
0.04
0.08
100
200
300
04:00
09:00
14:00

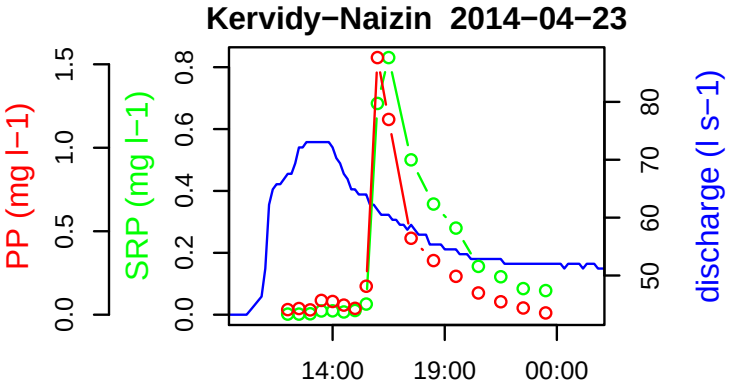
Kervidy−Naizin 2014−04−23
PP (mg l−1)
SRP (mg l−1)
discharge (l s−1)
0.0
0.5
1.0
1.5
0.0
0.2
0.4
0.6
0.8
50
60
70
80
14:00
19:00
00:00

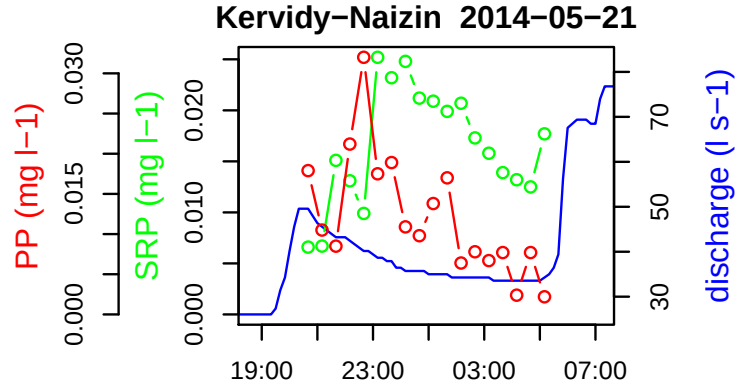
Kervidy−Naizin 2014−05−21
PP (mg l−1)
SRP (mg l−1)
discharge (l s−1)
0.000
0.015
0.030
0.000
0.010
0.020
30
50
70
19:00
23:00
03:00
07:00

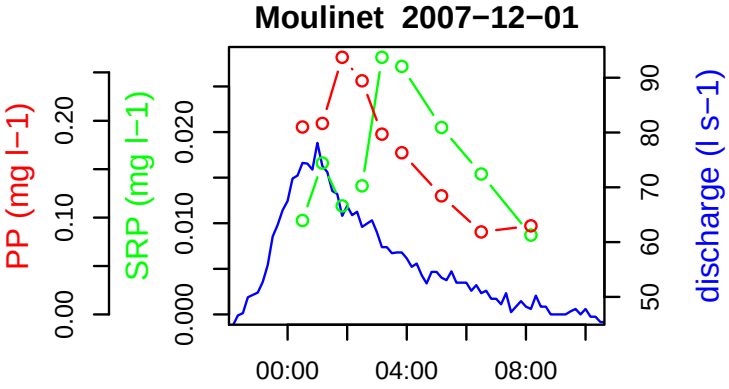
Moulinet 2007−12−01
PP (mg l−1)
SRP (mg l−1)
discharge (l s−1)
0.00
0.10
0.20
0.000
0.010
0.020
50
60
70
80
90
00:00
04:00
08:00

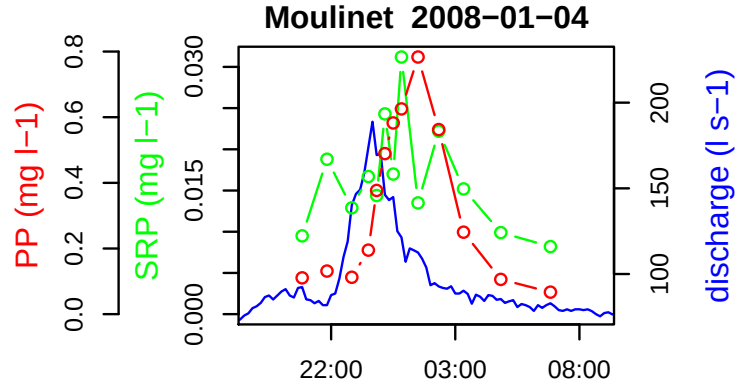
Moulinet 2008−01−04
PP (mg l−1)
SRP (mg l−1)
discharge (l s−1)
0.0
0.2
0.4
0.6
0.8
0.000
0.015
0.030
100
150
200
22:00
03:00
08:00

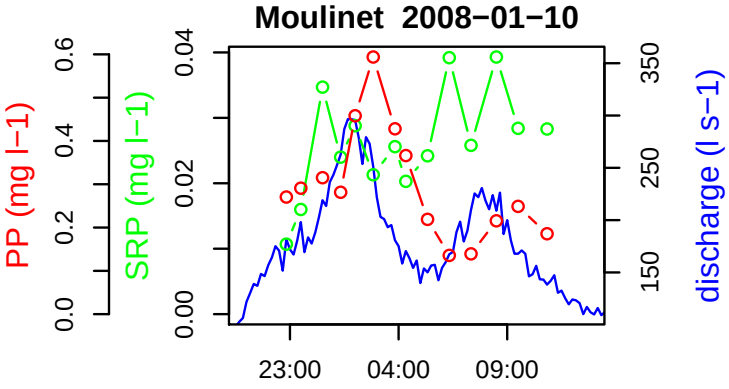
Moulinet 2008−01−10
PP (mg l−1)
SRP (mg l−1)
discharge (l s−1)
0.0
0.2
0.4
0.6
0.00
0.02
0.04
150
250
350
23:00
04:00
09:00

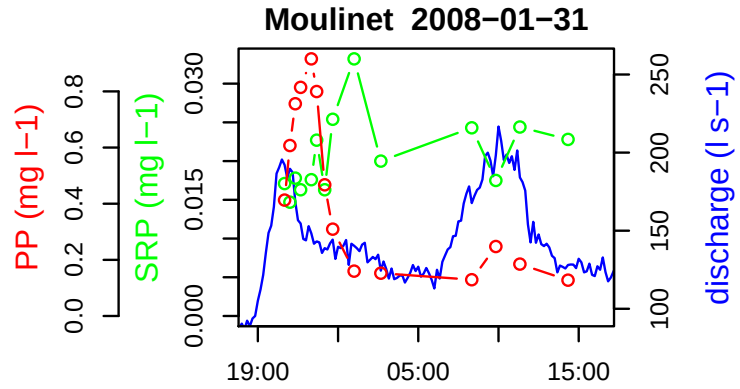
Moulinet 2008−01−31
PP (mg l−1)
SRP (mg l−1)
discharge (l s−1)
19:00
05:00
15:00

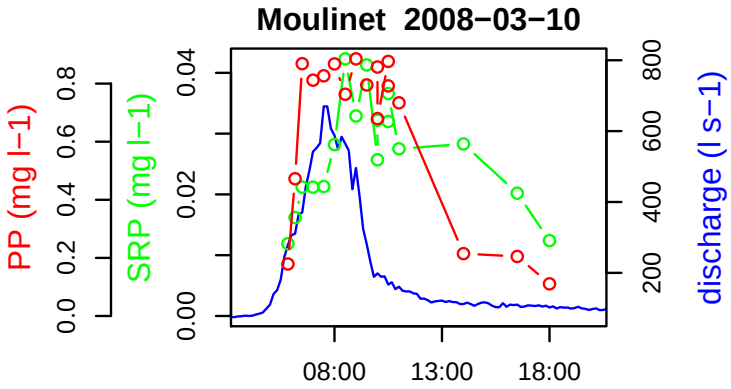
Moulinet 2008−03−10
PP (mg l−1)
SRP (mg l−1)
discharge (l s−1)
08:00
13:00
18:00

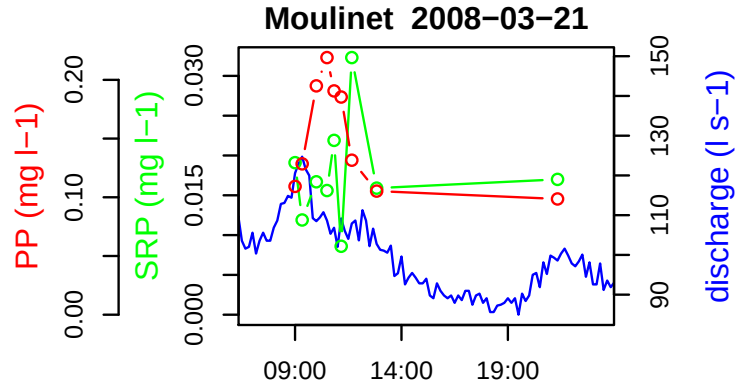
Moulinet 2008−03−21
PP (mg l−1)
SRP (mg l−1)
discharge (l s−1)
09:00
14:00
19:00

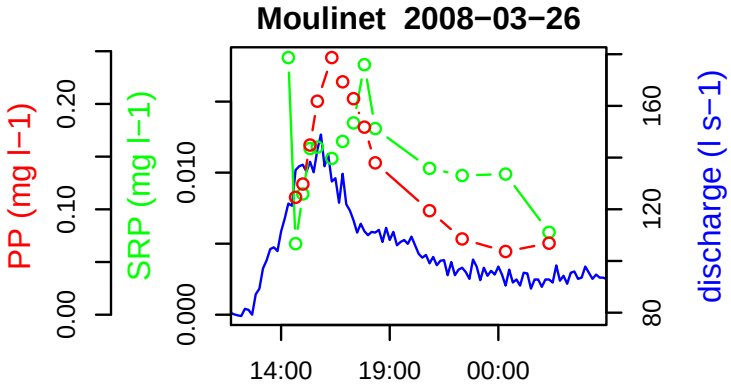
Moulinet 2008−03−26
PP (mg l−1)
SRP (mg l−1)
discharge (l s−1)
14:00
19:00
00:00

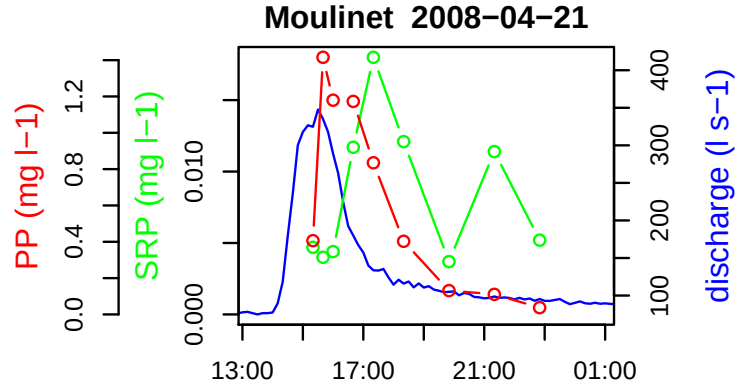
Moulinet 2008−04−21
PP (mg l−1)
SRP (mg l−1)
discharge (l s−1)
13:00
17:00
21:00
01:00

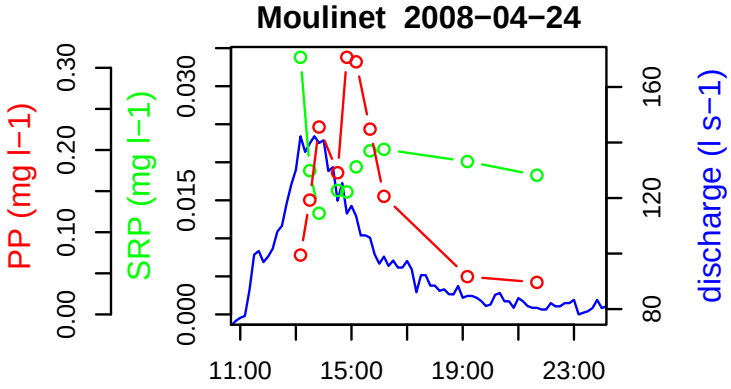
Moulinet 2008−04−24
PP (mg l−1)
SRP (mg l−1)
discharge (l s−1)
11:00
15:00
19:00
23:00

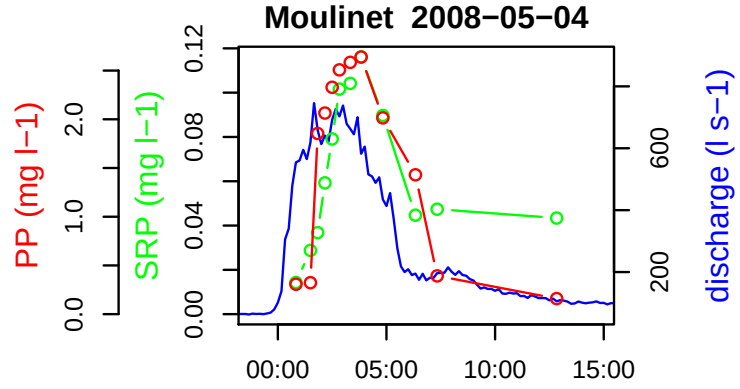
Moulinet 2008−05−04
PP (mg l−1)
SRP (mg l−1)
discharge (l s−1)
00:00
05:00
10:00
15:00

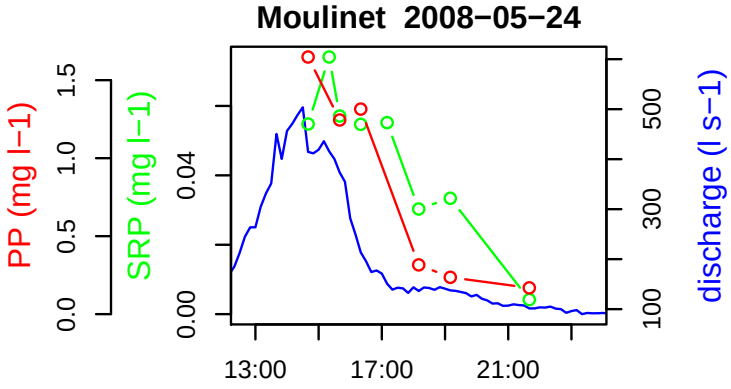
Moulinet 2008−05−24
PP (mg l−1)
SRP (mg l−1)
discharge (l s−1)
13:00
17:00
21:00

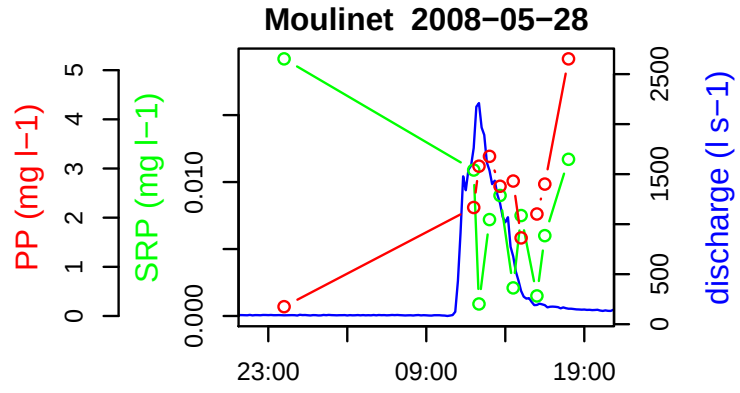
Moulinet 2008−05−28
PP (mg l−1)
SRP (mg l−1)
discharge (l s−1)
23:00
09:00
19:00

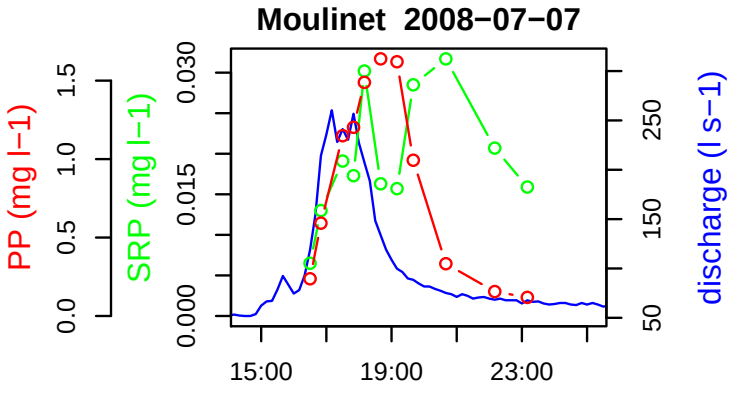
Moulinet 2008−07−07
PP (mg l−1)
SRP (mg l−1)
discharge (l s−1)
15:00
19:00
23:00

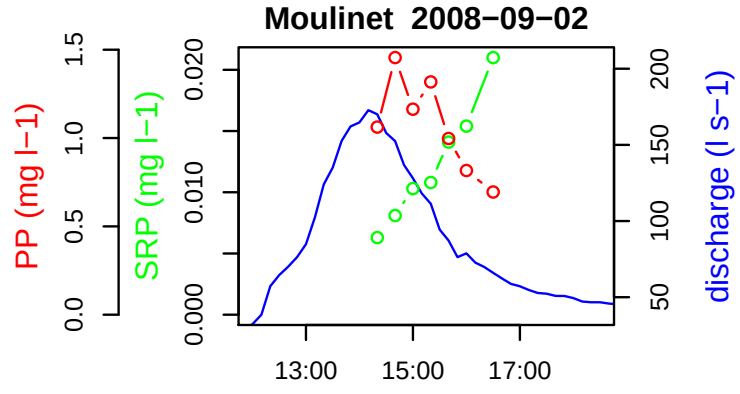
Moulinet 2008−09−02
PP (mg l−1)
SRP (mg l−1)
discharge (l s−1)
13:00
15:00
17:00

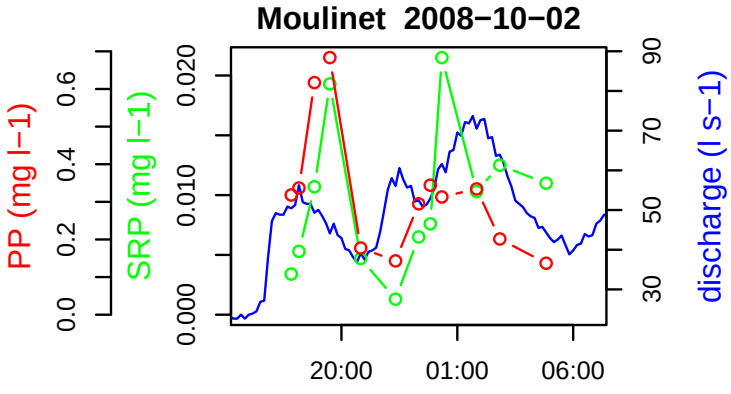
Moulinet 2008−10−02
PP (mg l−1)
SRP (mg l−1)
discharge (l s−1)
20:00
01:00
06:00

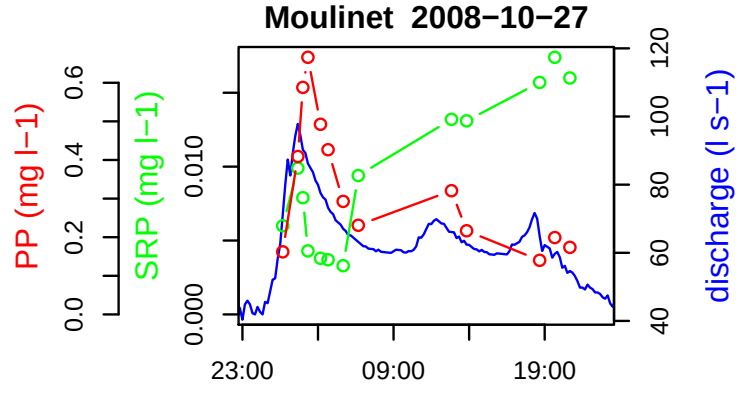
Moulinet 2008−10−27
PP (mg l−1)
SRP (mg l−1)
discharge (l s−1)
23:00
09:00
19:00

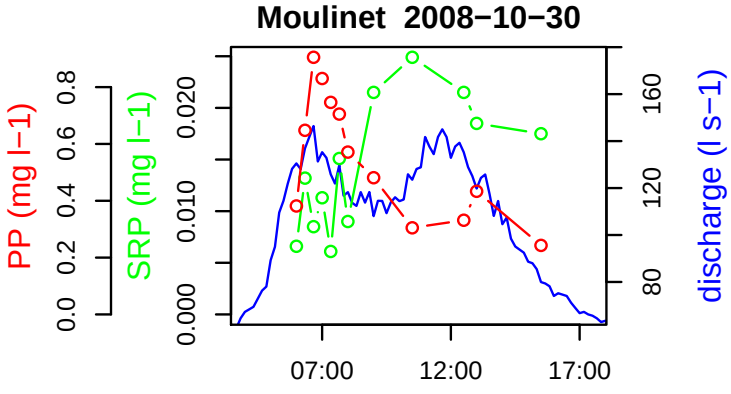
Moulinet 2008−10−30
PP (mg l−1)
SRP (mg l−1)
discharge (l s−1)
07:00
12:00
17:00

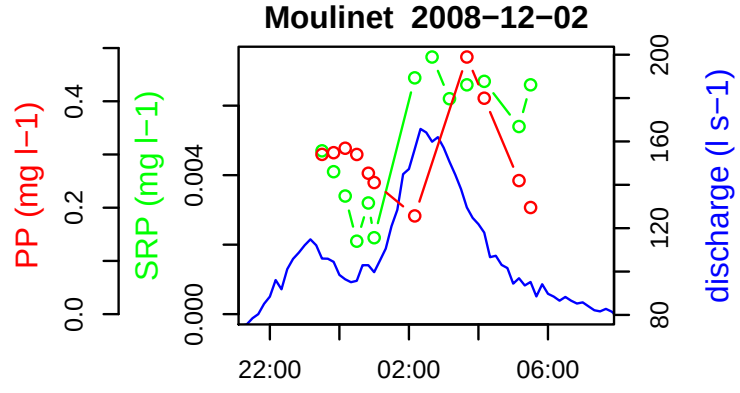
Moulinet 2008−12−02
PP (mg l−1)
SRP (mg l−1)
discharge (l s−1)
22:00
02:00
06:00

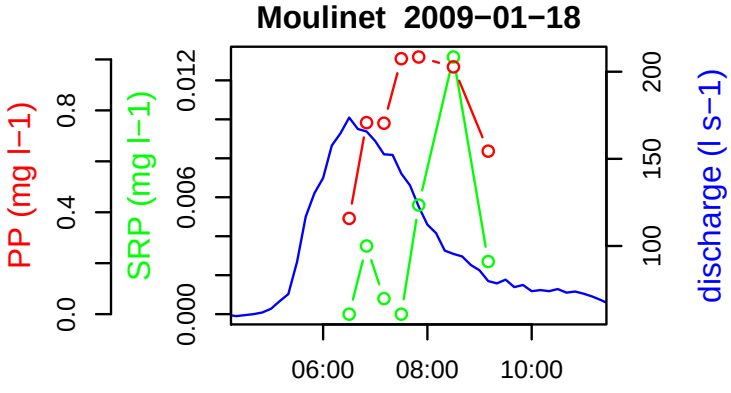
Moulinet 2009−01−18
PP (mg l−1)
SRP (mg l−1)
discharge (l s−1)
06:00
08:00
10:00

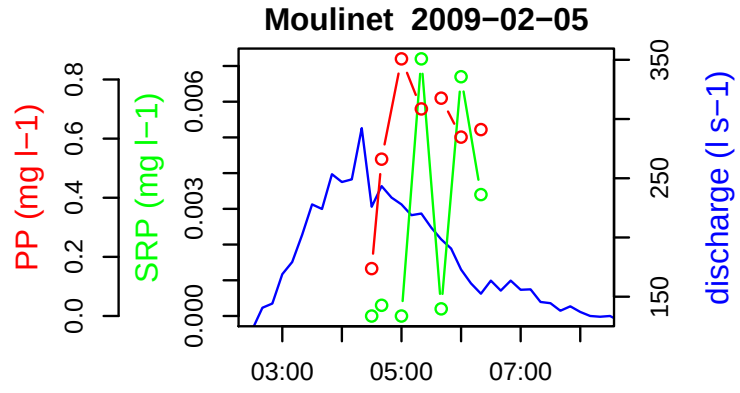
Moulinet 2009−02−05
PP (mg l−1)
SRP (mg l−1)
discharge (l s−1)
03:00
05:00
07:00

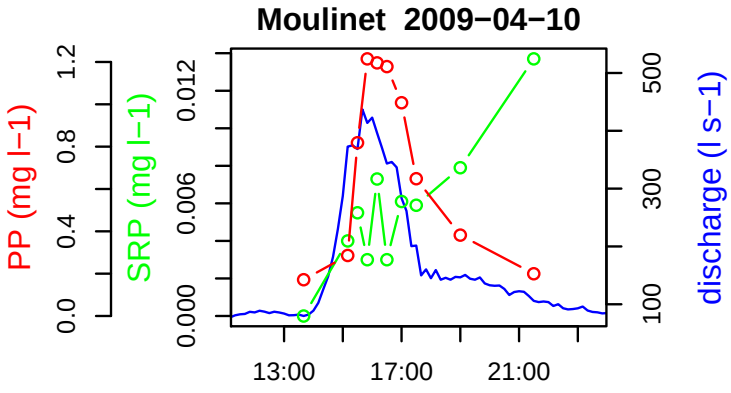
Moulinet 2009−04−10
PP (mg l−1)
SRP (mg l−1)
discharge (l s−1)
13:00
17:00
21:00

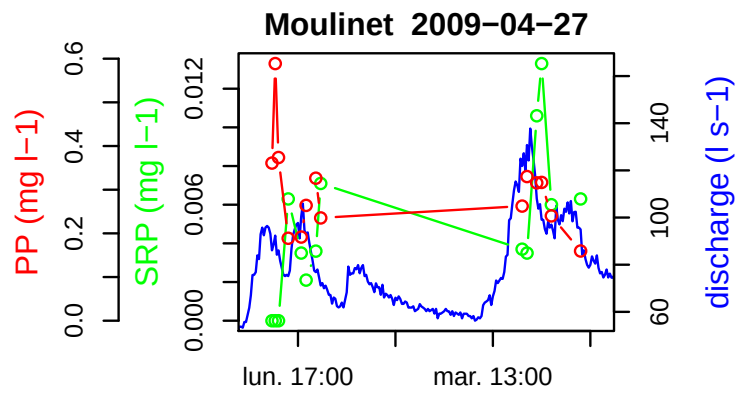
Moulinet 2009−04−27
PP (mg l−1)
SRP (mg l−1)
discharge (l s−1)
lun. 17:00
mar. 13:00

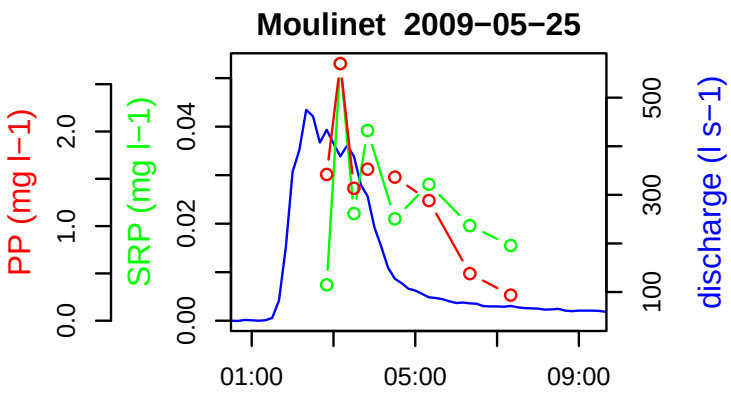
Moulinet 2009−05−25
PP (mg l−1)
SRP (mg l−1)
discharge (l s−1)
01:00
05:00
09:00

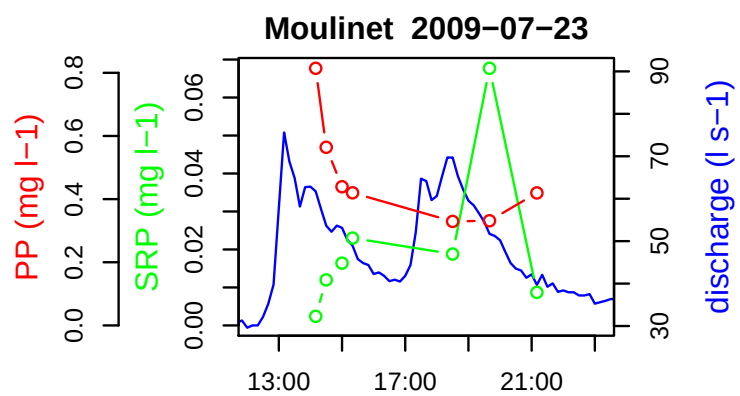
Moulinet 2009−07−23
PP (mg l−1)
SRP (mg l−1)
discharge (l s−1)
13:00
17:00
21:00

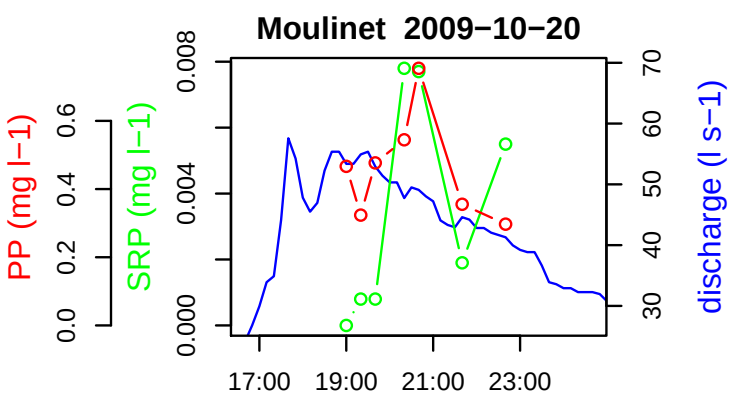
Moulinet 2009−10−20
PP (mg l−1)
SRP (mg l−1)
discharge (l s−1)
17:00
19:00
21:00
23:00

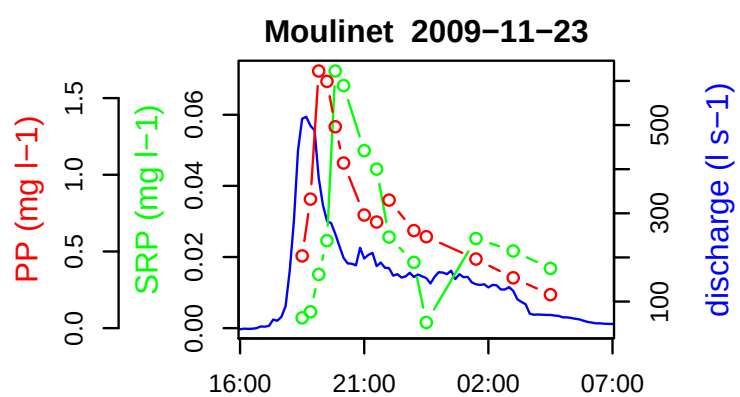
Moulinet 2009−11−23
PP (mg l−1)
SRP (mg l−1)
discharge (l s−1)
16:00
21:00
02:00
07:00

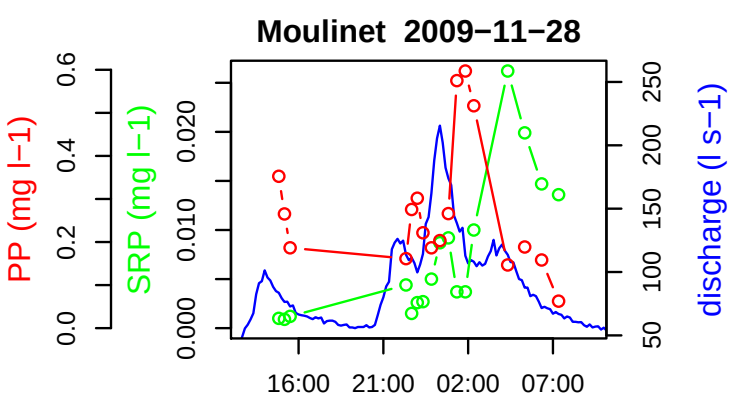
Moulinet 2009−11−28
PP (mg l−1)
SRP (mg l−1)
discharge (l s−1)
16:00
21:00
02:00
07:00

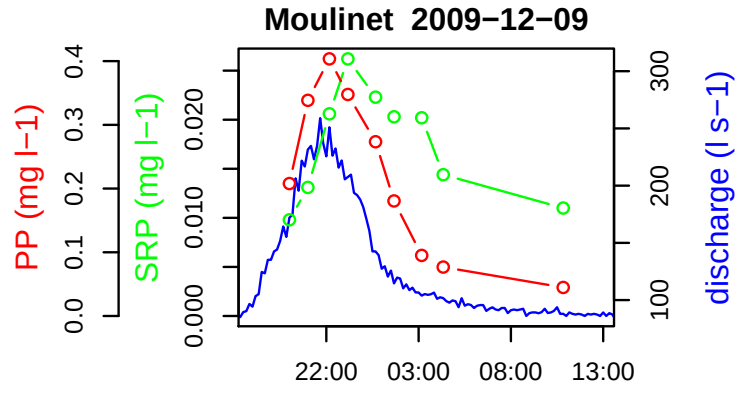
Moulinet 2009−12−09
PP (mg l−1)
SRP (mg l−1)
discharge (l s−1)
0.0 0.1 0.2 0.3 0.4
0.000 0.010 0.020
100 200 300
22:00 03:00 08:00 13:00

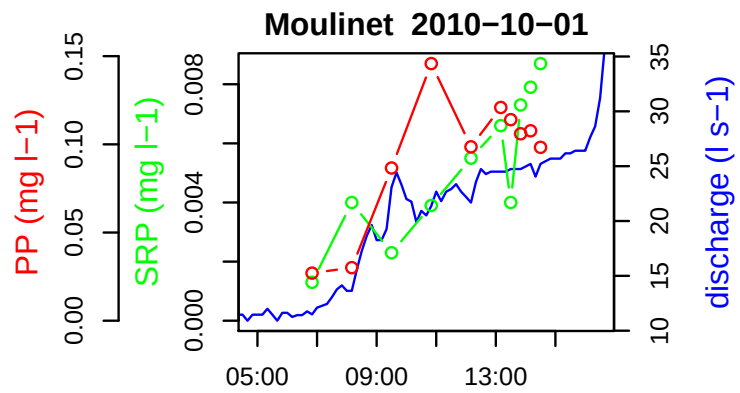
Moulinet 2010−10−01
PP (mg l−1)
SRP (mg l−1)
discharge (l s−1)
0.00 0.05 0.10 0.15
0.000 0.004 0.008
10 15 20 25 30 35
05:00 09:00 13:00

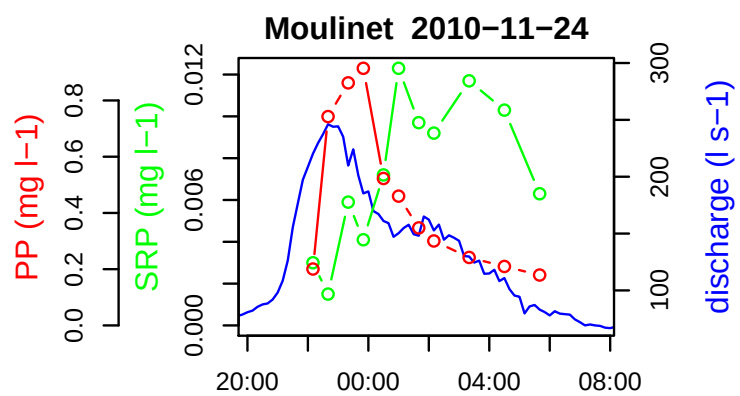
Moulinet 2010−11−24
PP (mg l−1)
SRP (mg l−1)
discharge (l s−1)
0.0 0.2 0.4 0.6 0.8
0.000 0.006 0.012
100 200 300
20:00 00:00 04:00 08:00

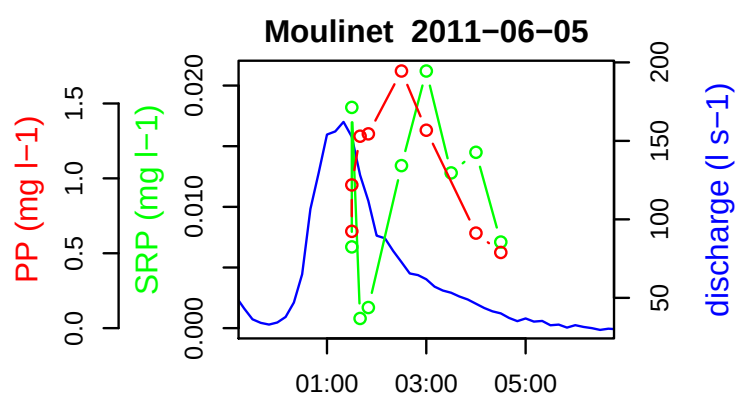
Moulinet 2011−06−05
PP (mg l−1)
SRP (mg l−1)
discharge (l s−1)
0.0 0.5 1.0 1.5
0.000 0.010 0.020
50 100 150 200
01:00 03:00 05:00

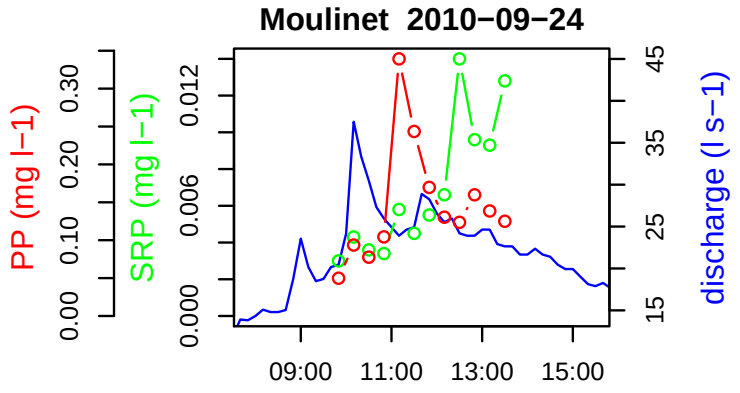
Moulinet 2010−09−24
PP (mg l−1)
SRP (mg l−1)
discharge (l s−1)
0.00 0.10 0.20 0.30
0.000 0.006 0.012
15 25 35 45
09:00 11:00 13:00 15:00

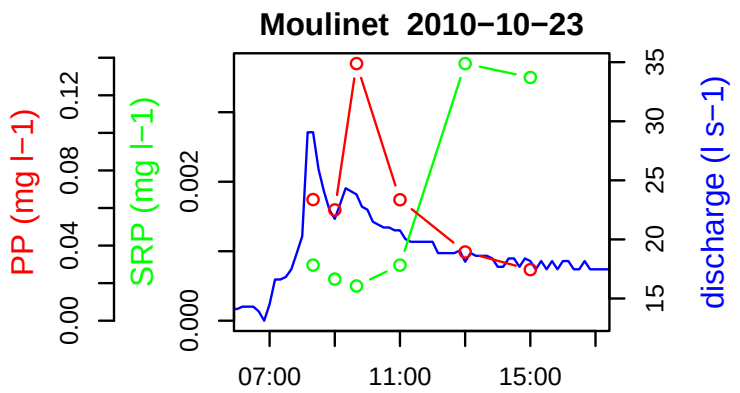
Moulinet 2010−10−23
PP (mg l−1)
SRP (mg l−1)
discharge (l s−1)
0.00 0.04 0.08 0.12
0.000 0.002
15 20 25 30 35
07:00 11:00 15:00

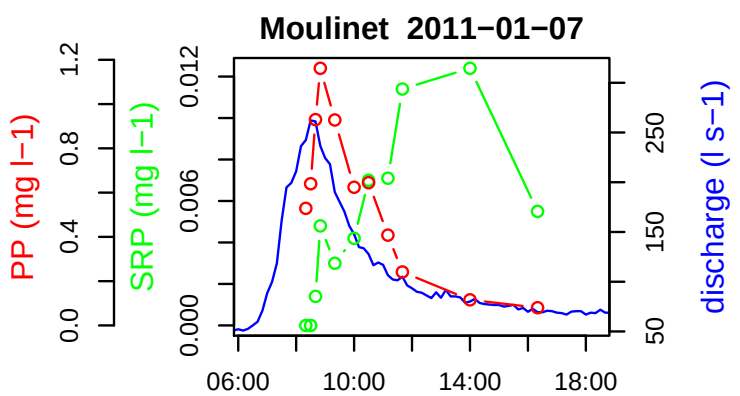
Moulinet 2011−01−07
PP (mg l−1)
SRP (mg l−1)
discharge (l s−1)
0.0 0.4 0.8 1.2
0.000 0.006 0.012
50 150 250
06:00 10:00 14:00 18:00

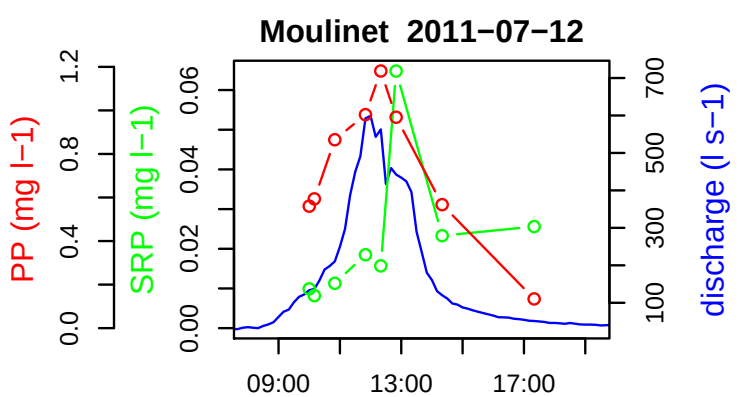
Moulinet 2011−07−12
PP (mg l−1)
SRP (mg l−1)
discharge (l s−1)
0.0 0.4 0.8 1.2
0.00 0.02 0.04 0.06
100 300 500 700
09:00 13:00 17:00

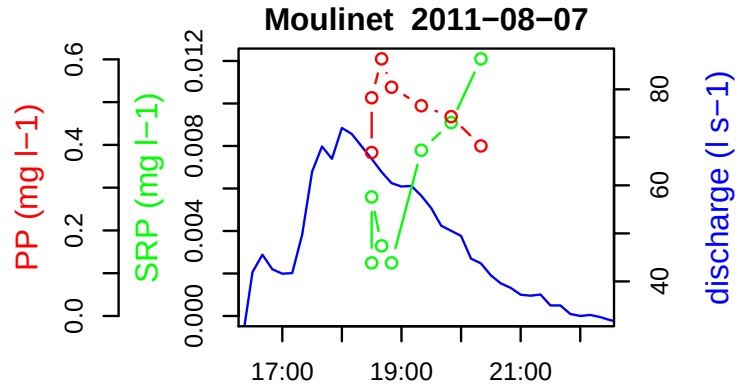
Moulinet 2011−08−07
PP (mg l−1)
SRP (mg l−1)
discharge (l s−1)
17:00
19:00
21:00

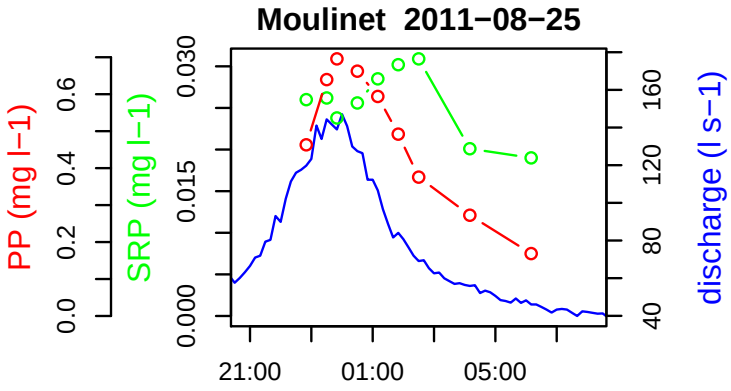
Moulinet 2011−08−25
PP (mg l−1)
SRP (mg l−1)
discharge (l s−1)
21:00
01:00
05:00

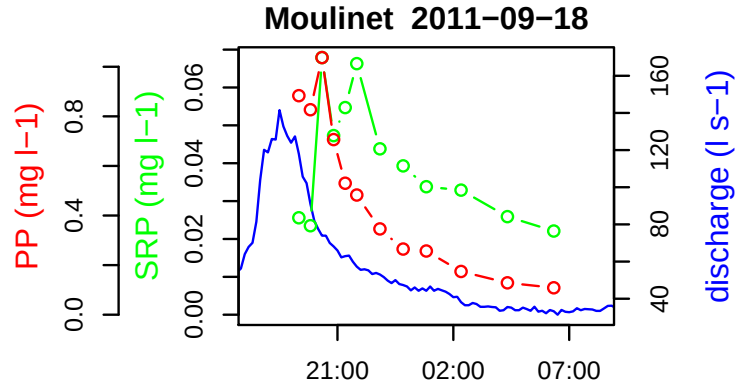
Moulinet 2011−09−18
PP (mg l−1)
SRP (mg l−1)
discharge (l s−1)
21:00
02:00
07:00

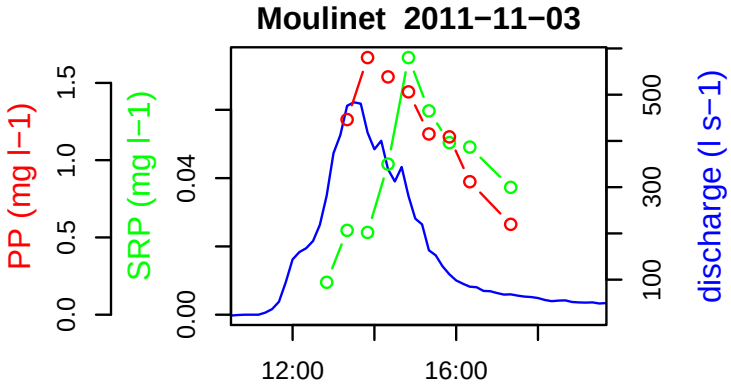
Moulinet 2011−11−03
PP (mg l−1)
SRP (mg l−1)
discharge (l s−1)
12:00
16:00

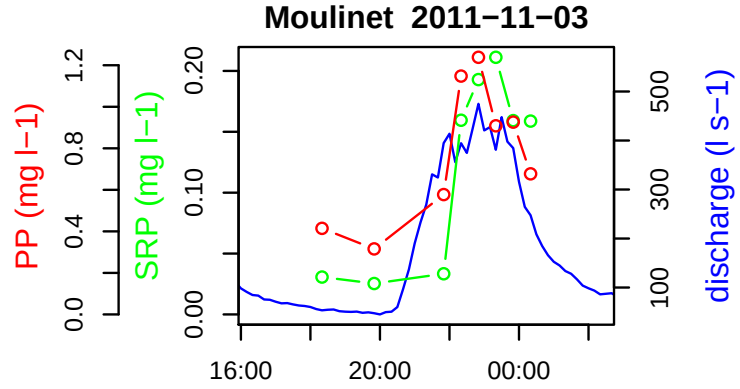
Moulinet 2011−11−03
PP (mg l−1)
SRP (mg l−1)
discharge (l s−1)
16:00
20:00
00:00

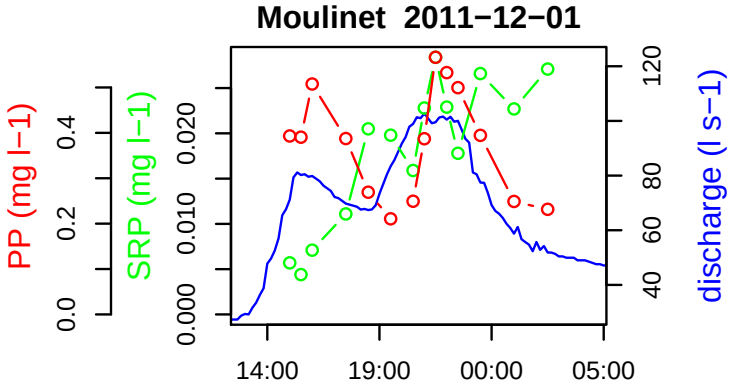
Moulinet 2011−12−01
PP (mg l−1)
SRP (mg l−1)
discharge (l s−1)
14:00
19:00
00:00
05:00

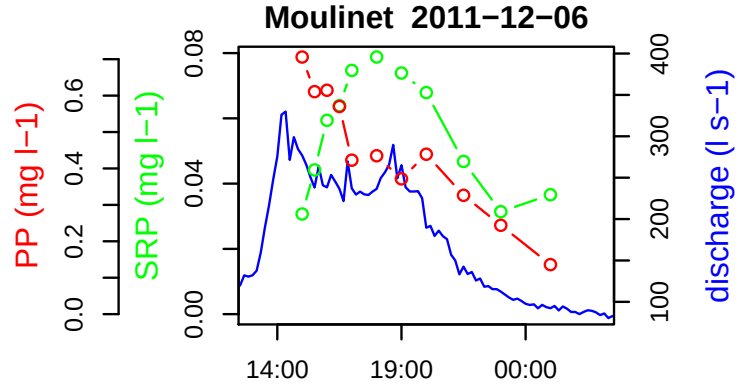
Moulinet 2011−12−06
PP (mg l−1)
SRP (mg l−1)
discharge (l s−1)
14:00
19:00
00:00

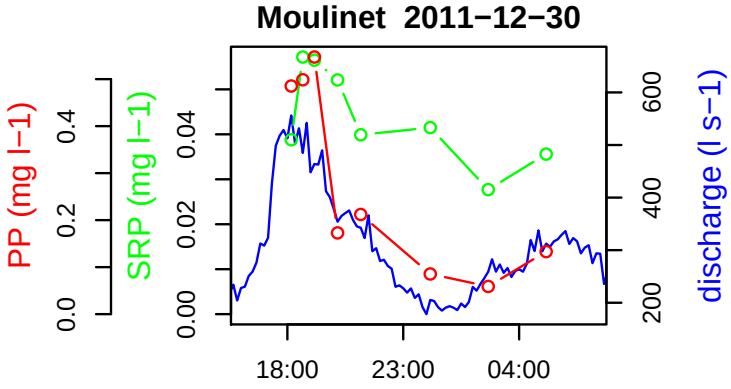
Moulinet 2011−12−30
PP (mg l−1)
SRP (mg l−1)
discharge (l s−1)
18:00
23:00
04:00

4.2 Conclusion du chapitre

Ce chapitre a permis de confirmer par une méthode différente les observations du chapitre 3 dans un bassin versant à dominance de terres arables, et de généraliser ces mécanismes à un bassin versant herbager. La non-synchronisation de l'export des formes particulaires (PP) et dissoutes (SRP) apparaît être la norme à la fois dans le bassin versant en terres arables et le bassin versant herbager. L'origine spatiale des sources et les mécanismes de transfert dominants semblent donc être les mêmes pour les deux types d'occupation du sol : le PP est majoritairement exporté par érosion de berges ou remobilisation de sédiments présents dans le cours d'eau ; le SRP est transféré depuis les zones humides ripariennes par la sub-surface.

Seuls différent entre les deux bassins versants les facteurs de contrôle responsables de la minorité d'évènements où les transferts de PP et de SRP sont synchrones, et que nous avons interprété comme résultant de transferts de surface par érosion et ruissellement dans les versants. Dans le bassin versant en terres arables, la saisonnalité des pratiques agricoles semble être un facteur de risque : l'implantation de culture de printemps peut dégrader la structure des sols et générer du ruissellement à une période de l'année où ont lieu les épandages. Dans le bassin versant herbager, il apparaît que l'occurrence de ces évènements est surtout contrôlée par l'amplitude des crues : seules les plus grosses pluies sont à même de générer des transferts de surface entre les versants et le cours d'eau. Au-delà des mécanismes mis en évidence, ce chapitre a présenté une méthode d'analyse des données en crue utile pour étudier plusieurs paramètres à la fois et quand les hydrogrammes ont des formes différentes. Cette méthode devrait s'avérer particulièrement utile avec la mise en place de dispositifs de suivi à très haute fréquence et multi-paramètres dans plusieurs bassins versants de recherche dans le monde, qui s'accompagne d'un grand nombre de données à analyser. Dans ce chapitre, les données utilisées proviennent de prélèvements par échantillonneurs automatiques, ce qui pose la question de leur qualité du fait des problèmes de stockage des échantillons dans ces préleveurs, de la difficulté à bien suivre les crues, et de la taille limité de l'échantillon de crues malgré un travail de terrain de longue haleine. Il serait intéressant d'appliquer cette méthode à d'autres jeux de données, où le nombre de crues suivies est plus élevé et où d'autres éléments sont suivis en crue (C, N).

Le chapitre suivant (chapitre 5) vise à préciser les mécanismes biogéochimiques mis en évidence aux chapitres 3 et 4, par un suivi des concentrations en phosphore dans la solution libre du sol dans le bassin versant de Kervidy-Naizin.

Chapitre 5

Rôle de la nappe dans le transfert de phosphore dissous

Ce chapitre s'appuie sur un article publié dans Water Research.

> Dupas R, Gruau G, Gu S, Humbert G, Jaffrezic A, Gascuel-Odoux C. Groundwater control of biogeochemical processes causing phosphorus release from riparian wetlands. Water Research 2015 ; 84.

Il repose sur le suivi in-situ de la chimie de l'eau du sol dans deux zones humides du bassin de Kervidy-Naizin au cours de l'année hydrologique 2013 – 2014. Ce suivi a été rendu possible grâce à une collaboration avec l'ANR MOSAIC, en particulier le travail de thèse de Guillaume Humbert. Des analyses complémentaires sont présentées à la suite de cet article ; elles présentent le suivi de voies de transfert non présentées dans l'article (drainage, ruissellement de surface) et des perspectives pour une analyse couplée Carbone – Phosphore.

Ce chapitre apporte des éléments de réponse à la question 2, rappelée ici :

Question 2 : Quel est le rôle de la nappe dans le transfert de phosphore dissous ? Agit-elle uniquement sur le transfert en provoquant une connexion hydrologique entre les sols et la rivière, ou agit-elle aussi sur la solubilisation du phosphore dans les sols ?

5.1 Groundwater control of biogeochemical processes causing phosphorus release from riparian wetlands

Résumé

Du fait de la forte affinité d'adsorption du phosphore (P) pour la phase solide des sols, les plans d'actions pour réduire le transfert diffus de P se concentrent généralement sur les formes particulaires et le transfert de surface. On a donc encouragé la mise en place de zones tampon entre les parcelles cultivées et les cours d'eau, parfois dans des zones humides. Pour étudier le risque que ces zones humides ripariennes (ZHR), qui de par leur position dans les versants piègent et accumulent du P, relarguent du P dissous vers les cours d'eau, nous avons suivi la concentration en phosphore réactif au molybdate (MRP) dans la solution de sol de deux ZHR situées dans un bassin versant agricole. Deux mécanismes principaux relarguent du MRP sous le contrôle des fluctuations de nappe. Le premier mécanisme est lié au flush d'un pool de P mobile, de taille limitée, présent dans les sols au moment de leur réhumectation à l'automne. La mobilisation de ce pool a lieu en condition de saturation des sols en eau au moment de la première remontée de nappe. Le second mécanisme intervient en conditions anoxiques à la fin de l'hiver, quand la réduction des (hydr)oxydes de Fer s'accompagne d'un relarguage de MRP. La comparaison des sites d'échantillonnage montre que le premier pic ne se produit que dans les ZHR où la une teneur en P du sol est élevée, tandis que le second est observé également dans les ZHR où la teneur en P du sol est basse. Les variations saisonnières de concentration dans la solution du sol des ZHR sont similaires à celles observées dans le cours d'eau. Ainsi, les ZHR sont un compartiment important dans la cascade du phosphore dans les paysages agricoles, en permettant la conversion du P particulaire qu'elles reçoivent en P dissous transféré au cours d'eau.

Abstract

Because of the high sorption affinity of phosphorus (P) for the soil solid phase, mitigation options to reduce diffuse P transfer usually focus on trapping particulate P delivered via surface flow paths. Therefore, placing riparian buffers between croplands and watercourses has been promoted worldwide, sometimes in wetland areas. To investigate the risk of P-accumulating riparian wetlands (RWs) releasing dissolved P into streams, we monitored molybdate-reactive P (MRP) in the soil pore water of two RWs in an agricultural watershed. Two main mechanisms released MRP under the control of groundwater dynamics. First, soil rewetting after the dry summer period was associated with the presence of a pool of mobile P, limited in size. Its mobilization started under water saturated conditions caused by a rise in groundwater. Second, anoxic conditions at the end of winter caused reductive dissolution of Fe (hydr)oxides along with a release of MRP. Comparison of sites revealed that the first MRP release occurred only in RWs with P-enriched soils, whereas the second was observed even in RWs with low soil P status. Seasonal variations in stream MRP concentrations were similar to concentrations in RW soils. Hence, RWs can act as a key component of the P transfer continuum in agricultural landscapes by converting particulate P from croplands into MRP transferred to streams.

5.1.1 Introduction

In agricultural landscapes, riparian wetlands (RWs) are highly reactive biogeochemical interfaces located between croplands and watercourses (Vidon *et al.*, 2010).

Due to their topographic position in valley bottoms, fluxes of sediments, nutrients and pesticides converge in these zones. Therefore, establishment of vegetated buffers has been promoted in riparian areas worldwide to reduce pollutant transfer to streams. Riparian wetlands have proved effective in sediment retention (Ockenden *et al.*, 2014), denitrification (Anderson *et al.*, 2014 ; Oehler *et al.*, 2007) and microbial degradation of pesticides (Maillard and Imfeld, 2014). Their role in the phosphorus transfer continuum is less clear. Generally, RWs help decrease P delivery to watercourses by trapping particulate P and, to a lesser extent, sorbing dissolved P forms (Dorioz *et al.*, 2006 ; Hoffmann *et al.*, 2009).

However, RWs may also act as P sources for surface waters. This is due to the periodic water table fluctuations that affect these zones, which lead to a succession of dry periods and water-saturated periods (Obour *et al.*, 2011 ; Song *et al.*, 2007). Such unstable hydraulic conditions can increase P release from soil microbial biomass (Blackwell *et al.*, 2010). Several laboratory studies have shown that soil rewetting after a dry period could lead to osmotic shock, causing microbial cell lysis and subsequent release of microbial P (e.g. Turner and Haygarth, 2001). According to Blackwell *et al.* (2009), up to ca. 70% of soil microbial biomass can be killed by osmotic shock caused by rewetting, with large variability in the amount of P released, depending on its recycling rate. Additionally, the periodic water table rises that affect RWs can modify the redox status of Fe (hydr)oxides, i.e. an important P sorbing compound in acidic soils (Li *et al.*, 2012 ; Surridge *et al.*, 2012). Anoxic conditions resulting from a high water table and low flow velocity can cause reductive dissolution of Fe (hydr)oxides in RW soils (Jeanneau *et al.*, 2014 ; Knorr, 2013 ; Lambert *et al.*, 2013 ; Li *et al.*, 2012), which may cause release of previously adsorbed P (Carlyle and Hill, 2001 ; Hoffmann *et al.*, 2009).

The presence of permanent vegetation in RWs can make biological P cycling in soils more intense than that in croplands as a result of more diversified plant and microbial communities (Roberts *et al.*, 2012 ; Stutter *et al.*, 2009). Permanent vegetation also results in high organic matter levels in RW soils, i.e. an important source of colloids (Haygarth *et al.*, 2006), and provides favorable conditions for macropore formation. Hence, subsurface transfer of mobile P forms via preferential flow can be increased (Gachter *et al.*, 1998 ; Haygarth *et al.*, 1997).

Although several laboratory experiments have highlighted mechanisms potentially involved in P solubilization and mobilization in RW soils (references above), a thorough literature search showed a lack of evidence regarding their contribution to diffuse P transfer in field conditions or the role of water table dynamics. In this study, we used zero-tension lysimeters to monitor molybdate-reactive P (MRP) concentrations in the free soil solution of two RWs in an intensively farmed watershed. The research questions addressed are : i) Does soil rewetting after a dry period and Fe (hydr)oxides reduction release MRP in RWs, and how are these production mechanisms linked to water table dynamics ? ; ii) Can we relate MRP concentrations in streams with P-release mechanisms in RW soils ? ; and, iii) Which soil factors control the spatial variability of P-release mechanisms in RWs ?

5.1.2 Materials Methods

Study sites

The monitored RWs were located in Kervidy-Naizin, a 5 km^2 agricultural watershed belonging to the Agrhys environmental research observatory (http ://www6.inra.fr/ ore_agrhys_eng) in Brittany, France (Aubert *et al.*, 2013 ; Aubert *et al.*, 2014). The Kervidy-Naizin watershed is drained by a stream of second Strahler order. Climate is temperate oceanic, with a mean annual (2007 – 2013) temperature of 10.6 ° C and annual rainfall of 867 mm. Lithology consists of impervious Brioverian schists capped by up to 30 m of unconsolidated weathered materials, in which a shallow aquifer develops. The schist contains mainly quartz, muscovite and chlorite and, to a lesser extent, K-feldspar and plagioclase (Pauwels *et al.*, 1998). The weathered schist is not likely to be a source of MRP in the watershed as mean MRP concentration measured below the soil depth (1m) was 7 $\mu g\ l^{-1}$ (unpublished results), which is lower than the long term mean baseflow concentration in the stream (18 $\mu g\ l^{-1}$, Dupas *et al.*, 2015). Soils are silty loams, classified as Luvisols. They are well-drained in the upland domain and hydromorphic in valley bottoms, where RWs develop. Agricultural activities are dominated by arable crops (cereals, maize) and animal production (pigs, dairy cows).

We confined investigations to two RWs at the footslope of two transects equipped with piezometers (Molenat *et al.*, 2008)(Fig 1). Transect A ranged in elevation from 110 to 120 m a.s.l. with a mean slope of 3.8% (max=6%). The RW in transect A was 51 m wide, and its vegetation consisted of unfertilized herbaceous species (Dactylis glomerata and Agrostis canina). Winter barley (Hordeum vulgare) was grown in the adjacent field during the study period (October 2013 – May 2014). Soil P content (0 – 15 cm) in this field was 315 mg P kg^{-1} extractable P (Dyer method NF X 31-160) and 1283 mg P kg^{-1} total P (NF X 31-147). Pig slurry was applied on this field on April 9, 2014 (61 kg P ha^{-1}). Transect B ranged in elevation from 104 to 109 m a.s.l. with a mean slope of 2.8% (max=4.5%). The RW in transect B was 64 m wide, and its vegetation consisted of shrubs and trees (Populus negro, Salix caprea, Betula alba). The adjacent field was left fallow during the study period, but maize (Zea mays) residues remained on the soil surface. Soil P content (0 – 15 cm) in this field was 157 mg P kg^{-1} extractable P (Dyer method NF X 31-160) and 1244 mg P kg^{-1} total P (NF X 31-147). Pig slurry was applied on this field on May 2, 2014 (52 kg P ha^{-1}). Both RWs were managed as unfertilized riparian buffers for 20 years without exportation of biomass. Prior to conversion into a buffer-zone, RW A received up to 60 kg P ha^{-1} yr^{-1} as pig slurry and mineral fertilizer, whereas RW B received P input from grazing cattle (unquantified inputs).

Soil and water sampling

Soil cores and soil pore water were sampled at two sites within each of the two RWs (WetUp and WetDown). In transect A, WetUp A was 13 m downslope from the wetland-field interface and WetDown A was 40 m downslope from the interface. In transect B, distances from the wetland-field interface were 9 m and 52 m for WetUp B and WetDown B, respectively. The aim of this sampling design was to investigate the variability of soil P content and water table level, and their effect on soil MRP concentrations, along the flowpaths between the upslope and downslope side of the RWs (Figure 5.1).

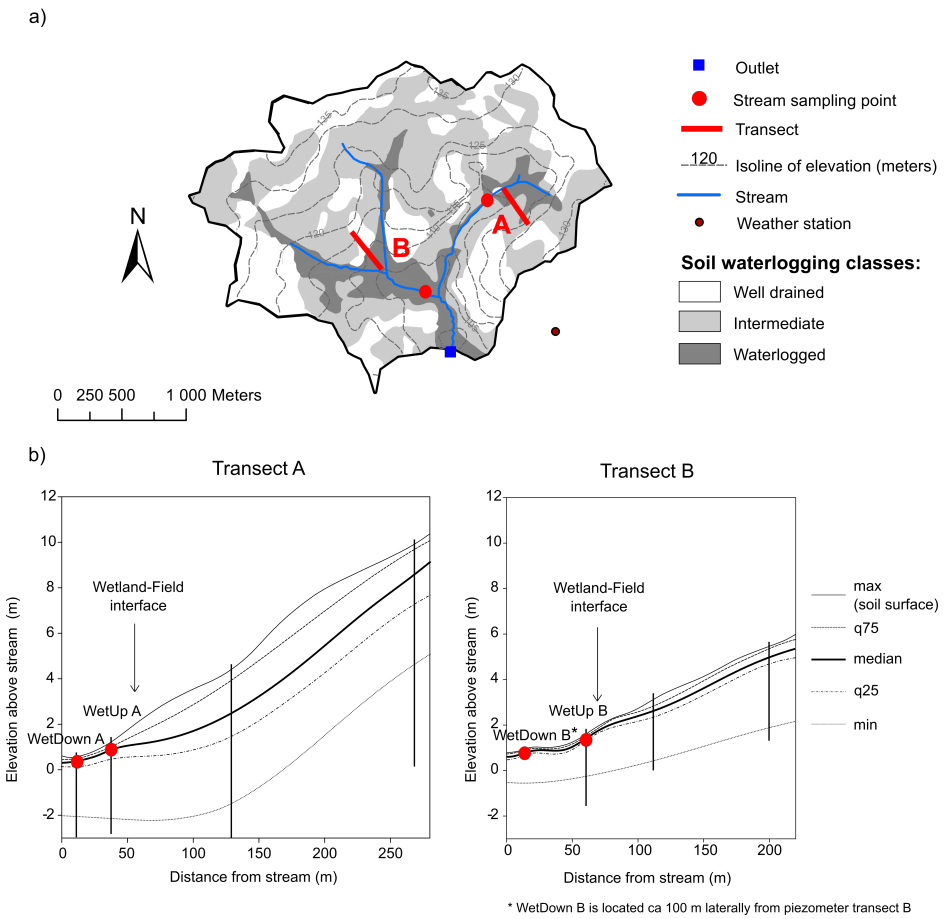

FIGURE 5.1 – a) map of the Kervidy-Naizin catchment ; b) location of the sampling sites (red dots) and variability in water table level along the two transects. Vertical lines represent piezometers (depth 3 – 8 m ; screening 1.5 – 4 m).

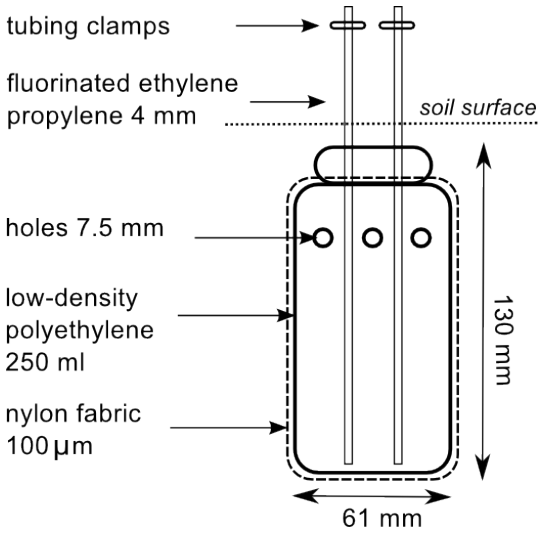

FIGURE 5.2 – Zero-tension lysimeter (adapted from Bourrie *et al.*, 1999)

Soil cores in the 0 – 15 cm and 25 – 40 cm horizons were collected with a 75 mm diameter sampler at each of the four sites in April 2014. WetDown B was only sampled in the surface due to water saturated soils below 15 cm. Soil pore water was collected with zero-tension lysimeters placed in triplicates (spaced ca. 1 m apart) at 10 – 15 cm and 50 – 55 cm depths, i.e. in the same soil horizons as the soil cores. The lysimeters were designed to collect free soil solution while maintaining in-situ anoxic conditions (Figure 5.2). After an equilibration period of three months, the 24 lysimeters were sampled weekly from October 2013 to January 2014 and every two weeks from February 2014 to May 2014. From June to October, soil moisture was too low to collect soil solution.

Grab samples of stream water were collected at the same frequency downstream of the monitored RWs, and daily at the outlet of the 5 km^2 watershed. Because we were interested in subsurface transfer, we focused analyses on baseflow concentrations by discarding grab samples collected during storms (surface runoff may contribute to storm flow). We considered storms as events with $>$ 10% discharge rise and $>$ 20 l s^{-1} discharge (Dupas *et al.*, 2015). All samples were filtered ($<$ 0.45 μm cellulose acetate filter) within 6 h after collection and kept refrigerated until analysis within 3 days.

Soil and water chemical analyses

Soil samples were air-dried, sieved to $<$ 2 mm and analyzed for particle size fractions (NF X 31-107), organic matter/nitrogen/carbon contents (NF ISO 13878, NF ISO 10694), pH in water (1 :5 v :v water extraction NF ISO 10390) , extractable P (Dyer method, i.e. 1 :5 w/v extraction with citric acid 20 g l^{-1} NF X 31-160), total P (ICP-AES after total solubilization with hydrofluoric and perchloric acid NF X 31-147), Al and Fe (ICP-AES after extraction with ammonium oxalate and oxalic acid, according to Tamm 1922) (Table 5.1). Equilibrium P concentration (EPCo) and maximum sorption capacity (Qmax) were estimated from 6-point batch isotherms (0, 0.1, 0.5, 50, 100, 200 mg P l^{-1} ; 1 :25 w :v)

in 0.01M CaCl2 according to Graetz and Nair (2000). One drop of chloroform was added to inhibit microbial activity. After 24 h equilibration at 20±2 ° C, samples were centrifuged (3000 rpm ; 10 min), filtered (< 0.45 μm) and analyzed for MRP. Qmax was determined by fitting a Langmuir equation (Van der Zee and Bolt, 2001) to the last three points (50, 100, 200 mg P l^{-1}) :

$$Q = (c * K * Qmax)/(1 + K * c)$$

where c is the concentration of P in the equilibrium solution (mg l^{-1}), Q is the total amount of P sorbed (mg mg^{-1}) and K is an affinity parameter (l mg^{-1}). EPCo represents the solution P concentration at which no net sorption or desorption of P would occur between soil and solution (Stutter and Lumsdon, 2008). EPCo was determined by fitting a linear equation to the first three points (0, 0.1, 0.5 mg P l^{-1}). We consider EPCo as a reference MRP concentration in the soil solution, which we can compare to the actual MRP concentration of soil solution collected in-situ. Qmax served to calculate "Degree of P Saturation" (DPS), defined here as the ratio of Extractable P to Qmax. DPS is an index of P accumulation in the soil, either via direct application of fertilizers or enrichment via erosion (Schoumans and Chardon, 2015).

For each water sample collected in lysimeters or in the stream, MRP was determined colorimetrically by reaction with ammonium molybdate (ISO 15681). Because filtrates $<$ 0.45 μm can contain colloidal forms of molybdate reactive phosphorus, we chose to use the term MRP rather than soluble reactive phosphorus (Haygarth and Sharpley, 2000). Precision of MRP measurement was ±4 μg l^{-1}. Fe^{2+} was analyzed using the 1.10 phenantroline colorimetric method, according to AFNOR NF T90-017, with a precision of 5%. Nitrate concentration was measured by ionic chromatography (DIONEX DX 100), with a precision of 2.5%.

5.1.3 Results and discussion

Soil P content and water table depths in riparian wetlands

Soil total P content at WetUp A and B was 13% and 33% higher than that at WetDown A and B, respectively (Figure 5.3). A probable explanation for the higher soil P levels on the upslope side of the RWs is that P delivery from the adjacent fields has enriched RWs in P (Ockenden *et al.*, 2014). Previous studies in the Kervidy-Naizin watershed have indeed evidenced that its loamy soils are vulnerable to erosion, which leads to spatial redistribution of soil and nutrients across the landscape (Le Bissonnais *et al.*, 2002). Long-term monitoring in a larger number of sites would be necessary to quantify the importance of P accumulation in RWs at the watershed scale. Such a monitoring is however beyond the scope of this study, which focuses on the role of groundwater dynamics in P remobilization in RWs.

Overall, data show contrasting hydrologic and soil conditions between the two RWs and within each RW. Mean water table level was shallower in RW B than in RW A (Figure 5.1), whereas soil P content and DPS were lower in RW B than in RW A (Figure 5.3). The legacy of past P inputs prior to conversion of these zones into unfertilized buffers, along with different rates of P enrichment from adjacent fields, are two possible explanations for the differences in soil P content between RW A and RW B (Dunne *et al.*, 2011 ; Jarvie *et*

TABLE 5.1 – Soil properties in the riparian wetlands studied

Site	WetUp A		WetDown A		WetUp B		WetDown B
Depth (cm)	0 – 15	25 – 40	0 – 15	25 – 40	0 – 15	25 – 40	0 – 15
Clay ($<$ 2 μm) g kg^{-1}	241	263	233	250	288	248	354
Silt (2 – 50 μm) g kg^{-1}	615	584	589	574		599	583
603							
Sand (50 – 2000 μm) g kg^{-1}	205	223	268	271	169	265	57
Organic carbon g kg^{-1}	40.9	9.5	37.1	10.7	60.2	14.8	89.1
Organic nitrogen g kg^{-1}	3.7	1.2	3.3	1.4	4.7	1.4	6.4
C :N ratio	11.2	7.7	11.2	7.9	12.9	10.3	14.0
Organic matter g kg^{-1}	70.7	16.5	64.2	18.5	104.0	25.6	154.0
pH	6.1	6.3	6.1	6.4	6.2	6.0	5.9
Dyer P mg kg^{-1}	288.5	65.9	241.8	62.8	47.6	4.4	12.2
Al (Tamm method) mg kg^{-1}	1690	1470	1410	1570	1710	1090	1560
Fe (Tamm method) mg kg^{-1}	4250	3340	6000	7220	7710		1480
10200							
Total P mg kg^{-1}	1213.2	375.3	1051.7	384.5	680.8	198.6	458.2
DPS %	21	10	14	7	3	1	1
EPCo μg l^{-1}	127.2	21.0	83.1	4.3	4.1	$<$ 4	$<$ 4
Soil solution MRP (mean$\pm$standard deviation) μg l^{-1}	220$\pm$86	60$\pm$73	126$\pm$43	60$\pm$81	16$\pm$20	6$\pm$8	6$\pm$6

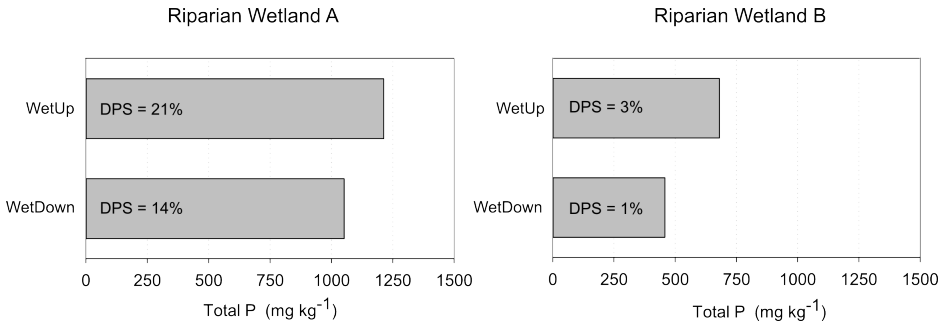

FIGURE 5.3 – Total P content and Degree of P Saturation (DPS) in the 0-15 cm soil layer in four wetland sites.

al., 2013 ; Sharpley *et al.*, 2013). Within each RW, opposite gradients of mean water table and soil P content were observed, with higher soil P content on the upslope side close to the cropped field (WetUp) and a shallower water table on the downslope side (WetDown).

Groundwater level controls P release in riparian wetlands

In both RW A and B, MRP concentrations in the soil solution appeared strongly linked to water table dynamics and/or stagnancy (Figure 5.4 and 5.5).

At the beginning of the hydrological year (October – December), when the water table level was below -15 cm, soil MRP concentrations displayed a decreasing vertical gradient at all sites, reflecting the vertical gradient of soil extractable P (Table 1). Mean MRP concentrations from October 17th to December 10th were strongly correlated to the theoretical concentration EPCo (r=0.98), which suggests that the soil solution was at equilibrium with the soil solid phase at this time of the year, as is usually observed in well-drained soils (Vadas *et al.*, 2007). Starting from December, MRP dynamics at the four sampling sites were dominated by the occurrence of two concentration peaks, whose amplitude depended on soil characteristics.

A first MRP peak (December – January) was observed concomitantly with the sudden water table rise in the uppermost soil horizons of the wetlands. This peak was on average 31 times higher in RW A than RW B and, within each RW, it was higher in upslope sites than downslope sites (respectively 1.6 and 1.8 times in RW A and RW B). In RW A, MRP concentrations increased both at -15 cm and -50 cm, and the vertical concentration gradient disappeared. Concentrations at that time were also much higher than EPCo values, which suggest initiation of a P-release process. Most likely, the observed vertical homogenization of MRP concentrations was caused by the water table rising. Vadas *et al.* (2007) also observed that under conditions of water saturation, P mobilization into groundwater could result in MRP concentrations exceeding those in equilibrium with soils because of P leaching from the topsoil. In RW B, concentrations increased slightly and only at -15 cm at site WetUp, indicating limited P mobility compared to that in RW A ; MRP concentrations did not vary in the other RW B lysimeters. Thus, it appears that this MRP peak was the highest at sites with high soil P content. This first MRP peak was followed by several weeks of gradually decreasing MRP concentrations (January – February), although

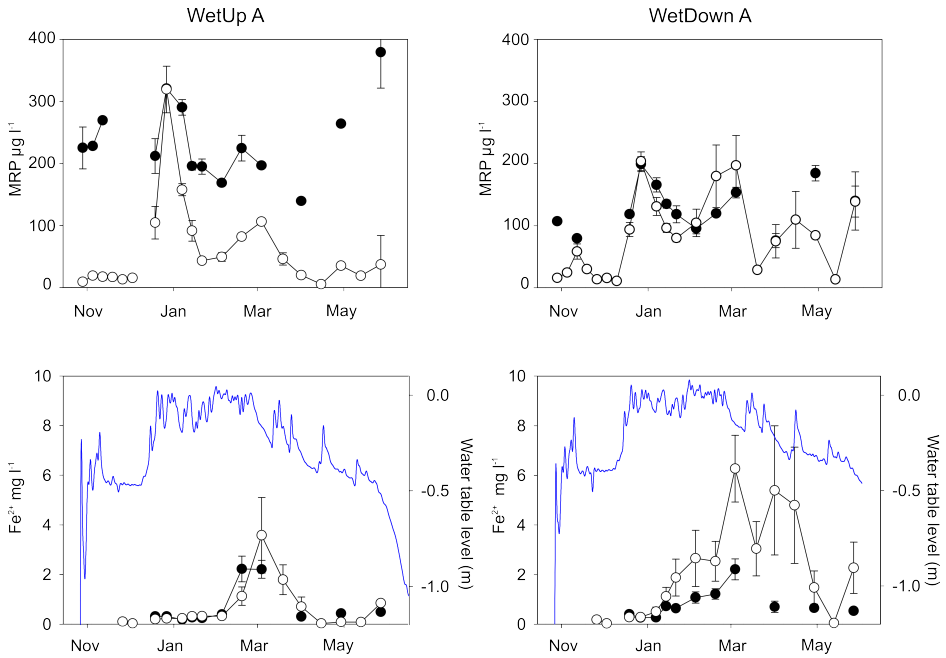

FIGURE 5.4 – Water table level, molybdate-reactive P (MRP) and Fe^{2+} concentrations in soil solutions of riparian wetland A. Solid circles : 10 – 15 cm depth ; empty circles : 50 – 55 cm depth. Error bars represent standard errors of triplicate samples.

the water table remained near the soil surface. This decrease suggests exhaustion of a pool of mobile P present in the soil at the beginning of the hydrological year. Exhaustion of this P pool may be caused by its flushing or by its readsorption onto the soil matrix. Our observations are consistent with previous laboratory experiments that have shown that soil rewetting after a dry period could release organic and inorganic P as a result of microbial biomass being killed by osmotic shock (Blackwell *et al.*, 2010 ; Turner and Haygarth, 2001). Previous monitoring campaigns in the same watershed, but focusing on the composition of dissolved organic matter using ultraviolet spectrometry, carbon isotopes and molecular biomarkers highlighted the release of microbial-derived organic compounds in the soil solution at the same time of the year (Jeanneau *et al.*, 2014 ; Lambert *et al.*, 2013). Hence, the most probable mechanism causing P release when the water table rose at the beginning of the hydrological season was mobilization of a P pool of microbial origin, limited in size, which can migrate under water saturated conditions (McGechan *et al.*, 2005). Further work on P speciation (with a particular focus on organic forms) will help test the hypothesis that the P pool flushed at the beginning of the hydrological season is microbial-derived.

A second MRP peak (February – March in RW A, April – May in RW B) was observed concomitantly with an increase in Fe^{2+} concentrations in periods of low NO_3^- concentrations (< 1 mg l^{-1}) in the soil solution (Supplementary material). This peak was again higher in RW A than RW B. In both RW A and B, MRP concentrations increased at 15 cm and -50 cm. At WetDown A, MRP concentrations at -50 cm exceeded that at -15 cm and that at -50 cm at WetUp A, similar to Fe^{2+} concentrations. In RW B, MRP concentrations increa-

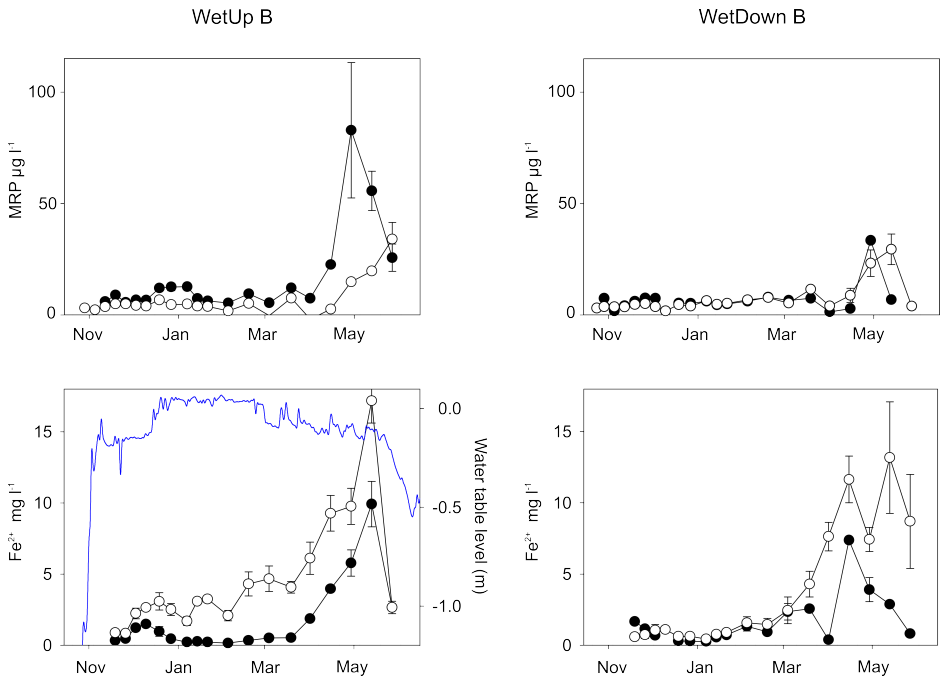

FIGURE 5.5 – Water table level, molybdate-reactive P (MRP) and Fe^{2+} concentrations in soil solutions of riparian wetland B. Solid circles : 10 – 15 cm depth ; empty circles : 50 – 55 cm depth. Error bars represent standard errors of triplicate samples.

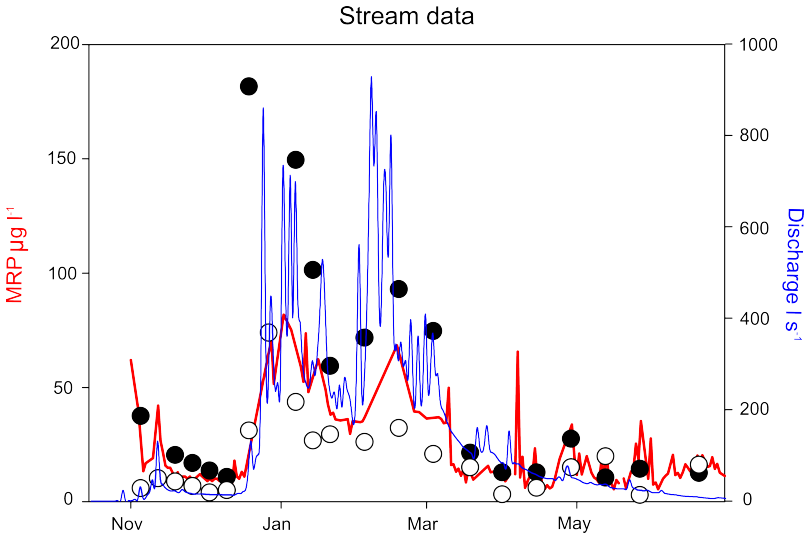

FIGURE 5.6 – Discharge (blue line) and stream molybdate-reactive P (MRP) concentrations during baseflow periods near RW A (solid circles), RW B (empty circles) and at the watershed outlet (red line).

sed the most at WetUp -15 cm, *i.e.* where soil P content was the highest. Hence, P release seemed more a function of the amount of Fe^{2+} being dissolved in RW A but more a function of soil P status in RW B. This indicates that reductive dissolution of Fe (hydr)oxides is the mechanism causing the P release observed under anoxic conditions (Carlyle and Hill, 2001). Anoxic conditions at this time of year were due to low rainfall in a period of high water table, which decreased water velocity and thus water oxygenation (Jeanneau *et al.*, 2014). As a result, Fe (hydr)oxides became solubilized as Fe^{2+} (Bourrié *et al.*, 1999), which released previously adsorbed P (Hoffmann *et al.*, 2009 ; Vidon *et al.*, 2010). The amount of P released by Fe (hydr)oxide reductive dissolution appeared to be controlled by both the amount of P sorbing sites that were solubilized and the amount of P previously adsorbed on them. The timing of this second peak appeared to be influenced by NO_3^- dynamics, as reductive dissolution of Fe (hydr)oxides started after NO_3^- had been consumed arguably through denitrification. Overall, seasonal variation in groundwater MRP concentration was controlled by water table fluctuation, and spatial variability among wetland sites depended on soil P status and propensity of Fe (hydr)oxides solubilization.

Linking MRP concentration in riparian wetlands and in the stream

In-situ observations of soil solution MRP concentrations can be directly linked to stream concentrations. We used stream MRP concentration measured downstream of the two RWs and at the watershed outlet. This combined soil and stream observation could provide a complete view of the solubilization-mobilization-transport continuum from RWs soil to surface water (Haygarth *et al.*, 2005 ; Haygarth *et al.*, 2012 ; Mellander *et al.*, 2012).

The water table rise in December – January was accompanied by a sudden increase in discharge (Figure 5.6). Stream MRP concentrations also increased downstream of both

RW A and B and at the watershed outlet. They were higher downstream of RW A than RW B, similar to differences observed at the same time in the soil solution (Figures 5.4 and 5.5). Stream MRP concentrations then decreased, probably as a result of exhaustion of the previously mobilized P pool in wetland soils. They increased again in February – March downstream of RW A and in April – May downstream of RW B. Again, the timing of these MRP peaks and their relative amplitude between RW A and B was consistent with observations of P release caused by reductive dissolution of Fe (hydr)oxides in wetland soils. Hence, variation in stream MRP concentrations could be related to the two successive P-release mechanisms identified in RWs. Despite this synchronization of peaks between wetland soils and the stream, differences in the relative amplitude of the peaks suggest that retention processes occurred : for example, the second peak was not as large as the first one in the stream downstream of RW A, whereas the amplitude of P release within the soil was similar during the first and second peak. This suggests that some of the MRP released in wetland soils via Fe (hydr)oxides reductive dissolution was not transferred to the stream, probably because of Fe^{2+} re-oxidation on its way to the stream and re-adsorption of P on the newly formed Fe (hydr)oxides (Baken *et al.*, 2015 ; van der Grift *et al.*, 2014).

This connection between MRP concentrations in RWs and streams completely explains stream observations made earlier by (Dupas *et al.*, 2015) that periods of high MRP concentrations coincided with the first water table rise in RWs and periods of anoxic conditions in RW soils. This study also confirms that RWs can be major sources of MRP in agricultural watersheds through their enrichment in particulate P delivered from upland fields via erosion followed by the solubilization-mobilization of this allochthonous P in water saturated conditions (Roberts *et al.*, 2012 ; Stutter *et al.*, 2009).

5.1.4 Conclusion

Riparian wetlands are commonly promoted as buffer zones to reduce P transfer to streams. This study demonstrates that enriched and/or periodically anoxic RWs can actually be hotspots of MRP in agricultural watersheds. “Hot moments” of P release were related to water table dynamics, which activated two successive release mechanisms :

- Soil rewetting after the dry summer caused mobilization of a pool of mobile P, probably of microbial origin. Soil P status appeared to be the main controlling factor of the spatial variability in autumn flush ;
- Anoxic conditions at the end of winter caused reductive dissolution of Fe (hydr)oxides, which released MRP into soil pore water. Propensity of Fe (hydr)oxides solubilization (determined by soil wetness, Fe content of the soil and presence of NO_3^-) appeared to be the main controlling factor of the spatial variability in end of winter P release.

Phosphorus release mechanisms in wetlands produced a clearly discernable signal in the stream both downstream of the monitored RWs and at the outlet of the watershed. To further investigate the biogeochemical processes taking place in RW soils, future monitoring in the Kervidy-Naizin catchment will focus on P speciation in soil and soil pore water, with a particular focus on organic P and colloidal P forms.

Given the risk of P remobilization in P-accumulating RWs, management options should focus on :

- Preventing P mobilization in upslope fields to avoid further enrichment of RWs by erosion ;
- Recovering legacy P from RWs by exporting biomass ;
- In highly sensitive areas, emerging technologies involving the use of P-sorbing materials could be implemented to increase P immobilization in riparian zones.

5.1.5 Acknowledgement

This work was funded by the 'Agence de l'Eau Loire Bretagne' via the 'Trans-P project', by the 'Agence Nationale de la Recherche' via the 'MOSAIC project' and by the 'EC2CO PHOSNAP project'. Long-term monitoring in the Kervidy-Naizin watershed is supported by 'ORE AgrHyS'. We would like to thank all those who helped with the field and lab work : Laurence Carteaux, Nicolas Gilliet, Laurent Jeanneau, Valentin Lemée, Patrice Petitjean, Armelle Racapé ; and Michael and Michelle Corson for English editing of the manuscript.

5.1.6 References

Anderson TR, Groffman PM, Kaushal SS, Walter MT. Shallow Groundwater Denitrification in Riparian Zones of a Headwater Agricultural Landscape. Journal of Environmental Quality 2014 ; 43 : 732-744. DOI : 10.2134/jeq2013.07.0303.

Aubert AH, Gascuel-Odoux C, Gruau G, Akkal N, Faucheux M, Fauvel Y, *et al.* Solute transport dynamics in small, shallow groundwater-dominated agricultural catchments : insights from a high-frequency, multisolute 10 yr-long monitoring study. Hydrology and Earth System Sciences 2013 ; 17 : 1379-1391. DOI : 10.5194/hess-17-1379-2013.

Aubert AH, Kirchner JW, Gascuel-Odoux C, Faucheux M, Gruau G, Merot P. Fractal Water Quality Fluctuations Spanning the Periodic Table in an Intensively Farmed Watershed. Environmental Science Technology 2014 ; 48 : 930-937. DOI : 10.1021/es403723r.

Baken S, Verbeeck M, Verheyen D, Diels J and Smolders E. Phosphorus losses from agricultural land to natural waters are reduced by immobilization in iron-rich sediments of drainage ditches. Water Research 2015 ; 71, 160-170. DOI : 10.1016/j.watres.2015.01.008

Blackwell MSA, Brookes PC, de la Fuente-Martinez N, Murray PJ, Snars KE, Williams JK, *et al.* Effects of soil drying and rate of re-wetting on concentrations and forms of phosphorus in leachate. Biology and Fertility of Soils 2009 ; 45 : 635-643. DOI : 10.1007/s00374-009-0375-x.

Blackwell MSA, Brookes RC, de la Fuente-Martinez N, Gordon H, Murray PJ, Snars KE, *et al.* Phosphorus solubilization and potential transfer to surface waters from the soil microbial biomass following drying-rewetting and freezing-thawing. In : Sparks DL, editor. Advances in Agronomy, Vol 106. 106, 2010, pp. 1-35. DOI : 10.1016/s0065-2113(10)06001-3.

Bourrie G, Trolard F, Genin JMR, Jaffrezic A, Maitre V, Abdelmoula M. Iron control by equilibria between hydroxy-Green Rusts and solutions in hydromorphic soils. Geochimica Et Cosmochimica Acta 1999 ; 63 : 3417-3427. DOI : 10.1016/s0016-7037(99)00262-8.

Carlyle GC, Hill AR. Groundwater phosphate dynamics in a river riparian zone : effects of hydrologic flowpaths, lithology and redox chemistry. Journal of Hydrology 2001 ; 247 : 151-168. DOI : 10.1016/s0022-1694(01)00375-4.

Dorioz JM, Wang D, Poulenard J, Trevisan D. The effect of grass buffer strips on phosphorus dynamics - A critical review and synthesis as a basis for application in agricultural landscapes in France. Agriculture Ecosystems Environment 2006 ; 117 : 4-21. DOI : 10.1016/j.agee.2006.03.029.

Dunne EJ, Clark MW, Corstanje R, Reddy KR. Legacy phosphorus in subtropical wetland soils : Influence of dairy, improved and unimproved pasture land use. Ecological Engineering 2011 ; 37 : 1481-1491. DOI : 10.1016/j.ecoleng.2011.04.003.

Dupas R, Gascuel-Odoux C, Gilliet N, Grimaldi C, Gruau G. Distinct export dynamics for dissolved and particulate phosphorus reveal independent transport mechanisms in an arable headwater catchment. Hydrological Processes 2015. DOI : 10.1002/hyp.10432.

Gachter R, Ngatiah JM, Stamm C. Transport of phosphate from soil to surface waters by preferential flow. Environmental Science Technology 1998 ; 32 : 1865-1869. DOI : 10.1021/es9707825.

Graetz DA, Nair VD. Phosphorus sorption isotherm determination. In : Pierzynski, G.M. (Ed.), Methods of Phosphorus Analaysis for Soils, Sediments, Residuals and Waters. Southern Cooperative Series Bulletin No. 396. Kansas State University. 2000.

Haygarth PM, Bilotta GS, Bol R, Brazier RE, Butler PJ, Freer J, *et al.* Processes affecting transfer of sediment and colloids, with associated phosphorus, from intensively farmed grasslands : an overview of key issues. Hydrological Processes 2006 ; 20 : 4407-4413. DOI : 10.1002/hyp.6598.

Haygarth PM, Condron LM, Heathwaite AL, Turner BL, Harris GP. The phosphorus transfer continuum : Linking source to impact with an interdisciplinary and multi-scaled approach. Science of the Total Environment 2005 ; 344 : 5-14. DOI : 10.1016/j.scitotenv.2005.02.001.

Haygarth PM, Page TJC, Beven KJ, Freer J, Joynes A, Butler P, *et al.* Scaling up the phosphorus signal from soil hillslopes to headwater catchments. Freshwater Biology 2012 ; 57 : 7-25. DOI : 10.1111/j.1365-2427.2012.02748.x

Haygarth PM and Sharpley AN. Terminology for phosphorus transfer. J. Environ. Qual. 2000 ; 29, 10–15.

Haygarth PM, Warwick MS, House WA. Size distribution of colloidal molybdate reactive phosphorus in river waters and soil solution. Water Research 1997 ; 31 : 439-448. DOI : 10.1016/s0043-1354(96)00270-9.

Hoffmann CC, Kjaergaard C, Uusi-Kamppa J, Hansen HCB, Kronvang B. Phosphorus Retention in Riparian Buffers : Review of Their Efficiency. Journal of Environmental Quality 2009 ; 38 : 1942-1955. DOI : 10.2134/jeq2008.0087.

ISO 15681. 2003. Determination of orthophosphate and total phosphorus contents by flow analysis (FIA and CFA)

Jarvie HP, Sharpley AN, Spears B, Buda AR, May L, Kleinman PJA. Water Quality Remediation Faces Unprecedented Challenges from "Legacy Phosphorus". Environmental Science Technology 2013 ; 47 : 8997-8998. DOI : 10.1021/es403160a.

Jeanneau L, Jaffrezic A, Pierson-Wickmann AC, Gruau G, Lambert T, Petitjean P. Constraints on the Sources and Production Mechanisms of Dissolved Organic Matter in Soils from Molecular Biomarkers. Vadose Zone Journal 2014 ; 13. DOI : 10.2136/vzj2014.02.0015.

Knorr KH. DOC-dynamics in a small headwater catchment as driven by redox fluctuations and hydrological flow paths - are DOC exports mediated by iron reduction/oxidation cycles ? Biogeosciences 2013 ; 10 : 891-904. DOI : 10.5194/bg-10-891-2013.

Lambert T, Pierson-Wickmann AC, Gruau G, Jaffrezic A, Petitjean P, Thibault JN, *et al.* Hydrologically driven seasonal changes in the sources and production mechanisms of dissolved organic carbon in a small lowland catchment. Water Resources Research 2013 ; 49 : 5792-5803. DOI : 10.1002/wrcr.20466.

Le Bissonnais Y, Cros-Cayot S, Gascuel-Odoux C. Topographic dependence of aggregate stability, overland flow and sediment transport. Agronomie 2002 ; 22 : 489-501. DOI : 10.1051/agro :2002024.

Li YC, Yu S, Strong J, Wang HL. Are the biogeochemical cycles of carbon, nitrogen, sulfur, and phosphorus driven by the "Fe-III-Fe-II redox wheel" in dynamic redox environments ? Journal of Soils and Sediments 2012 ; 12 : 683-693. DOI : DOI : 10.1007/s11368-012-0507-z.

Maillard E, Imfeld G. Pesticide Mass Budget in a Stormwater Wetland. Environmental Science Technology 2014 ; 48 : 8603-8611. DOI : 10.1021/es500586x.

McGechan MB, Lewis DR, Hooda PS. Modelling through-soil transport of phosphorus to surface waters from livestock agriculture at the field and catchment scale. Science of the Total Environment 2005 ; 344 : 185-199. DOI : 10.1016/j.scitotenv.2005.02.015.

Mellander PE, Jordan P, Wall DP, Melland AR, Meehan R, Kelly C, *et al.* Delivery and impact bypass in a karst aquifer with high phosphorus source and pathway potential. Water Research 2012 ; 46 : 2225-2236. DOI : 10.1016/j.watres.2012.01.048.

Molenat J, Gascuel-Odoux C, Ruiz L, Gruau G. Role of water table dynamics on stream nitrate export and concentration. in agricultural headwater catchment (France). Journal of Hydrology 2008 ; 348 : 363-378. DOI : 10.1016/j.jhydrol.2007.10.005.

NF ISO 10390. 2005. Détermination du pH

NF ISO 10694. 1995. Dose du carbone organique et du carbone total par combustion sèche.

NF ISO 13878. 1998. Détermination de la teneur totale en azote par combustion sèche.

NF X 31-107. 2003. Détermination de la distribution granulométrique des particules du sol.

NF X 31-147. 1996. Mise en solution totale par attaque acide.

NF X 31-160. 1999. Détermination du phosphore soluble dans une solution à 20 g.l-1d'acide citrique monohydraté

Obour AK, Silveira ML, Vendramini JMB, Sollenberger LE, O'Connor GA. Fluctuating water table effect on phosphorus release and availability from a Florida Spodosol. Nutrient Cycling in Agroecosystems 2011 ; 91 : 207-217. DOI : 10.1007/s10705-011-9456-y.

Ockenden MC, Deasy C, Quinton JN, Surridge B, Stoate C. Keeping agricultural soil out of rivers : Evidence of sediment and nutrient accumulation within field wetlands in the UK. Journal of Environmental Management 2014 ; 135 : 54-62. DOI : 10.1016/j.jenvman.2014.01.015.

Oehler F, Bordenave P, Durand P. Variations of denitrification in a farming catchment area. Agriculture, Ecosystems Environment 2007 ; 120 : 313-324. DOI : 10.1016/j.agee.2006.10.007.

Pauwels, H., Kloppmann, W., Foucher, J.C., Martelat, A. and Fritsche, V. (1998) Field tracer test for denitrification in a pyrite-bearing schist aquifer. Applied Geochemistry .13(6), 767-778. DOI : 10.1016/s0883-2927(98)00003-1

Roberts WM, Stutter MI, Haygarth PM. Phosphorus Retention and Remobilization in Vegetated Buffer Strips : A Review. Journal of Environmental Quality 2012 ; 41 : 389-399. DOI : 10.2134/jeq2010.0543.

Schoumans OF, Chardon WJ. Phosphate saturation degree and accumulation of phosphate in various soil types in The Netherlands. Geoderma 2015 ; 237 : 325-335. DOI : 10.1016/j.geoderma.2014.08.015.

Sharpley A, Jarvie HP, Buda A, May L, Spears B, Kleinman P. Phosphorus Legacy : Overcoming the Effects of Past Management Practices to Mitigate Future Water Quality Impairment. Journal of Environmental Quality 2013 ; 42 : 1308-1326. DOI : 10.2134/jeq2013.03.0098.

Song KY, Zoh KD, Kang H. Release of phosphate in a wetland by changes in hydrological regime. Science of the Total Environment 2007 ; 380 : 13-18. DOI : 10.1016/j.scitotenv.2006.11.035.

Stutter MI, Langan SJ, Lumsdon DG. Vegetated Buffer Strips Can Lead to Increased Release of Phosphorus to Waters : A Biogeochemical Assessment of the Mechanisms. Environmental Science Technology 2009 ; 43 : 1858-1863. DOI : 10.1021/es8030193.

Stutter MI, Lumsdon DG. Interactions of land use and dynamic river conditions on sorption equilibria between benthic sediments and river soluble reactive phosphorus concentrations. Water Research 2008 ; 42 : 4249-4260. DOI : 10.1016/j.watres.2008.06.017.

Surridge BWJ, Heathwaite AL, Baird AJ. Phosphorus mobilisation and transport within a long-restored floodplain wetland. Ecological Engineering 2012 ; 44 : 348-359. DOI : 10.1016/j.ecoleng.2012.02.009.

Tamm O. Determination of the inorganic components of the gel-complex in soils (in German). Medd. Statens skogforsoksanst 1922, 19, 385-404. Turner BL, Haygarth PM. Biogeochemistry - Phosphorus solubilization in rewetted soils. Nature 2001 ; 411 : 258-258. DOI : 10.1038/35077146.

Vadas PA, Srinivasan MS, Kleinman PJA, Schmidt JP, Allen AL. Hydrology and groundwater nutrient concentrations in a ditch-drained agroecosystem. Journal of Soil and Water Conservation 2007 ; 62 : 178-188.

van der Grift B, Rozemeijer JC, Griffioen J, van der Velde Y. Iron oxidation kinetics and phosphate immobilization along the flow-path from groundwater into surface water. Hydrology and Earth System Sciences 2014 ; 18 : 4687-4702. DOI : 10.5194/hess-18-4687-2014.

Van der Zee SEATM and Bolt GH. Deterministic and stochastic modeling of reactive solute transport. Journal of Contaminant Hydrology 1991, 7, 75–93.

Vidon P, Allan C, Burns D, Duval TP, Gurwick N, Inamdar S, et al. Hot Spots and Hot Moments in Riparian Zones : Potential for Improved Water Quality Management1. Journal of the American Water Resources Association 2010 ; 46 : 278-298. DOI : 10.1111/j.1752-1688.2010.00420.x.

5.1.7 Supplementary materials

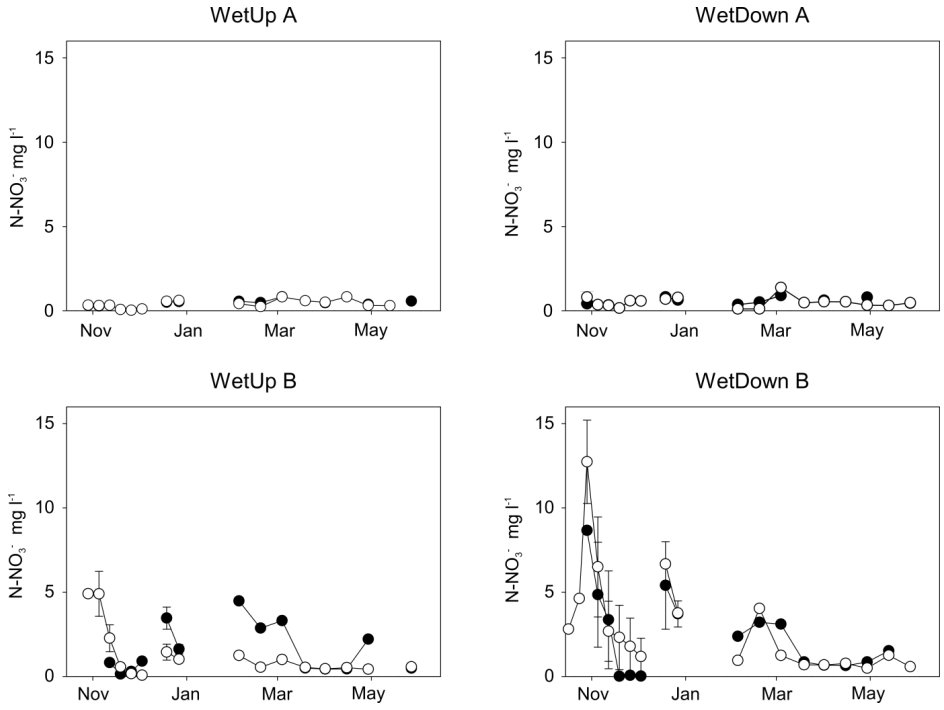

FIGURE 5.7 – Nitrate concentrations in soil solutions of riparian wetland A and B. Solid circles : 10-15 cm depth ; empty circles : 50-55 cm depth. Error bars represent standard errors of triplicate samples.

5.2 Suivis d'autres voies de transfert et lien avec le carbone

Comme mentionné dans l'article, la dynamique du SRP est similaire à celle du DOC pour certains pièges à eau, sans être parfaitement synchrone (Figure 5.8). Le lien entre carbone et phosphore est à explorer plus en détails pour comprendre les mécanismes sous-jacents.

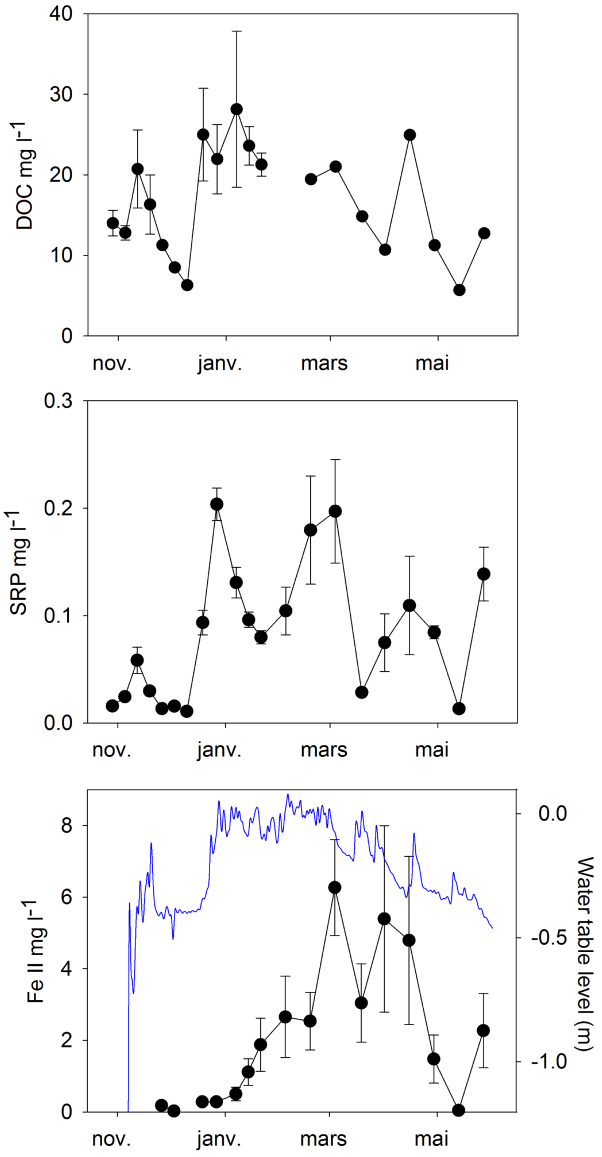

FIGURE 5.8 – Water table level, dissolved organic carbon (DOC), molybdate-reactive phosphorus (MRP) and Fe^{2+} concentration in soil solutions of riparian wetland A 15 cm depth. Error bars represent standard errors of triplicate samples.

En plus des données de pièges à eau présentées dans l'article, d'autres sites ont été suivis pour étudier d'autres voies de transfert. Si les données sont trop peu nombreuses pour une analyse solide des résultats, quelques pistes d'interprétation peuvent être évoquées ici. Les concentrations à la sorties de deux drains (situé dans les sous-bassins versants A et B), montrent une évolution saisonnière similaire aux données de solution de sol en zone non drainée, à savoir un flush automnal-hivernal suivi de concentrations plus basses (Figure 5.9). Les drains suivis ont cessé de couler avant la période de réduction et la période

d'épandage, ce qui a compromis l'étude de ces deux évènements sur le flux en sortie de drains.

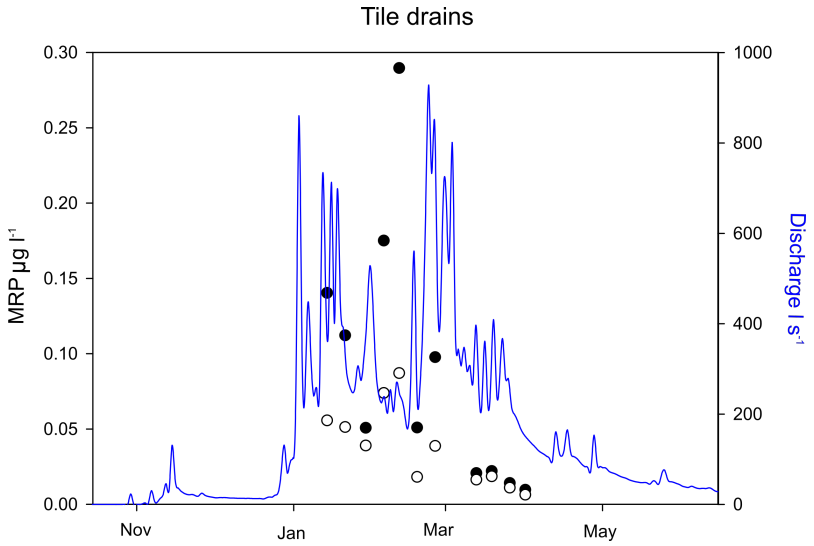

FIGURE 5.9 – Discharge (blue line) and molybdate-reactive phosphorus (MRP) concentrations in water flowing from two drains, in sub-watershed A (solid circles) and sub-watershed B (empty circles).

Des mini-piezomètres placé à 4-5 cm le long du transect A en trois sites (WetUp A, WetDown A et dans la parcelle adjacente à 1m de l'interface avec la bande enherbée) montrent des concentrations plus élevées dans la partie bande enherbée (WetUp A et WetDown A) que dans la partie cultivée de la zone humide, malgré des teneurs en phosphore du sol plus élevées dans cette dernière (Figure 5.1). Ces résultats laissent penser que la solubilité du phosphore est accrue du fait de la présence de végétation permanente.

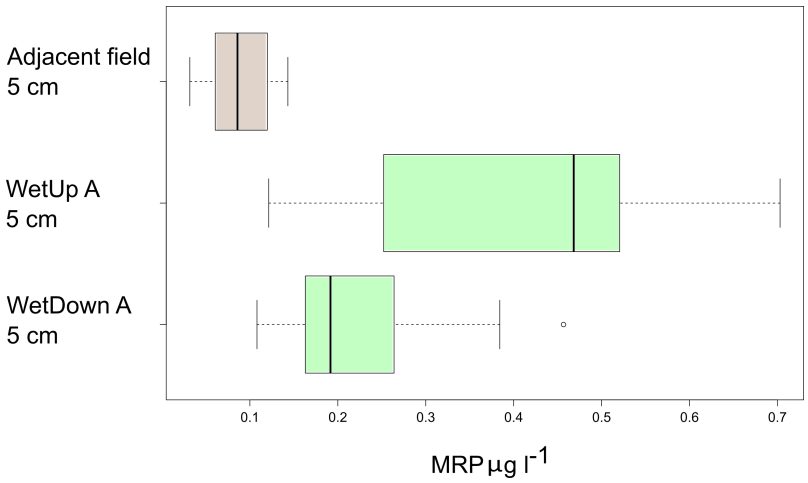

FIGURE 5.10 – Molybdate-reactive phosphorus concentration (MRP) in the soil pore water at 5 cm depth at three point along transect A (triplicate samples ; 5 sampling dates between January and March 2014). Green boxes show concentrations within the grass buffer strip and the brown box shows concentration in the adjacent field.

Un dispositif de collecte des eaux de ruissellement, installé en triplicat à l'interface entre la parcelle et la bande enherbé du transect A, a permis de quantifier le flux de P dissous et particulaire ayant atteint la bande enherbée au cours de l'année hydrologique 2013-2014. En 7 évènements, le flux cumulé rapporté au linéaire d'interface s'est élevé à 49.4 mg SRP m^{-1} yr^{-1} et 244.5 mg TP m^{-1} yr^{-1}. Dans le même temps, le flux annuel à l'exutoire du bassin versant s'est élevé à 0.35 kg SRP ha^{-1} yr^{-1} et 0.66 mg TP ha^{-1} yr^{-1}, soit, rapporté au linéaire de berge 87.7 mg SRP m^{-1} yr^{-1} et 165.2 mg SRP m^{-1} yr^{-1}. En faisant l'hypothèse que le versant A est représentatif du bassin, et que la bande enherbée comme le cours d'eau et ses berges sont à un état stationnaire, on constate alors que la bande enherbée reçoit et émet respectivement 83% et 47% de P sous forme particulaire. En réalité, les 47% de P particulaire émis par la bande enherbée incluent l'érosion des berges, donc il est probable que la part du P particulaire émis de manière vraiment diffuse soit inférieure à 47%. Ces chiffres semblent confirmer l'hypothèse formulée dans le chapitre 3, selon laquelle les bandes enherbées en zone humide sont des bioréacteurs qui convertissent du P émis depuis les versants principalement sous forme particulaire en P dissous transféré vers le cours d'eau. Il serait intéressant de confirmer ces chiffres par un suivi long-terme des entrées et sortie de P particulaire et dissous au niveau de plusieurs bandes enherbées.

5.3 Conclusion du chapitre

Ce chapitre a permis de confirmer le rôle de la nappe dans le transfert de phosphore réactif « dissous » (MRP) en provenance de la zone humide riparienne. Des observations in-situ de la concentration en MRP dans la solution libre du sol de zones humides ripariennes ont mis en évidence que les fluctuations saisonnières de la nappe avaient un effet non seulement sur le transfert, mais aussi sur les processus biogéochimique à l'origine de la

solubilisation du P. L'alternance de périodes sèches et de périodes saturées en eau est un des facteurs à l'origine d'une mobilité accrue du phosphore dans ces zones.

La présence d'un pool de P mobile dans les sols après la période de sècheresse estivale a été confirmée. Les mécanismes à l'origine de la constitution de ce pool restent à préciser, mais nous en avons identifié des facteurs de contrôle temporels (la sécheresse) et spatial (la teneur en P des sols). De précédentes observations sur le même site d'étude ont montré que la lyse bactérienne causée par la sécheresse (ou par la réhumectation) était à l'origine d'un pool de carbone organique dissous (COD) à la même période de l'année ; il est alors probable que le même mécanisme soit à l'origine du pool de P mobile. La réduction des (hydr)oxydes de Fer à la fin de l'hiver est accompagnée d'un deuxième relarguage de MRP, cette fois aussi visible dans une zone humide à faible teneur en P des sols. Ce relarguage a lieu lorsque tout le nitrate a été consommé, vraisemblablement par dénitrification. Ces deux mécanismes produisent un signal visible à la fois dans la solution libre du sol et dans la rivière, ce qui suggère que le phosphore mobilisé dans la zone humide est transmis, au moins en partie, au cours d'eau.

Pour confirmer et affiner la connaissance des processus en jeu, il serait utile de poursuivre le suivi de la solution de sol en engageant des moyens pour connaître la spéciation du MRP. En effet, il serait intéressant de connaître la part du MRP de nature colloïdale, et la spéciation des colloïdes (organiques ou minéraux). Enfin, la comparaison avec d'autres éléments, telle qu'initiée dans ce chapitre, peut être source d'enseignements. Les similitudes entre dynamiques du COD et du MRP laissent penser à des mécanismes de production communs. Les méthodes de spéciation chimique déjà mises en œuvre pour connaître la nature du COD devrait donc permettre de connaître celle du MRP. Enfin, nous avons ignoré, faute de données, l'effet de la végétation et des microorganismes du sol sur la solubilisation du P. Pourtant, les éléments présentés en analyses complémentaires laissent penser que l'occupation du sol joue un rôle puisque, dans des conditions hydrologiques similaires, la solubilisation P est accrue en présence de végétation permanente dans une bande enherbée par rapport à une parcelle cultivée.

Les résultats présentés dans les trois premiers chapitres questionnent la pertinence des modèles existants pour simuler les transferts de P dissous dans notre contexte d'étude. En effet, aucun de ces modèles ne simule explicitement le niveau de nappe, moteur principal des transferts et aucun ne simule les deux mécanismes de solubilisation mis en évidence dans le chapitre 5. Les mécanismes simulés par les modèles, pour la plupart en lien avec les pratiques de fertilisation, ne produisent pas de signal visible dans le contexte des bassins étudiés. Ceci est probablement dû au fait que la zone tampon entre les parcelles et le cours d'eau masque le signal « agricole » en provenance des parcelles et le remplace par un signal « biogéochimique » indépendant des pratiques. Le chapitre 6 propose donc un nouveau modèle simulant les processus dominants identifiés aux chapitres 3 à 5.

Chapitre 6

Modélisation et analyse d'incertitude

Ce chapitre est rédigé sous la forme d'un article soumis.

Dupas R, Salmon-Monviola J, Beven K, Durand P, Haygarth P, Hollaway M, Gascuel-Odoux C. Uncertainty assessment of a dominant-process catchment model of dissolved phosphorus transfer.

Ce chapitre apporte des éléments de réponse à la question 3, rappelée ici :

Question 3 : Comment raisonner la complexité d'un modèle en fonction de la quantité d'information contenue dans les données ? Comment quantifier l'incertitude des données et la propager dans les prédictions d'un modèle ?

Le travail de modélisation présenté a été rendu possible d'une part grâce à l'existence du modèle TNT2 et à tous ces développeurs, et d'autre part grâce à une collaboration avec Keith Beven, Phil Haygarth et Michael Hollaway de l'Université de Lancaster (Royaume-Uni).

6.1 Uncertainty assessment of a dominant-process catchment model of dissolved phosphorus transfer

Résumé

Nous avons développé un modèle hydrologique parcimonieux à base topographique couplé à un module biogéochimique pour améliorer la connaissance et la prédiction des transferts de phosphore réactif dissous (SRP) dans les bassins versants agricoles. La structure du modèle a pour but de représenter les principaux processus hydrologiques et biogéochimiques identifiés grâce à un suivi multi échelle dans un bassin versant de recherche (Kervidy-Naizin, 5 km^2). Les fluctuations de nappe, responsables de la mise en connexion des zones de production de SRP dans les sols avec le cours d'eau, sont simulées par un module hydrologique distribué à une résolution de 20 m. La variabilité spatiale de la teneur en P des sols et la variabilité temporelle des conditions d'humidité et de température, qui ont été identifiées comme les facteurs de contrôle principaux de la solubilisation du SRP dans les sols, ont donc été incluses dans le module biogéochimique. L'approche de modélisation mise en œuvre inclus une évaluation de l'information contenue dans les données de calibration et une propagation de l'incertitude dans les prédictions du modèle par une méthode reposant sur des limites d'acceptabilité GLUE. D'une manière générale, les performances du modèle se sont révélées satisfaisantes au vu de l'incertitude dans les données, avec des coefficients de Nash-Sutcliffe sur le flux journalier prédit par les modèles acceptables entre 0.1 et 0.8. Le rôle de la connectivité hydrologique provoquée par les fluctuations de nappe et la solubilisation accrue du SRP suite à des périodes chaudes et sèches sont bien reproduits. On peut conclure qu'en l'absence de suivi haute fréquence, la quantité d'information contenue dans les données est limitée donc des modèles parcimonieux visant à simuler les processus dominants sont plus adaptés que des modèles avec un grand nombre de paramètres. Une analyse de l'incertitude dans les données est recommandée pour la calibration des modèles afin d'obtenir des prédictions fiables.

Abstract

We developed a parsimonious topography-based hydrologic model coupled with a soil biogeochemistry sub-model in order to improve understanding and prediction of Soluble Reactive Phosphorus (SRP) transfer in agricultural headwater catchments. The model structure aims to capture the dominant hydrological and biogeochemical processes identified from multiscale observations in a research catchment (Kervidy-Naizin, 5 km^2). Groundwater fluctuations, responsible for the connection of soil SRP production zones to the stream, were simulated with a fully-distributed hydrologic model at 20 m resolution. The spatial variability of the soil phosphorus status and the temporal variability of soil moisture and temperature, which had previously been identified as key controlling factor of SRP solubilisation in soils, were included as part of an empirical soil biogeochemistry sub-model. The modelling approach included an analysis of the information contained in the calibration data and propagation of uncertainty in model predictions using a GLUE "limits of acceptability" framework. Overall, the model appeared to perform well given the uncertainty in the observational data, with a Nash-Sutcliffe efficiency on daily SRP loads between 0.1 and 0.8 for acceptable models. The role of hydrological connectivity via groundwater fluctuation,

and the role of increased SRP solubilisation following dry/hot periods were captured well. We conclude that in the absence of near continuous monitoring, the amount of information contained in the data is limited hence parsimonious models are more relevant than highly parameterised models. An analysis of uncertainty in the data is recommended for model calibration in order to provide reliable predictions.

6.1.1 Introduction

Excessive phosphorus (P) concentrations in freshwater bodies result in increased eutrophication risk worldwide (Carpenter *et al.*, 1998 ; Schindler *et al.*, 2008). Eutrophication restricts economic use of water and poses a serious health hazard to humans, due to the potential development of harmful cyanobacteria (Bradley *et al.*, 2013 ; Serrano *et al.*, 2015). In western countries, reduction of point source P emissions in the last two decades has resulted in a proportionally increasing contribution of diffuse sources, mainly from agricultural origin (Alexander *et al.*, 2008 ; Grizzetti *et al.*, 2012 ; Dupas *et al.*, 2015a). Of particular concern are dissolved P forms, often measured as Soluble Reactive Phosphorus (SRP), because they are highly bioavailable and therefore a likely contributor to eutrophication.

To reduce SRP transfer from agricultural soils it is important to identify the spatial origin of P sources in agricultural landscapes, the biogeochemical mechanisms causing SRP solubilisation in soils and the dominant transfer pathways. Research catchments provide useful data to investigate SRP transport mechanisms : typically, the temporal variations in water quality parameters at the outlet, together with hydroclimatic variables, are investigated to infer spatial origin and dominant transfer pathways of SRP (Haygarth *et al.*, 2012 ; Outram *et al.*, 2014 ; Dupas *et al.*, 2015b ; Mellander *et al.*, 2015 ; Perks *et al.*, 2015). Hypotheses drawn from analysis of water quality time series can be further investigated through hillslope monitoring and/or laboratory experiments (Heathwaite and Dils, 2000 ; Siwek *et al.*, 2013 ; Dupas *et al.*, 2015c). When dominant processes are considered reasonably known, it is possible to develop computer models, for two main purposes : first, to validate scientific conceptual models, by testing whether model predictions can produce reasonable simulations compared to observations. Of particular interest is the possibility to test the capability of a computer model to upscale P processes observed at fine spatial resolution (soil column, hillslope) to a whole catchment. Second, if the models survive such validation tests, then they can be useful tools to simulate the response of a catchment system to a future perturbation such as changes in agricultural management and climate changes.

However, process-based P models generally perform poorly compared to, for example, nitrogen models (Wade *et al.*, 2002 ; Dean *et al.*, 2009 ; Jackson-Blake *et al.*, 2015a). This is of major concern because poor model performance suggests poor knowledge of dominant processes at the catchment scale, and poor reliability of the modelling tools used to support management. The origin of poor model performance might be conceptual misrepresentations, structural imperfection, calibration problems, irrelevant model evaluation criteria and difficulties in properly assessing the information content of the available data when it is subject to epistemic error. All five causes of poor model performance are intertwined, e.g. model calibration strategy depends on model performance evaluation criteria, which depend on the way the information contained in the observation data is assessed (Beven

and Smith, 2015).

A key issue in environmental modelling is the level of complexity one should seek to incorporate in a model structure. Several existing P transfer models, such as INCA (Wade *et al.*, 2002), SWAT (Arnold *et al.*, 1998) and HYPE (Lindstrom *et al.*, 2010) seek to simulate many processes, with the view that complex models are necessary to understand processes and to predict the likely consequences of land-use or climate changes. However, these complex models include many parameters that need to be calibrated, while the amount of data available for calibration is often low. An imbalance between calibration requirement and the amount of available observation data can lead to equifinality issues, i.e. when many model structures or parameter sets lead to acceptable simulation results (Beven, 2006). A consequence of equifinality is the risk of unreliable prediction when an "optimal" set of parameters is used (Kirchner, 2006), and large uncertainty intervals when Monte Carlo simulations are performed (Dean *et al.*, 2009). In this situation, it will be worth exploring parsimonious models that aim to capture the dominant hydrological and biogeochemical processes controlling SRP transfer in agricultural catchment. For example, Hahn *et al.* (2013) used a soil-type based rainfall-runoff model (Lazzarotto *et al.*, 2006) combined with an empirical model of soil SRP release derived from rainfall simulation experiments over soils with different P content and manure application level/timing (Hahn *et al.*, 2012) to simulate daily SRP load from critical sources areas.

A second key issue, linked to the question of model complexity, concerns model calibration and evaluation. Both calibration and evaluation require assessing the fit of model outputs with observation data. However, observation data are generally not directly comparable with model outputs, because of incommensurability issues and/or because they contain errors (Beven, 2006 ; 2009). Typically, predicted daily concentrations and/or loads are evaluated against data from grab samples collected on a daily or weekly basis. The information content of these data must be carefully evaluated to propagate uncertainty in the data into model predictions. Uncertainty in grab sample data might stem from i) sampling frequency problems and ii) measurement problems (Lloyd *et al.*, 2015). Grab sample data represent a snapshot of the concentration at a given time of the day, which can differ from the flow weighted daily concentration. This difference between observation data and simulation output can be large during storm events in small agricultural catchments, as P concentrations can vary by several orders of magnitudes during the same day (Heathwaite and Dils, 2000 ; Sharpley *et al.*, 2008). Model evaluation can be severely penalised by this difference, because many popular evaluation criteria such as the Nash-Sutcliffe efficiency (NSE) are sensitive to extreme values and errors in timing (Moriasi *et al.*,2007). During baseflow periods, it is more likely that grab sample data are comparable to flow-weighted mean daily concentrations, as concentrations vary little during the day and they are usually low in the absence of point sources. However, measurement errors are expected to occur at low concentrations, either due to too long storage times or laboratory imprecision when concentrations come close to detection/quantification limits (Jarvie *et al.*, 2002 ; Moore and Locke, 2013). Uncertainty in the data can also relate to discharge measurement and input data (e.g. maps of soil P content and rainfall data). In this paper we strive to identify and quantify the different sources of uncertainty in the data when the required quality check tests have been performed. A Generalised Likelihood Uncertainty Estimation (GLUE) "limits of acceptability" approach (Beven, 2006 ; Beven and Smith,

2015) is used to calibrate/evaluate the model.

This paper presents a dominant-process model that couples a topography-based hydrologic model with a soil biogeochemistry sub-model able to simulate daily discharge and SRP loads. The dominant processes included in the hydrologic and soil biogeochemistry sub-models have been identified in previous analyses of multiscale observational data, which have demonstrated on the one hand the control of groundwater fluctuation on connecting soil SRP production zones to the stream (Haygarth *et al.*, 2012 ; Jordan *et al.*, 2012 ; Dupas *et al.*, 2015b ; 2015d ; Mellander *et al.*, 2015), and on the other hand the role of antecedent soil moisture and temperature conditions on SRP solubilisation in soils (Turner and Haygarth, 2001 ; Blackwell *et al.*, 2009 ; Dupas *et al.*, 2015c). Model development and application was performed in the Kervidy-Naizin catchment in western France with the objectives of : i) testing if the model was capable of capturing daily variation of SRP load, thus confirming hypotheses on dominant processes ; ii) develop a methodology to analyse and propagate uncertainty in the data into model prediction using a "limits of acceptability" approach. Model development and analysis of uncertainty in the data are interlinked in this approach.

6.1.2 Materials and methods

Study catchment

Site description Kervidy–Naizin is a small (4.94 km^2) agricultural catchment located in central Brittany, Western France (48 ° N, 3 ° W). It belongs to the AgrHyS environmental research observatory, which studies the impact of agricultural activities and climate change on water quality (Molenat *et al.*, 2008 ; Aubert *et al.*, 2013 ; Salmon-Monviola *et al.*, 2013 ; Humbert *et al.*, 2014). The catchment (Figure 6.1) is drained by a stream of second Strahler order, which generally dries up in August and September. The climate is temperate oceanic, with annual cumulative precipitation and specific discharge averaging 854 ± 179 mm and 290 ± 106 mm, respectively, from 2000 to 2014. Mean annual temperature is 11.2 ± 0.6 ° C. Elevation ranges from 93 to 135 m above sea level. Topography is gentle, with maximum slopes not exceeding 5%. The bedrock consists of impervious, locally fractured Brioverian schists and is capped by several metres of unconsolidated weathered material and silty, loamy soils. The hydrological behaviour is dominated by the development of a water table that varies seasonally along the hillslope. In the upland domain, consisting of well drained soils, the water table remains below the soil surface throughout the year, varying in depth from 1 to > 8 m. In the wetland domain, developed near the stream and consisting of hydromorphic soils, the water table is shallower, remaining near the soil surface generally from October to April each year. The land use is mostly agriculture, specifically arable crops and confined animal production (dairy cows and pigs). A farm survey conducted in 2013 led to the following land use subdivisions : 35% cereal crops, 36% maize, 16% grassland and 13% other crops (rape seed, vegetables). Animal density was estimated as high as 13 livestock units ha-1 in 2010. Estimated soil P surplus is 13.1 kg P ha^{-1} yr^{-1} (Dupas *et al.*, 2015b) and soil extractable P in 2013 (Olsen *et al.*, 1954) is 59 ± 31 mg P kg^{-1} (n = 89 samples). A survey targeting riparian areas highlighted the legacy of high soil P content in these currently unfertilized areas (Dupas *et al.*, 2015c). No point source emissions are recorded but scattered dwellings with septic tanks are present in the catchment.

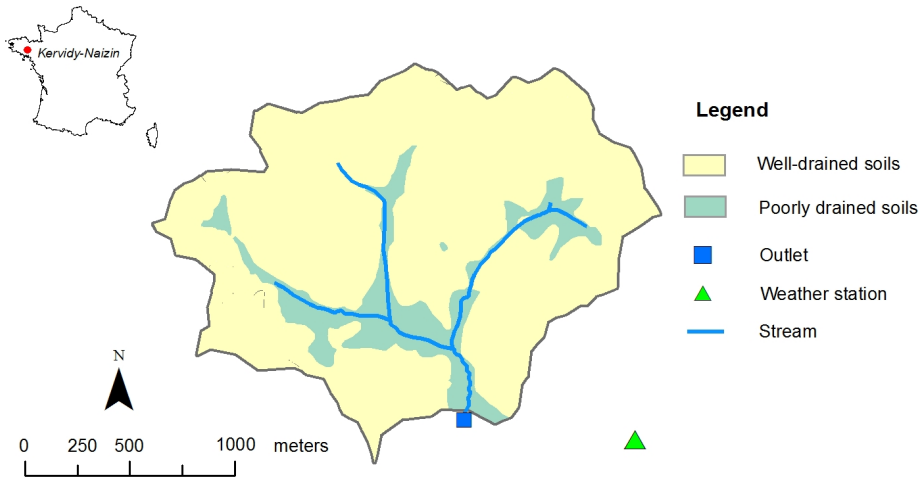

FIGURE 6.1 – Soil drainage classes in the Kervidy-Naizin catchment, Curmi *et al.* (1998)

Hydroclimatic and chemical monitoring Kervidy-Naizin was equipped with a weather station (Cimel Enerco 516i) located 1.1 km from the catchment outlet. It recorded hourly precipitation, air and soil temperatures, air humidity, global radiation, wind direction and speed, and estimates Penman evapotranspiration. Stream discharge was estimated at the outlet with a rating curve and stage measurements from a float-operator sensor (Thalimèdes OTT) upstream of a rectangular weir.

To record both seasonal and within storm dynamics in P concentration, two monitoring strategies complemented each other from October 2013 to August 2015 : a daily manual grab sampling at approximately the same time (between 16 :00 – 18 :00 local time) and automatic high frequency sampling during 14 storm events (autosampler ISCO 6712 Full-Size Portable Sampler, 24 one litre bottles filled every 30 min). The water samples were filtered on-site, immediately after grab sampling and after 1-2 days in the case of autosampling. They were analysed for SRP (ISO 15681) within a fortnight. To assess uncertainty in daily SRP concentration related to sampling time, storage and measurement errors, a second grab sample was taken at a different time of the day (between 11 :00 – 15 :00 local time) in 36 instances during the study period. The second sample was analysed within 24h with the same method ; this second dataset is referred to as verification dataset, as opposed to the reference dataset. Among the 36 pairs of comparable daily samples, 12 were taken during storm events and 24 during baseflow periods. To assess uncertainty in high frequency SRP concentration during storm events due to delayed filtration of autosampler bottles, 5 grab samples were taken during the course of 4 distinct storms and were filtered immediately. The same lab procedure was used to analyse SRP.

Identification of dominant processes from multiscale observations Observations in the Kervidy-Naizin catchment have highlighted that the temporal variability in stream SRP concentrations could not be related to the calendar of agricultural practices, but rather

to hydrological and biogeochemical processes (Dupas *et al.*, 2015b). The primary control of hydrology on SRP transfer has also been evidenced in several other small agricultural catchments (e.g. Haygarth et al, 2012 ; Jordan *et al.*, 2012 ; Mellander *et al.*, 2015). In the Kervidy-Naizin catchment, groundwater fluctuations in valley bottom areas was identified as the main driving factor of SRP transfer, through the hydrological connectivity it creates when it intercepts shallow soil layers (Dupas *et al.*, 2015b).

In-situ monitoring of soil pore water at 4 sites (15 cm and 50 cm depths) in the Kervidy-Naizin catchment has shown that mean SRP concentration in soils was a linear function of Olsen P (Olsen *et al.*, 1954). This reflects current knowledge that a soil P test, or alternatively estimation of a degree of P saturation, can be used to assess solubilisation in soils (Beauchemin and Simard, 1999 ; McDowell *et al.*, 2002 ; Schoumans *et al.*, 2015). This linear relationship derived from the data contrasts however with other studies, where threshold values above which SRP solubilisation increases greatly have been identified (Heckrath *et al.*, 1995 ; Maguire *et al.*, 2002).

Soluble Reactive Phosphorus solubilisation in soil varies seasonally according to antecedent conditions of temperature and soil moisture. Dry and/or hot conditions are favourable to accumulation of mobile P forms in soils, while water saturated conditions lead to their flushing (Turner *et al.*, 2001 ; Blackwell *et al.*, 2009 ; Dupas *et al.*, 2015c).

Description of the Topography-based Nutrient Transfer and Transformation – Phosphorus (TNT2-P)

TNT2 was originally developed as a process-based and spatially explicit model simulating water and nitrogen fluxes at a daily time step (Beaujouan *et al.*, 2002) in meso-scale catchments (< 50 km^2). TNT2-N has been widely used for operational objectives, to test the effect of mitigation options proposed by local stakeholders or public policy-makers (Moreau *et al.*, 2012 ; Durand *et al.*, 2015), on nitrate fluxes and concentrations in rivers.

TNT2-P uses a modified version of the hydrological sub-model in TNT2-N, to which a biogeochemistry sub-model was added to simulate SRP solubilisation in soils.

Hydrological sub-model The assumptions in the hydrological sub-model are derived from TOPMODEL which has previously been applied to the Naizin catchment (Bruneau *et al.*, 1995 ; Franks *et al.*, 1998) : 1) the effective hydraulic gradient of the saturated zone is approximated by the local topographic surface gradient ($tan\beta$). It is calculated in each cell of a Digital Elevation Model (DEM) at the beginning of the simulation ; 2) the effective downslope transmissivity (parameter T) of the soil profile in each cell of the DEM is a function of the soil moisture deficit (Sd). Hydraulic conductivity decreases exponentially with depth (parameter m, Figure 6.2). Hence water fluxes (q) are computed as :

$$q = T * tan\beta * exp(-Sd/m) \tag{6.1}$$

Based on these assumptions, TNT2 computes an explicit cell-to-cell routing of fluxes, using a D8 algorithm. This explicit cell-to-cell routing of fluxes increases computation times compared to TOPMODEL, for which calculations are grouped according to a distribution of hydrologically similar points, but it allows taking account of spatial interactions between

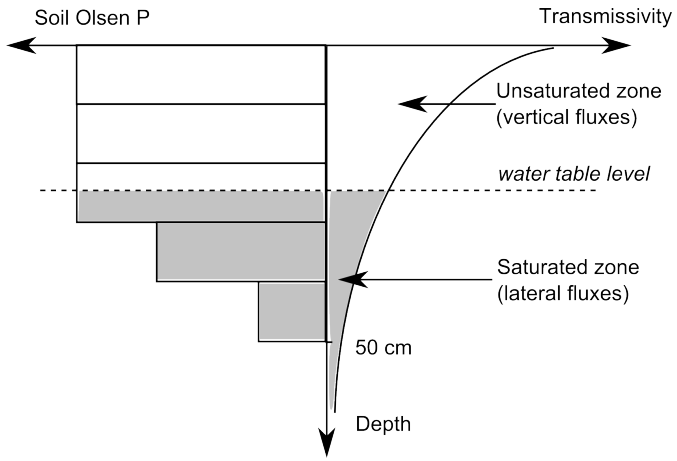

FIGURE 6.2 – Description of soil hydraulic properties and P content with depth

soil and groundwater, which has been shown to improve representation of nutrients fluxes and transformations (Beaujouan *et al.*, 2002).

To simulate SRP fluxes, the only modification to the hydrological sub-model aimed to compute water fluxes from each soil layer by integrating equation (6.1) between the maximum depth of the soil layer considered and :

- estimated groundwater level, if the groundwater table is within the soil layer considered

or

- the minimum depth of the soil layer considered, if the groundwater table above the soil layer considered.

In this application of the TNT2-P model, 5 soil layers with a thickness of 10 cm are considered. Hence, 7 flow components are computed in the model :

- overland flow on saturated surface ;
- 5 sub-surface flow components, for each soil layer ;
- deep flow, *i.e.* flow below the 5 soil layers.

Soil-P sub-model The soil-P sub-model consists in an empirical function derived from soil pore water monitoring data (Dupas *et al.*, 2015c) :

- Background SRP concentration in the soil pore water of a given layer is proportional to soil Olsen P ;
- Seasonal increases in P availability compared to background conditions are determined by biogeochemical processes controlled by antecedent temperature and soil moisture. Data show that SRP availability in the soil pore water increases following periods of dry and hot conditions.

Hence, SRP transfer is modelled with calibrated coefficients that describe both mobilisation and transfer to the stream. A different coefficient value is used to simulate transfer via overland flow and sub-surface flow.

$$F_{SRPoverland} = Coef_{SRPoverland} * P_{Olsen} * q_{overland} \tag{6.2}$$

$$F_{SRPsub-surface} = Coef_{SRPsub-surface} * P_{Olsen} * q_{sub-surface} \tag{6.3}$$

Where $F_{SRPoverland}$ and $F_{SRPsub-surface}$ are SRP transfer via overland flow and sub-surface flow for a given soil layer respectively, $q_{overland}$ and $q_{sub-surface}$ are water flows from the same pathways. $Coef_{SRPoverland}$ and $Coef_{SRPsub-surface}$ are coefficients which vary according to antecedent temperature and soil moisture conditions, such as :

$$Coef_{SRP} = Coef_{background} * (1 + F_T * F_S) \tag{6.4}$$

Where $Coef_{SRP}$ is either $Coef_{SRPoverland}$ or $Coef_{SRPsub-surface}$, and F_T and F_S are temperature and soil moisture factors, respectively. F_T and F_S are expressed as :

$$F_T = exp((mean(temperature, idays) - T1)/T2) \tag{6.5}$$

$$F_S = 1 - (mean(waterconcentent, idays)/(maximumwatercontent))^{S1} \tag{6.6}$$

Where $T1$, $T2$ and $S1$ are calibrated coefficients. The antecedent condition time length consists in a period of i=100 days. Both soil temperature and soil moisture are estimated by TNT2 soil module (Moreau *et al.*, 2013). Because soil moisture in the deep soil layers can differ significantly from that of shallow soil layers, two values of FS are calculated for two soil depth 0 - 20 cm and 20 - 50 cm. The temperature factor F_T was calculated as an average value for the entire soil profile 0 - 50 cm. Contrary to water fluxes, SRP fluxes are not routed cell-to-cell, because we lacked knowledge of the rate of SRP re-adsorption in downslope cells, and on the long term fate of re-adsorbed SRP. Hence, all the SRP emitted from each cell through overland flow and sub-surface flow reaches the stream on the same day. For deep flow, only the immediate riparian flux is used in determining SRP inputs to the river.

Input data and parameters Spatial input data include :

- A DEM in raster format. Here, a 20 m resolution DEM was used, hence model calculations were made in 12.348 grid cells in a 4.94 km2 catchment ;
- A map of soils with homogeneous hydrological parameter value, in raster format. Here, two soil classes were considered by differentiating well-drained (86%) and poorly drained soils (14%) according to Curmi *et al.* (1998) (Figure 6.1) ;
- A map of surface P Olsen in raster format and description of decrease in P Olsen with depth for five soil layers between 0 – 50 cm. Here, the map of P Olsen in the 0 – 15 cm soil layer was obtained from statistical modelling with the rule-based regression

algorithm CUBIST (Quinlan, 1992) using data from 198 soil samples (2013) in an area of 12 km^2 encompassing the 4.94 km^2 catchment (Matos-Moreira *et al.*, 2015). To describe how P Olsen decreases with depth, land use information was used. In tilled fields, *i.e.* all crop rotations including arable crops, Olsen P was assumed to be constant between 0 – 30 cm and to decrease linearly with depth between 30 – 50 cm. In no-till fields, *i.e.* permanent pasture and woodland, Olsen P was assumed to decrease linearly with depth between 0 – 50 cm. An exponential decrease with depth is more commonly adopted in untilled land, but a specific sampling in currently untilled areas in the Kervidy-Naizin catchment (Dupas *et al.*, 2015c) has shown that a linear function is more appropriate, probably because of these areas having been ploughed in the past.

Climate input data include minimum and maximum air temperature, precipitation, potential evapotranspiration, global radiation on a daily basis. The TNT2 model allows for several climate zones to be considered, in which case a raster map of climate zone must be provided to the model. Here, only one climate zone is considered.

In total, the TNT2-P model includes 15 parameters for each soil type, *i.e.* 30 parameters in total if two soil drainage classes are considered. To reduce the number of model runs necessary to explore the parameter space using Monte Carlo simulations, several parameters were given fixed values, or a constant ratio between the two soil types was set (Table

Finally, only 12 parameters were varied independently. Initial parameter ranges for the hydrological sub-model were based on literature-derived values (Moreau *et al.*, 2013) and those for the soil sub-model were based on a preliminary manual trial and error procedure. The SRP concentration for deep flow water was based on actual measurement of SRP in the weathered schist (Dupas *et al.*, 2015c). A constant flux value for domestic sources was set at the 1% percentile of the daily flux between 2007 and 2013 (Dupas *et al.*, 2015b).

Derivation of limits of acceptability from data uncertainty assessment

The Monte Carlo based Generalized Likelihood Uncertainty Estimation (GLUE) methodology has been widely used in hydrology and is described elsewhere (Beven and Freer, 2001 ; Beven, 2006, 2009). Briefly, the rationale of GLUE is that many model structures and parameter sets can give "acceptable" results, according to one or several performance measures, due to equifinality. Hence, GLUE considers that all models that give acceptable results should be used for prediction. A key issue in GLUE is to decide on a performance threshold to define acceptable models ; typically, modellers set a threshold value of a measure such as the Nash-Sutcliffe Efficiency based on their subjective appreciation of data uncertainty or on previously used values. To allow for a more explicit justification of the performance threshold values used, the limits of acceptability approach outlined by Beven (2006) relies on an assessment of uncertainty in the calibration/evaluation data. According to this approach, all model realisations that fall within the limits of acceptability are used for prediction, weighted by a score calculated based on overall performance.

Details on how the limits of acceptability for daily discharge and daily SRP load were derived from uncertainty assessment of the observational data are presented below. Input data, such as weather and soil data, also contained uncertainty which were not accounted for in the limits of acceptability due to a lack of data to quantifying them.

.	Abbreviation	Unit	Hydrological (H), Phosphorus model (P)	Range poorly drained soils (min-max)	Range well drained soils (min-max)
Lateral transmissivity at saturation	T	m^2 d^{-1}	H	4-8	-> x1.5
Exponential decay rate of hydraulic conductivity with depth	m	m^2 d^{-1}	H	0.02-0.2	0.02-0.2
Soil depth	ho	m	H	0.3-0.8	-> x1
Drainage porosity of soil	po	cm^3 cm^{-3}	H	0.1-0.4	-> x1
Regolith layer thickness	h1	m	H	5-10	-> x4
Exponent for evaporation limit	α	.	H	8 (fixed)	-> x1
kRC parameter for capillary rise	kRC	.	H	0.001 (fixed)	-> x1
n parameter for capillarity rise	n	.	H	2.5 (fixed)	-> x1
Drainage porosity of regolith layer	p1	cm^3 cm^{-3}	H	0.01-0.05	-> x1
Background P release coefficient for subsurface flow	$Coef_{overland}$	.	P	0-0.015	-> x1
Background P release coefficient for overland flow	$Coef_{sub-surface}$		P	0-0.25	-> x1
Temperature coefficient 1	T1	.	P	5-10	-> x1
Temperature coefficient 2	T2	.	P	2-10	-> x1
Soil moisture coefficient	S1	.	P	0-2	-> x1
SRP concentration in deep flow	SRP_{deep}	mg l^{-1}	P	0-0.007	-> x1

TABLE 6.1 – Initial parameter ranges in the hydrological and soil phosphorus sub models.

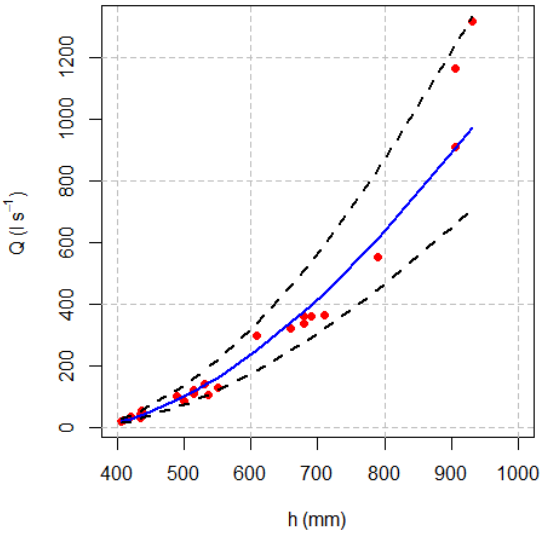

FIGURE 6.3 – Rating curve in Kervidy-Naizin ; acceptability bounds derived from 90% prediction interval (blue line : fitting regression ; black dots : 90% prediction interval). Red dots represent the original discharge measurements used to calibrate the stage-discharge rating curve (Carluer, 1998).

Discharge Error in discharge measurement data was assessed from the original discharge measurements used to calibrate the stage-discharge rating curve (Carluer, 1998). The rating curve used in this study was :

$$Q = a * (h - h_0)^b \tag{6.7}$$

Where Q is discharge, h is stage reading, h0 is stage reading at zero discharge, a and b are calibrated coefficients. Limits of acceptability were defined as the 90% prediction interval of log-log linear regression (Figure 6.3). Estimated acceptability range was ±39% on average. For daily discharge values below 2 mm d^{-1}, fixed acceptability limits were set at the 90% prediction interval for a stage measurement corresponding to 2 mm d^{-1}.

SRP load Uncertainty in "observed" daily load includes uncertainty in discharge and uncertainty in SRP concentration. Uncertainty in daily load was estimated summing up relative uncertainty assessed for discharge and SRP concentration. Uncertainty in SRP concentration stems from sampling frequency problems as one grab sample collected on a specific day is incommensurable with the mean daily concentration or load simulated by the model. Further, measurement errors exist that include the effect of storage time (Haygarth *et al.*, 1995). During baseflow periods, measurement error was expected to be the main source of uncertainty because relative measurement error is large for low concentrations,

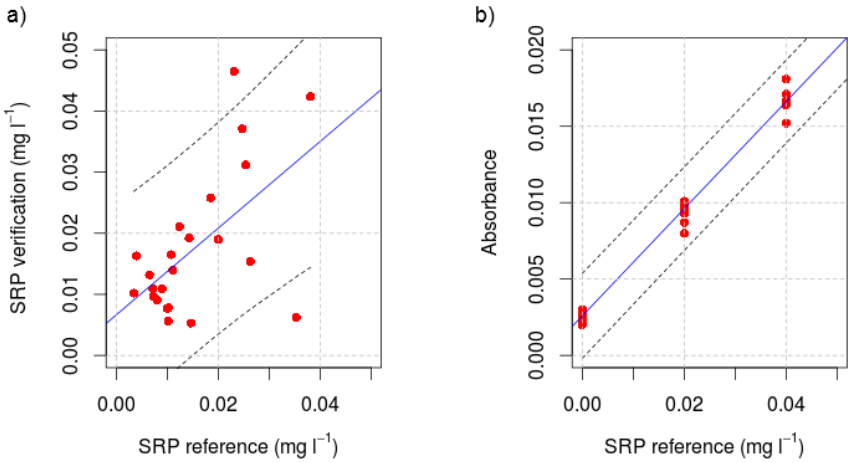

FIGURE 6.4 – a) linear regression model linking the reference data and a verification dataset ; b) measurement error as estimated from a repeatability test performed by the lab in charge of producing reference data (blue line : fitting regression ; black dots : 90% prediction interval).

especially when sample storage time exceeds 48h (Jarvie *et al.*, 2002), while concentrations vary little. During storm events, sampling frequency was expected to be the main source of uncertainty because SRP concentration can vary by one order of magnitude within a few hours. Therefore, different acceptability limits were set for both flow conditions. We considered storms as events with $>$ 20 l s^{-1} increase in discharge and the following 24h.

During baseflow periods, the acceptability limits were derived from the 90% prediction interval of a linear regression model linking pairs of data points sampled on the same day (reference sample between 16 :00 - 18 :00, verification sample between 11 :00 - 15 :00) and analysed independently (within a fortnight for the reference sample and within 1 - 2 days for the verification sample). It was assumed that there was no systematic bias between the two datasets due to different sampling time. The reference SRP concentrations were on average 13% lower than the verification value but this difference was not statistically significant (Mann-Whitney Rank Sum Test, $p > 0.05$). Hence, the expected underestimation of SRP concentration due to long sample storage appears to be overshadowed by other sources of uncertainty such as variability in SRP concentration during the day of sampling or analytical imprecision at low concentrations. This method encompasses all various sources of uncertainty, which results in prediction intervals much wider than what would result from a mere repeatability test : at the median concentration (0.02 mg l^{-1}), estimated prediction interval was 166% with this method versus 57% with a repeatability test (Figure 6.4).

During storm events, acceptability limits were derived from the 90% prediction interval of concentration discharge empirical models $C = a * Q^b$ using high frequency autosampler data. A distinct empirical model was used to fit to each storm event monitored and a delay term was introduced manually in the empirical model when a time lag existed between concentration and discharge peaks. The empirical models were then applied to extrapolate

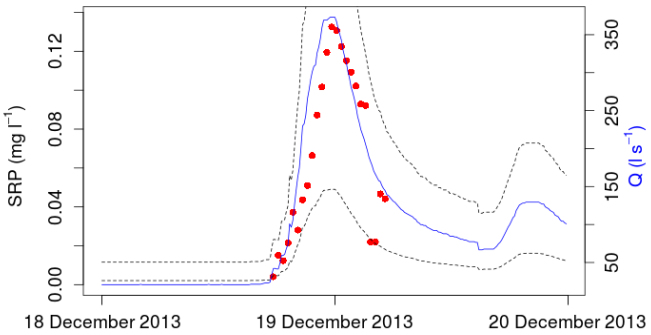

FIGURE 6.5 – Example of an empirical concentration – discharge model; acceptability bounds derived from 90% prediction interval. Red circles represent the SRP measurements.

concentration estimation during two days at 10 min resolution, for each of the 14 storm events monitored. Finally the 2-day mean "observed" load was estimated as the mean of 10 min loads and uncertainty limits were derived from the 90% prediction interval. In model evaluation, the mean of simulated loads during 2 consecutive days was evaluated against the 2-day mean "observed" load for which prediction intervals have been calculated. A 2-day acceptability limit enables to cover the whole of storm events (Figure 6.5 and Supplementary Materials).

When comparing autosampler data with data from immediately filtered samples, the ratio obtained ranged 1-1.6 (mean = 1.3), hence autosampler data were underestimated arguably through adsorption or biological consumption. We used the mean ratio to correct all storm uncertainty intervals by 30% and the range values to extend the upper limit by 60%. During days with a storm event not monitored at high frequency with an autosampler, we considered that the grab sample data did not contain enough information to derive an acceptability interval for daily SRP load.

Model runs and selection of acceptable models To explore the parameter space, 15,000 Monte Carlo realisations were performed to simulate daily discharge and SRP load during the water years 2013 - 2014 and 2014 - 2015. A 7-month initialisation period was run to reduce the impact of initial conditions on simulated results during the study period, from 1 October 2013 to 31 July 2015.

To be considered acceptable, model runs must fall within the acceptability limits defined in 2.3.1 and 2.3.2. More specifically, 100% of simulated daily discharge, 100% of simulated baseflow SRP load and 100% of simulated storm SRP load had to fall within the acceptability limits. Thus, 572 acceptability tests were performed for discharge, 378 for baseflow SRP load and 14 for storm SRP loads, *i.e.* 964 evaluation criteria.

To evaluate the model performance in more detail, normalized scores were calculated during 6 periods (Table 6.2). To calculate the scores, a difference was calculated between each of the daily simulated discharge, baseflow SRP load and 2-day storm SRP loads and the corresponding observation. This difference was then normalized by the width of the acceptability limit defined for that day, so the score has a value of 0 in the case of a perfect

Name	Starting date	Ending date
Autumn 2013	01-10-2013	31-12-2013
Winter 2014	01-01-2014	31-03-2014
Spring 2014	01-04-2014	31-07-2014
Autumn 2014	01-10-2014	31-12-2014
Winter 2015	01-01-2015	31-03-2015
Spring 2015	01-04-2015	31-07-2015

TABLE 6.2 – Starting and ending dates of the periods studied.

match with observation, -1 at the lower limit and +1 at the upper limit (Figure 6.6a). Finally, the median of this ratio was calculated for each of the 6 periods to investigate whether the model tended to underestimate or overestimate discharge and loads at different moments of the year and between the two years.

Model runs were successively evaluated for discharge, baseflow SRP load and storm SRP load. To use the models for prediction, each accepted model was given a likelihood weight according to how well it has performed for each of the 964 evaluation criteria. Here a triangular weight was calculated for each evaluation criteria (Figure 6.5b), with the base of the triangle corresponding to the acceptability limit. Calculated weights were then averaged for discharge, baseflow SRP load and storm SRP load respectively and the final likelihood was calculated as the sum of all three averages.

The model's sensitivity to each hydrological and soil parameter was performed with a Hornberger-Spear-Young Generalised Sensitivity Analysis (HSY GSA, Whitehead and Young, 1979 ; Hornberger and Spear, 1981). For each evaluation criteria (daily discharge, daily baseflow SRP load, 2-day storm SRP load), the model runs were split into acceptable and non-acceptable runs according to the above-mentioned acceptability limits. Then a Kolmogorov-Smirnov test is performed to assess whether the distribution of each of the three evaluation criteria differ between acceptable and non-acceptable models for each parameter. The p value of the Kolmogorov-Smirnov test is used to discriminate whether the model is critically sensitive ($p<0.01$ '***'), importantly sensitive ($p<0.1$ '*') or insignificantly sensitive ($p>0.1$ '.') to each parameter and for each of the three evaluation criteria. Because the Kolmogorov-Smirnov test might suggest that small differences in distribution are very significant when there are larger number of runs, this method is a qualitative guide to relative sensitivity.

In addition to acceptability limit approach, a NSE (Moriasi *et al.*, 2007) was calculated for daily discharge and daily load and concentration to allow comparison with other modelling studies where is has been taken as an evaluation criteria.

6.1.3 Results

Presentation of observation data and calculation of acceptability limits

The two water years studied were highly contrasted in terms of hydrology and SRP loads. Water year 2013 - 2014 was the wettest in the last 10 years, with cumulative rainfall 1289 mm and cumulative runoff 716 mm. Water year 2014 - 2015 was an average year

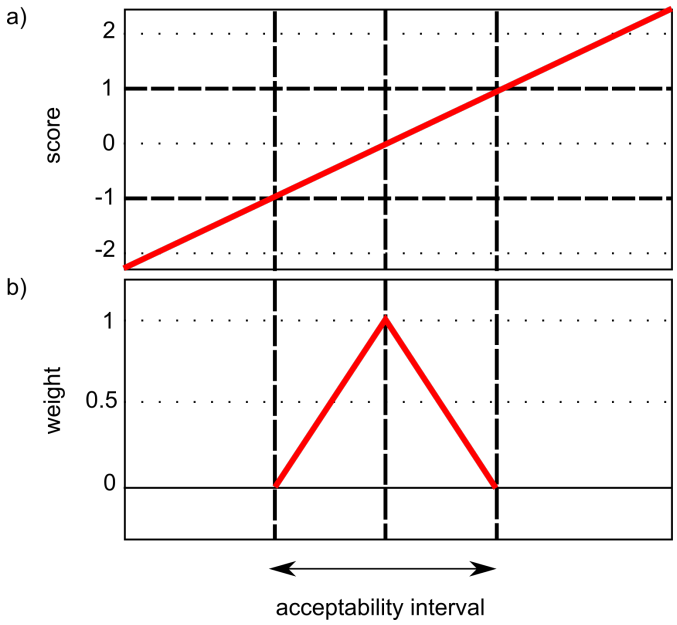

FIGURE 6.6 – a) normalized scores ; b) triangular weighting function.

(5th wettest in the last 10 years), with cumulative rainfall 677 mm and cumulative runoff 383 mm. Annual SRP load was 0.35 kg P ha^{-1} yr^{-1} in 2013-2014 and 0.17 kg P ha^{-1} yr^{-1} in 2014-2015, *i.e.* a difference 10% higher than that of discharge. Observed mean SRP concentration during the study period was 0.024 mg l^{-1}.

Figure 6.7 shows acceptability limits for daily discharge and daily SRP loads. Note that acceptability limits for discharge were calculated every day, while acceptability limits for SRP load was calculated on a daily basis during baseflow periods and on a 2-day basis during storm events monitored at high frequency. No SRP load acceptability limit was calculated during storm events when no high frequency autosampler data was available.

Model evaluation

First, model runs were evaluated against acceptability limits defined for discharge (Figure 6.8a). 4,120/15,000 models fulfilled the selection criterion for discharge, *i.e.* they had 100% of simulated daily discharge within the acceptability limits. The NSE estimated for these models ranged from 0.78 to 0.92. The normalized scores calculated seasonally (Figure 6.9a) show that simulated discharge is often overestimated in autumn and spring, and underestimated in winter.

Then, model runs were evaluated against acceptability limits defined for SRP loads (Figure 6.8b). During baseflow periods, 3,730/15,000 models fulfilled the selection criterion for SRP loads, *i.e.* they had 100% of simulated daily SRP load within the acceptability limits. Among them, 1,210 also fulfilled the previous selection criterion for discharge. Normalized scores for baseflow SRP load showed the same trend as for discharge (Figure 6.9b), *i.e.* overestimation in autumn and spring, and underestimation in winter. During storm

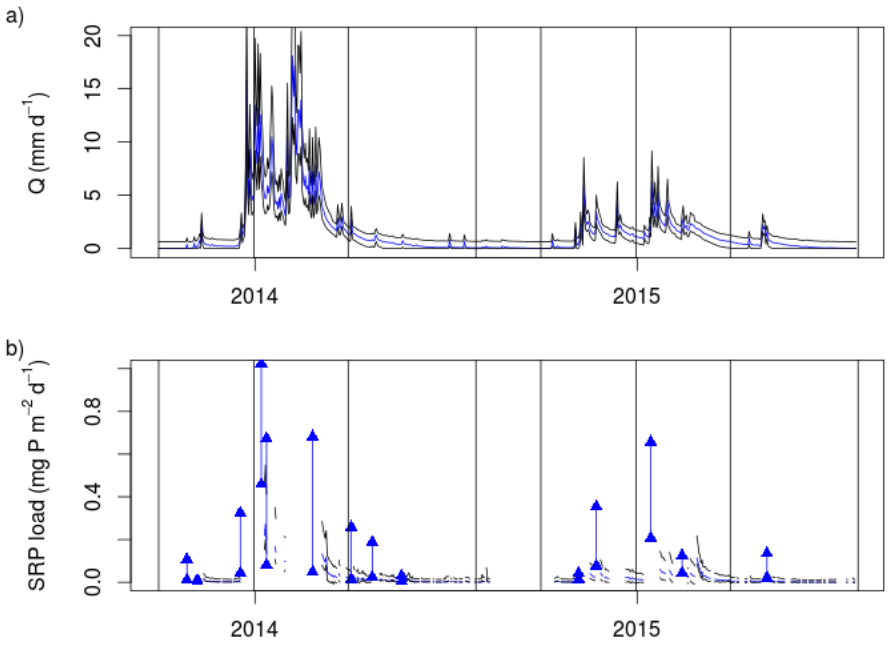

FIGURE 6.7 – Acceptability limits for daily discharge (a) and SRP load (b). Blue lines represent best estimates ; black lines represent the acceptability limits. Storm loads acceptability limits are represented by vertical blue lines. Black vertical lines represent the starting and ending dates for each season (Table 6.2).

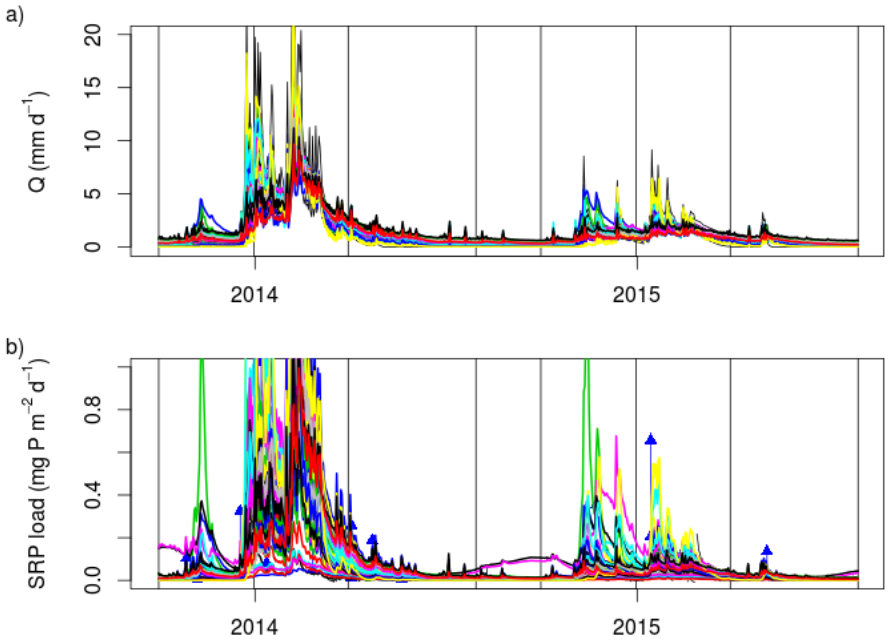

FIGURE 6.8 – Example of 50 model runs simulating discharge (a) and daily load (b). Vertical lines represent the starting and ending dates for each season (Table 6.2).

events, only 5 models fulfilled the selection criterion for SRP loads, *i.e.* they had 14/14 of simulated 2-day storm SRP loads within the acceptability limits, but none of them also fulfilled the selection criteria for discharge and baseflow SRP loads. Two storm events were particularly difficult to simulate (number 2 and number 9, Figure 6.9c), probably because their acceptability interval was very narrow as a result of only small changes in discharge and concentration. To obtain a reasonable number of acceptable models, we relaxed the selection criterion so that the acceptable models had to simulate 12/14 of storm loads within the acceptability limits, in addition to the selection criteria defined for discharge and baseflow SRP load : 418 models were then accepted. Estimated NSE of these 418 models ranged from 0.09 to 0.80 for daily load and from negative values to 0.53 for daily concentrations (this includes all data from the regular sampling).

Sensitivity analysis and prediction results

According to the HSA generalised sensitivity analysis, simulated discharge was critically sensitive to 10 out of the 12 hydrological parameters varied. Simulated SRP load was critically sensitive to the sub-surface and overland flow parameters during baseflow periods and to the overland flow parameter during storm events. During baseflow periods, SRP load was insignificantly sensitive to the parameter associated with deep flow load. Both baseflow and storm SRP loads were critically sensitive to the parameter related to soil moisture and soil temperature dependent SRP solubilisation (S1, T1 and T2), in addition to respectively 11 and 8 hydrological parameters.

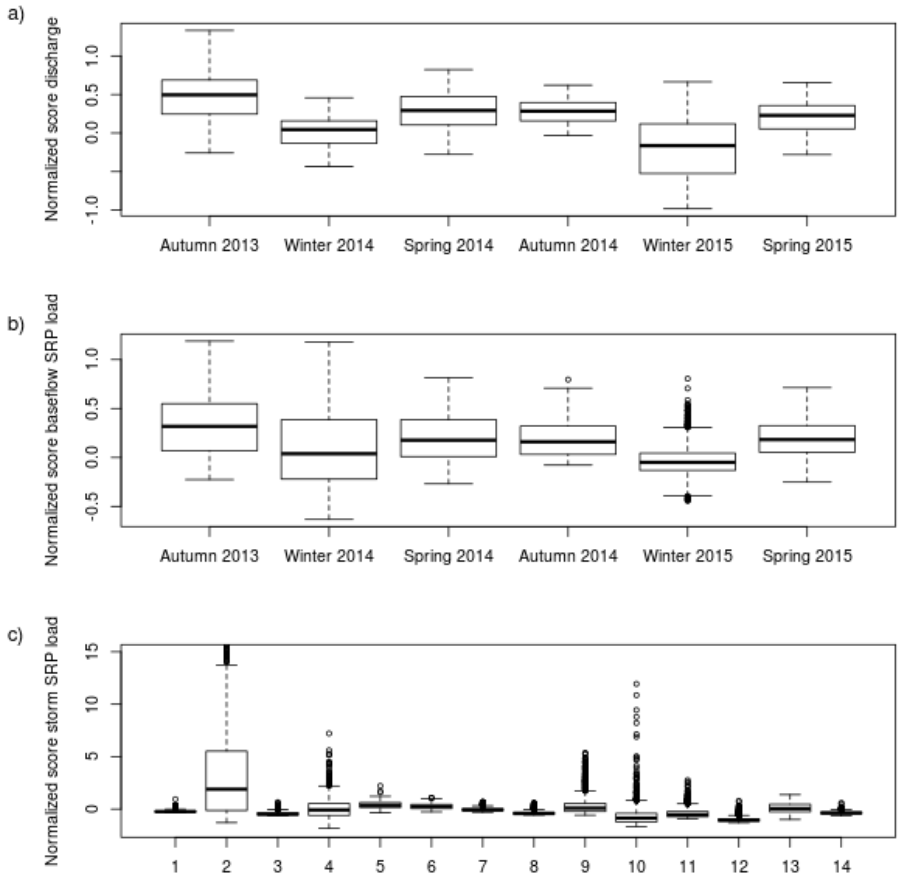

FIGURE 6.9 – Normalized score for daily discharge (a), baseflow SRP load (b) and storm SRP load (c).

.	discharge	baseflow load	SRP	storm SRP load
T (poorly drained soils)	.	***		***
m (poorly drained soils)	***	***		***
ho (poorly drained soils)	***	***		.
po (poorly drained soils)	***	***		***
h1 (poorly drained soils)	***	.		.
p1 (poorly drained soils)	***	***		*
T (well drained soils)	.	***		***
m (well drained soils)	***	***		***
ho (well drained soils)	***	***		.
po (well drained soils)	***	***		***
h1 (well drained soils)	***	***		.
p1 (well drained soils)	***	***		*
$Coef_{sub-surface}$	.	***		.
$Coef_{overland}$	.	.		***
SRP_{deep}	.	.		*
S1	.	***		***
T1	.	***		***
T2	.	***		***

TABLE 6.3 – Sensitivity analysis of the model to 18 model parameters (insignificant ., important *, critical ***)

Figure 6.10 shows the daily discharge, SRP load and concentration as simulated by the acceptable models. Simulated SRP load during the water year 2013 – 2014 ranged 0.77 – 3.28 kg P ha^{-1} yr^{-1} (median = 1.62 kg P ha^{-1} yr^{-1}) ; simulated SRP load during the water year 2014 – 2015 ranged 0.14 – 0.73 kg P ha^{-1} yr^{-1} (median = 0.32 kg P ha^{-1} yr^{-1}). Best estimate of SRP load according to observation data was 0.35 kg P ha^{-1} yr^{-1} in 2013 – 2014 and 0.17 kg P ha^{-1} yr^{-1} in 2014 – 2015. According to the model, 56 – 61% (median = 58%) of water discharge and 71 – 75% (median = 62%) of SRP load occurred during storm events. Mean SRP concentrations during the two water years ranged 0.013 – 0.043 mg l^{-1} (median = 0.028 mg l^{-1}), while mean observed SRP concentration was 0.024 mg l^{-1}.

6.1.4 Discussion

Role of hydrology and biogeochemistry in determining SRP transfer

The fairly good performance of TNT2-P at simulating SRP loads confirms that the hydrological and biogeochemical processes included into the model are dominant controlling factors in the Kervidy-Naizin catchment. The primary control of hydrology in controlling connectivity between soils and streams has been highlighted by many studies analysing water quality time series at the outlet of agricultural catchments (Haygarth *et al.*, 2012 ; Jordan *et al.*, 2012 ; Dupas *et al.*, 2015c ; Mellander *et al.*, 2015). This modelling exercise also confirmed that SRP solubility was determined by the soil P Olsen content and could vary according to temperature and moisture conditions. The underlying processes have not been identified precisely in the Kervidy-Naizin catchment : independent laboratory experiments have shown that microbial cell lysis resulting from alternating dry and water saturated periods in the soil could be the cause of increased SRP mobility (Turner and Haygarth, 2001 ; Blackwell *et al.*, 2009). This could explain the moisture dependence of SRP solubility in the model. Furthermore, net mineralisation of soil organic phosphorus could explain the temperature dependence of SRP solubility in the model. These two hypotheses may explain increased SRP solubility in soils in periods of dry and hot conditions and will be further explored by incubation experiment with soils from the Kervidy-Naizin catchments.

Potential improvements to the model structure according to modelling purpose

The TNT2-P model was designed to test hypotheses about dominant processes and for this purpose, a parsimonious model structure was chosen to include only the processes which were to be tested. This parsimonious model structure might contain some conceptual misrepresentations due to oversimplification, and it might not include all the processes necessary for the purpose of evaluating management scenarios. This section discusses whether the simplifications made are acceptable in the context of different catchment types, and to which conditions the model could be made more complex by including additional routines for the purpose of evaluating management scenarios.

From a conceptual point of view, the lack of cell-to-cell routing of SRP fluxes might result in erroneous results in some contexts. The fact that all the SRP emitted from each cell through overland flow and sub-surface flow reaches the stream on the same day is acceptable for the catchment studied because groundwater interception of shallow soil layers occurs in the riparian zone only, hence the signal of SRP mobilisation in these soils is

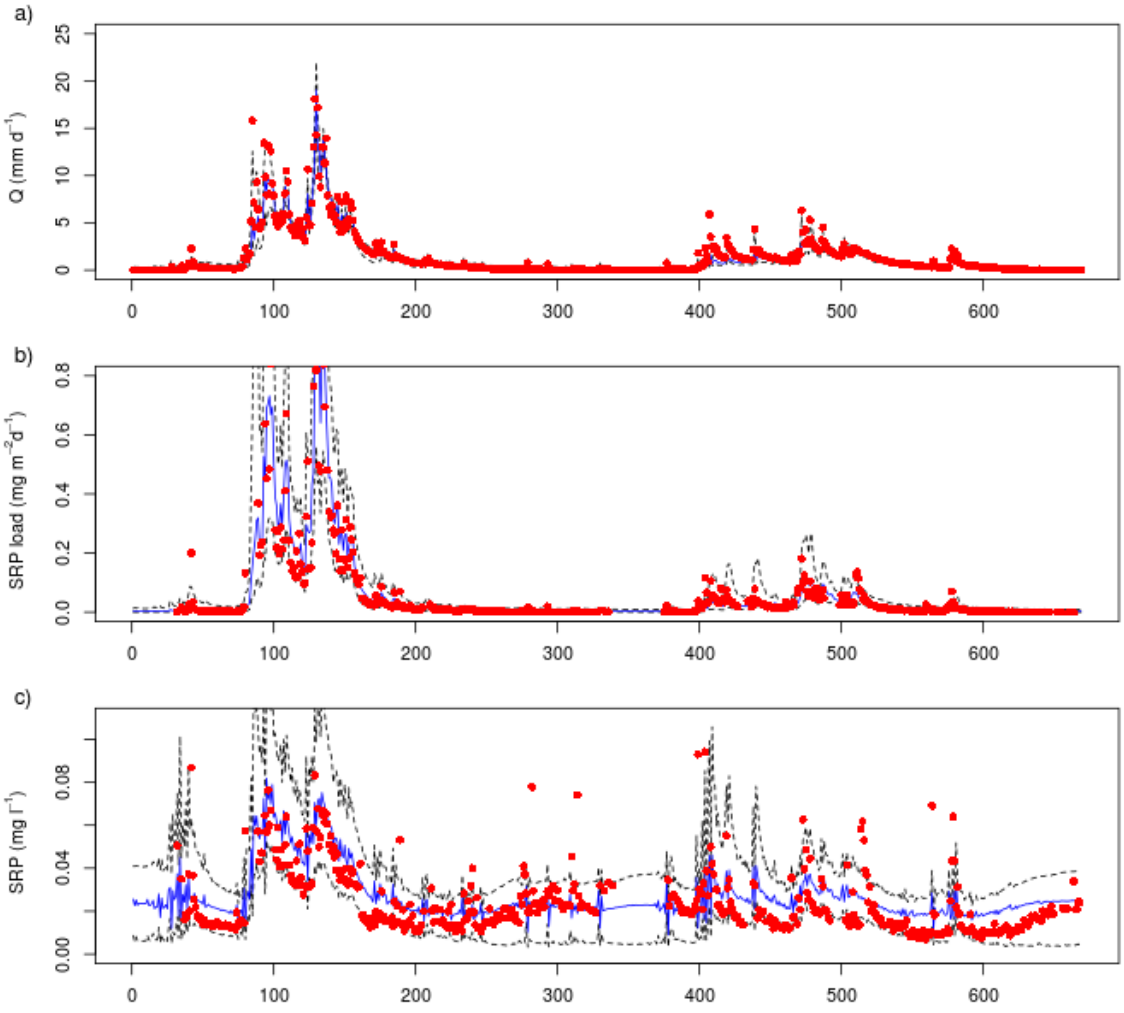

FIGURE 6.10 – Median and 95% credibility interval for daily discharge (a), SRP load (b) and SRP concentration (c). Red circles represent observational data.

generally transmitted to the stream (Dupas *et al.*, 2015c). This simplification would not be acceptable in catchments where soil-groundwater interactions are taking place throughout the landscape, e.g. due to topographic depressions or poorly drained soils. In the latter type of catchment, transmission of the SRP mobilisation signal to the stream is more complex to comprehend (Haygarth *et al.*, 2012), hence a more complex model structure would be required.

The reason for this simplification was that we lacked knowledge of SRP re-adsorption in downslope cells and on the long-term fate of re-adsorbed SRP. For a more physically realistic representation of processes, it is likely that an explicit representation of flow velocities and pathways would be necessary, along with an explicit representation of several soil P pools. However, such an explicit representation of processes contradicts the idea of a parsimonious model, which was adopted here for the purpose of identifying dominant processes. In this respect, TNT2-P is an aggregative model rather than a fully distributed model although it is based on a fully distributed hydrological model (Beaujouan *et al.*, 2002). The current spatial distribution allows finer representation of soil-groundwater interactions than semi-distributed models such as SWAT (Arnold *et al.*, 1998), INCA-P (Wade *et al.*, 2002) and HYPE (Lindstrom *et al.*, 2010) but at higher computation cost. It would be interesting to test to which extent moving from an aggregative model with fully distributed information to a semi-distributed model would degrade the model performance and in the same time reduce computation cost. This could be achieved by grouping cells according to a hydrological similarity criterion like in the original TOPMODEL and Dynamic Topmodel (Beven and Freer, 2001 ; Metcalfe *et al.*, 2015) and do the same for similarity in soil P content.

If reducing the number of calculation units proved to reduce computation cost without degrading quality of prediction, it would be possible to include more parameters in the model, for example to simulate SRP re-absorption in downslope cells or include routines to simulate the evolution of soil P content under different management scenarios (Vadas *et al.*, 2011 ; 2012), and still perform a Monte-Carlo based analysis of uncertainty. The question of coupling or not such a soil P routine with the current TNT2-P model will depend on available data and on the length of available time series : studying the evolution of the soil P content requires at least a decade of soil observation data (Ringeval *et al.*, 2014) and probably a longer period of stream data to account for the time delay for a perturbation in the catchment to become visible in the stream (Wall *et al.*, 2013). Thus, the two years of daily stream SRP in the Kervidy-Naizin catchment are not enough to build a coupled soil-hydrology model with an elaborate soil P routine. Therefore, as things stand, it is more reasonable to generate new soil P Olsen maps with a separate model such as the APLE model (Vadas *et al.*, 2012 ; Benskin *et al.*, 2014) or the 'soil P decline' model used by Wall *et al.* (2013), and use these maps as input to TNT2-P.

Because the current model can simulate response to rainfall, soil moisture and temperature, it could be used to test the effect of climate scenarios on SRP transfer. In Western France, and more generally in Western Europe, the climate for the next few decades is expected to consist of hotter, drier summers and warmer, wetter winter (Jacob *et al.*, 2007 ; Macleod *et al.*, 2012 ; Salmon-Monviola *et al.*, 2013) with increased frequency of high intensity rainfall events (Dequé 2007). In these conditions, SRP concentrations and load will seemingly increase compared to today's climate as a result of both an increase in SRP

solubility in soil due to higher temperature and more severe drought and an increase in transfer due to wetter winter and more frequent high intensity rainfall events. TNT2-P could be used to confirm and quantify the expected increase in SRP transfer from diffuse sources in future climate conditions.

Improving information content in the data

Despite relatively large uncertainty in the data used in this study, it was possible to build a parsimonious catchment model of SRP transfer for the purpose of testing hypotheses about dominant processes, namely the role of hydrology in controlling connectivity between soils and streams and the role of temperature and moisture conditions in controlling soil SRP solubilisation. However, the large uncertainties in the calibration data lead to large prediction uncertainty. For example, the SRP load estimated by the behavioural models from 2013 to 2015 ranged from 0.45 to 2.0 kg P ha^{-1} yr^{-1}; hence the width of the credibility interval was 160% of the median (0.97 kg P ha-1 yr-1). Similarly, the mean SRP concentration estimated by the behavioural models from 2013 to 2015 ranged from 0.013 to 0.045 mg l^{-1}; hence the width of the credibility interval was 110% of the median (0.028 mg l^{-1}). The large uncertainty in the calibration data, along with a lack of long-term information, also prevents including more detailed processes in the soil routine.

To reduce uncertainty in prediction and to build more complex models, several options exist to improve information content in the data. As stated by Jackson-Blake *et al.* (2015b), "the key to obtaining a realistic model simulation is ensuring that the natural variability in water chemistry is well represented by the monitoring data". The monitoring strategy adopted in the Kervidy-Naizin catchment should theoretically enable to capture the natural variability in stream SRP concentration, because sampling took place during two contrasting water years, during different seasons and at a high frequency during 14 storm events. The analysis of uncertainty in the data shows that a large part of uncertainty in "observed" SRP concentration originates from sample storage, both unfiltered between the time of autosampling and manual filtration and between filtration and analysis. This is due to SRP being non-conservative. Thus, there is room for improvement in reducing storage time, without increasing further the monitoring frequency. In this respect, the primary interest of investing in high frequency bankside analysers would lie in their ability to analyse water samples immediately in addition to providing near continuous data. Because bankside analysers perform measurements in relatively homogeneous conditions, unlike the manual and autosampler data for which storage time of filtered and unfiltered samples vary, a finer quantification of uncertainty in the measurement data would be possible (e.g. Lloyd *et al.*, 2015).

6.1.5 Conclusion

The TNT2-P model was capable of capturing daily variation of SRP loads, thus confirming the dominant processes identified in previous analyses of observation data in the Kervidy-Naizin catchment. The role of hydrology in controlling connectivity between soils and streams, and the role of soil Olsen P, soil moisture and temperature in controlling SRP solubility have been confirmed. The lack of any representation of the short-term effect of management practices did not seem to penalize the model's performance. Their long-term

effect on the soil Olsen P could be simulated with an independent model or through an additional sub-model if a longer period of data was available to calibrate it. The modelling approach presented in this paper included an assessment of the information content in the data, and propagation of uncertainty in the model's prediction. The information content of the data was sufficient to explore dominant processes, but the relatively large uncertainty in SRP concentrations would seemingly limit the possibility for including more detailed processes into the model. Data from near continuous bankside analyser will probably allow calibrating more detailed models in the near future.

6.1.6 References

Alexander RB, Smith RA, Schwarz GE, Boyer EW, Nolan JV, Brakebill JW. Differences in phosphorus and nitrogen delivery to the gulf of Mexico from the Mississippi river basin. Environmental Science Technology 2008 ; 42 : 822-830.

Arnold JG, Srinivasan R, Muttiah RS, Williams JR. Large area hydrologic modeling and assessment - Part 1 : Model development. Journal of the American Water Resources Association 1998 ; 34 : 73-89.

Aubert AH, Gascuel-Odoux C, Gruau G, Akkal N, Faucheux M, Fauvel Y, et al. Solute transport dynamics in small, shallow groundwater-dominated agricultural catchments : insights from a high-frequency, multisolute 10 yr-long monitoring study. Hydrology and Earth System Sciences 2013 ; 17 : 1379-1391.

Beauchemin S, Simard RR. Soil phosphorus saturation degree : Review of some indices and their suitability for P management in Quebec, Canada. Canadian Journal of Soil Science 1999 ; 79 : 615-625.

Beaujouan V, Durand P, Ruiz L, Aurousseau P, Cotteret G. A hydrological model dedicated to topography-based simulation of nitrogen transfer and transformation : rationale and application to the geomorphology-denitrification relationship. Hydrological Processes 2002 ; 16 : 493-507.

Benskin CMH, Roberts W. M, Wang Y, Haygharth PM. Review of the Annual Phosphorus Loss Estimator tool – a new model for estimating phosphorus losses at the field scale. Soil Use and Management 2014 ; 30 : 337-341.

Beven K. A manifesto for the equifinality thesis. Journal of Hydrology 2006 ; 320 : 18-36.

Beven K. Environmental Modelling – An Uncertain Future ? Routledge : London 2009.

Beven K, Freer J. Equifinality, data assimilation, and uncertainty estimation in mechanistic modelling of complex environmental systems using the GLUE methodology. Journal of Hydrology 2001 ; 249 : 11-29.

Beven K, Smith P. Concepts of Information Content and Likelihood in Parameter Calibration for Hydrological Simulation Models. Journal of Hydrologic Engineering 2015 ; 20.

Beven KJ. Distributed hydrological modelling : applications of the TOPMODEL concept, 1997.

Blackwell MSA, Brookes PC, de la Fuente-Martinez N, Murray PJ, Snars KE, Williams JK, et al. Effects of soil drying and rate of re-wetting on concentrations and forms of phosphorus in leachate. Biology and Fertility of Soils 2009 ; 45 : 635-643.

Blazkova S, Beven K. A limits of acceptability approach to model evaluation and uncertainty estimation in flood frequency estimation by continuous simulation : Skalka catchment, Czech Republic. Water Resources Research 2009 ; 45.

Bradley WG, Borenstein AR, Nelson LM, Codd GA, Rosen BH, Stommel EW, et al. Is exposure to cyanobacteria an environmental risk factor for amyotrophic lateral sclerosis and other neurodegenerative diseases ? Amyotrophic Lateral Sclerosis and Frontotemporal Degeneration 2013 ; 14 : 325-333.

Bruneau P, Gascuel-Odoux C, Robin P, Merot P, Beven KJ. Sensitivity to space and time resolution of a hydrological model using digital elevation data. Hydrological Processes 1995 ; 9 : 69-82.

Carluer N. Vers une modélisation hydrologique adaptée à l'évaluation des pollutions diffuses : prise en compte du réseau anthropique. Application au bassin versant de Naizin (Morbihan). PhD thesis Université Pierre et Marie Curie 1998.

Carpenter SR, Caraco NF, Correll DL, Howarth RW, Sharpley AN, Smith VH. Nonpoint pollution of surface waters with phosphorus and nitrogen. Ecological Applications 1998 ; 8 : 559-568.

Curmi P, Durand P, Gascuel-Odoux C, Merot P, Walter C, Taha A. Hydromorphic soils, hydrology and water quality : spatial distribution and functional modelling at different scales. Nutrient Cycling in Agroecosystems 1998 ; 50 : 127-142.

Dean S, Freer J, Beven K, Wade AJ, Butterfield D. Uncertainty assessment of a process-based integrated catchment model of phosphorus. Stochastic Environmental Research and Risk Assessment 2009 ; 23 : 991-1010.

Deque M. Frequency of precipitation and temperature extremes over France in an anthropogenic scenario : Model results and statistical correction according to observed values. Global and Planetary Change 2007 ; 57 : 16-26.

Dupas R, Delmas M, Dorioz JM, Garnier J, Moatar F, Gascuel-Odoux C. Assessing the impact of agricultural pressures on N and P loads and eutrophication risk. Ecological Indicators 2015a ; 48 : 396–407.

Dupas R, Gascuel-Odoux C, Gilliet N, Grimaldi C, Gruau G. Distinct export dynamics for dissolved and particulate phosphorus reveal independent transport mechanisms in an arable headwater catchment. Hydrological Processes 2015b.

Dupas R, Gruau G, Gu S, Humbert G, Jaffrezic A, Gascuel-Odoux C. Groundwater control of biogeochemical processes causing phosphorus release from riparian wetlands. Water Research 2015c.

Dupas R, Tavenard R, Fovet O, Gilliet N, Grimaldi C, Gascuel-Odoux C. Identifying seasonal patterns of phosphorus storm dynamics with Dynamic Time Warping. Water Resources Research 2015d.

Durand P, Moreau P, Salmon-Monviola J, Ruiz L, Vertes F, Gascuel-Odoux C. Modelling the interplay between nitrogen cycling processes and mitigation options in farming catchments. Journal of Agricultural Science 2015 ; 153 : 959-974.

Franks SW, Gineste P, Beven KJ, Merot P. On constraining the predictions of a distributed model : the incorporation of fuzzy estimates of saturated areas into the calibration process, Water Resources Research 1998 ; 34 : 787-797.

Grizzetti B, Bouraoui F, Aloe A. Changes of nitrogen and phosphorus loads to European seas. Global Change Biology 2012 ; 18 : 769-782.

Hahn C, Prasuhn V, Stamm C, Lazzarotto P, Evangelou MWH, Schulin R. Prediction of dissolved reactive phosphorus losses from small agricultural catchments : calibration and validation of a parsimonious model. Hydrology and Earth System Sciences 2013 ; 17 : 3679-3693.

Hahn C, Prasuhn V, Stamm C, Schulin R. Phosphorus losses in runoff from manured grassland of different soil P status at two rainfall intensities. Agriculture Ecosystems Environment 2012 ; 153 : 65-74.

Haygarth PM, Ashby CD, Jarvis SC. Short-term changes in the molybdate reactive phosphorus of stored soil waters. Journal of Environmental Quality 1995 ; 24 : 1133-1140.

Haygarth PM, Hepworth L, Jarvis SC. Forms of phosphorus transfer in hydrological pathways from soil under grazed grassland. European Journal of Soil Science 1998 ; 49 : 65-72.

Haygarth PM, Page TJC, Beven KJ, Freer J, Joynes A, Butler P, et al. Scaling up the phosphorus signal from soil hillslopes to headwater catchments. Freshwater Biology 2012 ; 57 : 7-25.

Heathwaite AL, Dils RM. Characterising phosphorus loss in surface and subsurface hydrological pathways. Science of the Total Environment 2000 ; 251 : 523-538.

Heckrath G, Brookes PC, Poulton PR, Goulding KWT. Phosphorus leaching from soils containing different phosphorus concentrations in the broadbalk experiment. Journal of Environmental Quality 1995 ; 24 : 904-910.

Hornberger GM, Spear RC. An approach to the preliminary analysis of environmental systems. J. Environmental Management 1981 ; 12 : 7-18.

Jackson-Blake LA, Dunn SM, Helliwell RC, Skeffington RA, Stutter MI, Wade AJ. How well can we model stream phosphorus concentrations in agricultural catchments ? Environmental Modelling Software 2015a ; 64 : 31-46.

Jackson-Blake LA, Starrfelt J. Do higher data frequency and Bayesian auto-calibration lead to better model calibration ? Insights from an application of INCA-P, a process-based river phosphorus model. Journal of Hydrology 2015b ; 527 : 641-655.

Jacob D, Barring L, Christensen OB, Christensen JH, de Castro M, Deque M, et al. An inter-comparison of regional climate models for Europe : model performance in present-day climate. Climatic Change 2007 ; 81 : 31-52.

Jarvie HP, Withers PJA, Neal C. Review of robust measurement of phosphorus in river water : sampling, storage, fractionation and sensitivity. Hydrology and Earth System Sciences 2002 ; 6 : 113-131.

Jordan P, Melland AR, Mellander PE, Shortle G, Wall D. The seasonality of phosphorus transfers from land to water : implications for trophic impacts and policy evaluation. Sci Total Environ 2012 ; 434 : 101-9.

Kirchner JW. Getting the right answers for the right reasons : Linking measurements, analyses, and models to advance the science of hydrology. Water Resources Research 2006 ; 42.

Humbert G, Jaffrezic A, Fovet O, Gruau G, Durand P. Dry-season length and runoff control annual variability in stream DOC dynamics in a small, shallow groundwater-dominated agricultural watershed. Water Resources Research 2015.

Lazzarotto P, Stamm C, Prasuhn V, Flühler H. A parsimonious soil-type based rainfall-runoff model simultaneously tested in four small agricultural catchments. Journal of Hy-

drology 2006 ; 321 : 21-38.

Lindstrom G, Pers C, Rosberg J, Stromqvist J, Arheimer B. Development and testing of the HYPE (Hydrological Predictions for the Environment) water quality model for different spatial scales. Hydrology Research 2010 ; 41 : 295-319.

Lloyd CEM, Freer JE, Johnes PJ, Coxon G, Collins AL. Discharge and nutrient uncertainty : implications for nutrient flux estimation in small streams. Hydrological processes 2015.

Macleod CJA, Falloon PD, Evans R, Haygarth PM. The effects of climate change on the mobilization of diffuse substances from agricultural systems. In : Sparks DL, editor. Advances in Agronomy, Vol 115. 115, 2012, pp. 41-77.

Maguire RO, Sims JT. Soil testing to predict phosphorus leaching. Journal of Environmental Quality 2002 ; 31 : 1601-1609.

Matos-Moreira M, Lemercier B, Michot D, Dupas R, Gascuel-Odoux C. Using agricultural practices information for multiscale environmental assessment of phosphorus risk. Geophysical Research Abstracts 2015 ; 17.

McDowell R, Sharpley A, Withers P. Indicator to predict the movement of phosphorus from soil to subsurface flow. Environmental Science Technology 2002 ; 36 : 1505-1509.

Mellander PE, Jordan P, Shore M, Melland AR, Shortle G. Flow paths and phosphorus transfer pathways in two agricultural streams with contrasting flow controls. Hydrological Processes 2015.

Metcalfe P, Beven BJ, and Freer J. Dynamic Topmodel : a new implementation in R and its sensitivity to time and space steps. Environmental Modelling and Software 2015 ; 72 : 155-172.

Molenat J, Gascuel-Odoux C, Ruiz L, Gruau G. Role of water table dynamics on stream nitrate export and concentration. in agricultural headwater catchment (France). Journal of Hydrology 2008 ; 348 : 363-378.

Moore MT, Locke MA. Effect of Storage Method and Associated Holding Time on Nitrogen and Phosphorus Concentrations in Surface Water Samples. Bulletin of Environmental Contamination and Toxicology 2013 ; 91 : 493-498.

Moreau P, Ruiz L, Mabon F, Raimbault T, Durand P, Delaby L, et al. Reconciling technical, economic and environmental efficiency of farming systems in vulnerable areas. Agriculture Ecosystems Environment 2012 ; 147 : 89-99.

Moreau P, Viaud V, Parnaudeau V, Salmon-Monviola J, Durand P. An approach for global sensitivity analysis of a complex environmental model to spatial inputs and parameters : A case study of an agro-hydrological model. Environmental Modelling Software 2013 ; 47 : 74-87.

Moriasi DN, Arnold JG, Van Liew MW, Bingner RL, Harmel RD, Veith TL. Model evaluation guidelines for systematic quantification of accuracy in watershed simulations. Transactions of the Asabe 2007 ; 50 : 885-900.

Olsen SR, Cole CV, Watanbe FS, Dean LA. Estimation of available phosphorus in soils by extraction with sodium bicarbonate 1954.. Circ. 939. USDA, Washington, DC.

Outram FN, Lloyd CEM, Jonczyk J, Benskin CMH, Grant F, Perks MT, et al. High-frequency monitoring of nitrogen and phosphorus response in three rural catchments to the end of the 2011-2012 drought in England. Hydrology and Earth System Sciences 2014 ; 18 : 3429-3448.

Page T, Haygarth PM, Beven KJ, Joynes A, Butler T, Keeler C, et al. Spatial variability of soil phosphorus in relation to the topographic index and critical source areas : Sampling for assessing risk to water quality. Journal of Environmental Quality 2005 ; 34 : 2263-2277.

Perks MT, Owen GJ, Benskin CMH, Jonczyk J, Deasy C, Burke S, et al. Dominant mechanisms for the delivery of fine sediment and phosphorus to fluvial networks draining grassland dominated headwater catchments. Science of the Total Environment 2015 ; 523 : 178-190.

Quinlan, J.R. Learning with continuous classes. Proceedings of the 5th Australian Joint Conference On Artificial Intelligence 1992, 343-348.

Ringeval B, Nowak B, Nesme T, Delmas M, Pellerin S. Contribution of anthropogenic phosphorus to agricultural soil fertility and food production. Global Biogeochemical Cycles 2014 ; 28 : 743-756.

Salmon-Monviola J, Moreau P, Benhamou C, Durand P, Merot P, Oehler F, et al. Effect of climate change and increased atmospheric CO2 on hydrological and nitrogen cycling in an intensive agricultural headwater catchment in western France. Climatic Change 2013 ; 120 : 433-447.

Schindler DW, Hecky RE, Findlay DL, Stainton MP, Parker BR, Paterson MJ, et al. Eutrophication of lakes cannot be controlled by reducing nitrogen input : Results of a 37-year whole-ecosystem experiment. Proceedings of the National Academy of Sciences of the United States of America 2008 ; 105 : 11254-11258.

Schoumans OF, Chardon WJ. Phosphate saturation degree and accumulation of phosphate in various soil types in The Netherlands. Geoderma 2015 ; 237 : 325-335.

Serrano T, Dupas R, Upegui E, Buscail C, Grimaldi C, Viel J-F. Geographical modeling of exposure risk to cyanobacteria for epidemiological purposes. Environment International 2015 ; 81 : 18-25.

Sharpley AN, Kleinman PJ, Heathwaite AL, Gburek WJ, Folmar GJ, Schmidt JP. Phosphorus loss from an agricultural watershed as a function of storm size. J Environ Qual 2008 ; 37 : 362-8.

Siwek J, Siwek JP, Zelazny M. Environmental and land use factors affecting phosphate hysteresis patterns of stream water during flood events (Carpathian Foothills, Poland). Hydrological Processes 2013 ; 27 : 3674-3684.

Turner BL, Haygarth PM. Biogeochemistry - Phosphorus solubilization in rewetted soils. Nature 2001 ; 411 : 258-258.

Vadas PA, Joern BC, Moore PA. Simulating soil phosphorus dynamics for a phosphorus loss quantification tool. J Environ Qual 2012 ; 41 : 1750-7.

Vadas PA, Jokela WE, Franklin DH, Endale DM. The Effect of Rain and Runoff When Assessing Timing of Manure Application and Dissolved Phosphorus Loss in Runoff1. JAWRA Journal of the American Water Resources Association 2011 ; 47 : 877-886.

Wade AJ, Whitehead PG, Butterfield D. The Integrated Catchments model of Phosphorus dynamics (INCA-P), a new approach for multiple source assessment in heterogeneous river systems : model structure and equations. Hydrology and Earth System Sciences 2002 ; 6 : 583-606.

Wall DP, Jordan P, Melland AR, Mellander PE, Mechan S, Shortle G. Forecasting the decline of excess soil phosphorus in agricultural catchments. Soil Use and Management 2013 ; 29 : 147-154.

Whitehead P, Young P. Water-quality in river systems – Monte-Carlo analysis. Water Resources Research 1979 ; 15 : 451-459.

6.1.7 Supplementary materials

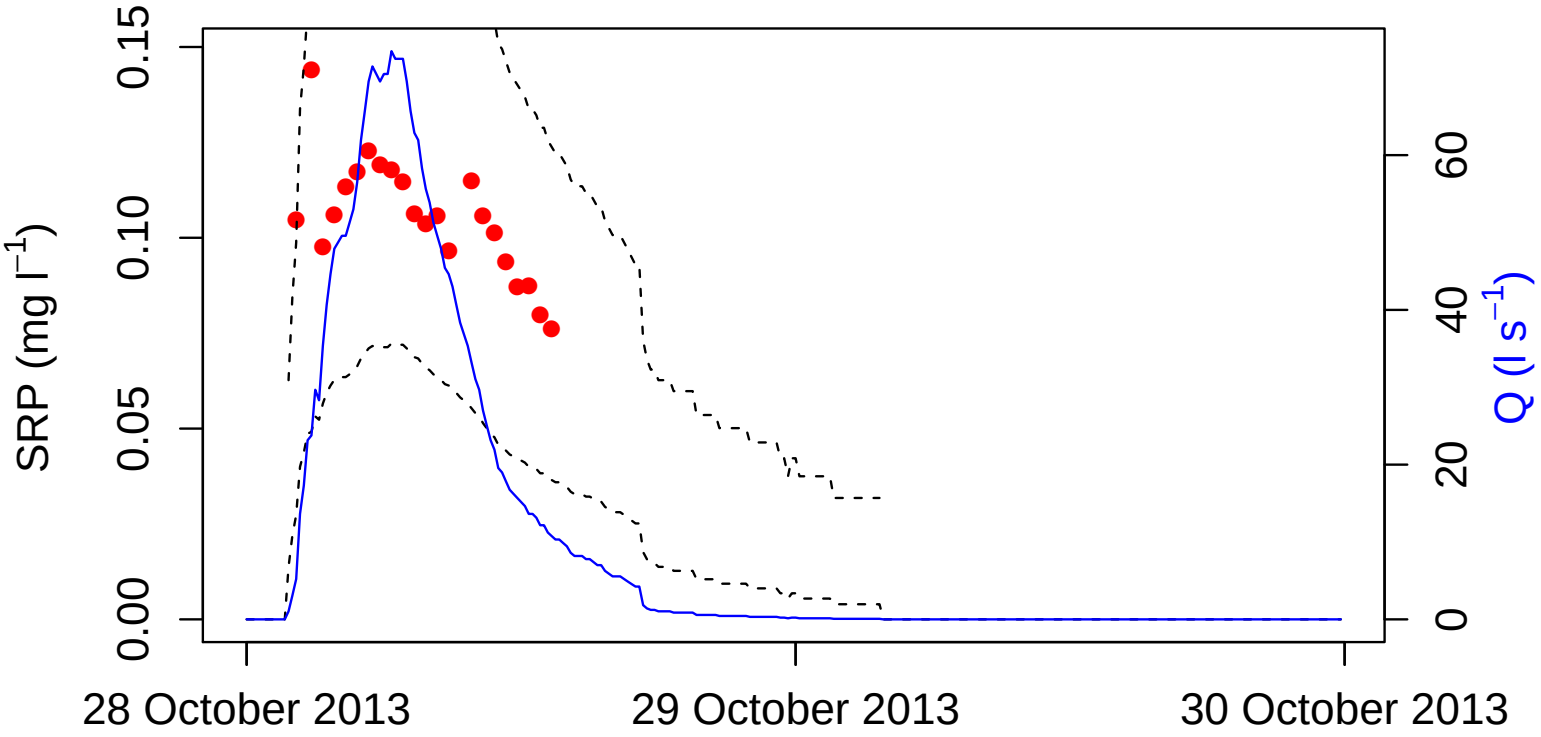
SRP (mg l^{-1})
0.00
0.05
0.10
0.15
Q (l s^{-1})
0
20
40
60
28 October 2013
29 October 2013
30 October 2013

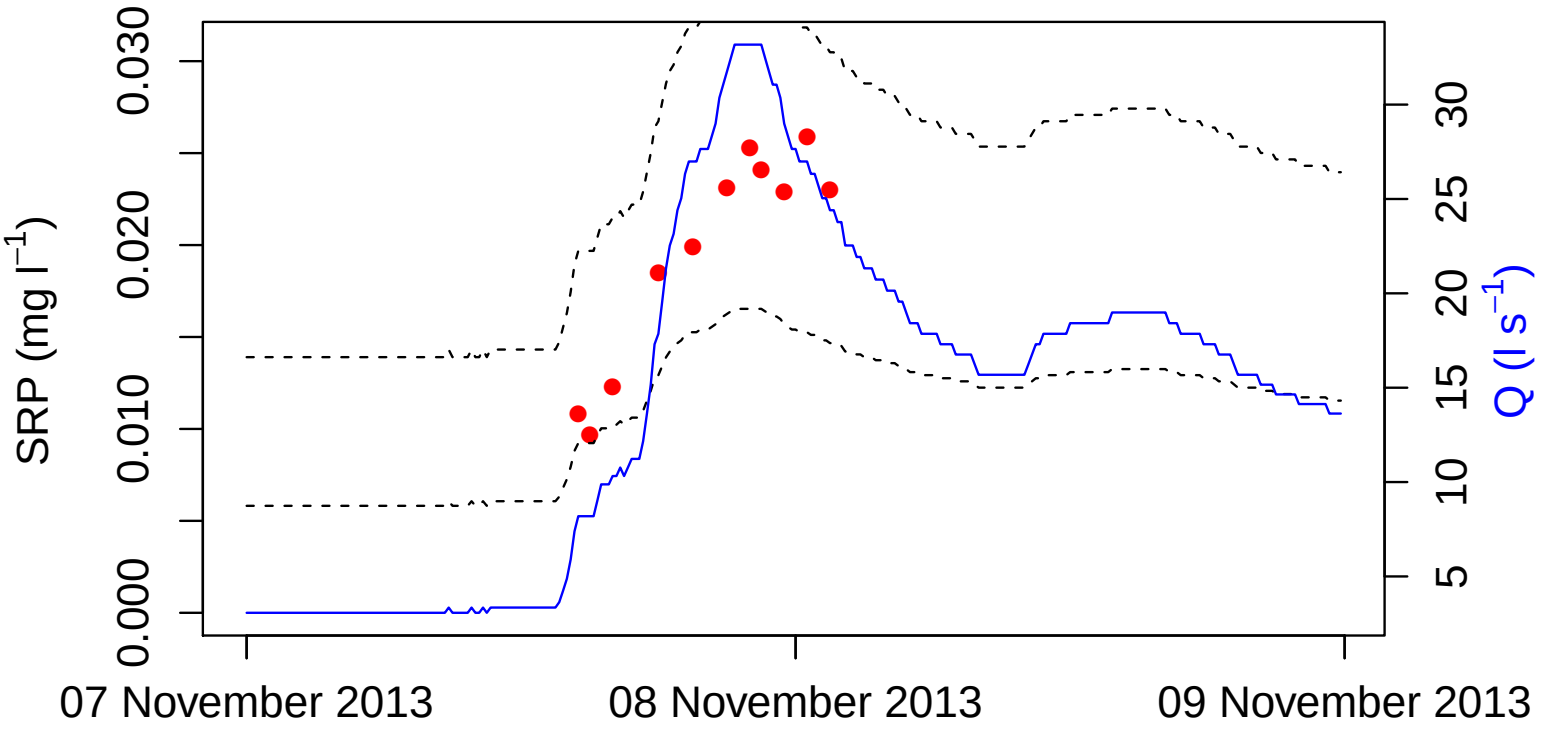
SRP (mg l^{-1})
0.000
0.010
0.020
0.030
Q (l s^{-1})
5
10
15
20
25
30
07 November 2013
08 November 2013
09 November 2013

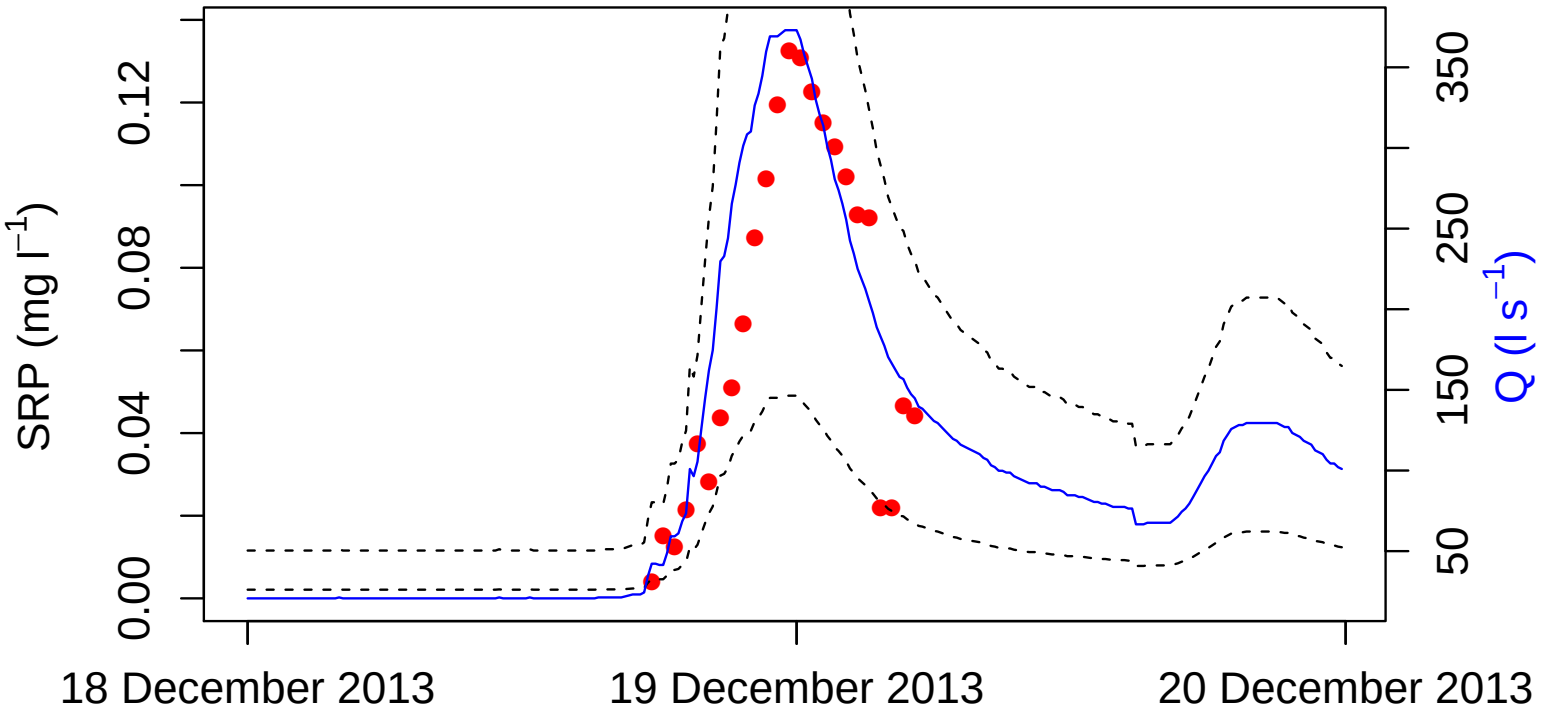
SRP (mg l^{-1})
0.00
0.04
0.08
0.12
Q (l s^{-1})
50
150
250
350
18 December 2013
19 December 2013
20 December 2013

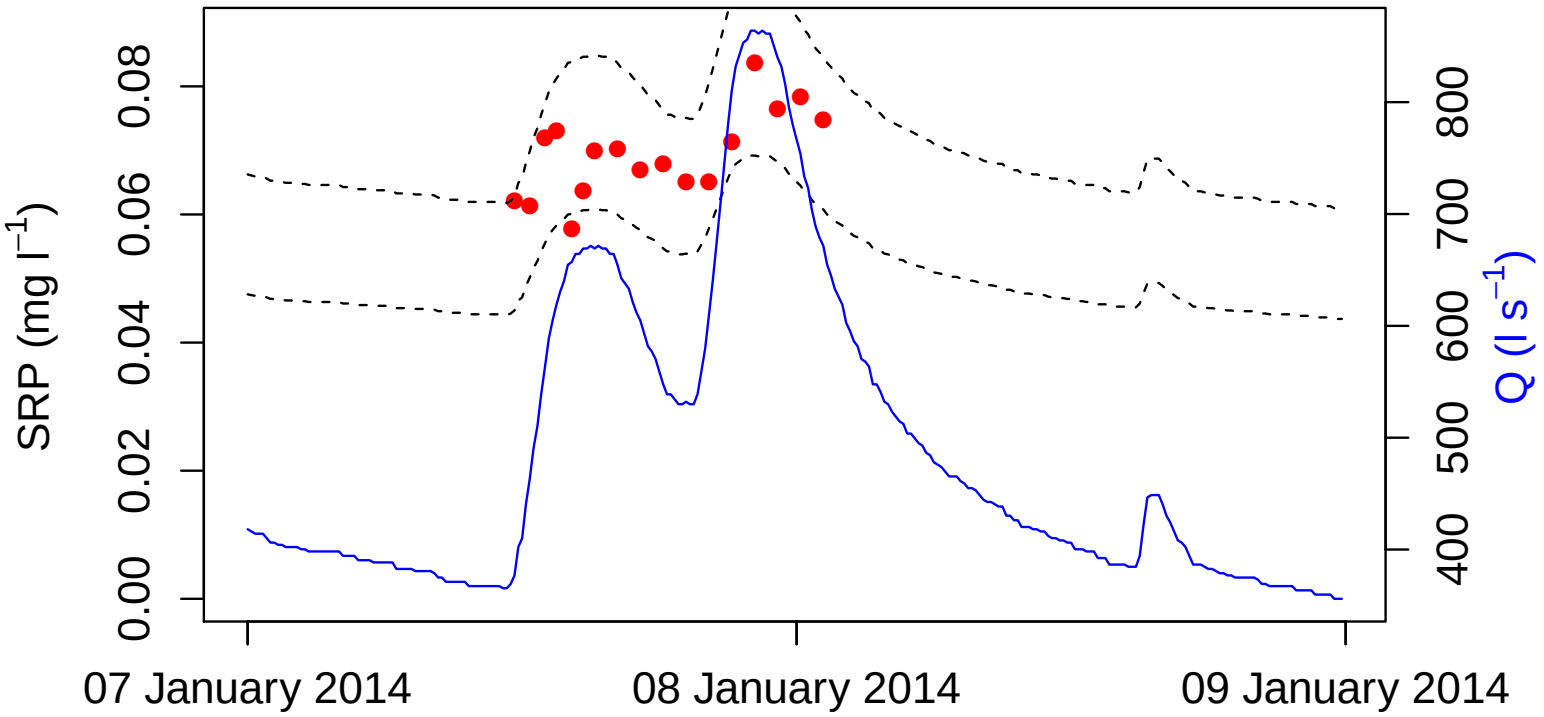
SRP (mg l^{-1})
0.00
0.02
0.04
0.06
0.08
Q (l s^{-1})
400
500
600
700
800
07 January 2014
08 January 2014
09 January 2014

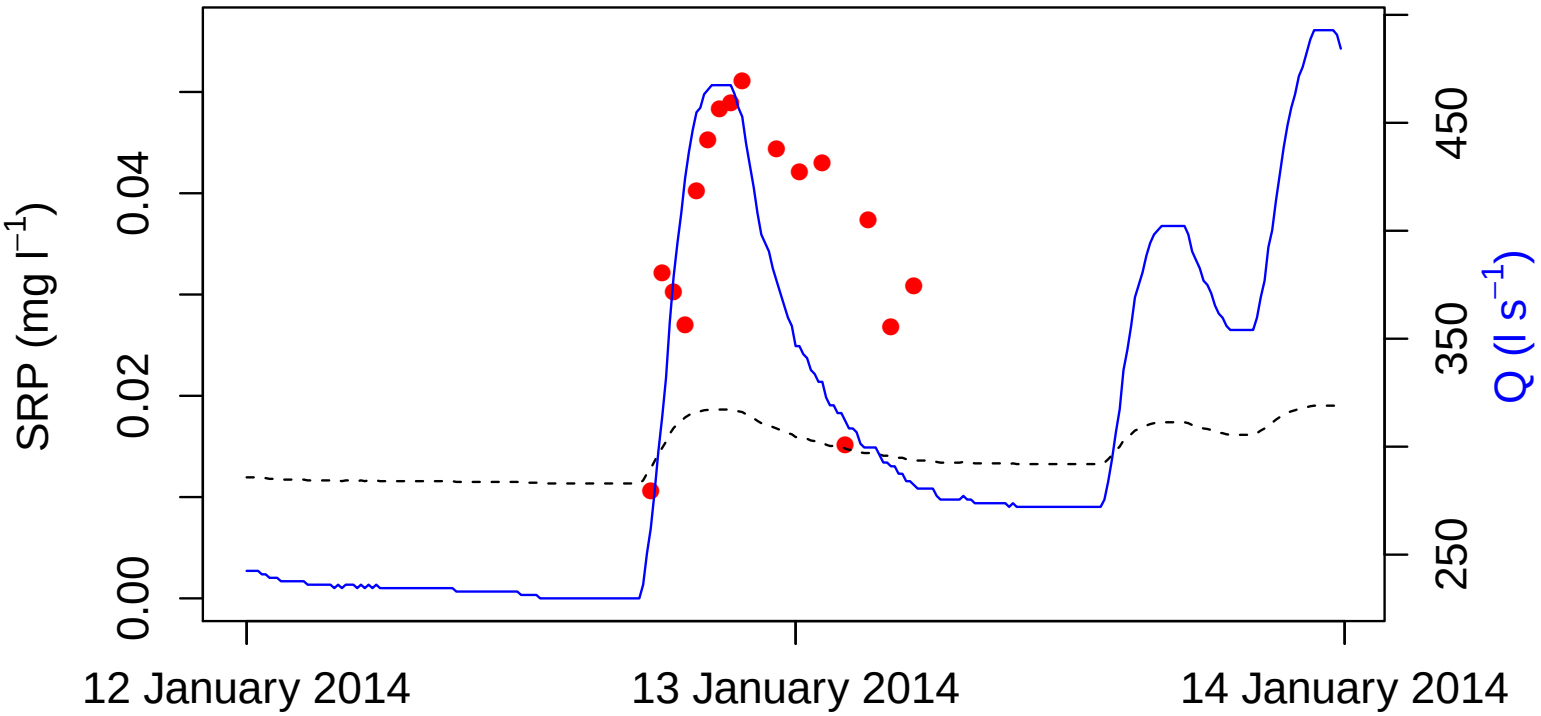
SRP (mg l^{-1})
0.00
0.02
0.04
Q (l s^{-1})
250
350
450
12 January 2014
13 January 2014
14 January 2014

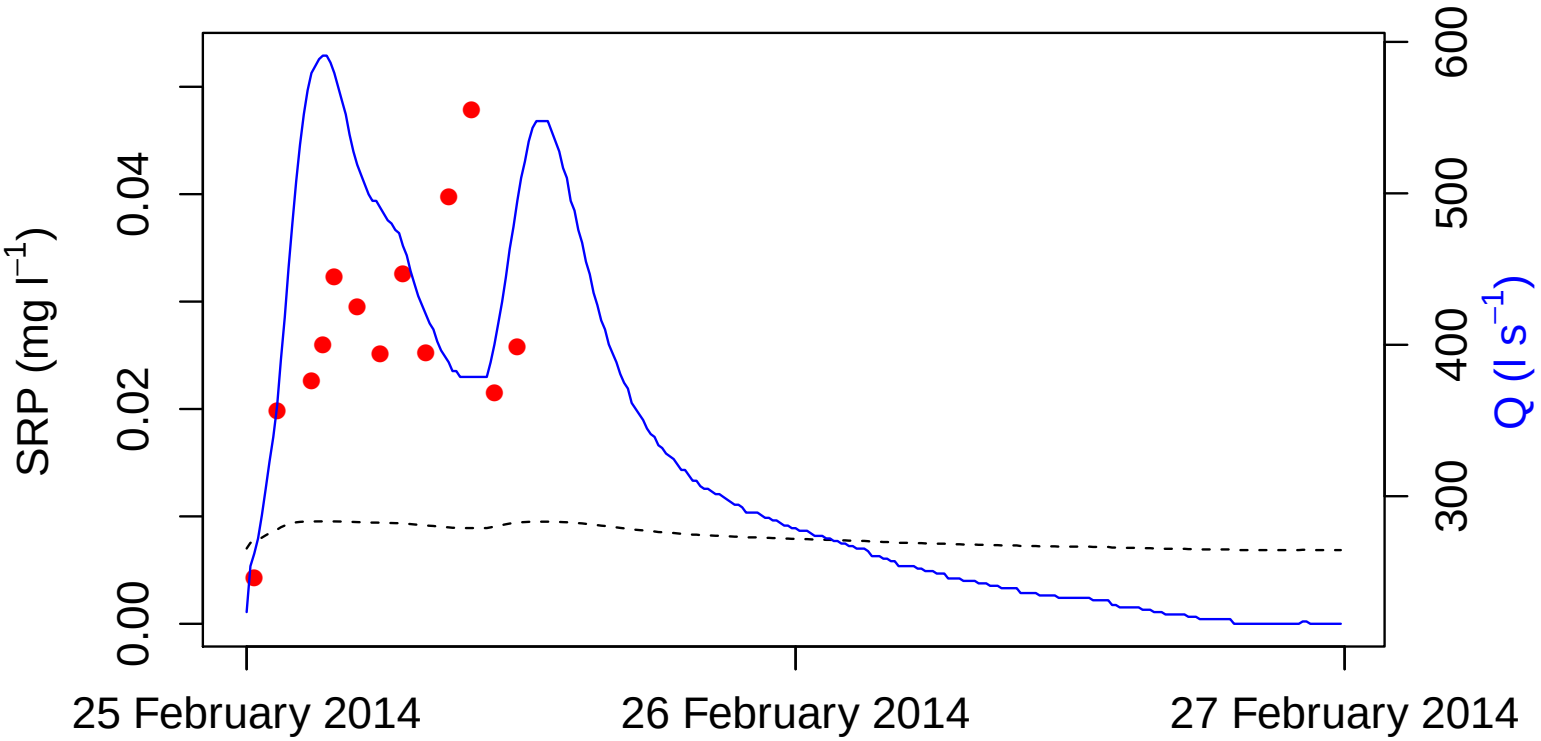
SRP (mg l^{-1})
0.00
0.02
0.04
Q (l s^{-1})
300
400
500
600
25 February 2014
26 February 2014
27 February 2014

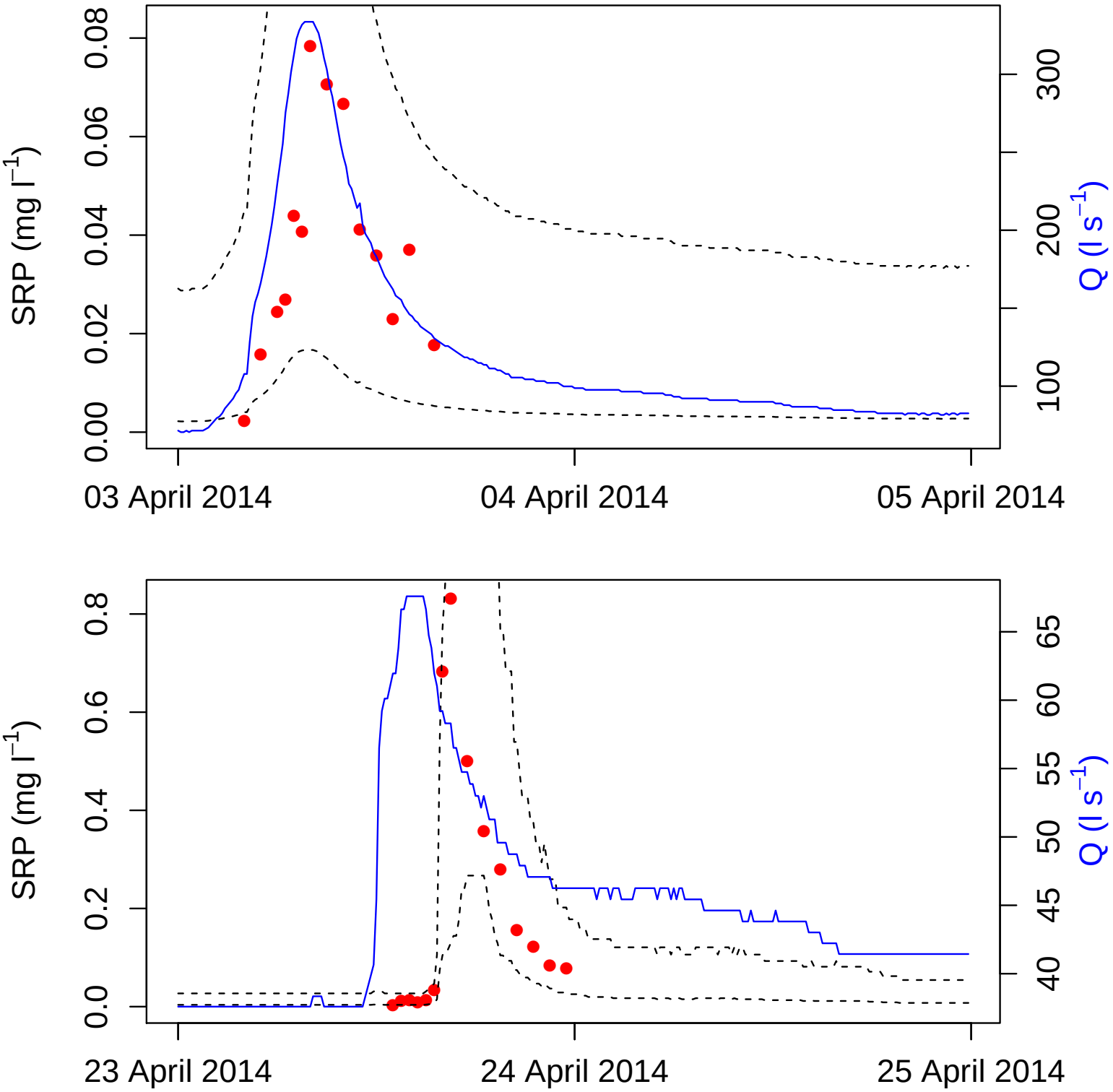
SRP (mg l^{-1})
0.00
0.02
0.04
0.06
0.08
Q (l s^{-1})
100
200
300
03 April 2014
04 April 2014
05 April 2014
SRP (mg l^{-1})
0.0
0.2
0.4
0.6
0.8
Q (l s^{-1})
40
45
50
55
60
65
23 April 2014
24 April 2014
25 April 2014

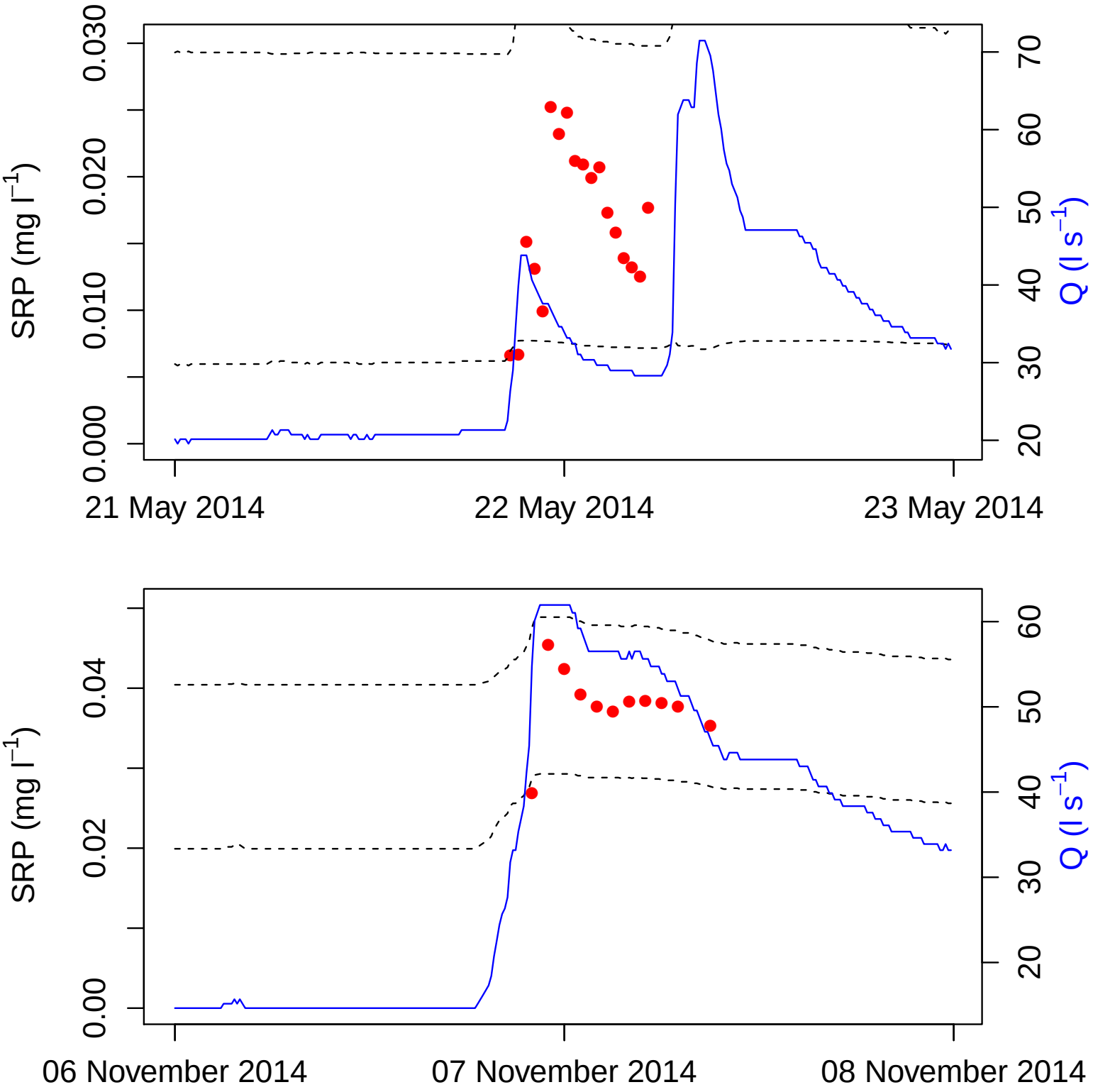
SRP (mg l^{-1})
0.000
0.010
0.020
0.030
Q (l s^{-1})
20
30
40
50
60
70
21 May 2014
22 May 2014
23 May 2014
SRP (mg l^{-1})
0.00
0.02
0.04
Q (l s^{-1})
20
30
40
50
60
06 November 2014
07 November 2014
08 November 2014

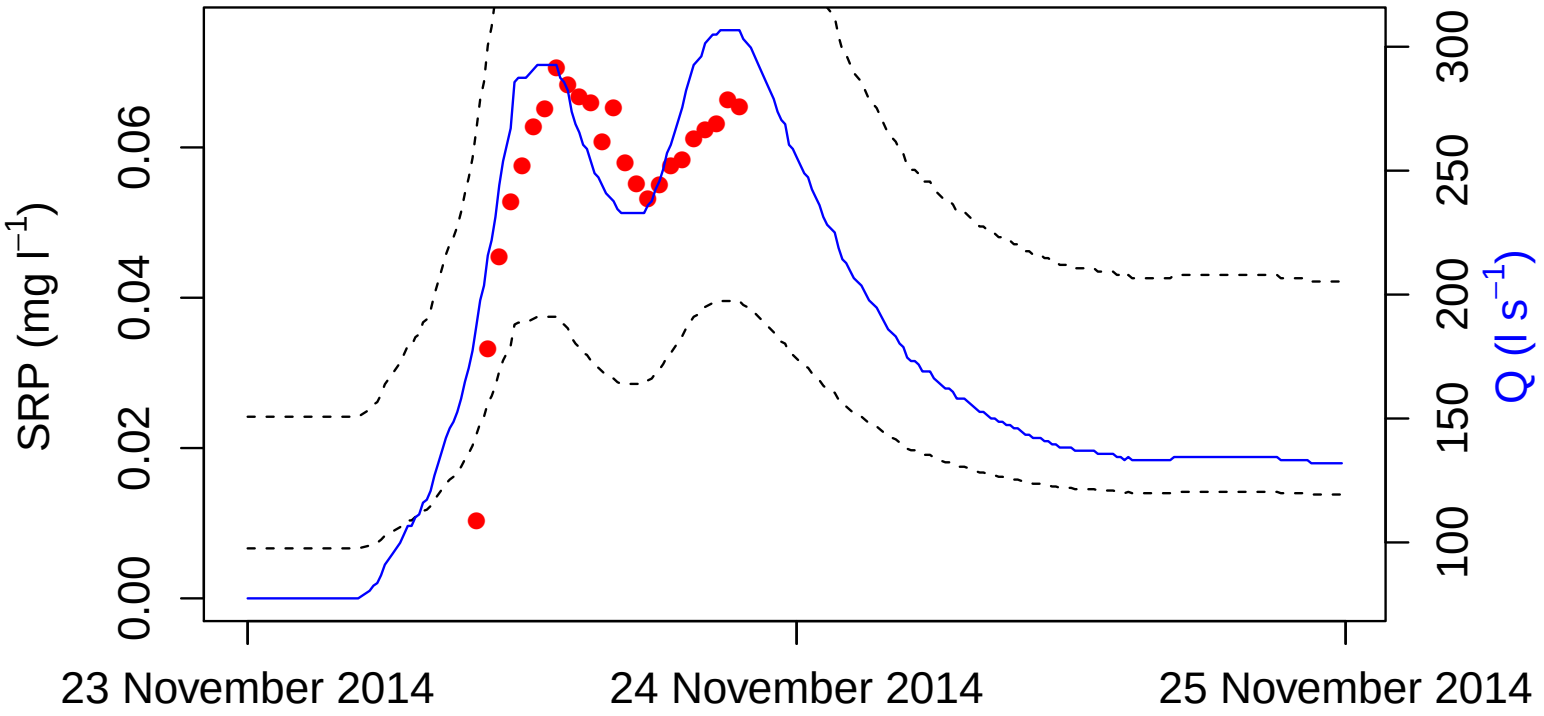
SRP (mg l^{-1})
0.00
0.02
0.04
0.06
100
150
200
250
300
Q (l s^{-1})
23 November 2014
24 November 2014
25 November 2014

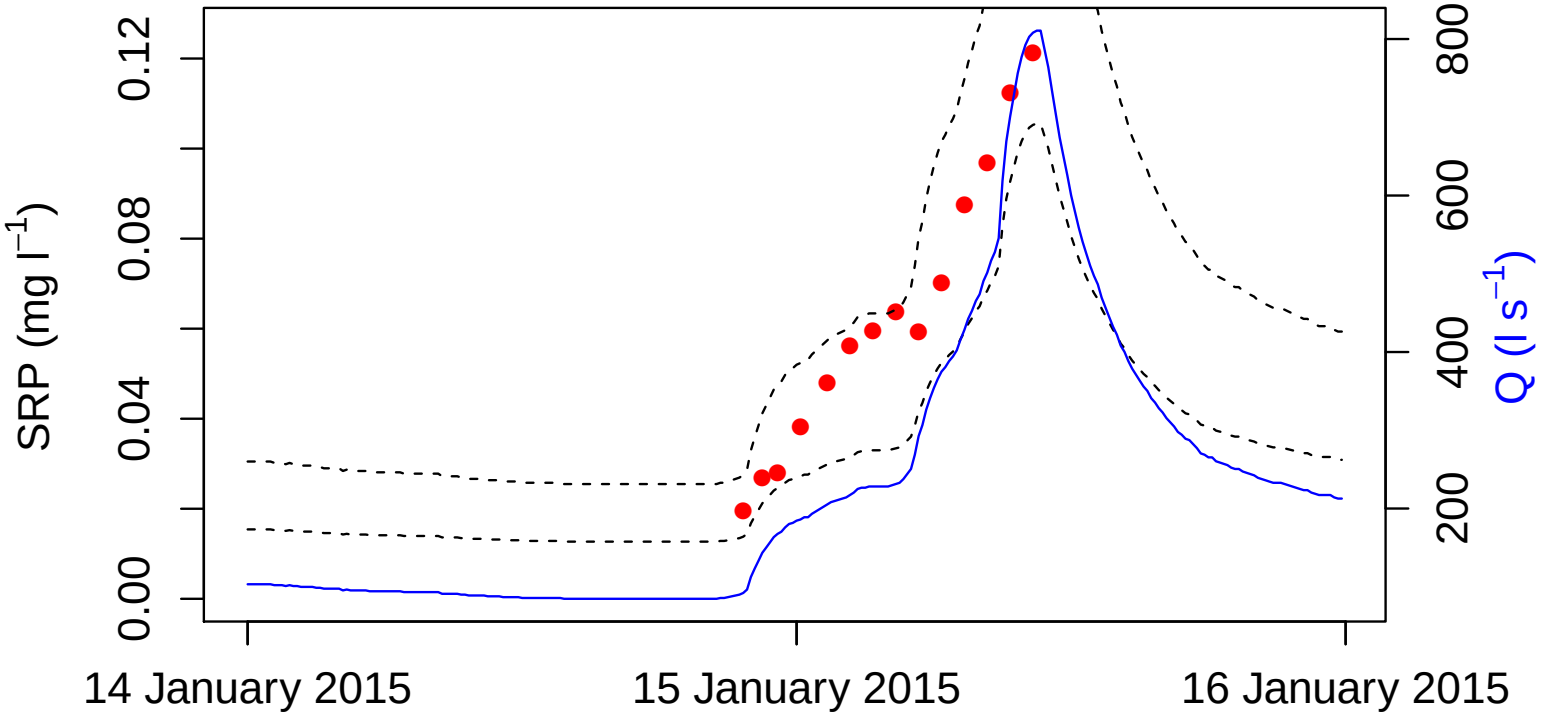
SRP (mg l^{-1})
0.00
0.04
0.08
0.12
200
400
600
800
Q (l s^{-1})
14 January 2015
15 January 2015
16 January 2015

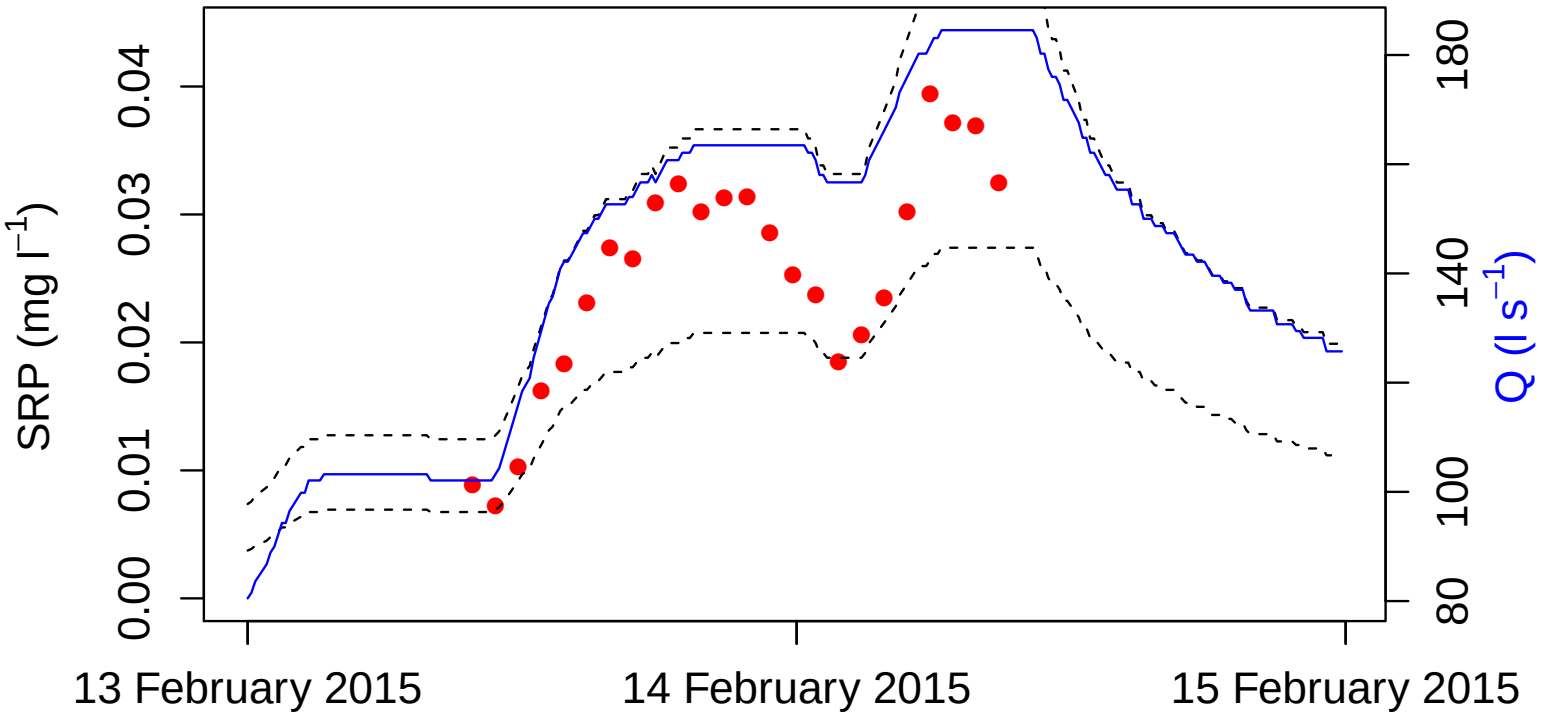
SRP (mg l^{-1})
0.00
0.01
0.02
0.03
0.04
Q (l s^{-1})
80
100
140
180
13 February 2015
14 February 2015
15 February 2015

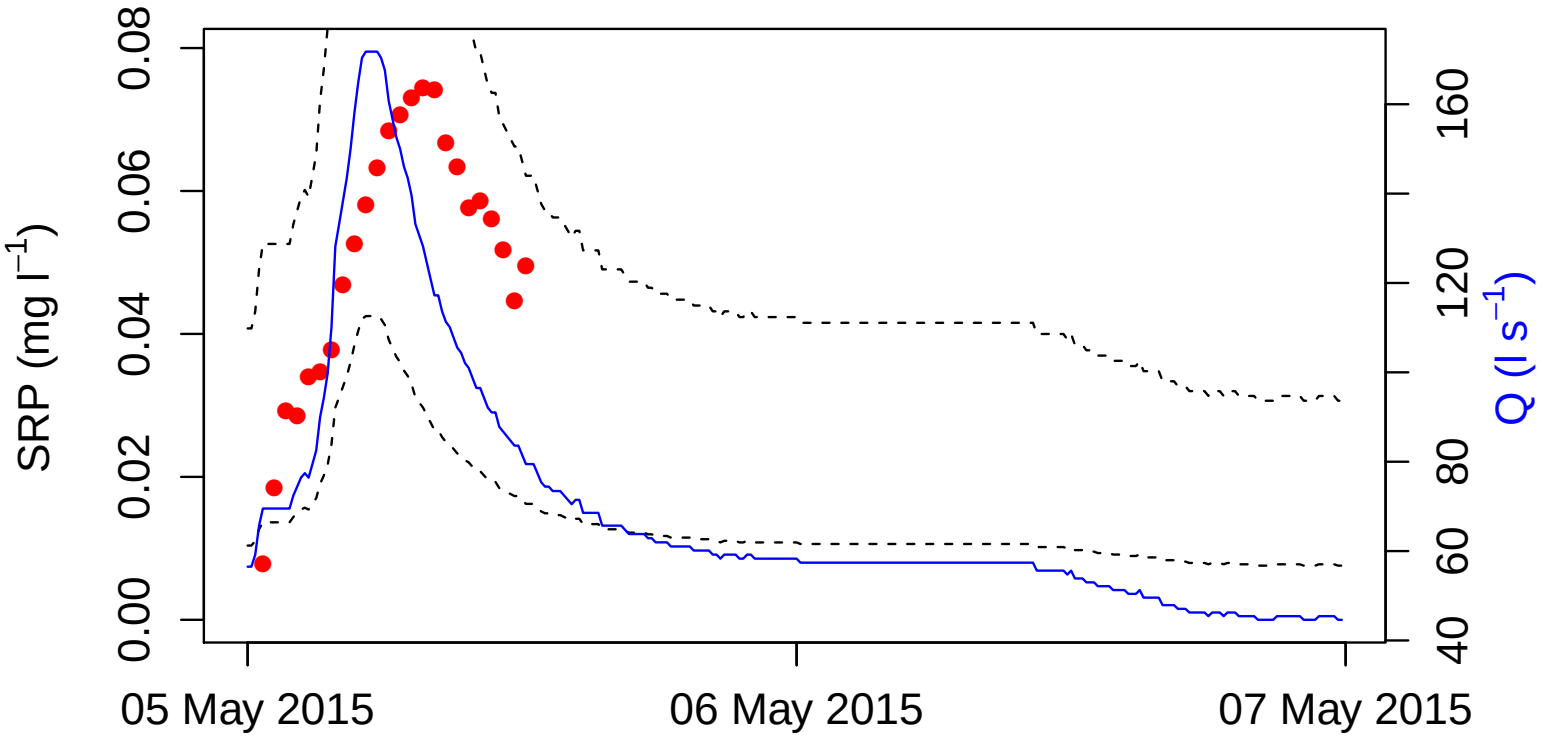
SRP (mg l^{-1})
0.00
0.02
0.04
0.06
0.08
Q (l s^{-1})
40
60
80
120
160
05 May 2015
06 May 2015
07 May 2015

6.2 Conclusion du chapitre

Dans ce chapitre, le modèle TNT2-P a été utilisé pour tester les hypothèses formulées dans les chapitres 3 à 5. Le rôle de la nappe dans la mise en connexion hydrologique entre les sols des zones ripariennes et la rivière semble bien reproduit, tout comme celui des conditions de température et d'humidité sur la solubilisation du P dans les sols. TNT2-P devrait permettre de simuler l'effet de scenarios climatiques sur les transferts de SRP ; il serait cependant recommandable de calibrer et d'évaluer TNT2-P sur un plus grand nombre d'années climatiques avant de procéder à la simulation de scénarios climatiques. TNT2-P ne permet pas de simuler des scénarios de pratiques agricoles, puisqu'aux échelles de temps couvertes par nos données observation, l'effet des pratiques agricoles n'est pas visible dans le cours d'eau. Il serait intéressant d'utiliser un autre modèle pour simuler l'évolution du P Olsen dans les sols, et utiliser les nouvelles cartes de P Olsen générées comme entrée de TNT2-P. Coupler un modèle un modèle d'évolution du P des sols avec TNT2-P est à déconseiller pour deux raisons : i) pour éviter d'augmenter le nombre de paramètres et ii) parce que la nature et la résolution temporelle des données à acquérir pour calibrer chacun des deux modèles sont différentes.

Des évolutions à apporter dans la structure du modèle pourraient permettre i) de définir des unités de réponse homogènes basées sur la similarité hydrologique et de teneur en P des sols, pour réduire les temps de calcul à la manière du TOPMODEL original ; ii) d'améliorer le routage des flux de P dissous cellule-à-cellule en introduisant des paramètres de cinétiques d'adsorption et tenant compte de la vélocité des écoulements au sein des couches de sol, et iii) de créer un modèle du carbone organique dissous (COD) basé sur la même structure et un modèle nitrate en simplifiant TNT2 pour avoir un ensemble de modèles raisonnablement paramétrés permettant de simuler les flux de C, N, P de manière intégrée.

Au-delà de la structure même du modèle, ce dernier chapitre pose la question de comment réduire l'incertitude dans les données. On constate en effet que, malgré l'importante quantité de travail que représente la constitution de la base de données P de AgryHys, cette dernière contient relativement peu d'information par rapport à ce que permettent les équipements de suivi haute fréquence utilisés aujourd'hui dans certains bassins de recherche. Ces équipements permettent de réduire l'incertitude liée à la fréquence d'échantillonnage et au stockage des échantillons (identifiés comme les premières sources d'incertitude) même s'il est possible que la qualité de la mesure en elle-même soit moins bonne. Il serait donc intéressant d'appliquer la démarche d'analyse d'incertitude présentée dans ce chapitre à ces données haute fréquence et d'étudier comment cette incertitude se propagerait dans un modèle.

Chapitre 7

Conclusion générale

7.1 Rappel des objectifs

L'objectif de cette thèse était d'identifier et de quantifier les mécanismes à l'origine des transferts de phosphore dissous dans un bassin agricole sur socle, par une démarche intégrant analyse d'observations multi-échelle et modélisation.

Les trois questions de recherche principales sont rappelées ici :

- Question 1 : Les mécanismes à l'origine du transfert des formes dissoutes et particulaires du phosphore sont-ils communs ou distincts ? Y a-t-il une saisonnalité dans le couplage/découplage des transferts de phosphore dissous et particulaire ? Dans quelle mesure la variabilité du signal peut-elle être reliée aux pratiques agricoles ou à des processus hydrologiques et biogéochimiques ?
- Question 2 : Quel est le rôle de la nappe dans le transfert de phosphore dissous ? Agit-elle uniquement sur le transfert en provoquant une connexion hydrologique entre les sols et la rivière, ou agit-elle aussi sur la solubilisation du phosphore dans les sols ?
- Question 3 : Comment raisonner la complexité d'un modèle en fonction de la quantité d'information contenue dans les données ? Comment quantifier l'incertitude des données et la propager dans les prédictions d'un modèle ?

7.2 Synthèse des résultats

7.2.1 Analyse de chroniques

Les chapitres 3 et 4 ont porté sur l'analyse de chroniques de chimie de l'eau, pour en déduire des connaissances sur les mécanismes de transfert de PP et de SRP.

Une première étude sur les données du bassin versant de Kervidy-Naizin a révélé une nette désynchronisation entre l'exportation de PP et de SRP, à l'échelle des saisons comme à l'échelle des crues. Cette désynchronisation pendant une grande partie de l'année suggère que les deux formes de phosphore proviennent de sources et/ou suivent des voies de transfert indépendantes. Le fait que les exportations de PP et SRP soient contrôlées par des facteurs hydroclimatiques différents renforce l'idée de mécanismes de transferts distincts.

L'exportation du PP apparaît contrôlée par la disponibilité des sédiments et la capacité de transport du cours d'eau, tandis que celle du SRP apparaît contrôlée par les fluctuations de nappe dans les sols de fonds de vallée. Les concentrations en PP sont donc les plus élevées en début d'année hydrologique, quand des sédiments facilement mobilisables sont présents dans le lit du cours d'eau, et pendant les crues hivernales, où les débits élevés sont favorables à l'érosion des berges voire à l'apport de sol érodé au niveau des versants. Les données dont nous disposions n'ont pas permis de distinguer nettement ces deux origines. Les concentrations en SRP sont les plus élevées en début d'année hydrologique puis diminuent alors même que l'augmentation des niveaux de nappe connecte des portions de bassin versant de plus en plus étendues. Comme ces concentrations automnales élevées sont observables en crue comme hors crue, nous avons écarté l'hypothèse d'une contribution importante d'une source ponctuelle en période de basses eaux, pour privilégier celle d'une disponibilité élevée de phosphore mobilisable dans les sols de fond de vallée à l'automne. Les concentrations en SRP diminuent ensuite au cours de l'hiver, à mesure que ce pool de phosphore mobilisable est épuisé par les crues successives. Au printemps et au début de l'été, des processus différents se mettent en place. En crue, des exportations synchrones de PP et SRP laissent penser à une source commune des deux formes de phosphore, probablement mobilisée par ruissellement et érosion dans les versants, à une période de l'année où les épandages augmentent le risque de transfert direct au cours d'eau. Hors crue, les concentrations en SRP augmentent au cours des derniers mois avant le tarissement du cours d'eau, alors même que la baisse du niveau de nappe déconnecte les horizons de sol riches en phosphore de la rivière. La cause de l'augmentation SRP au printemps/été n'est pas tranchée : les épandages printaniers et/ou la minéralisation de la matière organique peuvent augmenter la quantité de phosphore soluble dans les sols, se pose alors la question des mécanismes de transfert de cette source. Il ne faut pas exclure la possibilité d'une source domestique ou de processus internes au cours d'eau libérant du SRP à la faveur de l'augmentation des températures et des temps de résidence dans le cours d'eau. Ce flux printanier/estival inexpliqué, extrapolé à l'année, ne représente que 1,5% du flux annuel ; il est donc négligeable si l'on s'intéresse à réduire le flux annuel alimentant une retenue. Pourtant ce flux est la cause de concentrations élevées à une période de l'année où les conditions de température et de luminosité sont favorables à l'eutrophisation ; il serait donc crucial de mieux comprendre son origine si l'on cherche à réduire les concentrations dans le cours d'eau au printemps (Stamm *et al.*, 2014).

A l'exception de certaines crues printanières où des effluents d'élevage récemment épandus peuvent être transférés au cours d'eau de manière directe, le signal phosphore dans la rivière semble résulter de processus hydrologiques et biogéochimiques indépendants des pratiques agricoles. Ces dernières, et notamment les apports de phosphore à l'origine de l'enrichissent les sols, influencent les niveaux globaux de concentration, mais pas les dynamiques temporelles. L'absence de couplage entre transfert de PP et SRP contraste avec la vision courante des transferts de phosphore diffus, selon laquelle le phosphore serait principalement transféré sous forme particulaire et que le phosphore dissous proviendrait en grande partie de la solubilisation du phosphore de ces particules. Cette vision des transferts de PP et SRP, encore peu prise en compte par les gestionnaires de bassin versant, est en revanche déjà connue de la communauté scientifique puisqu'elle a déjà été démontrée dans de nombreux bassins versant herbagers. L'apport de cette thèse a été de montrer qu'elle

est aussi valable dans un bassin versant à dominance de terres arables.

La méthode de clustering k-means couplée avec Dynamic Time Warping (DTW) a permis d'identifier des motifs de crue dans deux bassins versants, avant d'en analyser la répartition saisonnière et d'en tirer des hypothèses sur les mécanismes de transfert de PP et SRP. L'intérêt de DTW a été de recaler des séries temporelles (Q, SRP, PP) par rapport à une série temporelle de référence en fonction de la forme des hydrogrammes. Ainsi, les relations concentration-débit peuvent être étudiées pour des crues avec des hydrogrammes de formes différentes, en perdant moins d'information qu'avec des descripteurs de relation concentration-débit (ou descripteurs d'hystérèse) classiques. Un algorithme de clustering k-means a été appliqué sur les séries temporelles de crue ainsi recalées. Deux motifs principaux ont été identifiés dans deux clusters, et des motifs rares ont été isolés dans un troisième cluster hétérogène. Le premier motif, majoritaire dans chacun des deux bassins, se caractérise par un pic de PP en phase de montée du débit, et un pic de SRP en phase de descente ; il s'agit du principal motif interprété précédemment comme résultant d'une mobilisation de PP en provenance du lit du cours d'eau, suivie d'une mobilisation et transfert de SRP en provenance des sols de bas de versant contrôlée par la nappe. Le deuxième motif, minoritaire, se caractérise par des pics de PP et de SRP synchrones entre eux et avec le débit ; il s'agit du motif interprété précédemment comme résultant d'une mobilisation et d'un transfert commun du PP et du SRP depuis les versants. Les facteurs de contrôle de ce motif, et donc des mécanismes sous-jacents, sont différents entre les deux bassins versants. Dans le bassin de Kervidy-Naizin, à dominance de terres arables, il apparaît majoritairement au printemps quelle que soit l'amplitude des crues ; la cause des transferts couplés de PP et SRP pourrait être liée au calendrier des pratiques agricoles : en cette saison, la préparation des lits de semence avant culture de printemps peut poser un risque de dégradation de la structure des sols, et donc de ruissellement et d'érosion, éventuellement à l'origine d'exportations directes d'effluents récemment épandus. Dans le bassin versant du Moulinet, à dominance herbagère, ce motif n'a pas pu être relié au calendrier des pratiques agricoles mais plutôt à l'amplitude des crues : seules les plus grosses crues permettent le transfert direct et couplé de PP et SRP en provenance des versants.

7.2.2 Suivi des concentrations dans la zone d'interaction sol-nappe

L'objectif de ce suivi a été d'étudier plus en détails le rôle de l'interaction sol-nappe dans les sols de bas-fond sur les transferts de SRP. Plus précisément, il s'est agit d'établir si la nappe contrôlait uniquement le transfert de SRP, en créant une connexion hydrologique entre sol et rivière, ou si elle contrôlait aussi la solubilisation du SRP.

Nos observations suggèrent que les fluctuations saisonnières de la nappe contrôlent en effet la solubilisation du SRP, par l'alternance de périodes sèches et de périodes saturées en eau. La période de sécheresse estivale permet la constitution d'un pool de phosphore mobile dans les sols, exporté et progressivement épuisé lorsque la nappe monte dans les sols de bas-fond à l'automne. Cette mobilisation automnale est d'autant plus importante que la teneur en phosphore des sols est élevée. La réduction des (hydr)oxydes de Fer causée par une stagnation prolongée de la nappe dans les sols à la fin de l'hiver est accompagnée d'un deuxième relargage de SRP lui aussi transféré, du moins en partie, au cours d'eau.

L'épisode de mobilisation-transfert automnal semble bien correspondre à la période de concentrations élevées en SRP à la reprise des écoulements, identifiée précédemment par analyse de la chronique initiale de 6 ans. L'épisode de mobilisation-transfert suite à la réduction des oxydes de fer ne peut pas être relié à une période de concentrations élevées en SRP identifiée dans la chronique. Les concentrations élevées dans la rivière au printemps-été ne correspondent pas à une épisode de mobilisation observé dans les sols.

Le suivi des concentrations dans les sols de bas-fond se poursuit pour les années hydrologiques 2014 – 2015 et 2015 – 2016 grâce au projet PHOSNAP, et en particulier la thèse de Sen Gu à Géosciences Rennes. L'objectif est de préciser la spéciation des formes de phosphore mobilisées, et d'étudier le couplage des processus avec la matière organique dissoute et les nitrates.

7.2.3 Modélisation et analyse d'incertitude

L'analyse de données à plusieurs échelles de temps (année, saison, crue) et d'espace (bassins versants dans leur ensemble, versants) a permis d'identifier les facteurs de contrôle principaux des transferts de SRP. Il s'agit en premier lieu de l'interaction sol-nappe dans le zones de bas-fond, à l'origine de transferts de sub-surface ou par ruissellement sur surface saturée et en second lieu de la disponibilité en phosphore mobile, qui varie spatialement en fonction de la teneur en phosphore des sols et temporellement en fonction des conditions antérieures d'humidité du sol. L'effet des pratiques agricoles ne produit pas de signal visible directement dans le cours d'eau, à l'exception d'épisodes accidentels de transfert d'effluents récemment épandus. En l'absence d'un suivi haute-fréquence, ces épisodes accidentels sont rarement échantillonnés ; aussi il nous a semblé difficile de construire un modèle permettant de les simuler. La démarche de modélisation adoptée dans cette thèse reste au plus près des données, avec une structure de modèle reflétant le schéma conceptuel élaboré par l'interprétation d'observations de terrain, et avec une propagation de l'incertitude sur les données dans les prédictions du modèle. Les deux principaux facteurs de contrôle identifiés, à savoir la connexion hydrologique par fluctuation de nappe et la solubilisation du SRP en fonction de la teneur en phosphore des sols et des conditions antérieures d'humidité et de température, ont été confirmés grâce au modèle. Cependant, l'incertitude sur les données reste importante, ce qui risque de compromettre l'élaboration de modèles plus détaillés avec les données actuelles.

7.3 Implications opérationnelles

Les objectifs scientifiques de cette thèse avaient pour but de répondre à un enjeu opérationnel de gestion, pour les bassins versants 3B-1 du SDAGE Loire Bretagne, et plus généralement pour des bassins versants sur socle en climat tempéré océanique, avec une nappe superficielle, des apports aux sols et des teneurs en P des sols élevés, en contexte peu érosif.

Dans ce type de contexte agro-pédo-climatique, les transferts de PP et SRP sont généralement indépendants, c'est-à-dire qu'ils proviennent de sources différentes et/ou suivent des voies de transfert différentes. Des stratégies de gestion différentes sont donc à mettre en place pour cibler l'une ou l'autre des formes de phosphore. Il serait utile de mieux connaître

la biodisponibilité des formes particulaires transférées, pour décider si la priorité doit être donnée aux formes dissoutes seulement, ou si les formes particulaires présentent aussi un risque pour l'eutrophisation. Il faut aussi garder en tête que des processus de rétention temporaire – remobilisation et des changements de spéciation chimique vont se produire dans le réseau hydrographique aval et au sein des plan d'eau.

Outre les formes de phosphore à traiter en priorité, les stratégies de gestion peuvent aussi différer selon que l'objectif est de réduire la concentration moyenne, ou la concentration printanière/estivale (c'est le cas si l'écosystème que l'on cherche à protéger est une rivière), ou si l'objectif est de réduire le flux annuel total (c'est le cas si l'écosystème que l'on cherche à protéger est un plan d'eau). Dans le premier cas, les résultats de cette thèse apportent peu d'éléments puisque nous n'avons pas identifié avec certitude la cause des concentrations élevées au printemps/été. Dans le contexte de bassins de plus grande taille, il a été prouvé que les émissions domestiques dominent à cette période de l'année (Serrano *et al.*, 2015), même quand elles représentent une part minoritaire du flux annuel (Legeay *et al.*, 2015). Dans le second cas, les résultats de cette thèse ont bien permis d'identifier les causes principales de flux annuels de PP et SRP ; des pistes pour la gestion sont suggérées ci-dessous.

Concrètement, il est possible de réduire les exportations de PP en limitant l'érosion des berges, par exemple en implantant une végétation ripisylve, en restaurant l'hydro morphologie naturelle du cours d'eau, ou en restreignant l'accès du bétail à la rivière. Dans les sites d'étude de cette thèse, les épisodes de transfert direct de sol érodé dans les versants sont plutôt rares, même si des phénomènes d'érosion sont bien visibles dans les parcelles (Le Bissonnais *et al.*, 2002). Il y a donc re déposition en certains endroits du paysage des sols érodés dans les parcelles, à la faveur de zones plus plates dans les bas-fonds et des bandes enherbées déjà en place le long des cours d'eau en application de la réglementation. Si l'érosion des terres arables ne produit pas un signal visible directement dans la rivière, elle reste un problème à traiter, d'une part parce qu'elle représente une perte de terre arable dommageable pour l'agriculture, et d'autre part parce que les sols érodés et redéposés dans les bas-fonds enrichissent ces derniers en phosphore remobilisable par des mécanismes biogéochimiques indépendants des pratiques agricoles.

Le transfert de phosphore dissous a lieu quand la nappe intercepte les horizons de sol de surface et provoque une connexion hydrologique entre ces sols et le cours d'eau. Les voies de transfert sont la sub-surface et le ruissellement sur surface saturée ; les quantités de SRP mobilisé par ces deux types d'écoulement augmentent avec la teneur en P des sols. Des tests agronomiques de teneur en P des sols, comme le P Olsen utilisé dans cette thèse, permettent bien d'évaluer le risque de solubilisation. Pour affiner cette évaluation du risque de solubilisation, il serait intéressant de définir les bases de calcul d'un taux de saturation pour les sols de Bretagne, et de fixer des valeurs cibles de ce taux de saturation. Une fois identifiées les zones où coïncident risques de transfert (par une carte des zones humides) et risques liés à la source (par une carte de teneur en P des sols ou d'un taux de saturation en phosphore), on peut agir de trois manières :

- Eviter que les sols de ces zones s'enrichissent davantage, en limitant les apports dans le cas des parcelles cultivées, et en limitant l'érosion dans les parcelles amont dans le cas des bandes enherbées ;

- Diminuer la teneur en P des sols de ces zones, en exportant de la biomasse ;
- Favoriser l'immobilisation du phosphore, en utilisant des matériaux adsorbant sous la forme de « permeable reactive barriers », en les épandant à la surface ou en les plaçant autour de drains.

La solution consistant à drainer ces zones pour abaisser les niveaux de nappe n'a pas fait ces preuves puisque il y a été montré que l'augmentation du flux de phosphore transféré par les drains compense la diminution des transferts par écoulement de sub-surface et à la surface du sol (Castillon 2007). Par ailleurs, les services écosystémiques rendus par les zones humides (épuration des nitrates, biodiversité, etc) seraient perdus si on les drainait.

Le modèle développé pour cette thèse n'a pas été conçu pour être utilisé comme un outil de gestion. S'agissant d'un modèle distribué à la résolution du MNT, il ne peut pas être utilisé sur des bassins versant de taille opérationnelle (> 100 km^2), d'autant plus que le module hydrologique inspiré de TOPMODEL supporte mal les résolutions supérieures à 50 m. Le modèle n'inclut pas non plus les émissions domestiques, ponctuelles ou diffuses, ni les processus in-stream qui ont de l'importance dans des bassins versants de grande taille. Enfin, il ne simule pas l'effet des pratiques agricoles sur l'évolution du P Olsen dans les sols. Il serait possible d'utiliser un autre modèle pour générer des cartes d'évolution du P Olsen sous différents scenarios de gestion et d'utiliser ces cartes comme donnée d'entrée de notre modèle. Chercher à coupler un modèle d'évolution du P des sols avec notre modèle ne semble pas une option à recommander : i) pour éviter d'augmenter le nombre de paramètres et ii) parce que la nature et la résolution temporelle des données à acquérir pour calibrer chacun des deux modèles sont différentes. Finalement, le temps de calcul pour une simulation (environ 4 minutes par année de simulation pour un petit bassin versant comme Kervidy-Naizin) est long si l'on veut assortir les prédictions du modèle d'une estimation de l'incertitude par la méthode GLUE. Des approches semi-distribuées sont donc plus adaptées pour les bassins de gestion, même si les modèles existants comptent souvent beaucoup de paramètres par rapport à la quantité d'information contenue dans les données généralement disponibles pour les calibrer. Finalement, aucune structure existante de modèle à base physique n'est satisfaisante pour être utilisée en gestion, et la question des données reste problématique pour l'application des modèles. Rappelons qu'en France, aucun bassin versant n'est actuellement équipé pour un suivi haute fréquence des concentrations en phosphore.

Les approches statiques « indices phosphore », comme l'approche Territ'eau en Bretagne https ://agro-transfert-bretagne.univ-rennes1.fr/, sont peut-être les plus utiles pour la gestion à l'heure actuelle, même si elles ne permettent pas une évaluation quantitatives des flux et des concentrations. Au vu des conclusions de cette thèse, le module phosphore de Territ'eau pourrait être amélioré, en particulier en prenant en compte la carte des zones humides dans le facteur « transfert ».

7.4 Perspectives scientifiques

7.4.1 Vers une vision intégrée des cycles C, N, P

Cette thèse sur les transferts de phosphore vient compléter la connaissance sur les éléments majeurs carbone et azote d'ores et déjà acquise, en se basant sur un même site d'étude : le bassin versant de Kervidy-Naizin. Résumons la connaissance actuelle sur les sources et voies de transfert de ces trois éléments sous la forme de schémas (Figure 7.1 – 7.4) :

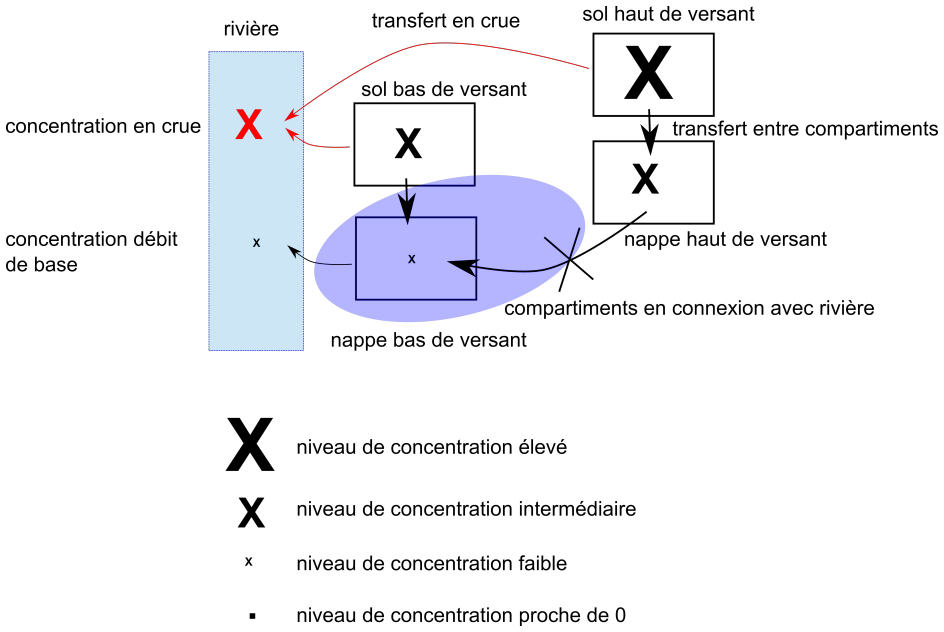

FIGURE 7.1 – Représentation schématique des différents compartiments contribuant aux flux de C, N, P dans un bassin versant agricole sur socle.

- L'azote, transféré en grande partie sous forme de nitrate, provient des apports d'engrais et de la minéralisation des sols, à l'origine de reliquats lixiviés pendant la période automnale/hivernale. Le nitrate lixivié s'accumule dans la nappe, notamment dans les versants cultivés, tandis que l'eau interstitielle des zones humides est pauvre en nitrate du fait du prélèvement par les plantes et de la dénitrification (Figure 7.2). La concentration en nitrate dans la rivière est donc plus élevée en hiver, du fait d'une forte contribution à l'écoulement de la nappe de haut de versant par rapport à l'eau interstitielle des zones humides qui elles contribuent à l'écoulement à l'automne et au printemps ;
- Les sources de carbone sont la photosynthèse et les apports d'effluents au sol. La teneur en carbone des sols est plus élevée dans les sols de zone humide que dans les hauts de versants (Figure 7.3). Les concentrations en matière organique dissoute (MOD) sont donc plus élevées à l'automne qu'en hiver, du fait d'une forte contribution de l'eau interstitielle des zone humides par rapport à la nappe profonde de haut

de versant, qui elle est pauvre en COD. Au sein des zones humides, le pool de COD mobile se constitue pendant l'été et est progressivement épuisé au cours de l'hiver ;

- Contrairement à la MOD, l'origine du phosphore mobile est en grande partie anthropique, mais les sources, mécanismes de solubilisation et les voies de transferts du MRP ont de nombreux points communs (détaillés précédemment et dans la Figure 7.4) avec la MOD.

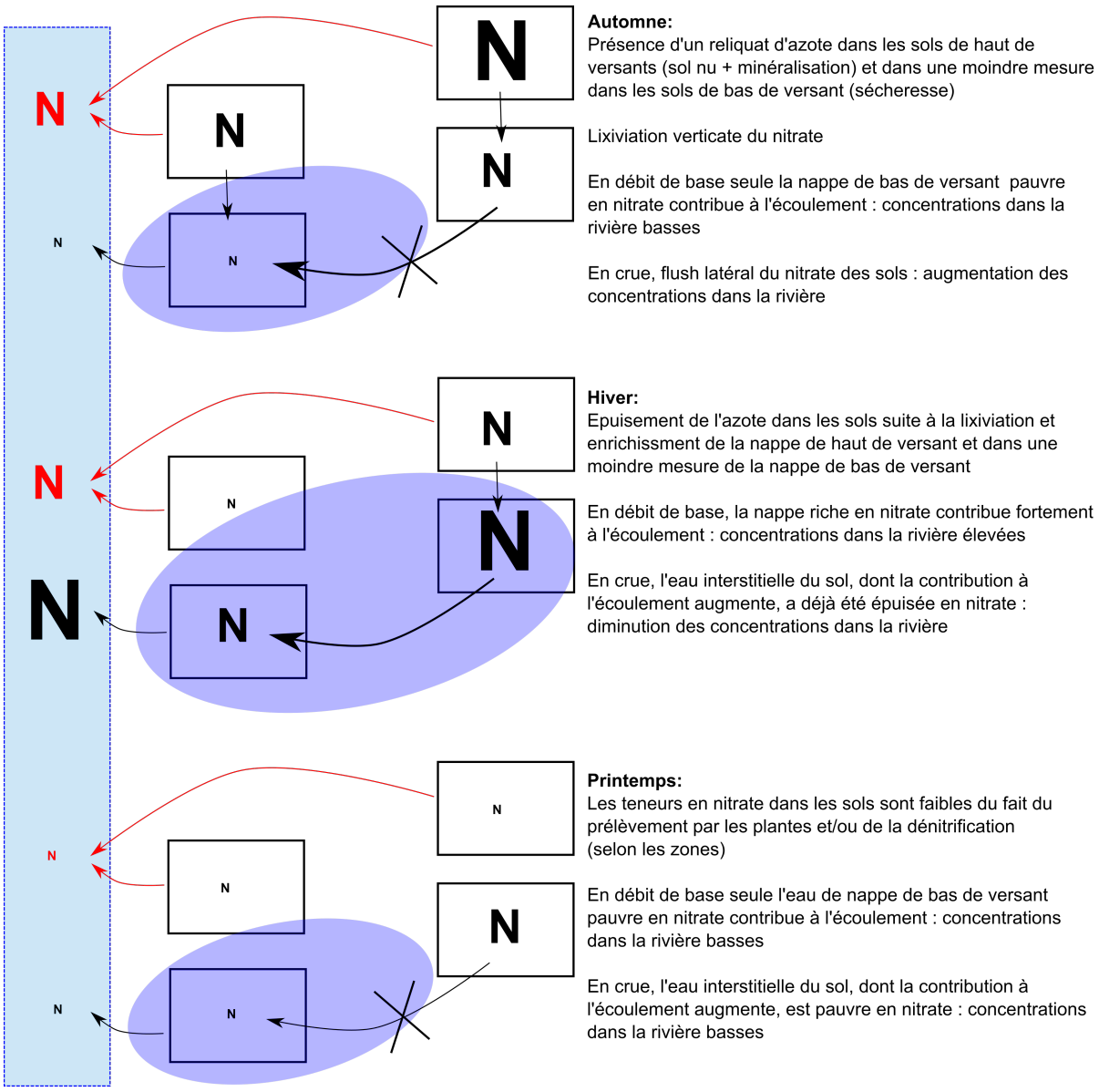

FIGURE 7.2 – Sources et voies de transfert de l'azote dans un bassin versant agricole sur socle.

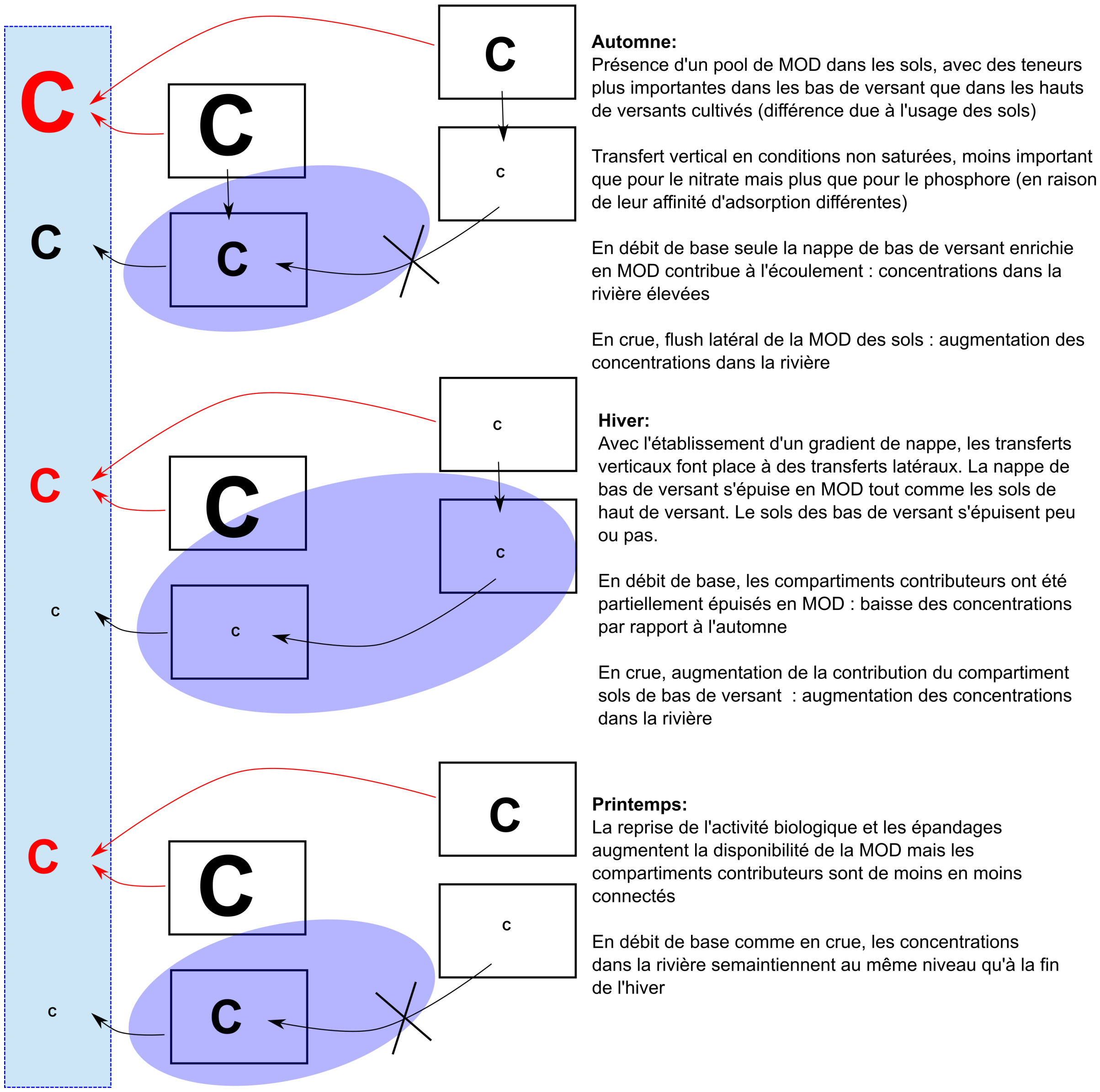

FIGURE 7.3 – Sources et voies de transfert du carbone organique dissous dans un bassin versant agricole sur socle.

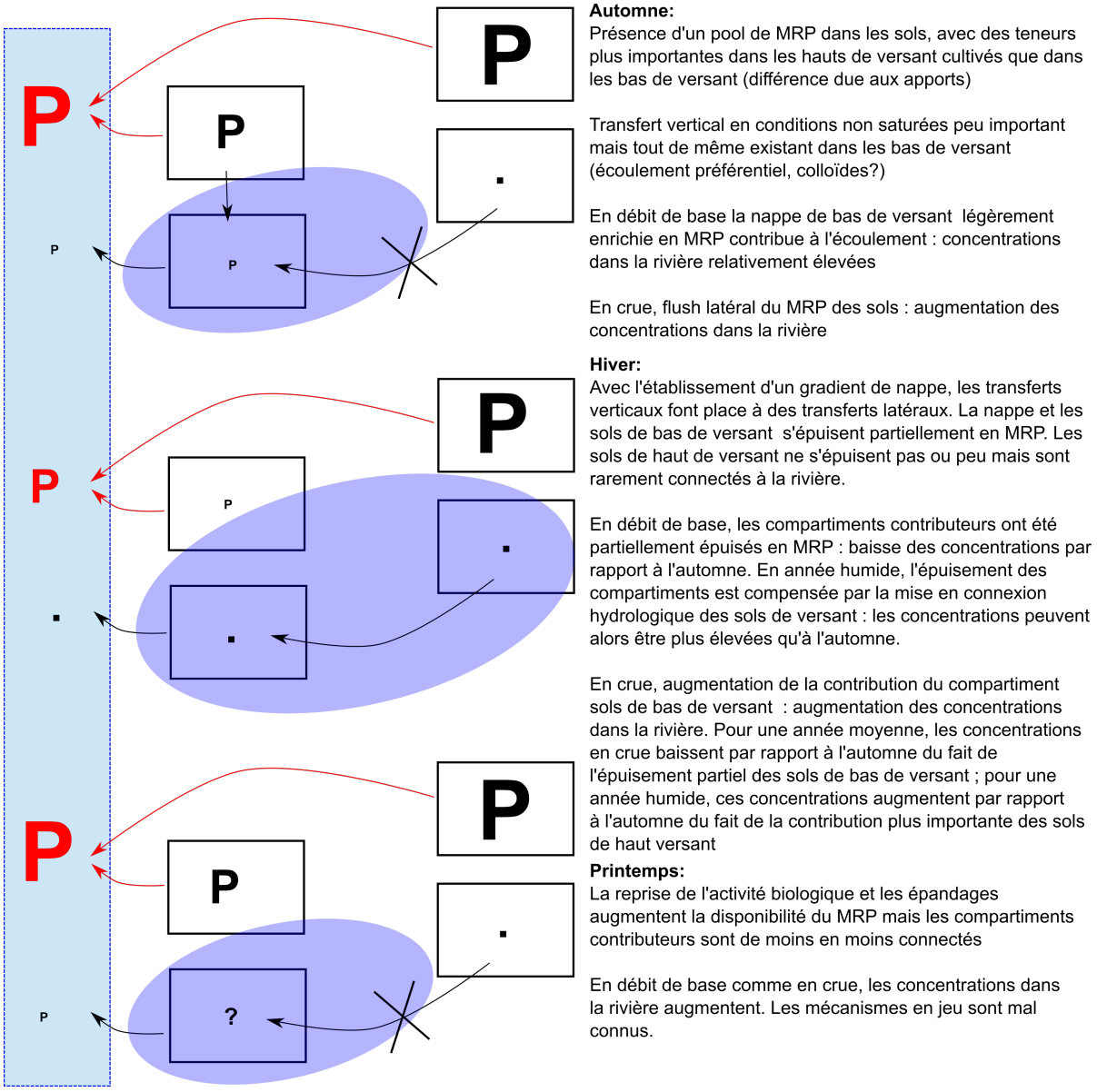

FIGURE 7.4 – Sources et voies de transfert du phosphore dissous dans un bassin versant agricole sur socle.

Si les cycles de chacun des éléments sont représentés séparément ici, des exemples d'interactions entre cycles ont été identifiés grâce au projet Trans-P entre autres.

Par exemple, la relative synchronisation des transferts de SRP et de MOD, à l'échelle annuelle comme à l'échelle des crues, laisse penser à des mécanismes de production et de transfert communs. Il est probable que le pool de MRP présent dans les sols en début d'année hydrologique résulte des mêmes processus biogéochimiques, voire soit constitué des mêmes molécules, que le pool de MOD présent dans les sols à la même période. Un travail

de thèse en cours (2014-2017), réalisé par Sen Gu sous l'encadrement de Gérard Gruau (Géosciences Rennes), vise à préciser la spéciation des formes chimiques de la MOD, du MRP et du phosphore total dissous dans différentes fractions après ultracentrifugation et ultrafiltration.

Un autre exemple d'interaction potentielle entre cycles, mis en évidence dans cette thèse, est le relargage de MRP suite à la dissolution réductrice des (hydr)oxides de Fer, elle-même influencée par la présence ou l'absence de nitrates dans les zones humides ripariennes. Tendre vers une vision intégrée des cycles C, N, P est une nécessité à la fois du point de vue scientifique (enrichissement des connaissances) et du point de vue de la gestion (éviter de remplacer une pollution par une autre en ciblant un élément sans prendre en compte les autres).

7.4.2 Les apports de la haute fréquence et de l'analyse sur site

Les transferts de phosphore sont sujets à des dynamiques infra journalières très importantes, notamment en crue. Partant de là, un échantillonnage journalier ne peut être considéré pour le phosphore comme de la haute fréquence dans des bassins versants de petite taille (< 10 km^2) ; dans l'exercice de modélisation présenté au chapitre 6, nous avons considéré que les échantillons du suivi journalier prélevés un jour de crue contenaient peu d'information, puisque qu'ils peuvent correspondre au pic de concentration comme être situés très loin de ce pic. Le problème de la fréquence d'échantillonnage est à même de compromettre une estimation précise des flux (Cassidy and Jordan, 2011) et donc de calculer des ratios entre flux de C/N/P, surtout sur des périodes de temps inférieures à l'année.

Une autre source d'incertitude dans la chronique phosphore de Kervidy-Naizin, mais aussi dans beaucoup de bassins versants de recherche ou opérationnels, est liée au stockage des échantillons. Nous avons identifié ce problème à la fois pour les échantillons non filtrés stockés dans les préleveurs automatiques et dans les échantillons filtrés immédiatement mais stockés jusqu'à deux semaines au réfrigérateur (chapitre 6). D'après Jarvie *et al.* (2002), des échantillons prélevés pour une analyse de MRP ne devraient pas être stockés plus de deux jours. Cet objectif est inatteignable dans le bassin versant de Kervidy-Naizin, du fait de la distance au laboratoire et des contraintes d'organisation du travail que cela représenterait pour les techniciens de terrain et de laboratoire.

Aujourd'hui, des appareils de mesure haute fréquence existent sur le marché et se répandent dans les bassins de recherche, notamment en Irlande (Jordan *et al.*, 2007 ; Mellander *et al.*, 2012) et en Angleterre (Outram *et al.*, 2014 ; Perks *et al.*, 2015). Ce type d'équipement apparaît incontournable pour atteindre les objectifs de l'UMR SAS de tendre vers une vision intégrée des cycles C, N, P. En complément de l'achat d'un équipement, il serait intéressant de poursuivre l'analyse d'incertitude entamée dans cette thèse (en répétant les expériences de stockage d'échantillons pendant des durées variables) et/ou produire un effort supplémentaire pour réduire les temps de stockage des échantillons non filtrés et filtrés. Une autre possibilité envisageable pour réduire les incertitudes liées à la mesure serait d'analyser le phosphore total dissous plutôt que le phosphore réactif dissous (après vérification que le phosphore total dissous est bien stable après filtration et stockage au réfrigérateur).

7.4.3 Vers une analyse comparative des bassins versants agricoles européens ?

Les bassins versants de l'ORE AgrHys font déjà partie du réseau national des bassins versants RBV (http ://rnbv.ipgp.fr/). Ce réseau permet de créer des synergies entre chercheurs et disciplines, d'accroître la visibilité des travaux menés sur chacun des sites d'étude et de permettre l'achat d'équipements. La diversité des problématiques et des contextes agropédoclimatiques au sein de RBV est une richesse, mais elle ne facilite pas toujours les travaux d'inter comparaison. Il existe des bassins de recherche en Europe dont les problématiques scientifiques et les contextes agropédoclimatiques sont plus proches de l'ORE AgrHys que les bassins versants français de RBV. Ils sont également organisés en réseaux nationaux, comme par exemple le « Demonstration Test Catchment » au Royaume-Uni (http ://www.demonstratingcatchmentmanagement.net/) ou le « Agricultural Catchments Programme » en Irlande (http ://www.teagasc.ie/agcatchments/), pour ne citer que ceux où le contexte est le plus similaire à la Bretagne. Dans ces bassins versants européens, les dispositifs de mesure haute fréquence et sur site se développent depuis 5 – 10 ans. Grâce aux relations existantes entre l'UMR SAS et les chercheurs européens en charge de ces réseau, il serait possible à moyen terme de créer un réseau européen des bassins versants agricoles, pour faciliter les échanges sur les équipements, étudier l'effet des différences de climat et d'agriculture, comparer les modèles, etc. Pour s'imposer parmi les bassins versants de pointe au niveau européen, il est urgent pour l'ORE AgrHys de rattraper le retard pris sur la mesure haute fréquence en s'équipant d'analyseurs sur site d'azote et de phosphore.

Chapitre 8

Références bibliographiques générales

Alexander, R.B., Smith, R.A., Schwarz, G.E., Boyer, E.W., Nolan, J.V., Brakebill, J.W., 2008. Differences in phosphorus and nitrogen delivery to the gulf of Mexico from the Mississippi river basin. Environmental Science Technology 42(3) 822-830.

Amery, F. and O.F. Schoumans, 2014. Agricultural phosphorus legislation in Europe. Merelbeke, ILVO, 45 p.

Arnold, J.G., Srinivasan, R., Muttiah, R.S., Williams, J.R., 1998. Large area hydrologic modeling and assessment - Part 1 : Model development. Journal of the American Water Resources Association 34(1) 73-89.

Aubert AH, Gascuel-Odoux C, Gruau G, Akkal N, Faucheux M, Fauvel Y, *et al.* Solute transport dynamics in small, shallow groundwater-dominated agricultural catchments : insights from a high-frequency, multisolute 10 yr-long monitoring study. Hydrology and Earth System Sciences 2013 ; 17 : 1379-1391.

Beauchemin, S., Simard, R.R., 1999. Soil phosphorus saturation degree : Review of some indices and their suitability for P management in Quebec, Canada. Canadian Journal of Soil Science 79(4) 615-625.

Beven, K., 2006. A manifesto for the equifinality thesis. Journal of Hydrology 320(1-2) 18-36.

Beven, K., Smith, P., 2015. Concepts of Information Content and Likelihood in Parameter Calibration for Hydrological Simulation Models. Journal of Hydrologic Engineering 20(1).

Bieroza, M.Z., Heathwaite, A.L., 2015. Seasonal variation in phosphorus concentration-discharge hysteresis inferred from high-frequency in situ monitoring. Journal of Hydrology 524 333-347.

Bolster, C.H., Vadas, P.A., Sharpley, A.N., Lory, J.A., 2012. Using a Phosphorus Loss Model to Evaluate and Improve Phosphorus Indices. Journal of Environmental Quality 41(6) 1758-1766.

Bouraoui, F., Grizzetti, B., 2011. Long term change of nutrient concentrations of rivers discharging in European seas. Sci Total Environ 409(23) 4899-4916.

Bowes, M.J., House, W.A., Hodgkinson, R.A., Leach, D.V., 2005. Phosphorus-discharge hysteresis during storm events along a river catchment : the River Swale, UK. Water Research 39(5) 751-762.

Bowes, M.J., Smith, J.T., Jarvie, H.P., Neal, C., 2008. Modelling of phosphorus inputs

to rivers from diffuse and point sources. Science of the Total Environment 395(2-3) 125-138.

Bundy, L.G., Tunney, H., Halvorson, A.D., 2005. Agronomic aspects of phosphorus management. Phosphorus : agriculture and the environment.

Carpenter, S.R., Caraco, N.F., Correll, D.L., Howarth, R.W., Sharpley, A.N., Smith, V.H., 1998. Nonpoint pollution of surface waters with phosphorus and nitrogen. Ecological Applications 8(3) 559-568.

Cassidy R, Jordan P. Limitations of instantaneous water quality sampling in surface-water catchments : Comparison with near-continuous phosphorus time-series data. Journal of Hydrology 2011 ; 405 : 182-193.

Castillon P. Transferts de phosphore hors des parcelles cultivées. L'impact des pratiques culturales. Perspectives agricoles 2007 ; 3366-7.

Chevassus-au-Louis, B., Femenias A., Andral B., Bouvier M., 2012. Bilan des connaissances scientifiques sur les causes de prolifération des macroalgues vertes. Applicatio à la situation de la Bretagne et propositions. Rapport 147p.

Collins, A.L., Stutter, M., Kronvang, B., 2014. Mitigating diffuse pollution from agriculture : International approaches and experience. Science of the Total Environment 468 1173-1177.

Cooper, R.J., Krueger, T., Hiscock, K.M., Rawlins, B.G., 2014. Sensitivity of fluvial sediment source apportionment to mixing model assumptions : A Bayesian model comparison. Water Resources Research 50(11) 9031-9047.

Cordell, D., Drangert, J.O., White, S., 2009. The story of phosphorus : Global food security and food for thought. Global Environmental Change-Human and Policy Dimensions 19(2) 292-305.

Cordell, D., White, S., 2011. Peak Phosphorus : Clarifying the Key Issues of a Vigorous Debate about Long-Term Phosphorus Security. Sustainability 3(10) 2027-2049.

Correll, D.L., 1998. The role of phosphorus in the eutrophication of receiving waters : A review. Journal of Environmental Quality 27(2) 261-266. Dean, S., Freer, J., Beven, K., Wade, A.J., Butterfield, D., 2009. Uncertainty assessment of a process-based integrated catchment model of phosphorus. Stochastic Environmental Research and Risk Assessment 23(7) 991-1010.

Delmas M, Saby N, Arrouays D, Dupas R, Lemercier B, Pellerin S, *et al.* Explaining and mapping total phosphorus content in French topsoils. Soil Use and Management 2015 ; 31 : 259-269.

Dorioz JM. Mechanisms and control of agricultural diffuse pollution : the case of phosphorus. Biotechnologie Agronomie Societe Et Environnement 2013 ; 17 : 277-291.

Dupas, R., Delmas, M., Gscuel-Odoux, C., Arrouays, D., Durand, P., Parneaudeau, V. 2011. Revue bibliographique des modèles d'émission de N et P vers les masses d'eau, rapport ONEMA 82p.

Dupas, R. and Gascuel-Odoux, C. 2013. Revue bibliographique sur les modèles de transfert du phosphore, de la parcelle au bassin versant, rapport ONEMA 37 p.

Dupas, R., Delmas, M., Dorioz, J.M., Garnier, J., Moatar, F., Gascuel-Odoux, C., 2015. Assessing the impact of agricultural pressures on N and P loads and eutrophication risk. Ecological Indicators 48 396–407.

Durand, P., Torres, J.L.J., 1996. Solute transfer in agricultural catchments : The interest and limits of mixing models. Journal of Hydrology 181(1-4) 1-22.

Gburek, W.J., Sharpley, A.N., 1998. Hydrologic controls on phosphorus loss from upland agricultural watersheds. Journal of Environmental Quality 27(2) 267-277.

Grizzetti, B., Bouraoui, F., Aloe, A., 2012. Changes of nitrogen and phosphorus loads to European seas. Global Change Biology 18(2) 769-782.

Hahn, C., Prasuhn, V., Stamm, C., Lazzarotto, P., Evangelou, M.W.H., Schulin, R., 2013. Prediction of dissolved reactive phosphorus losses from small agricultural catchments : calibration and validation of a parsimonious model. Hydrology and Earth System Sciences 17(10) 3679-3693.

Haygarth, P.M., 2005. Linking landscape sources of phosphorus and sediment to ecological impacts in surface waters. Science of the Total Environment 344(1-3) 1-3.

Haygarth, P.M., Jarvie, H.P., Powers, S.M., Sharpley, A.N., Elser, J.J., Shen, J.B., Peterson, H.M., Chan, N.I., Howden, N.J.K., Burt, T., Worrall, F., Zhang, F.S., Liu, X.J., 2014. Sustainable Phosphorus Management and the Need for a Long-Term Perspective : The Legacy Hypothesis. Environmental Science Technology 48(15) 8417-8419.

Haygarth, P.M., Page, T.J.C., Beven, K.J., Freer, J., Joynes, A., Butler, P., Wood, G.A., Owens, P.N., 2012. Scaling up the phosphorus signal from soil hillslopes to headwater catchments. Freshwater Biology 57 7-25.

Heathwaite, A.L., Dils, R.M., 2000. Characterising phosphorus loss in surface and subsurface hydrological pathways. Science of the Total Environment 251 523-538.

Heathwaite, A.L., Quinn, P.F., Hewett, C.J.M., 2005. Modelling and managing critical source areas of diffuse pollution from agricultural land using flow connectivity simulation. Journal of Hydrology 304(1-4) 446-461.

Heckrath, G., Brookes, P.C., Poulton, P.R., Goulding, K.W.T., 1995. PHOSPHORUS LEACHING FROM SOILS CONTAINING DIFFERENT PHOSPHORUS CONCENTRATIONS IN THE BROADBALK EXPERIMENT. Journal of Environmental Quality 24(5) 904-910.

House, W.A., Warwick, M.S., 1998. Hysteresis of the solute concentration/discharge relationship in rivers during storms. Water Research 32(8) 2279-2290.

Hyland C., Ketterings Q., Dewing D.,Stockin K., Czymmek K., Albrecht G., Geohring L. 2005. Phosphorus Basics – The Phosphorus Cycle. Agronomy Fact Sheet Series. Cornell University

Ide, J., Haga, H., Chiwa, M., Otsuki, K., 2008. Effects of antecedent rain history on particulate phosphorus loss from a small forested watershed of Japanese cypress (Chamaecyparis obtusa). Journal of Hydrology 352(3-4) 322-335.

Jackson-Blake, L.A., Dunn, S.M., Helliwell, R.C., Skeffington, R.A., Stutter, M.I., Wade, A.J., 2015. How well can we model stream phosphorus concentrations in agricultural catchments ? Environmental Modelling Software 64 31-46.

Jarvie HP, Withers PJA, Neal C. Review of robust measurement of phosphorus in river water : sampling, storage, fractionation and sensitivity. Hydrology and Earth System Sciences 2002 ; 6 : 113-131.

Jarvie, H.P., Sharpley, A.N., Spears, B., Buda, A.R., May, L., Kleinman, P.J.A., 2013. Water Quality Remediation Faces Unprecedented Challenges from "Legacy Phosphorus". Environmental Science Technology 47(16) 8997-8998.

Jin, L., Whitehead, P.G., Sarkar, S., Sinha, R., Futter, M.N., Butterfield, D., Caesar, J., Crossman, J., 2015. Assessing the impacts of climate change and socio-economic changes

on flow and phosphorus flux in the Ganga river system. Environmental Science-Processes Impacts 17(6) 1098-1110.

Jones, C.A. C.V. Cole, A.N. Sharpley, and J.R. Williams. 1984. A simplified soil and plant phosphorus model. I. Documentation. Soil Sci. Soc. Am. J. 48 :800-805.

Jordan-Meille, L., Dorioz, J.M., 2004. Soluble phosphorus dynamics in an agricultural watershed. Agronomie 24(5) 237-248.

Jordan-Meille, L., Rubaek, G.H., Ehlert, P.A.I., Genot, V., Hofman, G., Goulding, K., Recknagel, J., Provolo, G., Barraclough, P., 2012. An overview of fertilizer-P recommendations in Europe : soil testing, calibration and fertilizer recommendations. Soil Use and Management 28(4) 419-435.

Jordan, P., Arnscheidt, J., McGrogan, H., McCormick, S., 2005. High-resolution phosphorus transfers at the catchment scale : the hidden importance of non-storm transfers. Hydrology and Earth System Sciences 9(6) 685-691.

Jordan P, Arnscheidt A, McGrogan H, McCormick S. Characterising phosphorus transfers in rural catchments using a continuous bank-side analyser. Hydrology and Earth System Sciences 2007; 11 : 372-381.

Kirchner, J.W., 2006. Getting the right answers for the right reasons : Linking measurements, analyses, and models to advance the science of hydrology. Water Resources Research 42(3) n/a-n/a.

Krueger, T., Freer, J., Quinton, J.N., Macleod, C.J.A., 2007. Processes affecting transfer of sediment and colloids, with associated phosphorus, from intensively farmed grasslands : a critical note on modelling of phosphorus transfers. Hydrological Processes 21(4) 557-562.

Krueger, T., Quinton, J.N., Freer, J., Macleod, C.J., Bilotta, G.S., Brazier, R.E., Butler, P., Haygarth, P.M., 2009. Uncertainties in data and models to describe event dynamics of agricultural sediment and phosphorus transfer. J Environ Qual 38(3) 1137-1148.

Lambert, T., Pierson-Wickmann, A.C., Gruau, G., Jaffrezic, A., Petitjean, P., Thibault, J.N., Jeanneau, L., 2014. DOC sources and DOC transport pathways in a small headwater catchment as revealed by carbon isotope fluctuation during storm events. Biogeosciences 11(11) 3043-3056.

Lawler, D.M., Petts, G.E., Foster, I.D.L., Harper, S., 2006. Turbidity dynamics during spring storm events in an urban headwater river system : The Upper Tame, West Midlands, UK. Science of the Total Environment 360(1-3) 109-126.

Le Bissonnais, Y., Cros-Cayot, S., Gascuel-Odoux, C., 2002. Topographic dependence of aggregate stability, overland flow and sediment transport. Agronomie 22(5) 489-501.

Lefrancois, J., Grimaldi, C., Gascuel-Odoux, C., Gilliet, N., 2007. Suspended sediment and discharge relationships to identify bank degradation as a main sediment source on small agricultural catchments. Hydrological Processes 21(21) 2923-2933.

Legeay, P.-L., Gruau, G., Moatar, F., Gascuel-Odoux, C. 2015. Une analyse de la variabilité spatio-temporelle des flux et des sources du phosphore dans les cours d'eau bretons. Période 1987-2012. Rapport trans-P volet 1.

Li, B., Brett, M.T., 2013. The influence of dissolved phosphorus molecular form on recalcitrance and bioavailability. Environ Pollut 182 37-44.

Lindstrom, G., Pers, C., Rosberg, J., Stromqvist, J., Arheimer, B., 2010. Development and testing of the HYPE (Hydrological Predictions for the Environment) water quality model for different spatial scales. Hydrology Research 41(3-4) 295-319.

McDowell, R., Sharpley, A., Withers, P., 2002. Indicator to predict the movement of phosphorus from soil to subsurface flow. Environmental Science Technology 36(7) 1505-1509.

McDowell, R.W., Moreau, P., Salmon-Monviola, J., Durand, P., Leterme, P., Merot, P., 2014. Contrasting the spatial management of nitrogen and phosphorus for improved water quality : Modelling studies in New Zealand and France. European Journal of Agronomy 57 52-61.

McDowell, R.W., Sharpley, A.N., 2002. The effect of antecedent moisture conditions on sediment and phosphorus loss during overland flow : Mahantango Creek catchment, Pennsylvania, USA. Hydrological Processes 16(15) 3037-3050.

Mellander, P.-E., Melland, A.R., Jordan, P., Wall, D.P., Murphy, P.N.C., Shortle, G., 2012. Quantifying nutrient transfer pathways in agricultural catchments using high temporal resolution data. Environmental Science Policy 24 44-57.

Mellander, P.E., Jordan, P., Shore, M., Melland, A.R., Shortle, G., 2015. Flow paths and phosphorus transfer pathways in two agricultural streams with contrasting flow controls. Hydrological Processes.

Molenat J, Durand P, Gascuel-Odoux C, Davy P, Gruau G. Mechanisms of nitrate transfer from soil to stream in an agricultural watershed of French Brittany. Water Air and Soil Pollution 2002 ; 133 : 161-183.

Morel, B., Durand, P., Jaffrezic, A., Gruau, G., Molenat, J., 2009. Sources of dissolved organic carbon during stormflow in a headwater agricultural catchment. Hydrological Processes 23(20) 2888-2901.

Nemery, J., Garnier, J., Morel, C., 2005. Phosphorus budget in the Marne Watershed (France) : urban vs. diffuse sources, dissolved vs. particulate forms. Biogeochemistry 72(1) 35-66.

Neset, T.S.S., Cordell, D., 2012. Global phosphorus scarcity : identifying synergies for a sustainable future. Journal of the Science of Food and Agriculture 92(1) 2-6.

Outram, F.N., Lloyd, C.E.M., Jonczyk, J., Benskin, C.M.H., Grant, F., Perks, M.T., Deasy, C., Burke, S.P., Collins, A.L., Freer, J., Haygarth, P.M., Hiscock, K.M., Johnes, P.J., Lovett, A.L., 2014. High-frequency monitoring of nitrogen and phosphorus response in three rural catchments to the end of the 2011-2012 drought in England. Hydrology and Earth System Sciences 18(9) 3429-3448.

Pauwels H, Kloppmann W, Foucher JC, Martelat A, Fritsche V. Field tracer test for denitrification in a pyrite-bearing schist aquifer. Applied Geochemistry 1998 ; 13 : 767-778.

Perks, M.T., Owen, G.J., Benskin, C.M.H., Jonczyk, J., Deasy, C., Burke, S., Reaney, S.M., Haygarth, P.M., 2015. Dominant mechanisms for the delivery of fine sediment and phosphorus to fluvial networks draining grassland dominated headwater catchments. Science of the Total Environment 523 178-190.

Poirier, S.C., Whalen, J.K., Michaud, A.R., 2012. Bioavailable Phosphorus in Fine-Sized Sediments Transported from Agricultural Fields. Soil Science Society of America Journal 76(1) 258-267.

Pothig, R., Behrendt, H., Opitz, D., Furrer, G., 2010. A universal method to assess the potential of phosphorus loss from soil to aquatic ecosystems. Environ Sci Pollut Res Int 17(2) 497-504.

Radcliffe, D.E., Freer, J., Schoumans, O., 2009. Diffuse phosphorus models in the United

States and europe : their usages, scales, and uncertainties. J Environ Qual 38(5) 1956-1967.

Ringeval B, Nowak B, Nesme T, Delmas M, Pellerin S. Contribution of anthropogenic phosphorus to agricultural soil fertility and food production. Global Biogeochemical Cycles 2014 ; 28 : 743-756.

Rodriguez-Blanco, M.L., Taboada-Castro, M.M., Keizer, J.J., Taboada-Castro, M.T., 2013. Phosphorus Loss from a Mixed Land Use Catchment in Northwest Spain. Journal of Environmental Quality 42(4) 1151-1158.

Schindler, D.W., 2012. The dilemma of controlling cultural eutrophication of lakes. Proceedings of the Royal Society B-Biological Sciences 279(1746) 4322-4333.

Schindler, D.W., Hecky, R.E., Findlay, D.L., Stainton, M.P., Parker, B.R., Paterson, M.J., Beaty, K.G., Lyng, M., Kasian, S.E.M., 2008. Eutrophication of lakes cannot be controlled by reducing nitrogen input : Results of a 37-year whole-ecosystem experiment. Proceedings of the National Academy of Sciences of the United States of America 105(32) 11254-11258.

Schoumans, O.F., Chardon, W.J., 2015. Phosphate saturation degree and accumulation of phosphate in various soil types in The Netherlands. Geoderma 237 325-335.

Schoumans, O.F., Chardon, W.J., Bechmann, M.E., Gascuel-Odoux, C., Hofman, G., Kronvang, B., Rubaek, G.H., Ulen, B., Dorioz, J.M., 2014. Mitigation options to reduce phosphorus losses from the agricultural sector and improve surface water quality : A review. Science of the Total Environment 468 1255-1266.

Schroder, J.J., Smit, A.L., Cordell, D., Rosemarin, A., 2011. Improved phosphorus use efficiency in agriculture : A key requirement for its sustainable use. Chemosphere 84(6) 822-831.

Seeger, M., Errea, M.P., Begueria, S., Arnaez, J., Marti, C., Garcia-Ruiz, J.M., 2004. Catchment soil moisture and rainfall characteristics as determinant factors for discharge/suspended sediment hysteretic loops in a small headwater catchment in the Spanish pyrenees. Journal of Hydrology 288(3-4) 299-311.

Senthilkumar, K., Nesme, T., Mollier, A., Pellerin, S., 2012a. Conceptual design and quantification of phosphorus flows and balances at the country scale : The case of France. Global Biogeochemical Cycles 26.

Senthilkumar, K., Nesme, T., Mollier, A., Pellerin, S., 2012b. Regional-scale phosphorus flows and budgets within France : The importance of agricultural production systems. Nutrient Cycling in Agroecosystems 92(2) 145-159.

Serrano, T., Dupas, R., Upegui, E., Buscail, C., Grimaldi, C., Viel, J.-F., 2015. Geographical modeling of exposure risk to cyanobacteria for epidemiological purposes. Environment International 81 18-25.

Sharpley, A.N., T. Daniel, T. Sims, J. Lemunyon, R. Stevens, and R. Parry. 2003. Agricultural Phosphorus and Eutrophication, 2nd ed. U.S. department of Agriculture, Agricultural Research Service, ARS.149, 44 pp.

Sharpley, A., Jarvie, H.P., Buda, A., May, L., Spears, B., Kleinman, P., 2013. Phosphorus Legacy : Overcoming the Effects of Past Management Practices to Mitigate Future Water Quality Impairment. Journal of Environmental Quality 42(5) 1308-1326.

Shore, M., Jordan, P., Mellander, P.E., Kelly-Quinn, M., Wall, D.P., Murphy, P.N.C., Melland, A.R., 2014. Evaluating the critical source area concept of phosphorus loss from soils to water-bodies in agricultural catchments. Science of the Total Environment 490

405-415.

Simard, R.R., Beauchemin, S., Haygarth, P.M., 2000. Potential for preferential pathways of phosphorus transport. Journal of Environmental Quality 29(1) 97-105.

Siwek, J., Siwek, J.P., Zelazny, M., 2013. Environmental and land use factors affecting phosphate hysteresis patterns of stream water during flood events (Carpathian Foothills, Poland). Hydrological Processes 27(25) 3674-3684.

Smith, V.H., Schindler, D.W., 2009. Eutrophication science : where do we go from here ? Trends in Ecology Evolution 24(4) 201-207.

Soulsby, C., Petry, J., Brewer, M.J., Dunn, S.M., Ott, B., Malcolm, I.A., 2003. Identifying and assessing uncertainty in hydrological pathways : a novel approach to end member mixing in a Scottish agricultural catchment. Journal of Hydrology 274(1-4) 109-128.

Stamm C, Jarvie HP, Scott T. What's More Important for Managing Phosphorus : Loads, Concentrations or Both ? Environmental Science Technology 2014 ; 48 : 23-24.

Stromqvist, J., Arheimer, B., Dahne, J., Donnelly, C., Lindstrom, G., 2012. Water and nutrient predictions in ungauged basins : set-up and evaluation of a model at the national scale. Hydrological Sciences Journal-Journal Des Sciences Hydrologiques 57(2) 229-247.

Stutter, M.I., Langan, S.J., Cooper, R.J., 2008. Spatial contributions of diffuse inputs and within-channel processes to the form of stream water phosphorus over storm events. Journal of Hydrology 350(3-4) 203-214.

Vadas, P.A., Bolster, C.H., Good, L.W., 2013. Critical evaluation of models used to study agricultural phosphorus and water quality. Soil Use and Management 29 36-44.

Vadas, P.A., Joern, B.C., Moore, P.A., 2012. Simulating soil phosphorus dynamics for a phosphorus loss quantification tool. J Environ Qual 41(6) 1750-1757.

Vadas, P.A., White, M.J., 2010. VALIDATING SOIL PHOSPHORUS ROUTINES IN THE SWAT MODEL. Transactions of the Asabe 53(5) 1469-1476.

van der Salm, C., Dupas, R., Grant, R., Heckrath, G., Iversen, B.V., Kronvang, B., Levi, C., Rubaek, G.H., Schoumans, O.F., 2011. Predicting Phosphorus Losses with the PLEASE Model on a Local Scale in Denmark and the Netherlands. Journal of Environmental Quality 40(5) 1617-1626.

Van Drecht, G., Bouwman, A.F., Harrison, J., Knoop, J.M., 2009. Global nitrogen and phosphate in urban wastewater for the period 1970 to 2050. Global Biogeochemical Cycles 23.

Van Moorleghem, C., De Schutter, N., Smolders, E., Merckx, R., 2013. The bioavailability of colloidal and dissolved organic phosphorus to the alga Pseudokirchneriella subcapitata in relation to analytical phosphorus measurements. Hydrobiologia 709(1) 41-53.

Wade, A.J., Whitehead, P.G., Butterfield, D., 2002. The Integrated Catchments model of Phosphorus dynamics (INCA-P), a new approach for multiple source assessment in heterogeneous river systems : model structure and equations. Hydrology and Earth System Sciences 6(3) 583-606.

Wall, D.P., Jordan, P., Melland, A.R., Mellander, P.E., Mechan, S., Shortle, G., 2013. Forecasting the decline of excess soil phosphorus in agricultural catchments. Soil Use and Management 29 147-154.

Wellen, C., Kamran-Disfani, A.R., Arhonditsis, G.B., 2015. Evaluation of the Current State of Distributed Watershed Nutrient Water Quality Modeling. Environmental Science Technology 49(6) 3278-3290.

Annexe A

Etat des lieux des flux de N et P en France

Ecological Indicators 48 (2015) 396–407

Contents lists available at ScienceDirect

Ecological Indicators

journal homepage: www.elsevier.com/locate/ecolind

Assessing the impact of agricultural pressures on N and P loads and eutrophication risk

Rémi Dupas[a,b,*], Magalie Delmas[c], Jean-Marcel Dorioz[d], Josette Garnier[e], Florentina Moatar[f], Chantal Gascuel-Odoux[a,b]

[a] INRA, UMR1069, Sol Agro and hydroSystem, F-35000 Rennes, France
[b] Agrocampus Ouest, Sol Agro and hydroSystem, F-35000 Rennes, France
[c] INRA, Infosol, F-45075 Orléans, France
[d] INRA, UMR Carrtel, F74203 BP 11 Thonon les bains, France
[e] CNRS, Univ Paris 06, UMR Sisyphe 7619, F-75252 Paris, France
[f] Univ Tours, Fac Sci & Tech, EA 6293, F-37200 Tours, France

ARTICLE INFO

Article history:
Received 26 May 2014
Received in revised form 11 July 2014
Accepted 6 August 2014

Keywords:
Nitrogen
Phosphorus
Mass-balance model
Eutrophication
Indicator
Agriculture

ABSTRACT

Excessive nutrient delivery into freshwater bodies results in increased eutrophication risk worldwide. Because high-frequency monitoring cannot be generalised to all rivers, methods are needed to assess eutrophication risk in contexts with scarce data. To this end, we present an assessment framework which includes: (i) a mass-balance model to estimate diffuse N and P transfer/retention in unmonitored catchments and (ii) a set of indicators based on N:P:Si molar ratios to assess the risk of eutrophication in freshwaters. The model, called Nutting, integrates variables that describe both agricultural pressures and physical attributes of catchments (climate, topography, soil). Nutting refines previous mass-balance models by describing nutrient pressures with soil N surplus and soil P content instead of N and P inputs, and by considering physical attributes not only as lumped variables over the entire area but also within river corridors. The model was calibrated on a set of 160 independent catchments across France and applied to all headwater catchments. We found that apparent N and P retention represented 53 ± 24% and 95 ± 29% of soil N and P surplus, respectively, and was mainly controlled by the climate and a hydrology-related connectivity index. The spatial organisation of the landscape was of secondary importance compared to the refined description of agricultural pressures. Estimated eutrophication risk was highly sensitive to assumptions about P bioavailability, hence the potential range of headwaters at risk of eutrophication spanned 26–63% of the catchments, depending on assumptions. This framework provides a generic method to assess the relative contribution of agriculture to nutrient loads and the subsequent risk of eutrophication.

1. Introduction

Degradation of surface water resulting from excessive nitrogen (N) and phosphorus (P) inputs is a major concern for drinking water quality and ecosystem health (Carpenter et al., 1998; Vitousek et al., 1997). Due to improvement of point-source control in recent decades, research and management efforts to decrease nutrient pollution have been redirected towards diffuse sources (Van Drecht et al., 2009). In industrialised countries, most source apportionment studies have shown that agriculture is currently a major source of nutrients in surface waters (e.g. Bouraoui and Grizzetti, 2011; Grizzetti et al., 2012; Windolf et al., 2012). Nutrient transfers from agricultural landscapes result from combined hydrological and biogeochemical processes controlling their mobilisation and delivery in the terrestrial and aquatic compartments of catchments (Bouwman et al., 2013; Haygarth et al., 2005; Seitzinger et al., 2006). These processes are difficult to understand and to model due to the complexity of agricultural landscapes (Burt and Pinay, 2005; Strayer et al., 2003).

Low-order catchments (i.e. below Strahler order 5) are known to contribute large amounts of nutrient loads to downstream water bodies (Alexander et al., 2007; Lassaletta et al., 2010; Peterson et al., 2001). In terms of scientifically understanding the processes controlling N and P diffuse transfer/retention in agricultural landscapes, low-order catchments are relevant spatial units because

* Corresponding author at: INRA, UMR1069, Sol Agro and hydroSystem, F-35000 Rennes, France. Tel.: +33 223487047.
E-mail address: rdupas@agrocampus-ouest.fr (R. Dupas).

http://dx.doi.org/10.1016/j.ecolind.2014.08.007
1470-160X/

in-stream processes and point-source emissions are relatively less important than they are in larger river networks (Burt and Pinay, 2005; Montreuil et al., 2010). Since the 1980s, long-term observatories have been initiated in low-order catchments to identify both the hydrological and biogeochemical process controlling N and P transfer/retention in space and time (Aubert et al., 2013; Neal et al., 2011). These detailed observations of individual catchments have provided scientific understanding, which has served as a basis for the development of process-based models (e.g. Arnold et al., 1998; Beaujouan et al., 2002; Ferrant et al., 2011). However, such models require a large number of input data, which are generally not available for regional-scale assessments (Schoumans et al., 2009).

To determine which landscape features control nutrient diffuse transfer and retention, an alternative approach to process-based modelling consists of considering a large number of catchments, taken as lumped and steady-state entities, and developing statistical approaches (Preston et al., 2011; Tysmans et al., 2013). Models resulting from a statistical approach can be classified into two broad categories: export-coefficient models (e.g. Johnes, 1996; Worrall et al., 2009) and mass-balance models (e.g. Dupas et al., 2013; Grizzetti et al., 2008; Smith et al., 1997). They provide a means to assess water quality in unmonitored catchments and determine the factors controlling it (Kronvang et al., 2003; Wu and Chen, 2013; Zhou et al., 2012). Limits of such models include poor characterisation of agricultural pressures (limited to land-use/land-cover types in the export coefficient approach or N–P inputs in mass-balance models) and ignoring the spatial distribution of catchment attributes.

Additionally, linking N and P loads to the assessment of eutrophication risk in freshwaters is extremely challenging. Many authors consider that development of undesirable non-siliceous algae occurs when N and P levels exceed those of silica (Si), according to Redfield (1958) stoichiometric ratios. According to this view, Billen and Garnier (2007) introduced the Indicator for Coastal Eutrophication Potential (ICEP) to assess the risk of marine eutrophication resulting from excessive nutrient delivery (see also Garnier et al. (2010) and Romero et al. (2013) for applications in coastal catchments worldwide). The ICEP improves the commonly used N:P ratios by considering the stoichiometric C:N:P:Si composition of diatoms, but has never been adapted to freshwater ecosystems.

In this paper, we present an assessment framework which includes: (i) a refined mass-balance model, called Nutting, to estimate diffuse N and P transfer/retention in unmonitored catchments and identify attributes of the catchments controlling them and (ii) a set of indicators to assess the risk of eutrophication resulting from excessive nutrient delivery in freshwater bodies. We hypothesised that we could improve previous mass-balance models by: (i) describing diffuse nutrient sources in terms of soil N surplus and soil P content instead of N and P inputs and (ii) considering catchment attributes not only as lumped variables over the entire area but also within river corridors. Because eutrophication risk is highly dependent on P bioavailability, we tested the sensitivity of the indicators developed to three assumptions about the bioavailability of particulate P. The assessment framework was performed at the country level, and France was chosen as a typical country of Western Europe, with large variability in agricultural pressure intensity and climate conditions.

2. Materials and methods

The assessment framework described in this paper uses monitoring data from 160 independent catchments for calibration. The models developed are then applied to 2210 unmonitored catchments in France. Further description of both calibration and application catchments are given after a presentation of the general methodology.

2.1. Multivariate analysis

A multivariate analysis was performed to relate observed N and P transfer/retention of a set of catchments to spatial attributes describing N and P pressures and the physical environment of the catchment. Hierarchical Clustering on Principal Components (HCPC) combines principal component analysis (PCA), hierarchical clustering (HC) and partitional clustering (specifically *k*-means) (Husson et al., 2010). The PCA consists of projecting nutrient load variables and illustrative variables onto a factorial plan defined by two axes. In HCPC, PCA is a pre-processing step which reduces the number of dimensions in parameter space. In a second step, HC is performed on the PCA axes using Ward's criterion. The number of clusters is chosen visually from the hierarchical tree and is based on the increase of inertia. Finally, the clusters obtained from the hierarchical tree cut are used to initialise the *k*-means algorithm, which 'consolidates' the initial clustering. We performed the HCPC with functions from the R software (R Development Core Team, 2012) package 'FactoMineR'. This clustering method identifies different catchment types based on observed N and P loads in dissolved and particulate forms and relates this typology to the physical environment of the catchments.

2.2. Statistical modelling

2.2.1. Model structure: Nutting-N

Nutting-N (NUTrient Transfer modellING-Nitrogen) is a statistical model that links N sources and catchment land and river attributes to estimate mean annual total-N and nitrate-N loads. The name of the model, Nutting, means that it is constructed from few datasets which cannot completely represent all processes involved in N transport from land to rivers. The foundation of the Nutting-N model is to make the best use of available data at national or regional levels to optimise model accuracy. Total-N and nitrate-N specific loads (TNload and DNload, in kg N ha^{-1} yr^{-1}) at the outlet of each catchment are expressed as:

$$\text{TNload} = R_{TN} * (B_{TN} * \text{Nsurplus} + \text{Npoint}) \quad (1)$$

$$\text{DNload} = R_{DN} * (B_{DN} * \text{Nsurplus} + \text{Npoint}) \quad (2)$$

where Nsurplus is the soil N surplus [kg N ha^{-1} yr^{-1}], Npoint is the sum of all domestic and industrial point sources in the catchment [kg N ha^{-1} yr^{-1}], and R_{TN}/R_{DN} and B_{TN}/B_{DN} are river and catchment transfer factors, respectively. The river and catchment transfer factors express the percentage of the load that is transferred in the terrestrial part and the aquatic part of the catchment. They combine observed variables and calibrated parameters and vary from 0 to 1. In Eq. (1), $R_{TN} * B_{TN} *$ Nsurplus represents the contribution of agricultural diffuse source, and $R_{TN} * B_{TN} *$ Npoint represents the contribution of domestic and industrial point sources to total-N specific load.

In the original description of Nutting-N (Dupas et al., 2013), total runoff was partitioned into a shallow and a deep component to address the issue of catchments that are not at equilibrium, and included a benthic denitrification factor. Here, we considered only one flow component and no benthic denitrification factors in order to reduce the number of parameters in the model. The resulting simplified version of Nutting-N differs from earlier models (e.g. Grizzetti et al., 2008; Smith et al., 1997) because diffuse N sources are characterised by N surplus instead of N input and because the river-transfer factor was inspired by the denitrification function of

Boyer et al. (2006), adapted for lumped application in catchments. The river-transfer factor is calculated as:

$$R_{TN} \text{ or } R_{DN} = \exp\left(-\alpha j * \frac{T}{D}\right) \quad (3)$$

where αj is a mass-transfer coefficient to be calibrated, T is the specific residence time in the river network (s ha^{-1}) and D is the mean stream depth (m).

The catchment transfer factor B is calculated as:

$$B_{TN} \text{ or } B_{DN} = \exp\left(-\sum_i \alpha j * Xi\right) \quad (4)$$

where αi are coefficients to be calibrated and Xi are predictor variables selected from available catchment attributes. These are defined either as lumped variables or within river corridors (see Section 2.4.3). Predictor variables which are expected to have a positive effect on N transfer (e.g. effective rainfall) are entered as their reciprocals, so that all $\alpha i < 0$ and B_{TN}/B_{DN} vary between 0 and 1.

2.2.2. Model structure: Nutting-P

Nutting-P (NUTrient Transfer modellING-Phosphorus) was built similarly to Nutting-N, but diffuse P sources are characterised by the amount of P in the topsoil instead of P surplus. This choice relied on a trial-and-error procedure aiming to minimise the root mean squared error of prediction (RMSEP) with different combinations of candidate variables (Ptopsoil, Ptopsoil × erosion coefficient, P surplus). A benthic retention factor was added because it increased the accuracy of model prediction, unlike in Nutting-N. Total-P and dissolved-P specific loads (TPload and DPload, respectively) at the outlet of each catchment are expressed as:

$$\text{TPload} = (B_{TP} * \text{Ptopsoil} + \text{Ppoint}) - \text{Ret}_{\text{benthic}} \quad (5)$$

$$\text{DPload} = R_{DP} * (B_{TP} * \text{Ptopsoil} + \text{Ppoint}) - \text{Ret}_{\text{benthic}} \quad (6)$$

where Ptopsoil is the amount of P in the 0–0.3 m topsoil [kg P ha^{-1}]; Ppoint is the sum of all point-source emissions in the catchment [kg P ha^{-1} yr^{-1}]; $\text{Ret}_{\text{benthic}}$ is a benthic denitrification factor and R_{DP}, B_{DP} and B_{TP} are two river and one catchment transfer factors, respectively. They are computed in the same manner as R_{TN} and B_{TN}. Variables included in the factors B_{DP} and B_{TP} may differ from those in B_{TN} and B_{DN}, however. In Eq. (5), B_{TP} * Ptopsoil represents the contribution of agricultural diffuse source, and Ppoint represents the contribution of domestic and industrial point sources to total-P specific load.

Although the processes involved in long-term retention of dissolved-P in the river system (i.e. adsorption onto particles followed by sedimentation) differ from those involved in N retention (i.e. denitrification), R_{DP} remains a function of the same river geometry variable as R_{TN} and R_{DN} (Eq. (3)). We assumed that dissolved-P retention is a function of the contact time with river sediments and the height of the water column. $\text{Ret}_{\text{benthic}}$ is calculated from lakes' hydraulic residence times with the Euroharp nutrient retention tool (Euroharp-Nutret Tier 2; Kronvang et al. (2004)). We estimated lakes' hydraulic residence times with data on lake geometry (Folton and Lavabre, 2006). No river-transfer factor was included in the total-P model because we considered that the antagonistic processes controlling P retention (i.e. adsorption vs. desorption within the river bed, sedimentation vs. transport of sediments, biological uptake vs. release) balance each other on a pluri-annual basis. The only processes causing long-term P retention at equilibrium are overbank floodplain sedimentation and sedimentation in lakes and reservoirs (Demars et al., 2005). We ignored the former due to lack of data with which to estimate it, and the latter is already included in the $\text{Ret}_{\text{benthic}}$ factor.

2.2.3. Variable selection and model parameterisation

A wide range of catchment attributes (see Section 2.4.3.) was tested as potential variables to include in Nutting-N and Nutting-P catchment transfer factors B_{TN}, B_{DN}, B_{TP} and B_{DP}. The variable selection procedure aimed to select a limited number of independent variables to optimise model accuracy and avoid over-fitting (Dupas et al., 2013). It had two steps: (i) re-writing a "linearized" version of equations (1), (2), (5), (6) by log-transforming them and ignoring point sources. Variable selection in the "linearized" model was performed according to the Bayesian Information Criterion and parameters were calibrated by minimising a sum of square function. These optimised parameters were used as initial values for the final parameterisation; (ii) final variable selection and parameterisation in a leave-one-out cross-validation to minimise RMSEP. Final parameterisation relied on minimising a weighted least-squared objective function with a modified Gauss–Newton algorithm. Initial parameter values in the B factor were those estimated in the "linearized" model. Initial parameter values in the R factor were chosen to match the in-stream denitrification rate reported by Kronvang et al. (2004).

Additionally, we performed an uncertainty analysis of model parameters and model predictions. We used the R function 'boot' to draw the bootstrap 95% percentile confidence intervals of model parameters and predictions on the basis of 1000 bootstrap replicates.

2.3. The Indicator of Freshwater Eutrophication Potential

The Indicator of Freshwater Eutrophication Potential (IFEP) is an adaptation for freshwaters of the Indicator of Coastal Eutrophication Potential (ICEP) by Billen and Garnier (2007). Both are based on Redfield's (1958) molar C:N:P:Si composition of diatoms, i.e. 106:16:1:20 in marine waters and 106:16:1:40 in freshwaters. The IFEP measures the degree to which N and P concentrations exceed that of Si, assuming that excessive nutrient delivery causes development of undesirable non-siliceous algae instead of diatoms. The IFEP, which is converted into carbon units, can assess N and P independently (N-IFEP, P-IFEP), as follows:

$$\text{N-IFEP} = \left(\frac{\text{TNload}}{14 * 16} - \frac{\text{Siload}}{28 * 40}\right) * 106 * 12 \quad (7)$$

$$\text{P-IFEP} = \left(\frac{\text{TPload}}{31} - \frac{\text{Siload}}{28 * 40}\right) * 106 * 12 \quad (8)$$

where TNload, TPload and Siload are, respectively, the specific loads of total-N, total-P and Si in kg ha^{-1} yr^{-1}. Index values are expressed in kg C ha^{-1} yr^{-1}. A positive value of N-IFEP or P-IFEP indicates that the nutrient in question exceeds Si and that eutrophication may occur; the lower index indicates which nutrient is limiting.

The limiting nutrient can also be determined by comparing the molar N:P ratio to the Redfield N:P ratio of 16. We also analysed the sensitivity of IFEP to three assumptions about P bioavailability by testing three hypotheses: (i) only dissolved-P forms are bioavailable, (ii) dissolved-P + 30% of particulate-P is bioavailable, and (iii) 100% of total-P is bioavailable. The 30% bioavailability of particulate-P was a plausible estimate according to several authors (Dorioz and Trevisan, 2013; Poirier et al., 2012; Sharpley et al., 1992), despite the high variability observed in bioassay experiments.

2.4. The catchment database

2.4.1. Selection criteria

For the multivariate analysis and to calibrate the Nutting models, we established a dataset of 160 independent observation catchments using national public data from French environmental

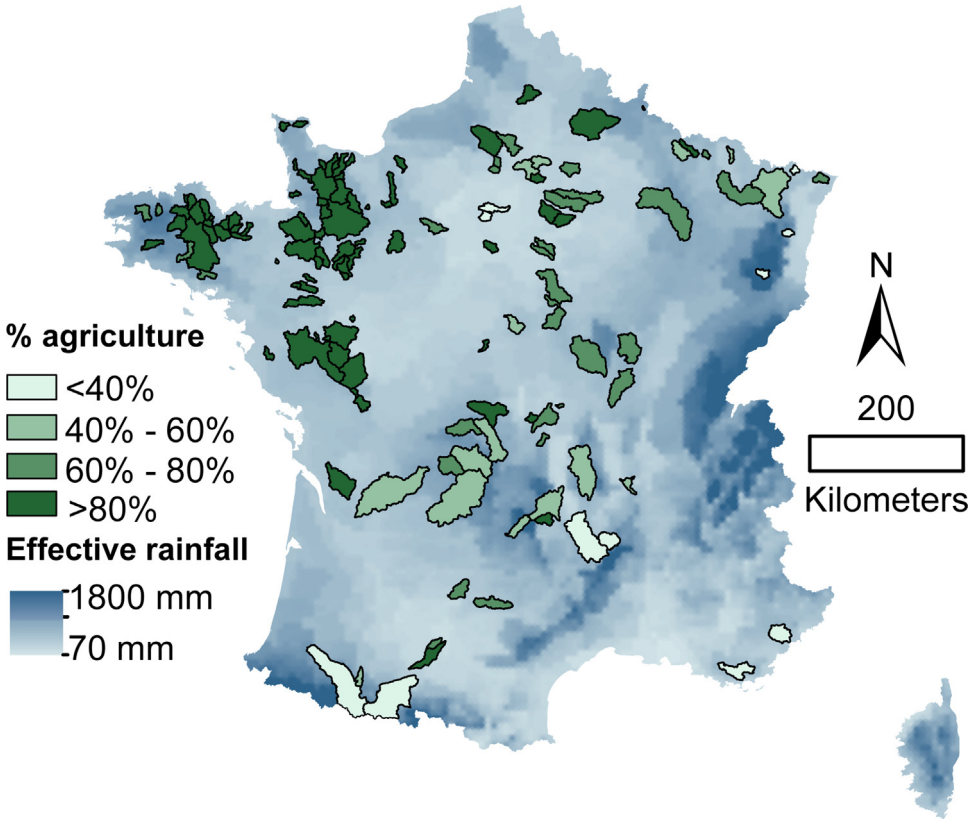

Fig. 1. Percentage of agricultural land use in the 160 catchments selected in France and effective rainfall (Météo France data).

agencies. Catchments were selected based on the ability to estimate mean annual N and P loads for the 2005–2009 period, according to five criteria: (i) presence of water flow and quality stations on the same reach, (ii) ≥1 total-N measurement per month from 2005 to 2009 and ≥100 total-P measurements from 1999 to 2009 to calibrate a rating curve and estimate P load from 2005 to 2009, (iii) <3 missing total-N data points per year, (iv) independence (two nested catchments could not share >20% surface area), and (v) point sources represented <10% of N pressure. Due to difficulties in finding catchments that complied with both N and P criteria, 79 catchments were kept for N- and P-load analysis and 160 for N loads only. Catchment sizes ranged from 10 to 3100 km^2 and cover a wide range of physical and agricultural conditions. Ninety two percent had a Strahler order below 5, but we included 8% of higher-order catchments to increase the variability of river-system size. Mean annual runoff ranged from 70 to 1400 mm and percentage of agricultural land use ranged from 10% to 99% (Fig. 1). Catchment boundaries were delineated with the GeoSAS tool (http://geowww.agrocampus-ouest.fr/web/) using a 50 m DEM.

After calibration, the Nutting models and IFEP indicators were applied to 2210 unmonitored catchments as part of a nation-wide assessment of eutrophication risk. These 2210 unmonitored catchments represent all headwater catchments in the French 'Carthage' database.

2.4.2. Nutrient loads and retention rates

We calculated mean annual specific loads in the 160 observation catchments for the following quality parameters: total-N, nitrate-N, total-P, particulate-P, and dissolved-P. We used water quality data from 2005 to 2009 to remain consistent with the reference years of catchment attributes (Corine Land Cover: 2006, N and P surplus: 2007, point sources: 2007). This time period included wet and dry hydrological years (Gascuel-Odoux et al., 2010; Romero et al., 2013) and was assumed to be short enough to avoid trends in water quality evolution that were not due to interannual climate variability. For N quality variables (total-N and nitrate-N), we used the discharge-weighted concentration method (Moatar and Meybeck, 2007; Moatar et al., 2013) to estimate mean annual loads, i.e. the product of discharge-weighted mean concentration and mean annual discharge. Apparent N retention rate was defined as:

$$\text{Ret } N_{\text{annual}} = 1 - \frac{\text{TNload}}{\text{Nsurplus}} \quad (9)$$

where TNload is the mean annual total-N load [kg N ha^{-1} yr^{-1}] and Nsurplus is the soil N surplus [kg N ha^{-1} yr^{-1}]. N point-source emissions were ignored since they represented a mean (±standard deviation) of only 1.8 ± 9.0% of N surplus.

Total-P load was calculated by summing estimates of dissolved-P load (discharge-weighted concentration method) and particulate-P load (improved rating curve of Delmas et al. (2011)). Among the 160 catchments in the database, we estimated P loads only for 79 due to monitoring that did not meet the previously defined criteria. Annual apparent P retention rate was defined as:

$$\text{Ret } P_{\text{annual}} = 1 - \frac{\text{TPload} - \text{Ppoint}}{\text{Psurplus}} \quad (10)$$

where TPload is the mean annual total-P load in [kg P ha^{-1} yr^{-1}], Psurplus is an estimate of P surplus [kg P ha^{-1} yr^{-1}] and Ppoint is the sum of all point-source emissions of P in the catchment [kg P ha^{-1} yr^{-1}].

Finally, we estimated Si concentrations by considering lithology and base flow index using reference values from Meybeck (1987). Annual Si loads were calculated by multiplying the estimated concentrations by runoff volumes.

Table 1
Catchment attributes and data sources. The last two columns indicate whether the variable was estimated for the entire catchment and/or the river corridor.

Attribute type	Description	Source	Catchment mean	River corridor mean
Diffuse N and P sources	N and P surplus (2007); topsoil P content	Solagro (2010); Delmas et al. (in review)	x	x
N and P point sources	N and P domestic and industrial emissions (2007)	Water agencies	x	
Land use	% artificial surfaces, % agricultural areas, % forest and semi-natural areas, % arable land, % pastures.	Corine Land Cover (2006)	x	x
Soil	Parent material: % Undifferentiated alluvial deposits, % Calcareous rocks, % Clayey materials, % Sandy materials, % Loamy materials,% Detrital formations, % Crystalline rocks and migmatites, % Volcanic rocks; soil texture: % Coarse, % Medium, % Medium fine, % Fine, % Very fine; estimates of hydraulic conductivity and plant-extractable water reserve derived from soil textures using pedotransfer rules of Wosten et al. (2001).	European soil database	x	x
Climate	Effective rainfall, calculated as P-ETP for the months when P-ETP > 0	SAFRAN database, Météo France	x	
Topography, topo-hydrology	Elevation, slope, stream density, topographic wetness index, mean distance to stream	50 m DEM Carthage database Beven and Kirkby (1979)	x	
Connectivity index	Index of Development and Persistence of River networks (IDPR)	Mardhel et al. (2004)	x	x
Catchment size and shape	Catchment size and compacity index (Gravelius)		x	
Stream flow	Annual flow, seasonal flow (four quarters), annual base flow index, seasonal base flow index (four quarters)	French Banque hydro		
River channel geometry	Channel slope, channel depth, channel width, streamflow velocity	ESTIMKART, Pella et al. (2012)	x	
Soil erosion	Annual soil erosion rate	Cerdan et al. (2010)		x

2.4.3. N–P pressure and transfer variables

A total of 110 variables characterising both N–P pressures and transfer risk were estimated for the 160 calibration catchments. Point-source variables included domestic and industrial N and P point-source emissions recorded by public water agencies (pers. comm.) for the 2007 reference year. Diffuse-source variables included estimation of N and P surplus as well as the total-P content in the topsoil. N surplus was calculated by the NOPOLU method (Schoumans et al., 2009; Solagro, 2010) as the sum of agricultural N balance (N inputs–N outputs) and atmospheric deposition. Agricultural N inputs consist of organic/inorganic fertiliser and N fixation; outputs represent the amount of N in harvested crops and grass/fodder. Input and output values were estimated with data from agricultural censuses (e.g., livestock, crops) and crop export coefficients/animal excretion coefficients. NOPOLU disaggregates these statistical agricultural data at administrative levels to the hydrological level using land-cover information. Atmospheric deposition was estimated over the entire area, including non-agricultural land use. Concerning P, an estimate of P surplus at the national level was performed for this study. The methodology was derived from the NOPOLU method, using crop export coefficients and animal excretion coefficients specific to P. Coefficient values used were the same as those of Senthilkumar et al. (2012). Mineral P fertiliser application was estimated by allocating the amount of fertiliser sold in 2005–2007 (statistical trade data) to agricultural areas using land-cover information. Total-P content in the topsoil (0–0.3 m in depth) was estimated with the method of Delmas et al. (in review), to account for P accumulation in soils.

Transfer variables were related to land cover, soil, climate, hydrology, topography, and river-channel geometry (Table 1). The IDPR (Index of Development and Persistence of River networks) connectivity index is a unitless number from 0 to 2000. It is based on comparing a theoretical river network deduced from elevation to the real network: high IDPR values indicate that surface runoff contributes more to water transfer than deep water percolation (Mardhel et al., 2004). In the database, we lumped catchment data into catchment-attribute variables by averaging quantitative variables (e.g. N surplus) according to surface area. Qualitative variables (e.g. land-cover classes) were considered as a percentage of the total surface area. Each variable in the dataset was averaged for the entire catchment and for the surface area in the river corridor, defined as a 200 m-wide zone on both sides of the streams. Soil variables where considered not only as average values in the catchments, but also in interaction with land-use (e.g. variable % sandy soils on arable land use). River corridors and land-cover/soil interactions are known to influence nutrient transfer/retention within catchments (Curie et al., 2011; Mengistu et al., 2014).

3. Results

3.1. N and P transfer/retention

The catchment database displayed high variability in nutrient loads: observed specific loads for total-N ranged from 4 to 59 kg N ha^{-1} yr^{-1} (mean = 18 ± 11 kg N ha^{-1} yr^{-1}) and observed total-P specific loads ranged from 0.1 to 1.4 kg P ha^{-1} yr^{-1} (mean = 0.5 ± 0.3 kg N ha^{-1} yr^{-1}). Nitrate-N was the dominant form of N (mean = 77 ± 14%), whereas P loads were dominated by particulate forms (mean = 65 ± 14%). The particulate-P:total-P load ratio increased with increasing Strahler order of the catchment (Fig. 2) due to biochemical transformation of dissolved-P into particulate-P in the river network. The Nutting-P model empirically integrates the underlying processes in the B_{DP} parameter.

Apparent retentions of N and P differed greatly, i.e. 53 ± 24% of N surplus versus 95 ± 29% of P surplus. Four of the 160 catchments exhibited a negative apparent N retention rate, either due to errors in N surplus or N load estimates or because these catchments were not at equilibrium (i.e. N loads determined by past N surplus stored within the catchment). Twelve out of 79 catchments exhibited apparent P retention rates outside the [0,1] interval, either because estimated P surpluses were negative or because calculated total-P loads exceeded P sources in the catchments.

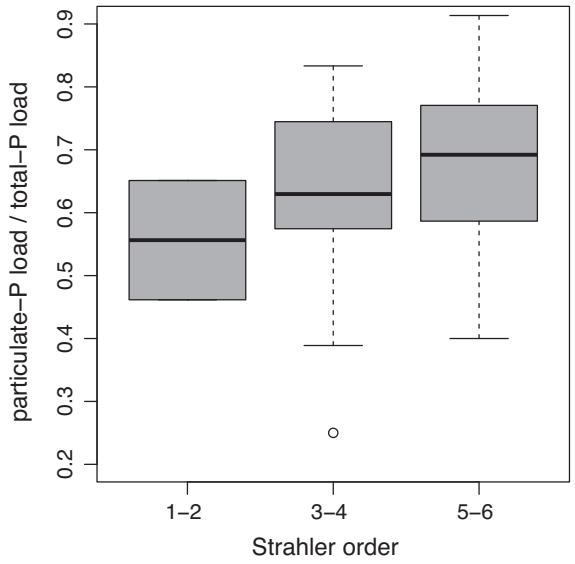

Fig. 2. Boxplots of annual proportion of particulate-P out of total-P in catchments as a function of Strahler order.

3.2. Relations between N and P transfer/retention and catchment attributes

Firstly, relations between N and P transfer/retention and catchment attributes were analysed variable per variable. Observed N loads increased with increasing percentage of agricultural land use (Fig. 3a). Below 60% agricultural land use, annual nitrate-N loads generally remained below 10 kg N ha^{-1} yr^{-1} (mean = 6.4 ± 3.8 kg N ha^{-1} yr^{-1}); above 60% agricultural land use, variability in the nitrate-N loads increased, ranging from 2.5 to 52.0 kg N ha^{-1} yr^{-1} (mean = 16.5 ± 10.2 kg N ha^{-1} yr^{-1}). The large scatter observed for N load when agricultural land use exceeded 60% was refined when considering the N surplus (Fig. 3c); the slope of the TNload = $a \times$ Nsurplus line equals 0.47, which is consistent with the 53% mean apparent retention. Forty eight percent of the variance was explained by this simple regression equation. The annual N retention (i.e. 1 − regression coefficient in Fig. 3c) was a negative function of annual runoff (Fig. 3e).

Such a clear trend was not observed between P loads and percentage of agricultural land use (Fig. 3b). P load is also a positive function of P surplus, but the linear regression fitted to the data explains only 11% of the variance (Fig. 3d). No apparent relation was visible between annual P retention and annual runoff (Fig. 3f).

Secondly, an HCPC multivariate analysis was performed to cluster catchments according to their N–P load features (Fig. 4). According to the PCA, total-N loads were positively correlated with nitrate-N:total-N ratios, i.e. nitrate was the dominant N form in catchments with high N loads. High N loads were associated with high runoff values and high N surplus (Fig. 4a). Total-P loads were negatively correlated with dissolved-P:total-P ratios, i.e. particulate P was the dominant P form in catchments with high P loads. High total-P loads were associated with high runoff and high IDPR values and negatively correlated with the base flow index. Conversely, the dissolved-P:total-P ratio was positively correlated with the base flow index. This suggests that P is mainly transferred to streams as particulate P via superficial runoff pathways in catchments where the connectivity between land and water is high. High IDPR and high runoff values characterise highly connected catchments. The least flashy catchments, characterised by a higher base flow index, had a larger proportion of dissolved-P in the total-P loads but transferred less P. N was transferred to streams mainly as nitrate-N, especially in catchments with high N surplus and high runoff. The IDPR index of surface connectivity was less influential for N than for P, which suggests that N was delivered to streams mainly via base flow transport pathways.

The HCPC resulted in three catchment clusters (Fig. 4b). Cluster 1 included catchments with high N and P loads, a relatively high percentage of nitrate-N and a low percentage of dissolved-P; they had low base-flow indices and high runoff values. Cluster 2 included catchments with low N and P loads and a relatively high percentage of dissolved forms; they had high base-flow indices and low runoff values. Cluster 3 included a greater variety of catchments, characterised by high P loads and low N loads. Hence, catchments can be prone to N or P problems depending on the cluster to which they belong.

3.3. Fate of N and P loads by statistical modelling

3.3.1. Load estimation with the Nutting model

The variables retained by the selection procedure with Nutting further identify which catchment attributes control N and P transfer/retention. Table 2 summarises optimal parameter values, standard errors and 95% bootstrap confidence interval. For the nitrate-N model, the basin transfer factor B_{DN} included effective rainfall and the percentage of forest and semi-natural areas in the catchment. The latter variable, which was not included in the original Nutting-N model (Dupas et al., 2013), reduced RMSEP from 6.3 to 5.9 kg N ha^{-1} yr^{-1}. It corresponds to an R^2 as high as 0.66 for specific nitrate load and 0.84 for global nitrate load estimation in a leave-one-out cross-validation. Bootstrap estimates of nitrate-N load ranged from −10% to +9% of the mean model prediction. For the total-N model, the basin transfer factor B_{TN} included only effective rainfall. R^2 equalled 0.59 for specific total-N load and 0.85 for the global load. Bootstrap estimates of total-N load ranged from −12% to +10% of the mean model prediction.

The basin transfer factors B_{DP} and B_{TP} were a function of the IDPR index for both dissolved-P and total-P models. R^2 equalled 0.45 for the dissolved-P model and 0.40 for the total-P model when predicting specific P load in the leave-one-out cross-validation. This corresponds to an R^2 as high as 0.83 and 0.70 when predicting the global load of dissolved-P and total-P, respectively. Bootstrap estimates of dissolved-P load ranged from −18% to +15% of the mean model prediction. Bootstrap estimates of total-P load ranged from −13% to +12% of the mean model prediction.

The variable selection procedure with Nutting did not result in the inclusion of any 'spatially-defined' variables in Nutting-N or -P. This suggests that lumped variables were better predictor variables than those defined within the river corridor or within specific soil types. Application of the Nutting-N and -P models on 2210 headwater catchments allowed us to estimate the contribution of agricultural diffuse emissions to N and P loads (Fig. 5). Diffuse agricultural sources represented 97% of total total-N load, on average, i.e. 12.4 ± 7.1 kg N ha^{-1} yr^{-1}. In contrast, they represented only 46% of total-P load, on average, i.e. 0.31 ± 0.14 kg P ha^{-1} yr^{-1}.

3.3.2. Eutrophication risk

N loads exceeded Si loads in 90% of the 2210 headwater catchments (i.e. N-IFEP > 0), which indicates that P availability generally controls the potential risk of eutrophication related to nutrients. Hence, estimated eutrophication risk was highly sensitive to assumptions about the bioavailability of particulate P. Fig. 6 shows the distribution of min (N-IFEP, P-IFEP), whose value indicates eutrophication risk when it exceeds 0, under three assumptions: when assuming that all P forms were bioavailable, 63% of the catchments were potentially at risk; this percentage dropped to 45% and 26% when assuming that 30% particulate P + dissolved P and only dissolved P forms were bioavailable, respectively. The greater difference in density functions on the right side indicates that

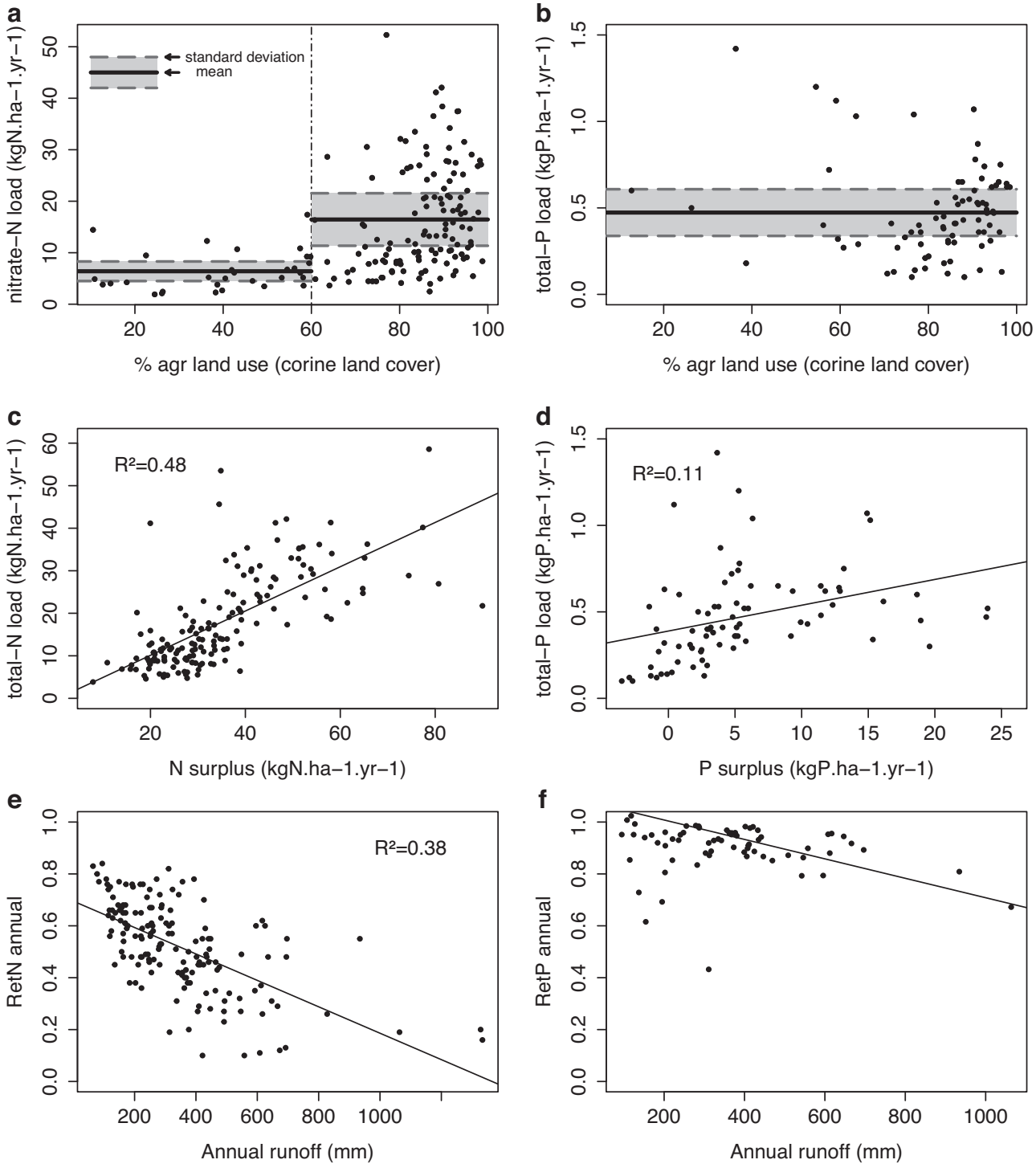

Fig. 3. Nutrient load and apparent retention as a function of catchment attributes: (a, b) land use, (c, d) nutrient surplus and (e, f) annual runoff.

uncertainties about eutrophication risk were highest in catchments with high P loads because they had a high percentage of particulate-P. Thus, they were highly sensitive to the fraction of particulate-P assumed to be bioavailable.

4. Discussion

4.1. Catchment attributes controlling nutrient transfer/retention

Both multivariate analysis and the variable selection procedure with Nutting indicate that N and P loads were more directly related to variables describing agricultural nutrient pressure, i.e. N and P surplus and topsoil P, than to land-use classes. N surplus and topsoil P content are relevant variables for describing agricultural pressures at large scales, provided that enough agricultural and soil data exist to estimate them in some detail (Windolf et al., 2011, 2012). The rate of N transfer is controlled mostly by effective rainfall, as suggested by the relation between annual runoff and apparent N retention rate. P transfer rate was more highly correlated with the IDPR index, a qualitative indicator of connectivity via surface or subsurface runoff. This agrees with the common understanding of N and P transfers: P is transported mostly via

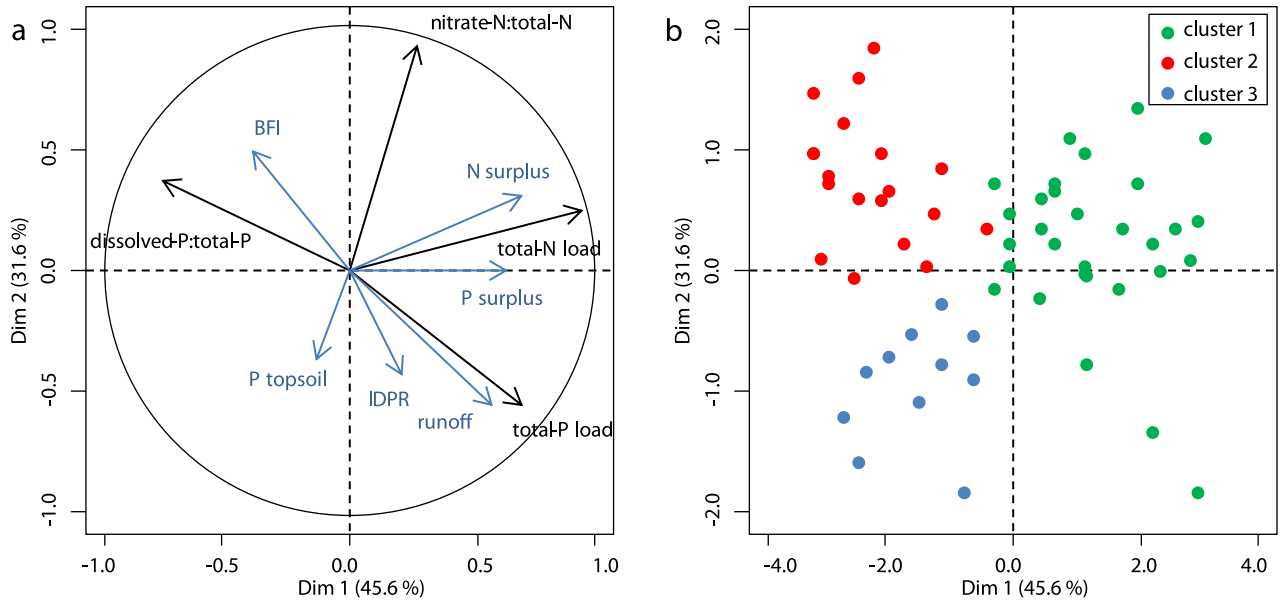

Fig. 4. Hierarchical Clustering on Principal Components (HCPC). (a) Variable factor map with 4 nutrient-load and nutrient-ratio variables (total-N load, total-P load, nitrate-N:total-N ratio, dissolved-P:total-P ratio) projected onto a factorial plan. Illustrative variables (in blue) were projected onto the same factorial plan but did not contribute to construction of the axes. (b) individual/cluster map of the Principal Component Analysis. (For interpretation of reference to color in this figure legend, the reader is referred to the web version of this article.)

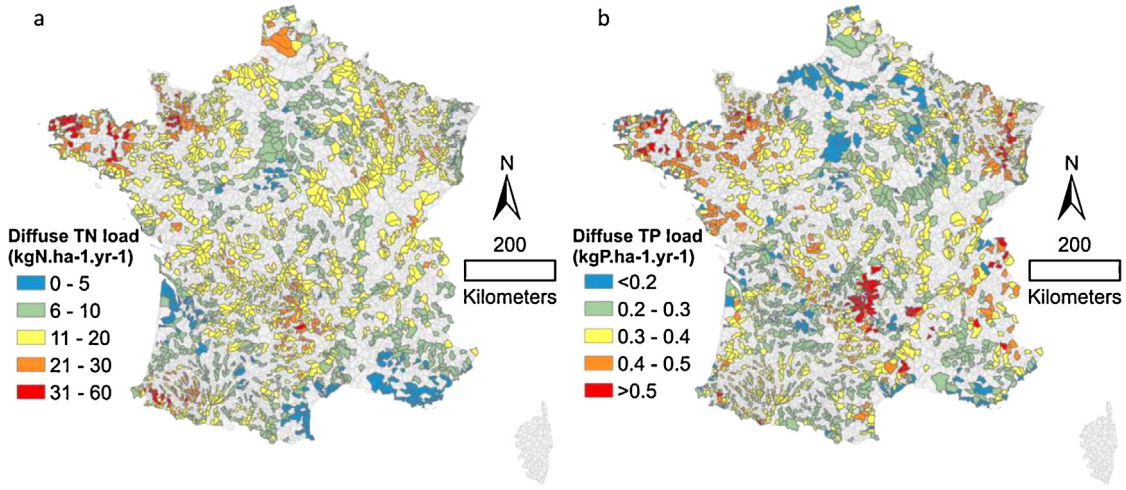

Fig. 5. Application of Nutting models on 2210 headwater catchments of the Carthage database. (a) total-N load of agricultural origin; (b) total-P load of agricultural origin.

surface or subsurface runoff and erosion from a P stock which has accumulated over years in soils; N is transported through annual leaching of N surplus via deeper transport pathways (Mellander et al., 2012; Parn et al., 2012). However, the fact that the proportion of particulate P forms increases with increasing stream order suggests that high particulate-P:total-P load ratios do not result only from erosion dominating P transfer but from stream processes that convert dissolved-P into particulate-P along the stream network

Table 2
Parameter estimates from Nutting-N and Nutting-P models. αi refer to the parameters included in the basin transfer factor and αj refer to the parameter included in the river-transfer factors.

	Model parameters	Units	Estimate	Standard error	*P* value	Bootstrap 95% CI lower bound	Bootstrap 95% CI upper bound
(a) Nutting-nitrate-N	αi (1/effective rainfall)	mm	1.45E+02	3.90E+01	2.72E-04	5.69E+01	2.73E+02
	αi (% forest and semi-natural areas)	–	1.05E−02	2.48E−03	3.53E−05	6.38E−03	1.55E−02
(b) Nutting-total-N	αj	s^{-1} ha m	4.06E-03	9.70E-04	4.82E-05	7.19E-04	5.99E-03
	αi (1/effective rainfall)	mm	1.43E+02	3.59E+01	1.05E-05	6.50E+01	2.47E+02
(c) Nutting-dissolved-P	αj	s^{-1} ha m	3.48E−03	9.55E−04	3.67E−04	7.80E−04	5.34E−03
	αi (1/IDPR)	-	1.22E+03	1.61E+02	6.46E−11	7.96E+02	1.48E+03
(d) Nutting-total-P	αj	s^{-1} ha m	6.17E−03	1.19E−03	1.53E−06	4.20E−03	9.66E−03
	αi (1/IDPR)	–	3.76E+02	6.16E+01	3.74E−08	2.66E+02	4.78E+02

* Index of Development and Persistence of River network.

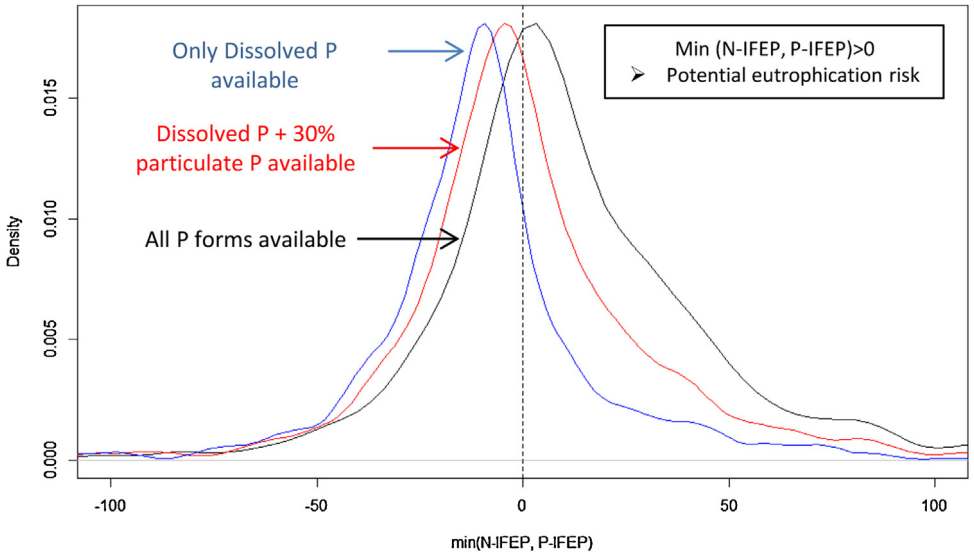

Fig. 6. Density functions of eutrophication risk min(N-IFEP, P-IFEP) in 2210 headwater catchments under 3 hypotheses.

(Kronvang et al., 2012, 2013). In this respect, the present statistical approach generalises the knowledge acquired from process-based studies based on observation of individual catchments.

To our knowledge, this study is the first attempt to consider the spatial organisation of the landscape in a mass-balance model. Whereas all catchment attributes were lumped variables estimated over the entire surface area in previous applications of mass-balance models, we included variables defined within river corridors, such as land use and IDPR. We also attempted to characterise not only average soils in the catchment but also their interaction with agricultural land use. None of these 'spatially-estimated' variables, however, helped to predict nutrient transfers more accurately than the corresponding 'lumped-estimated' variables. Several reasons can explain this negative result: (i) the resolution of national-level GIS datasets is too low for such a spatial approach; (ii) great uncertainties exist in the estimation of catchment attributes that explain most of the variance in nutrient transfer (e.g. N surplus), which prevents identification of the effect of secondary variables; and (iii) the assumption of a steady-state catchment is not correct, which induces imprecision and prevents identification of effects of secondary variables. Previous attempts to include landscape metrics based on proximity to the stream in multiple-regression models of water chemistry generally have not been successful (Jones et al., 2001; Zampella et al., 2007), except that of Johnson et al. (1997), in which attributes defined in upland ecotones explained total-P and suspended sediment loads better than lumped attributes.

The negative result of landscape metrics in Nutting-N and–P might be overcome by: (i) improving estimation and spatial resolution of all variables (e.g. by using recent remote-sensing data), (ii) developing new landscape metrics (e.g. by identifying critical source areas) (Gascuel-Odoux et al., 2011; Heathwaite et al., 2005) or topographic metrics (Creed and Beall, 2009; Mengistu et al., 2014), and (iii) identifying interfaces between source areas and buffer zones. Despite this, the fact that a lumped estimate of N surplus/topsoil P explained most of the variance in N and P loads highlights that reducing nutrient pressures, rather than reorganising agricultural landscapes, is the most powerful mechanism for decreasing nutrient transfer. Nonetheless, spatial organisation of the landscape and buffer zones remain relevant mitigation techniques when considering cost-effectiveness.

Nutting-P was less accurate than Nutting-N with lumped variables, which suggests that landscape connectivity is more crucial for P than for N (Schoumans et al., 2014). The IDPR index was useful for describing hydrology-related connectivity, but landscape-connectivity metrics adapted for a large spatial scale must be created. Potential improvement of Nutting-P may come from adapting distributed suspended sediment models developed for large scales (e.g. Delmas et al., 2009; Van Rompaey et al., 2001; Zhang, 2010).

4.2. Limits of mass-balance models in identifying processes

Mass-balance models such as Nutting are sometimes called hybrid statistical and process-based models because, despite their statistical nature, their structure reflects the understanding of dominant processes controlling nutrient loads. It is thus tempting to use these models to quantify how the apparent retention rate of nutrients is divided between terrestrial and aquatic compartments of catchments. This must be done with caution: equifinality in the calibration of the parameters included in Nutting's R and B factors might result in inaccurate estimates of the proportion of terrestrial and aquatic retention (Beven, 2006).

Schwarz et al. (2011) have imposed cross-regional constraints on SPARROW parameters to limit their variation between regionally calibrated SPARROW models. By doing so, their regionalised models were consistent with each other but do not ensure consistency with process-based models. In this study, we calibrated Nutting with an iterative algorithm that optimised parameter values to fit the data. As initial parameter values might influence the calibration when the algorithm converges to a local minimum, we chose an initial parameter value in the R factor to match the in-stream denitrification rate reported by Kronvang et al. (2004). Finally, the version of Nutting used in this study is more parsimonious than the original (Dupas et al., 2013) to avoid over-parameterisation. One to three calibrated parameters were enough to fit the data in a leave-one-out cross-validation with an R^2 ranging from 0.40 to 0.66 for specific N and P loads and 0.70–0.85 for global N and P loads.

The results of the mass-balance model are based on a steady-state hypothesis, i.e. the assumption of no temporary retention of N and P in any compartment of the catchment during the pluri-annual study period. There has been much discussion about whether some aquifers are temporary N sinks that delay N release or permanent sinks due to denitrification (Van Breemen et al., 2002). The fact that effective rainfall controls a catchment's rate of N transfer may be

interpreted as a transit-time effect, which supports the hypothesis of temporary retention, but longer transit time might also result in longer contact times between N and denitrifying conditions, which supports the hypothesis of permanent retention.

Similarly, the hypothesis of steady-state P retention in river systems (i.e. retention and release balancing each other on a pluri-annual basis) is contradicted by budget studies performed on large catchments (Jarvie et al., 2011; Nemery et al., 2005). A P budget performed on the Marne catchment (12,000 km^2) estimated P retention of 15–30% of the total-P input on a pluri-annual basis (Nemery and Garnier, 2007; Nemery et al., 2005). Jarvie et al. (2011), using an extended end-member mixing analysis, estimated 48% retention of total-P in the Sandusky River (3200 km^2) and 14% in the Thames River at Wallingford (3500 km^2). However, the headwater catchments included in our dataset were generally smaller, which led us to ignore permanent retention of total-P through overbank floodplain sedimentation.

4.3. The risk of eutrophication in freshwaters

The IFEP indicators represent a simple way to estimate the potential risk of eutrophication and determine which nutrient limits algal growth, based on 'external' nutrient loadings. The actual functioning of freshwater ecosystems such as lakes is more complex than what could be accounted for in this paper. 'Internal' loadings from anoxic sediments can contribute a large proportion of bioavailable P in lakes and atmospheric fixation by planktonic bacteria can represent a significant source of N (Schindler, 2012). Furthermore, the IFEP used in this study were simplified indicators of nutrient-related potential eutrophication but did not include the effect of other crucial environmental factors, such as light and temperature. Hence, they might fail to predict actual eutrophication, but they remain a useful means for managers to estimate potential eutrophication risk based on nutrient loadings from 'external' anthropogenic sources.

Because national water quality databases generally do not include an estimate of the bioavailable fraction of P on particles, we tested three hypotheses: all P forms bioavailable, dissolved-P + 30% of particulate-P bioavailable, and only dissolved-P bioavailable. We found that estimated eutrophication risk was highly sensitive to these hypotheses. Our recommendation to reduce this uncertainty is to measure P bioavailability in water-quality monitoring programmes, especially in catchments where uncertainty in IFEP results is high. Despite these uncertainties, the IFEP indicators showed that P availability generally controlled eutrophication risk, as N exceeded Si in 90% of headwaters. In this way, our results rather confirm the observations from long-term, whole-system experiments, which have shown that eutrophication in lakes was generally controlled by P availability (Schindler et al., 2008; Schindler, 2012). However, exceptions can exist, as highlighted by the 10% headwater catchments where N was limiting eutrophication. Dual-nutrient reduction strategies can thus be relevant to limit eutrophication in a minority of lakes (Conley et al., 2009). Because the ultimate destination of N and P riverine loads is coastal and marine ecosystems, i.e. N limited ecosystems (Garnier et al., 2010; Howarth and Marino, 2006; Conley et al., 2009), management strategies to reduce both N and P loadings are recommended.

5. Conclusion

We developed a methodology to address the issue of N and P pressure/impact assessment in contexts of scarce data. The methodology consists of (i) a mass-balance model to estimate diffuse N and P transfer/retention and identify the landscape attributes controlling them and (ii) a set of indicators to assess the risk of freshwater eutrophication resulting from excessive nutrient delivery. The Nutting model describes agricultural pressures in greater detail than previous statistical models, thanks to national level data on N and P surplus and P content of the topsoil. No effects of the spatial distribution of agricultural landscapes could be highlighted with this approach. We hypothesised that this was due to inaccurate estimation of variables that explained most of the variability in nutrient loads (e.g. N surplus), which masked the effects of secondary variables. The methodology developed provides a means for river basin district managers to identify the catchments at risk of eutrophication at regional or national level and informs whether nutrient control measures should be directed towards point sources or diffuse sources. Because conclusions drawn from the IFEP indicator were highly sensitive to P availability, we recommend introducing P bioavailability tests in water-quality monitoring programmes, especially when uncertainties in IFEP results are high.

Acknowledgments

This work was funded by ONEMA, the French National Agency for Water and Aquatic Environments. We would like to thank Catherine Grimaldi for her advice in writing this paper and Michelle and Michael Corson for correcting its English style.

References

Alexander, R.B., Boyer, E.W., Smith, R.A., Schwarz, G.E., Moore, R.B., 2007. The role of headwater streams in downstream water quality. J. Am. Water Resour. Assoc. 43, 41–59, http://dx.doi.org/10.1111/j. 1752-1688.2007.00005.x.

Arnold, J.G., Srinivasan, R., Muttiah, R.S., Williams, J.R., 1998. Large area hydrologic modeling and assessment – Part 1: model development. J. Am. Water Resour. Assoc. 34, 73–89, http://dx.doi.org/10.1111/j. 1752-1688.1998.tb05961.

Aubert, A.H., Gascuel-Odoux, C., Gruau, G., Akkal, N., Faucheux, M., Fauvel, Y., Grimaldi, C., Hamon, Y., Jaffrézic, A., Lecoz-Boutnik, M., Molénat, J., Petitjean, P., Ruiz, L., Merot, P., 2013. Solute transport dynamics in small, shallow groundwater-dominated agricultural catchments: insights from a high-frequency, multisolute 10 yr-long monitoring study. Hydrol. Earth Syst. Sci. 17, 1379–1391, http://dx.doi.org/10.1021/es403723r.

Beaujouan, V., Durand, P., Ruiz, L., Aurousseau, P., Cotteret, G., 2002. A hydrological model dedicated to topography-based simulation of nitrogen transfer and transformation: rationale and application to the geomorphology–denitrification relationship. Hydrol. Process. 16, 493–507, http://dx.doi.org/10.1002/hyp.327.

Beven, K., 2006. A manifesto for the equifinality thesis. J. Hydrol. 320, 18–36, http://dx.doi.org/10.1016/j.jhydrol.2005.07.007.

Beven, K.J., Kirkby, M.J., 1979. A physically based, variable contributing area model of basin hydrology. Hydrol. Sci. Bull. 24, 43–69.

Billen, G., Garnier, J., 2007. River basin nutrient delivery to the coastal sea: assessing its potential to sustain new production of non-siliceous algae. Mar. Chem. 106, 148–160, http://dx.doi.org/10.1016/j.marchem.2006.12.017.

Bouraoui, F., Grizzetti, B., 2011. Long term change of nutrient concentrations of rivers discharging in European seas. Sci. Total Environ. 409, 4899–4916, http://dx.doi.org/10.1016/j.scitotenv.2011.08.015.

Bouwman, A.F., Bierkens, M.F.P., Griffioen, J., Hefting, M.M., Middelburg, J.J., Middelkoop, H., Slomp, C.P., 2013. Nutrient dynamics, transfer and retention along the aquatic continuum from land to ocean: towards integration of ecological and biogeochemical models. Biogeosciences 10, 1–22, http://dx.doi.org/10.5194/bg-10-1-2013.

Boyer, E.W., Alexander, R.B., Parton, W.J., Li, C.S., Butterbach-Bahl, K., Donner, S.D., Skaggs, R.W., Del Gross, S.J., 2006. Modeling denitrification in terrestrial and aquatic ecosystems at regional scales. Ecol. Appl. 16, 2123–2142.

Burt, T.P., Pinay, G., 2005. Linking hydrology and biogeochemistry in complex landscapes. Progr. Phys. Geogra. 29, 297–316, http://dx.doi.org/10.1191/0309133305pp450ra.

Carpenter, S.R., Caraco, N.F., Correll, D.L., Howarth, R.W., Sharpley, A.N., Smith, V.H., 1998. Nonpoint pollution of surface waters with phosphorus and nitrogen. Ecol. Appl. 8, 559–568, http://dx.doi.org/10.2307/2641247.

Cerdan, O., Govers, G., Le Bissonnais, Y., Van Oost, K., Poesen, J., Saby, N., et al., 2010. Rates and spatial variations of soil erosion in Europe: a study based on erosion plot data. Geomorphology 122, 167–177, http://dx.doi.org/10.1016/j.geomorph.2010.06.011.

Conley, D.J., Paerl, H.W., Howarth, R.W., Boesch, D.F., Seitzinger, S.P., Havens, K.E., Lancelot, C., Likens, G.E., 2009. ECOLOGY controlling eutrophication: nitrogen and phosphorus. Science 323, 1014–1015, http://dx.doi.org/10.1126/science.1167755.

Creed, I.F., Beall, F.D., 2009. Distributed topographic indicators for predicting nitrogen export from headwater catchments. Water Resour. Res. 45, W10407, http://dx.doi.org/10.1029/2008wr007285.
Curie, F., Ducharne, A., Bendjoudi, H., Billen, G., 2011. Spatialization of denitrification by river corridors in regional-scale watersheds: case study of the Seine river basin. Phys. Chem. Earth 36, 530–538, http://dx.doi.org/10.1016/j.pce.2009.02.004.
Delmas, M., Cerdan, O., Cheviron, B., Mouchel, J.M., 2011. River basin sediment flux assessments. Hydrol. Process. 25, 1587–1596, http://dx.doi.org/10.1002/hyp.7920.
Delmas, M., Cerdan, O., Mouchel, J-M., Garcin, M., 2009. A method for developing a large-scale sediment yield index for European river basins. J. Soils Sedim. 9, 613–626, http://dx.doi.org/10.1007/s11368-009-0126-5.
Delmas, M., Saby, N., Gascuel-Odoux, C., Arrouays, D., Lemercier, B., Pellerin, S. Explaining and mapping total phosphorus content in the topsoil in France. Soil use and management, in review.
Demars, B.O.L., Harper, D.M., Pitt, J.A., Slaughter, R., 2005. Impact of phosphorus control measures on in-river phosphorus retention associated with point source pollution. Hydrol. Earth Syst. Sci. 9, 43–55.
Dorioz, J.M., Trevisan, D., 2013. Le transfert diffus du phosphore dans les bassins agricoles: ordres de grandeur, mécanismes, maîtrise. Revue EAT thématique, 27–47.
Dupas, R., Curie, F., Gascuel-Odoux, C., Moatar, F., Delmas, M., Parnaudeau, V., Durand, P., 2013. Assessing N emissions in surface water at the national level: comparison of country-wide vs regionalized models. Sci. Total Environ. 443, 152–162, http://dx.doi.org/10.1016/j.scitotenv.2012.10.011.
Ferrant, S., Oehler, F., Durand, P., Ruiz, L., Salmon-Monviola, J., Justes, E., et al., 2011. Understanding nitrogen transfer dynamics in a small agricultural catchment: comparison of a distributed (TNT2) and a semi distributed (SWAT) modeling approaches. J. Hydrol. 406, 1–15, http://dx.doi.org/10.1016/j.jhydrol.2011.05.026.
Folton, N., Lavabre, J. 2006. Regionalization of a monthly rainfall-runoff model for the southern half of France based on a sample of 880 gauged catchments. In: Andréassian, V., Hall, A., Chahinian, N., Schaake, J. (Eds.). Large sample basin experiments for hydrological model parameterization: results of the model parameter experiment (MOPEX). vol. 307, IAHS Publication, pp. 264-277. ISBN 1978-1-901502-73-2, Record Number 20073200668.
Garnier, J., Beusen, A., Thieu, V., Billen, G., Bouwman, L., 2010. N:P:Si nutrient export ratios and ecological consequences in coastal seas evaluated by the ICEP approach. Global Biogeochem. Cycles 24, GB0A05, http://dx.doi.org/10.1029/2009gb003583.
Gascuel-Odoux, C., Aurousseau, P., Durand, P., Ruiz, L., Molenat, J., 2010. The role of climate on inter-annual variation in stream nitrate fluxes and concentrations. Sci. Total Environ. 408, 5657–5666, http://dx.doi.org/10.1016/j.scitotenv.2009.05.003.
Gascuel-Odoux, C., Aurousseau, P., Doray, T., Squividant, H., Macary, F., Uny, D., Grimaldi, C., 2011. Incorporating landscape features to obtain an object-oriented landscape drainage network representing the connectivity of surface flow pathways over rural catchments. Hydrol. Process. 25, 3625–3636, http://dx.doi.org/10.1002/hyp.8089.
Grizzetti, B., Bouraoui, F., Aloe, A., 2012. Changes of nitrogen and phosphorus loads to European seas. Global Change Biol. 18, 769–782, http://dx.doi.org/10.1111/j.1365-2486.2011.02576.x.
Grizzetti, B., Bouraoui, F., De Marsily, G., 2008. Assessing nitrogen pressures on European surface water. Global Biogeochem. Cycles 2, 2, http://dx.doi.org/10.1029/2007gb003085.
Haygarth, P.M., Condron, L.M., Heathwaite, A.L., Turner, B.L., Harris, G.P., 2005. The phosphorus transfer continuum: linking source to impact with an interdisciplinary and multi-scaled approach. Sci. Total Environ. 344, 5–14, http://dx.doi.org/10.1016/j.scitotenv.2005.02.001.
Heathwaite, A.L., Quinn, P.F., Hewett, C.J.M., 2005. Modelling and managing critical source areas of diffuse pollution from agricultural land using flow connectivity simulation. J. Hydrol. 304, 446–461, http://dx.doi.org/10.1016/j.jhysrol.2004.07.043.
Howarth, R.W., Marino, R., 2006. Nitrogen as the limiting nutrient for eutrophication in coastal marine ecosystems: evolving views over three decades. Limnol. Oceanogr. 51, 364–376.
Husson, F., Josse, J., Pagès, J., 2010. Principal component methods–hierarchical clustering - partitional clustering: why would we need to choose for visualizing data? Technical Report–Agrocampus.
Jarvie, H.P., Neal, C., Withers, P.J.A., Baker, D.B., Richards, R.P., Sharpley, A.N., 2011. Quantifying phosphorus retention and release in rivers and watersheds using extended end-member mixing analysis (E-EMMA). J. Environ. Qual. 40, 492–504, http://dx.doi.org/10.2134/jeq2010.0298.
Johnes, P.J., 1996. Evaluation and management of the impact of land use change on the nitrogen and phosphorus load delivered to surface waters: the export coefficient modelling approach. J. Hydrol. 183, 323–349.
Johnson, L.B., Richards, C., Host, G.E., Arthur, J.W., 1997. Landscape influences on water chemistry in Midwestern stream ecosystems. Freshw. Biol. 37, 193–208, http://dx.doi.org/10.1046/j.1365-2427.1997.d01-539.x.
Jones, K.B., Neale, A.C., Nash, M.S., Van Remortel, R.D., Wickham, J.D., Riitters, K.H., et al., 2001. Predicting nutrient and sediment loadings to streams from landscape metrics: a multiple watershed study from the United States Mid-Atlantic Region. Landsc. Ecol. 16, 301–312, http://dx.doi.org/10.1023/a:1011175013278.
Kronvang, B., Andersen, H.E., Larsen, S.E., Audet, J., 2013. Importance of bank erosion for sediment input, storage and export at the catchment scale. J. Soils Sedim. 13 (1), 230–241, http://dx.doi.org/10.1007/s11368-012-0597-7.
Kronvang, B., Audet, J., Baattrup-Pedersen, A., Jensen, H.S., Larsen, S.E., 2012. Phosphorus load to surface water from bank erosion in a Danish lowland river basin. J. Environ. Qual. 41 (2), 304–313, http://dx.doi.org/10.2134/jeq2010.0434.
Kronvang, B., Bechmann, M., Pedersen, M.L., Flynn, N., 2003. Phosphorus dynamics and export in streams draining micro-catchments: development of empirical models. J. Plant Nutr. Soil Sci. 166 (4), 469–474.
Kronvang, B., Hezlar, J., Boers, P., Jensen, J.P., Behrendt, H., Anderson, T., et al., 2004. Nutrient retention handbook. In: Software Manual for EUROHARP-NUTRET and Scientific Review on Nutrient Retention, EUROHARP Report 9-2004, NIVA Report SNO 4878/2004, Oslo, Norway, p. 103.
Lassaletta, L., Garcia-Gomez, H., Gimeno, B.S., Rovira, J.V., 2010. Headwater streams: neglected ecosystems in the EU water framework directive implications for nitrogen pollution control. Environ. Sci. Policy 13, 423–433, http://dx.doi.org/10.1016/j.envsci.2010.04.005.
Mardhel, V., Frantar, P., Uhan, J., Mio, A., 2004. Index of development and persistence of the river networks as a component of regional groundwater vulnerability assessment in Slovenia. In: Int. Conf. Groundwater Vulnerability Assessment and Mapping, Ustron, Poland.
Mellander, P.-E., Melland, A.R., Jordan, P., Wall, D.P., Murphy, P.N.C., Shortle, G., 2012. Quantifying nutrient transfer pathways in agricultural catchments using high temporal resolution data. Environ. Sci. Policy 24, 44–57, http://dx.doi.org/10.1016/j.envsci.2012.06.004.
Mengistu, S.G., Creed, I.F., Webster, K.L., Enanga, E., Beall, F.D., 2014. Searching for similarity in topographic controls on carbon, nitrogen and phosphorus export from forested headwater catchments. Hydrol. Process. 28, 3201–3216, http://dx.doi.org/10.1002/hyp.9862.
Meybeck, M., 1987. Global chemical weathering of surficial rocks estimated from river dissolved loads. Am. J. Sci. 287, 401–428.
Moatar, F., Meybeck, M., 2007. Riverine fluxes of pollutants: towards predictions of uncertainties by flux duration indicators. Comptes Rendus Geoscience 339, 367–382, http://dx.doi.org/10.1016/j.crte.2007.05.001.
Moatar, F., Meybeck, M., Raymond, S., Birgand, F., Curie, F., 2013. River flux uncertainties predicted by hydrological variability and riverine material behaviour. Hydrol. Process. 27, 3535–3546, http://dx.doi.org/10.1002/hyp.9464.
Montreuil, O., Merot, P., Marmonier, P., 2010. Estimation of nitrate removal by riparian wetlands and streams in agricultural catchments: effect of discharge and stream order. Freshw. Biol. 55, 2305–2318, http://dx.doi.org/10.1111/j.1365-2427.2010.02439.x.
Neal, C., Reynolds, B., Norris, D., Kirchner, J.W., Neal, M., Rowland, P., et al., 2011. Three decades of water quality measurements from the Upper Severn experimental catchments at Plynlimon, Wales: an openly accessible data resource for research, modelling, environmental management and education. Hydrol. Process. 25, 3818–3830, http://dx.doi.org/10.1002/hyp.8191.
Nemery, J., Garnier, J., 2007. Origin and fate of phosphorus in the Seine watershed (France): agricultural and hydrographic P budgets. J. Geophys. Res.: Biogeosci. 112, G03012, http://dx.doi.org/10.1029/2006jg000331.
Nemery, J., Garnier, J., Morel, C., 2005. Phosphorus budget in the Marne Watershed (France): urban vs. diffuse sources, dissolved vs. particulate forms. Biogeochemistry 72, 35–66, http://dx.doi.org/10.1007/s10533-004-0078-1.
Parn, J., Pinay, G., Mander, U., 2012. Indicators of nutrients transport from agricultural catchments under temperate climate: a review. Ecol. Indic. 22, 4–15.
Pella, H., Lejot, J., Lamouroux, N., Snelder, T., 2012. Le réseau hydrographique théorique (RHT) français et ses attributs environnementaux. Géomorphologie 3, 317–336, http://dx.doi.org/10.4000/geomorphologie.9933.
Peterson, B.J., Wollheim, W.M., Mulholland, P.J., Webster, J.R., Meyer, J.L., Tank, J.L., et al., 2001. Control of nitrogen export from watersheds by headwater streams. Science 292, 86–90, http://dx.doi.org/10.1126/science.1056874.
Poirier, S.C., Whalen, J.K., Michaud, A.R., 2012. Bioavailable phosphorus in fine-sized sediments transported from agricultural fields. Soil Sci. Soc. Am. J. 76, 258–267, http://dx.doi.org/10.2136/sssaj2010.0441.
Preston, S.D., Alexander, R.B., Schwarz, G.E., Crawford, C.G., 2011. Factors affecting stream nutrient loads: a synthesis of regional SPARROW model results for the continental United States. J. Am. Water Resour. Assoc. 47, 891–915, http://dx.doi.org/10.1111/j.1752-1688.2011.00577.x.
R Development Core Team, 2012. R: A language and environment for statistical computing. R Foundation for Statistical Computing, Vienna, Austria, ISBN 3-900051-07-0, URL http://www.R-project.org/
Redfield, A.C., 1958. The biological control of chemical factors in the environment. Am. Scientist 46, 205–222.
Romero, E., Garnier, J., Lassaletta, L., Billen, G., Le Gendre, R., Riou, P., Cugier, P., 2013. Large-scale patterns of river inputs in southwestern Europe: seasonal and interannual variations and potential eutrophication effects at the coastal zone. Biogeochemistry 113, 481–505, http://dx.doi.org/10.1007/s10533-012-9778-0.
Schindler, D.W., 2012. The dilemma of controlling cultural eutrophication of lakes. Proc. R. Soc. B: Biol. Sci. 279, 4322–4333, http://dx.doi.org/10.1098/rspb.2012.1032.
Schindler, D.W., Hecky, R.E., Findlay, D.L., Stainton, M.P., Parker, B.R., Paterson, M.J., Beaty, K.G., Lyng, M., Kasian, S.E.M., 2008. Eutrophication of lakes cannot be controlled by reducing nitrogen input: results of a 37-year whole-ecosystem experiment. Proc. Natl. Acad. Sci. U. S. A. 105, 11254–11258, http://dx.doi.org/10.1073/pnas.0805108105.
Schoumans, O.F., Chardon, W.J., Bechmann, M.E., Gascuel-Odoux, C., Hofman, G., Kronvang, B., Rubæk, G.H., Uléng, B., Dorioz, J.M., 2014. Mitigation options

to reduce phosphorus losses from the agricultural sector and improve surface water quality: a review. Sci. Total Environ. 468-469, 1255–1266, http://dx.doi.org/10.1016/j.scitotenv.2013.08.061.
Schoumans, O.F., Silgram, M., Groenendijk, P., Bouraoui, F., Andersen, H.E., Kronvang, B., et al., 2009. Description of nine nutrient loss models: capabilities and suitability based on their characteristics. J. Environ. Monit. 11, 506–514, http://dx.doi.org/10.1039/b823240g.
Schwarz, G.E., Alexander, R.B., Smith, R.A., Preston, S.D., 2011. The regionalization of national-scale SPARROW models for stream nutrients. J. Am. Water Resour. Assoc. 47, 1151–1172, http://dx.doi.org/10.1111/j. 1752-1688.2011.00581.x.
Seitzinger, S., Harrison, J.A., Bohlke, J.K., Bouwman, A.F., Lowrance, R., Peterson, B., Tobias, C., Van Drecht, G., 2006. Denitrification across landscapes and waterscapes: a synthesis. Ecol. Appl. 16, 2064–2090.
Senthilkumar, K., Nesme, T., Mollier, A., Pellerin, S., 2012. Regional-scale phosphorus flows and budgets within France: the importance of agricultural production systems. Nutr. Cycl. Agroecosyst. 92, 145–159, http://dx.doi.org/10.1007/s10705-011-9478-5.
Sharpley, A.N., Smith, S.J., Jones, O.R., Berg, W.A., Coleman, G.A., 1992. The transport of bioavailable phosphorus in agricultural runoff. J. Environ. Qual. 21, 30–35.
Smith, R.A., Schwarz, G.E., Alexander, R.B., 1997. Regional interpretation of water-quality monitoring data. Water Resour. Res. 33, 2781–2798.
Solagro. NOPOLU volet Agricole–Guide méthodologique; 2010. p. 89.
Strayer, D.L., Beighley, R.E., Thompson, L.C., Brooks, S., Nilsson, C., Pinay, G., et al., 2003. Effects of land cover on stream ecosystems: roles of empirical models and scaling issues. Ecosystems 6, 407–423, http://dx.doi.org/10.1007/s10021-002-0170-0.
Tysmans, D.J.J., Lohr, A.J., Kroeze, C., Ivens, W., van Wijnen, J., 2013. Spatial and temporal variability of nutrient retention in river basins: a global inventory. Ecol. Indic. 34, 607–615, http://dx.doi.org/10.1016/j.ecolind.2013.06.022.
Van Breemen, N., Boyer, E.W., Goodale, C.L., Jaworski, N.A., Paustian, K., Seitzinger, S.P., et al., 2002. Where did all the nitrogen go? Fate of nitrogen inputs to large watersheds in the northeastern USA. Biogeochemistry 57, 267–293.
Van Drecht, G., Bouwman, A.F., Harrison, J., Knoop, J.M., 2009. Global nitrogen and phosphate in urban wastewater for the period 1970 to 2050. Global Biogeochem. Cycles 23, GB0A03, http://dx.doi.org/10.1029/2009gb003458.
Van Rompaey, A.J.J., Verstraeten, G., Van Oost, K., Govers, G., Poesen, J., 2001. Modelling mean annual sediment yield using a distributed approach. Earth Surf. Process. Landforms 26, 1221–1236, http://dx.doi.org/10.1002/esp.275.
Vitousek, P.M., Aber, J.D., Howarth, R.W., Likens, G.E., Matson, P.A., Schindler, D.W., et al., 1997. Human alteration of the global nitrogen cycle: sources and consequences. Ecol. Appl. 7, 737–750, http://dx.doi.org/10.2307/2269431.
Windolf, J., Blicher-Mathiesen, G., Carstensen, J., Kronvang, B., 2012. Changes in nitrogen loads to estuaries following implementation of governmental action plans in Denmark: a paired catchment and estuary approach for analysing regional responses. Environ. Sci. Policy 24, 24–33, http://dx.doi.org/10.1039/c1em10139k.
Windolf, J., Thodsen, H., Troldborg, L., Larsen, S.E., Bøgestrand, J., Ovesen, N.B., Kronvang, B., 2011. A distributed modelling system for simulation of monthly runoff and nitrogen sources, loads and sinks for ungauged catchments in Denmark. J. Environ. Monit. 13 (9), 2645–2658, http://dx.doi.org/10.1016/j.envsci.2012.08.009.
Worrall, F., Burt, T.P., Howden, N.J.K., Whelan, M.J., 2009. Fluvial flux of nitrogen from Great Britain 1974–2005 in the context of the terrestrial nitrogen budget of Great Britain. Global Biogeochem. Cycles 23, GB3017, http://dx.doi.org/10.1029/2008gb003351.
Wosten, J.H.M., Pachepsky, Y.A., Rawls, W.J., 2001. Pedotransfer functions: bridging the gap between available basic soil data and missing soil hydraulic characteristics. J. Hydrol. 251, 123–150.
Wu, Y.P., Chen, J., 2013. Investigating the effects of point source and nonpoint source pollution on the water quality of the East River (Dongjiang) in South China. Ecol. Indic. 32, 294–304, http://dx.doi.org/10.1016/j.ecolind.2013.04.002.
Zampella, R.A., Procopio, N.A., Lathrop, R.G., Dow, C.L., 2007. Relationship of land-use/land-cover patterns and surface-water quality in the Mullica River basin. J. Am. Water Resour. Assoc. 43, 594–604, http://dx.doi.org/10.1111/j. 1752-1688.2007.00045.x.
Zhang, T., 2010. A spatially explicit model for estimating annual average loads of nonpoint source nutrient at the watershed scale. Environ. Model. Assess. 15, 569–581, http://dx.doi.org/10.1007/s10666-010-9225-3.
Zhou, T., Wu, J.G., Peng, S.L., 2012. Assessing the effects of landscape pattern on river water quality at multiple scales: a case study of the Dongjiang River watershed, China. Ecol. Indic. 23, 166–175, http://dx.doi.org/10.1016/j.ecolind.2012.03.013.